

Regulatory and functional aspects of stress-inducible plant metabolite pathways



Inaugural-Dissertation

zur Erlangung des Doktorgrades

der Mathematisch-Naturwissenschaftlichen Fakultät
der Heinrich-Heine-Universität Düsseldorf

vorgelegt von

Elia Stahl
aus Werdohl

Düsseldorf, Mai 2016

Aus dem Institut für Molekulare Ökophysiologie der Pflanzen
der Heinrich-Heine-Universität Düsseldorf.

Gedruckt mit der Genehmigung der Mathematisch-
Naturwissenschaftlichen Fakultät der Heinrich-Heine-Universität
Düsseldorf.

Referent: Prof. Dr. Jürgen Zeier

Korreferent: Prof. Dr. Vlada B. Urlacher

Tag der mündlichen Prüfung: 01.07.2016

Summary

The plant immune system is multilayered and consists of constitutive and inducible defense mechanisms. The cruciferous model plant *Arabidopsis thaliana* responds to an infection by the bacterial plant-pathogen *Pseudomonas syringae* rapidly with changes in the plant metabolome. The produced metabolites have a broad structural diversity and include phenolics, protein and non-protein amino acids, indole derivatives, terpenoids, oxylipins, phytosterols, and others. Some of these metabolites possess a direct antimicrobial activity, whereas others act as signals, controlling the expression of defense-related genes and contributing to plant innate immunity by regulatory means. Here, it is reported that several previously uncharacterized metabolite pathways are activated in *A. thaliana* upon *P. syringae*-infection.

Tocopherols are lipid-soluble antioxidants with vitamin E activity that are synthesized exclusively by photosynthetic organisms and occur in plastids of higher plants. The four known tocopherols, α -, β -, γ - and δ -tocopherol, differ in number and position of methyl groups on their chromanol head group. We realized that inoculation of *Arabidopsis* leaves with virulent or avirulent *P. syringae* strains induces increased expression of several genes involved in early steps of tocopherol biosynthesis. Subsequent metabolite analyses revealed that *P. syringae* inoculation triggers a strong accumulation of β -tocopherol and quantitatively moderate production of γ - and δ -tocopherol in leaves, whereas α -tocopherol levels essentially remain constant. Notably, *vte2* which is fully impaired in basal and pathogen-induced tocopherol generation but not in the accumulation of other defense related metabolites, exhibits increased susceptibility towards virulent *P. syringae*. This is accompanied by increased levels of lipid peroxidation after *P. syringae* infection in this mutant. The lack of tri-unsaturated fatty acids in a *vte2-1 fad3-2 fad7-2 fad8* quadruple mutant prevents increased lipid peroxidation in the *vte2* background and restores pathogen resistance to wild-type levels. Our results therefore suggest that basal levels and induced production of tocopherols contribute to *Arabidopsis* basal resistance against *Pseudomonas syringae* by preventing oxidative damage of lipids.

Moreover, we could identify nine N-acetylated and N-formylated amino acids which accumulate in *Arabidopsis* in response to *P. syringae* infection. The *P. syringae*-inducible accumulation of those metabolites is influenced by JA- and ethylene-signaling. However, the functional relevance of the identified N-acetylated amino acids could not be clarified in this study and remains to be elucidated. Additionally, we could

Summary

identify scopoletin, a methyl coumarin, as a metabolite which accumulates in *Arabidopsis* upon *P. syringae* infection. Transcript levels of the 2 oxoglutarate-dependent dioxygenase *F6'H1*, which is essential for scopoletin biosynthesis in *Arabidopsis*, are increased upon *P. syringae* infection. An *Arabidopsis* mutant plant which is impaired in scopoletin biosynthesis via *F6'H1* exhibits a moderate increased susceptibility towards virulent and avirulent *P. syringae*, suggesting that scopoletin production to some extent contributes to *Arabidopsis* basal resistance against bacterial plant-pathogens.

Furthermore, it is shown that indolic metabolism is broadly activated in *P. syringae*-inoculated and in distant, non-inoculated leave tissue. We therefore investigated the functional role and the regulatory characteristics of indolic metabolism in systemic acquired resistance (SAR). At inoculation sites, camalexin, indol-3-ylmethylamine (I3A), and indole-3-carboxylic acid (ICA) are the major accumulating compounds, along with about 20 other detected indolics. Moreover, exogenous application of the defense hormone salicylic acid (SA) stimulates I3A generation at the expense of its precursor indol-3-ylmethylglucosinolate (I3M), and the SAR regulator pipecolic acid (Pip) primes plants for enhanced *P. syringae*-induced activation of distinct branches of indolic metabolism. In uninfected systemic tissue, the metabolic response is more specific and associated with enhanced levels of the indolics I3A, ICA, and indole-3-carbaldehyde (ICC). Systemic indole accumulation fully depends on functional *CYP79B2/3*, *PEN2*, and *MYB34/51/122*, and requires functional SAR signaling. Mutant analyses suggest that systemically elevated indoles are dispensable for SAR directed against *P. syringae* and associated systemic increases of salicylic acid. However, soil-grown but not hydroponically-cultivated *cyp79b2/3* and *pen2* plants, both defective in indolic secondary metabolism, exhibit pre-induced immunity, which abrogates their intrinsic ability to induce SAR.

The capability of SAR establishment in plants is dependent on Pip and SA signaling pathways. Thereby, Pip functions as the main regulator of SAR, controlling SAR establishment via SA-dependent and –independent pathways. SA acts downstream of Pip and *FLAVIN-DEPENDENT MONOOXYGENASE1* (FMO1) in defense-signal-amplification and is necessary for a full and strong SAR response. We therefore further investigated if the main SAR regulator Pip can serve as a precursor for new potential defense related metabolites and investigated a potential role of Pip as a long-distance signal in SAR establishment. We fed deuterium labeled Pip into distinct leaves in combination with an infection with *P. syringae*. Exogenous fed Pip at the

Summary

infection-site can be metabolized to N-formyl-Pip and partially also to α -amino adipic acid (Aad). Moreover, Pip can serve as a precursor for two until now not yet identified FMO1-generated metabolites. Furthermore, the exogenous fed Pip could be detected also in leaves distal to the site of application. However, this transport was not increased in wild-type plants which were in addition to Pip-infiltration also infected with *Psm*. Interestingly, *ald1* mutant plants, which are defective in endogenous Pip generation and SAR, could activate systemic defense responses to a certain extent when locally co-infiltrated with both Pip and *Psm*. By contrast, local Pip- or *P. syringae*-infiltrations alone were not sufficient to trigger systemic responses in the *ald1* mutant. Although able to partially complement SAR-deficiency of *ald1*, Pip and *P. syringae* co-treatments could not trigger any SAR response in *fmo1* mutant plants, which is consistent with the previously described central function of *FMO1* downstream of Pip in SAR activation.

Zusammenfassung

Das pflanzliche Immunsystem hat mehrere Stufen und beinhaltet konstitutive und induzierbare Abwehrmechanismen. Der Modellorganismus *Arabidopsis thaliana*, aus der Familie der Brassicaceae, reagiert auf eine Infektion des bakteriellen Pflanzenpathogen *Pseudomonas syringae* mit Änderungen im Metaboliten-Profil. Die produzierten Metaboliten sind strukturell divers und beinhalten Phenole, Aminosäuren, Indolalkaloide, Terpenoide, Oxylipine, Phytosterole und andere. Einige dieser Metaboliten wirken direkt antimikrobiell, während andere die Expression von Abwehrgenen kontrollieren und damit in regulatorischer Weise zur pflanzlichen Immunantwort beitragen. Diese Arbeit beschreibt weitere, bis jetzt nicht beschriebene, Metabolitenbiosynthesewege in *Arabidopsis*, die in Folge einer *Pseudomonas syringae*-Infektion aktiviert werden.

Tocopherole sind eine Gruppe von lipophilen Antioxidanten, die ausschließlich von Photosynthese-betreibenden Organismen synthetisiert werden können und in den Plastiden von höheren Pflanzen vorkommen. Man unterscheidet in Pflanzen zwischen vier verschiedenen Formen von Tocopherolen, α -, β -, γ - und δ -Tocopherol. Die vier Tocopherol-Derivate unterscheiden sich durch die Anzahl und die Position der Methylgruppen am Chromanolring. Gene, die für Enzyme kodieren die frühe Schritte der Tocopherol-Biosynthese katalysieren, zeigen erhöhte Transkript-Level in Blättern, die mit virulenten und avirulenten *P. syringae* infiziert sind. Metaboliten Analysen zeigten, dass eine *P. syringae*-Infektion zu einer starken Akkumulation von β -Tocopherol führt und zu einer moderaten Produktion von γ - und δ -Tocopherol, während die endogenen α -Tocopherol Level konstant bleiben. Die Mutante *vte2* ist vollständig beeinträchtigt in der basalen und *P. syringae*-induzierten Akkumulation von Tocopherolen, aber nicht in der Produktion von anderen Abwehrmetaboliten. Interessanterweise zeigt diese Mutante eine erniedrigte basale Resistenz gegen *P. syringae*, welche von erhöhter Lipid-Peroxidation im Falle einer *P. syringae*-Infektion begleitet ist. Das Fehlen von dreifach ungesättigten Fettsäuren in der *vte2-1 fad3-2 fad7-2 fad8* vierfach Mutante verhindert die erhöhte Lipid-Peroxidation im *vte2*-Hintergrund und stellt eine Resistenz auf Wildtyp Niveau wieder her. Die Ergebnisse zeigen, dass Tocopherole in *Arabidopsis* zur basalen Resistenz gegen *P. syringae* beitragen, indem sie Lipide vor oxidativem Schaden schützen.

Des Weiteren konnten im Rahmen dieser Arbeit neun N-acetylierte und N-formylierte Aminosäuren identifiziert werden, die in *P. syringae* infizierten *Arabidopsis* Pflanzen akkumulieren. Die Akkumulation dieser Aminosäuren ist beeinflusst von JA

und Ethylen Signalwegen, aber die funktionelle Relevanz dieser Metaboliten in Arabidopsis gegen bakterielle Pathogene konnte im Rahmen dieser Arbeit nicht aufgeklärt werden. Ein weiterer Metabolit, der in *P. syringae* infizierten Arabidopsis Pflanzen akkumuliert, ist Scopoletin. Die Transkript-Level der 2-Oxoglutarat-abhängigen Dioxygenase *F6'H1*, die für die Scopoletin-Biosynthese in Arabidopsis essentiell ist, sind im Falle einer *P. syringae*-Infektion erhöht. Eine Arabidopsis Mutante, die in der Scopoletin-Biosynthese via *F6'H1* beeinträchtigt ist, zeigt eine leicht erhöhte Anfälligkeit gegen virulente und avirulente *P. syringae* Stämme. Dieses Ergebnis weist darauf hin, dass die Scopoletin-Akkumulation zur basalen Resistenz von Arabidopsis gegen bakterielle Pathogene beitragen könnte.

Weiterhin konnte in dieser Arbeit gezeigt werden, dass der Indol-Metabolismus umfassend aktiviert wird. Die Akkumulation von Indolalkaloiden ist hierbei nicht nur auf den Infektionsort beschränkt, sondern kann auch in Blättern distal zu der Infektion beobachtet werden. Aus diesem Grund wurde die regulatorische Rolle des Indol-Metabolismus in der systemisch erworbenen Resistenz (SAR) untersucht. In infizierten Blättern konnte die Akkumulation von ca. 20 Indolalkaloiden beobachtet werden. Dabei sind die am stärksten akkumulierenden Indole Camalexin, Indol-3-ylmethylamin (I3A) und Indole-3-Carboxylsäure (ICA). Die exogene Gabe des Pflanzenabwehrhormons Salicylsäure (SA) stimuliert die Produktion von I3A auf Kosten des Biosynthesevorläuferstoffes Indol-3-Methylglucosinolat (I3M). Zudem induziert der SAR-Regulator Pipecolinsäure (Pip) das Priming einiger Zweige des Indol-Metabolismus. Die Akkumulation von Indolalkaloiden in Blättern distal zum Infektionsort ist spezifischer. Hier kann die Akkumulation von drei Indolen beobachtet werden; I3A, ICA und Indole-3-Carbaldehyd (ICC). Die systemische Indol-Akkumulation ist vollständig abhängig von *CYP79B2/3*, *PEN2* und *MYB34/51/122*, darüber hinaus benötigt sie funktionierende SAR-Signalwege. Die Analyse von Arabidopsis Mutanten zeigte, dass die systemische Indol-Akkumulation nicht zur SAR-Etablierung benötigt wird. Ferner konnte gezeigt werden, dass auf Erde kultivierte *cyp79b2/3* und *pen2* Mutanten, die beide im Indol-Metabolismus beeinträchtigt sind, eine präaktivierte Immunantwort zeigen, welche ihre Möglichkeit SAR zu etablieren beeinflusst. Dies ist nicht der Fall, wenn *cyp79b2/3* und *pen2* in einem hydroponischen Medium kultiviert werden.

Die Etablierung von SAR in Pflanzen ist abhängig von Pip und SA Signalwegen. Hierbei orchestriert Pip als Hauptregulator der SAR, welcher SAR über SA-abhängige und unabhängige Signalwege kontrolliert. In der Signalkette der SAR-Etablierung agiert

SA dabei hinter Pip und der Flavin abhängigen Monooxygenase 1 (FMO1) in der Amplifikation der Abwehrreaktion und ist für eine volle und starke SAR-Reaktion erforderlich. Im Rahmen dieser Arbeit wurde untersucht ob der SAR-Hauptregulator Pip als mobiles Langstreckensignal in der SAR-Etablierung fungiert und ob Pip als Vorstufe für andere abwehrrelevante Metaboliten dienen kann. Hierfür wurde mit Deuterium markiertes Pip, in Kombination mit *P. syringae*, in individuelle Blätter gefüttert. Am Infektionsort kann das gefütterte Pip zu N-formyl-Pip metabolisiert werden und teilweise auch zu α -Amino Adipinsäure (Aad). Des Weiteren kann das gefütterte Pip in zwei FMO1-abhängige Metaboliten umgewandelt werden, die im Rahmen dieser Arbeit nicht identifiziert werden konnten. Das gefütterte Pip kann darüber hinaus auch in Blättern distal zur Applikation detektiert werden. Obwohl dieser Transport nicht erhöht ist, wenn Pip in Kombination mit *P. syringae* in lokale Blätter infiltriert wird, induziert nur eine Co-Infiltration eine partielle systemische Aktivierung von Abwehrreaktionen in Pip-defizienten *ald1* Pflanzen, während eine Infiltration von Pip alleine keine systemische Reaktionen in *ald1* induziert. Passend zu der partiellen Aktivierung von Abwehrreaktionen in *ald1* und der Rolle von FMO1 in SAR, kann die Co-Infiltration von Pip und *P. syringae* partiell den SAR-Defekt von *ald1* Pflanzen kompensieren, aber nicht den von *fmo1* Pflanzen.

Content

Summary	I
Zusammenfassung	IV
Content	VII
List of figures	XI
1 Introduction	14
1.1 Constitutive defense layers and their role for nonhost resistance	15
1.2 Inducible defense mechanisms.....	17
1.2.1 PAMP-triggered immunity	17
1.2.2 Effector-triggered immunity.....	18
1.2.3 Systemic acquired resistance	19
1.2.4 Primary and secondary metabolism in plant defense	20
1.2.4.1 Phytohormones in plant defense.....	20
1.2.4.2 Salicylic acid (SA).....	20
1.2.4.3 Jasmonic acid (JA), abscisic acid (ABA), and ethylene	21
1.2.4.4 Phytohormone cross-talk in plant defense	23
1.2.4.5 Pipecolic acid (Pip)	25
1.2.4.6 Phytoalexins	27
1.2.4.7 Oxylipins	30
1.2.4.8 Stigmasterol.....	33
1.3 The model pathosystem <i>Arabidopsis thaliana</i> and <i>Pseudomonas syringae</i>	33
1.4 Aims and form of the thesis	34
2 Tocopherols in Arabidopsis basal resistance	35
2.1 Abstract	35
2.2 Introduction.....	36
2.3 Results	39
2.3.1 Tocopherol biosynthesis in Arabidopsis is induced upon <i>Pseudomonas syringae</i> inoculation.....	39
2.3.2 Pathogen-triggered tocopherol generation is independent of classical stress inducible signaling molecules SA, JA, ABA, ethylene, Pip and extracellular H ₂ O ₂	44
2.3.3 The <i>vte2-2</i> mutant exhibits increased susceptibility against <i>Psm</i> and is fully impaired in basal and pathogen-triggered Tocopherol accumulation but not in the accumulation of other defense-related metabolites.....	45

2.3.4 The <i>vte2-2</i> mutant exhibits an increased amount of non-enzymatic lipid peroxidation in leaves after <i>Psm</i> inoculation	49
2.3.5 Reduced non-enzymatic lipid peroxidation in the <i>vte2</i> background abolishes the <i>vte2</i> susceptibility phenotype	51
2.4 Discussion	53
2.4.1 The transcriptional reprogramming of tocopherol biosynthesis upon <i>P. syringae</i> infection leads to a strong accumulation of β -tocopherol in Arabidopsis	53
2.4.2 Pathogen-triggered tocopherol generation is independent from classical phytohormone defense-signaling	55
2.4.3 Constitutive and pathogen-induced tocopherols contribute to Arabidopsis basal resistance to <i>Psm</i> and protect tri-unsaturated fatty acids from non-enzymatic lipid peroxidation during infection	56
3 Amino acid metabolism in plant defense	61
3.1 Introduction.....	61
3.2 Results	63
3.2.1 Accumulation of acetylated and formylated amino acids upon <i>Psm</i> -infection. 63	
3.2.2 The <i>P. syringae</i> -induced accumulation of the identified acylated amino acids is influenced by stress-inducible phytohormone pathways and is activated by constitutive defense signaling	65
3.2.3 Investigating the role of amino acid acylation in inducible plant immunity	68
3.3 Discussion	70
3.3.1 Identification of nine N-acetylated and N-formylated amino acids which accumulate in Arabidopsis leaves in response to a <i>Psm</i> -infection	70
3.3.2 Regulation of <i>Psm</i> -inducible accumulation of the nine identified acylated amino acids.....	71
3.3.3 Investigations for a putative role of N-acetylated and N-formylated amino acids in Arabidopsis inducible immunity against <i>Psm</i>	72
4 Scopoletin in Arabidopsis initiate immunity	75
4.1 Introduction.....	75
4.2 Results	77
4.2.1 Scopoletin biosynthesis is activated in Arabidopsis upon <i>Psm</i> -infection	77
4.2.2 Coumarin metabolism moderately contributes to Arabidopsis basal resistance against <i>P. syringae</i>	79
4.3 Discussion	79
5 Indolic compounds in systemic acquired resistance	83

Content

5.1 Abstract	83
5.2 Introduction.....	84
5.3 Results	87
5.3.1 SAR establishment in Arabidopsis is associated with a strong activation of indolic metabolism.....	87
5.3.2 Temporal patterns of indolic metabolite accumulation in inoculated leaves.....	92
5.3.3 Biosynthetic and regulatory aspects of indolic metabolism at sites of bacterial inoculation	94
5.3.4 Systemic accumulation of I3A, ICA, and ICC is dependent on <i>CYP79B2/3</i> , <i>PEN2</i> , <i>MYB34/51</i> and requires functional SAR signaling	101
5.3.5 Pre-induced immunity of soil-grown <i>cyp79b2/3</i> and <i>pen2</i> plants mask their intrinsic ability for SAR establishment.....	105
5.3.6 Exogenous application of indole-3-carboxylic acid does not lead to a major resistance increase to <i>Psm</i> infection	108
5.4 Discussion.....	109
5.4.1 Activation and regulatory aspects of Trp-derived metabolism in <i>P. syringae</i> -inoculated leaves.....	109
5.4.2 Systemic indole accumulation and its functional relevance for SAR.....	114
5.4.3 Cultivation-dependent pre-induced immunity in <i>cyp79b2/3</i> and <i>pen2</i> dampens <i>P. syringae</i> -triggered SAR.....	117
6 Metabolism and transport of Pip in Arabidopsis SAR	119
6.1 Abstract	119
6.2 Introduction.....	120
6.3 Results	123
6.3.1 A co-infiltration of Pip and <i>Psm</i> leads to a partial SAR response in <i>ald1</i> but not in <i>fmo1</i>	125
6.3.2 Upon <i>P. syringae</i> -infection, Pip can be metabolized via FMO1-dependent and -independent pathways at the inoculation-site	126
6.3.3 D ₉ -Pip can be detected in leaf tissue distal to the site of infiltration.....	132
6.3.4 A local co-infiltration of Pip and <i>Psm</i> leads to a partial activation of defense responses in systemic leaf tissue in <i>ald1</i> which is absent in <i>fmo1</i>	133
6.4 Discussion.....	139
6.4.1 In <i>Psm</i> -infected leaf tissue Pip can be metabolized in FMO1-dependent and -independent manner.....	139
6.4.2 A local co-infiltration of Pip and <i>Psm</i> can partial complement SAR deficiency of <i>ald1</i> mutant plants in a FMO1-dependent manner.....	142

Content

7 Methods	148
7.1 Plant material and cultivation	148
7.2 Cultivation and inoculation of bacteria	148
7.3 Determination of basal resistance and SAR.....	149
7.4 flg22 and xanthine/xanthine oxidase treatments	149
7.5 Exogenous application of Pip via the leaf.....	150
7.6 Exogenous application of Pip, SA, and ICA for assessment of basal resistance	150
7.7 Microarray data.....	151
7.8 Quantitative real-time PCR analysis	151
7.9 Determination of nonenzymatic lipid peroxidation via MDA quantification	151
7.10 Determination of metabolites via GC/MS	151
7.11 Determination of free amino acids via GC/MS	152
7.12 Determination of metabolites via HPLC	152
7.13 Accession numbers	153
8 References	154
Supplemental Material	179
Curriculum vitae	205
Acknowledgements	208
Eidesstattliche Versicherung	209
Author contributions Chapter 5	210

List of figures

Figure 1.1 Schematic overview of defense layers a plant-pathogen has to conquer for a successful infection of his host.	15
Figure 1.2 Plant hormone crosstalk in plant defense signaling.	24
Figure 3.1 Possible scheme for the metabolism of the Lys catabolites Pip and Aad following pathogen attack.....	26
Figure 1.4 Structures of selected phytoalexins which are produced by members of the plant families Brassicaceae, Fabaceae, Vitaceae, Solanaceae, and Poaceae.	28
Figure 2.1 Scheme of tocopherol-biosynthesis in Arabidopsis and changes in tocopherol-biosynthesis upon <i>P. syringae</i> infection.....	40
Figure 2.2 Inoculation of Arabidopsis leaves with <i>Psm</i> and <i>Psm avrRpm1</i> triggers a transcriptional reprogramming of genes involved in tocopherol biosynthesis.	41
Figure 2.3 Temporal accumulation of tocopherols upon <i>Psm</i> - and <i>Psm avrRpm1</i> -inoculation.	43
Figure 2.4 Exogenous application of superoxide and flg22 is sufficient to trigger a moderate β -tocopherol accumulation.....	44
Figure 2.5 Pathogen-triggered generation of β -tocopherol is virtually independent of ethylene-, jasmonic acid-, salicylic acid, abscisic acid-, pipecolic acid-signaling and extracellular H ₂ O ₂	46
Figure 2.6 The <i>vte2-2</i> mutant exhibits increased susceptibility against <i>Psm</i>	46
Figure 2.7 The <i>vte2-2</i> mutant is fully impaired in basal and pathogen-triggered tocopherol generation but not in the accumulation of other defense-related metabolites.	48
Figure 2.8 The <i>vte2-2</i> mutant exhibits increased nonenzymatic lipid peroxidation upon <i>Psm</i> -inoculation.....	50
Figure 2.9 Reduced nonenzymatic lipid peroxidation in the <i>vte2</i> background complements the <i>vte2</i> susceptibility phenotype.	52
Figure 2.10 Proposed model for the role of tocopherols in Arabidopsis basal resistance against <i>Psm</i>	59

Figure 3.1 Changes in endogenous levels of identified N-acylated amino acids in Arabidopsis (Col-0) after inoculation with <i>Psm</i> at the infection-site.	64
Figure 3.2 Temporal accumulation of N-formyl-Leu upon <i>Psm</i>- and <i>Psm avrRpm1</i>-inoculation.	65
Figure 3.3 Pathogen-triggered generation of N-formyl-Leu in different phytohormone-biosynthesis and –signaling mutants.	66
Figure 3.4 Accumulation of the identified acylated amino acids in <i>etr1</i>, <i>dde2</i>, and <i>cpr5-2</i> after inoculation with <i>Psm</i> and <i>Psm avrRpm1</i>.	67
Figure 3.5 Basal resistance of <i>atf1</i>, <i>nata1</i>, <i>ivd1-a</i>, <i>din4-a</i>, and <i>din4-c</i> mutant plants against <i>Psm</i>.	69
Figure 4.1 Scopoletin biosynthesis is activated upon <i>P. syringae</i>-infection and coumarin metabolism contributes to Arabidopsis basal resistance against <i>P. syringae</i>.	78
Figure 4.2 Pathogen-triggered generation of scopoletin in mutants impaired in defence signaling pathways.	81
Figure 5.1 Chemical structure of selected indolics.	90
Figure 5.2 Indole accumulation in <i>P. syringae</i>-inoculated (1°) and in non-inoculated, systemic leaf tissue (2°) of Arabidopsis Col-0 plants.	91
Figure 5.3 Time course of indole accumulation in Col-0.	93
Figure 5.4 <i>P. syringae</i>-inducible indole accumulation in mutants impaired in indolic metabolism at the site of inoculation.	95
Figure 5.5 <i>P. syringae</i>-inducible indole accumulation in mutant plants affected in camalexin production.	96
Figure 5.6 Impact of exogenous salicylic acid and pipercolic acid treatments on basal and inducible levels of indolics in leaves of Col-0 plants.	100
Figure 5.7 <i>P. syringae</i>-inducible indole accumulation in mutants impaired in indolic metabolism in leaves distal from the inoculation site.	103
Figure 5.8 Levels of indolic metabolites in leaves of SAR-deficient mutant plants following <i>P.syringae</i> inoculation.	104

Figure 5.9 Pre-induced immunity of soil-grown <i>cyp79b2/3</i> and <i>pen2</i> plants dampens <i>P. syringae</i>-triggered SAR.	106
Figure 5.10 Soil-grown <i>myb34</i>, <i>myb51</i>, <i>myb122</i>, <i>myb51 myb122</i>, and <i>tmyb</i> plants display normal SAR.	108
Figure 5.11 Regulation of induced indolic metabolism in <i>P. syringae</i>-inoculated leaves, and possible consequences of dysfunctional, indole-related early immune layers on basal resistance and SAR.	115
Figure 6.1 Experimental setup for Pip and D₉-pip feeding via the leaf.	124
Figure 6.2 A co-infiltration of Pip + <i>Psm</i> partial complements SAR deficiency of <i>ald1</i> in a FMO1-dependent manner	125
Figure 6.3 Pip and D₉-Pip can be discriminated in infiltrated leave tissue.	127
Figure 6.4 Moderate amounts of exogenous fed D₉-Pip can endogenously be converted to D₆-Aad.	129
Figure 6.5 Pip can serve as a precursor for N-formyl-Pip.	130
Figure 6.6 Detection of potential D₉-Pip-derived metabolites generated by FMO1.	131
Figure 6.7 D₉-Pip can be detected in leaves distal to the leaves of exogenous application.	132
Figure 6.8 The local co-infiltration of D₉-Pip + <i>Psm</i> leads to a partial activation of systemic SA-biosynthesis in <i>ald1</i> but not in <i>fmo1</i>.	134
Figure 6.9 The local co-infiltration of D₉-Pip + <i>Psm</i> leads to an increased expression of SA-dependent and SA-independent SAR+ genes in <i>ald1</i> but not in <i>fmo1</i>.	136
Figure 6.10 The local co-infiltration of D₉-Pip + <i>Psm</i> leads to a partial activation of systemic indole metabolism in <i>ald1</i> but not in <i>fmo1</i>.	137
Figure 6.11 SAR upon the co-infiltration of Pip + <i>Psm</i> in mutants impaired in Pip and SA signaling.	138
Figure 6.12 Possible model for the transport and metabolism of exogenously applied Pip in combination with <i>Psm</i> inoculation in Col-0, <i>ald1</i>, and <i>fmo1</i>.	146

1 Introduction

By the conversion of light energy into chemical energy and the production of oxygen, plants are the basis of all life on earth. Plants live in fast changing environments and are exposed through their lifetime to several abiotic stressors such as variable light conditions, changing temperatures, nutrient availability, or changing water amounts, but also to biotic stressors. Biotic stress results from the interaction of plants with several insects, microorganism, or other plants, which can interact with above-grown plant parts but also with roots. Some of those microorganisms and insects have evolved structures that enable them to live and feed on plants.

During evolution, plants have evolved a multilayered immune system that counteracts pathogen attack. This plant immune system consists of constitutive and inducible defense layers, and a plant pathogen has to overcome all those barriers for a successful infection of its potential host (Fig. 1.1; Thordal-Christensen, 2003; Jones and Dangl, 2006; Spoel and Dong, 2012). Most interactions between plant-pathogens and plants remain symptom-free, caused by that a plant-pathogen is not adapted to a specific plant species, which makes the plant not suitable as a source of life for the pathogen. This phenomenon is described as nonhost resistance (Thordal-Christensen, 2003). In addition to the buildup of constitutive defense layers, plants can activate a broad range of inducible defense responses in cases of an imminent pathogen infection. Therefore, plants are able to recognize potential pathogens by so called microbe or pathogen associated molecular patterns (MAMPs; PAMPs). PAMPs are often highly conserved structures of a distinct group of pathogens and essential compounds of those microorganisms, such as flg22 which is a highly conserved peptide sequence from the bacterial flagellum (Felix et al., 1999; Gómez-Gómez et al., 1999; Chinchilla et al., 2007), or chitin which is an essential constituent of fungal cell walls (Felix et al., 1993; Kaku et al., 2006). Furthermore, plants can recognize damage-associated molecular patterns (DAMPs) which are released by a plant upon a pathogen infection or wounding (Lotze et al., 2007). A schematic scheme of defense layers which plant-pathogens have to conquer is depicted in Fig. 1.1. Notably, the development of all this defense layers is accompanied by the endogenous production of primary and secondary metabolites as described in the following.

1.1 Constitutive defense layers and their role for nonhost resistance

Constitutive defense layers comprises mechanical barriers such as trichomes on plant leaves and stems, reinforced plant cell walls, or the presence of a cuticle, but also antimicrobially-acting secondary metabolites and enzymes. The plant cuticle is a wax layer on several parts of the plant which is composed out of very long chain fatty acids (Kolattukudy, 1981; Nawrath, 2002). Beside to its role in the regulation of transpiration in leaves and the protection prior irradiation damage, the plant cuticle is also assigned with a role in plant-herbivore and plant-fungi interactions (Nawrath, 2002). Several pathogenic fungi have to produce and secrete cutinases, which are enzymes that degrade cutin polymers, for a successful penetration of their host plant (Kolattukudy, 1985; Kolattukudy et al 1995). However, it was also reported that several pathogenic fungi need

signals from the surface wax of their host to trigger infection, suggesting that the cuticle composition of the host is important for the host-identification of some adapted pathogens (Kolattukudy, et al 1995; Tsuba et al., 2002 Hansjakob et al 2011). In addition to mechanical barriers, constitutive defense layers also consist of antimicrobial secondary metabolites, such as saponins. Saponins are glycosylated secondary metabolites which are found in several crop plants and are produced by them in high quantities. They can bind and extract sterols from fungal cell walls and are therefore harmful for several fungi. Consistent with that, saponin-deficient (*sad*) mutant plants of wild oat (*Avena strigosa*) are more susceptible to the pathogenic fungus *Gaeumannomyces graminis* var. *tritici* than the saponin-producing wild-type (Papadopoulou et al., 1999). Saponins in oat plants are also an example for the co-

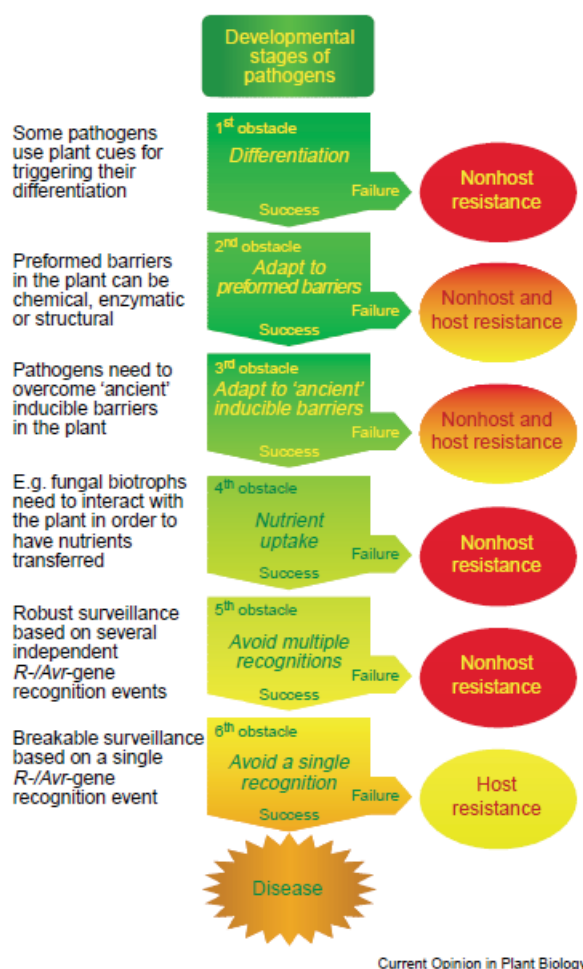


Figure 1.1 **Schematic overview of defense layers a plant-pathogen has to conquer for a successful infection of his host.**

Figure from: Thordal-Christensen, 2003

evolution between a plant pathogen and its host. The pathogenic fungi *Stagonospora avenae* is able to infect oat plants despite the presence of saponins produced by the host. *S. avenae* produces and secretes multiple enzymes which can hydrolyze oat saponins. However, even the biosynthesis of the saponin-hydrolyzing β -glucosidase on the site of *S. avenae* is not essential for the infection of oat plants, this process could contribute to pathogenicity of *S. avenae* against oat plants (Morrissey et al., 2000).

Other secondary metabolites which are constitutively synthesized by plant species belonging to the family Brassicales and contribute to plant resistance are glucosinolates (Piasecka et al., 2015). Glucosinolates are derived from different amino acids, including Val, Leu, Ile, Met, Phe, Tyr, and Trp, and contain for example allyl, benzyl, or hydroxy-butenyl functional groups (Halkier and Gershenzon, 2006). Therefore glucosinolates in cruciferous plants have a brought structural diversity (Agerbirk and Olsen, 2012). Arabidopsis mainly generates two groups of those metabolites, the Trp-derived indolic glucosinolates (IGs) and the Met-derived aliphatic glucosinolates (AGs). Glucosinolates represent chemically stable and biological inactive metabolites which are stored in vacuoles. In separated but adjacent cells plants store β -thioglucoside glucohydrolases (TGGs), which are also described as myrosinases. Upon plant-tissue disruption, glucosinolates and TGGs are released and the TGGs initiate a rapid glucosinolate hydrolysis. This process results in the generation of chemically unstable aglycones, such as isothiocyanates. Those metabolites are chemical highly reactive and possess protection prior insects and some microbial plant-pathogens (Piasecka et al., 2015).

Metabolites which are constitutively produced by different plant species and contribute to resistance against different plant pathogens are also designated as phytoanticipins (VanEtten et al., 1994). Other plant natural products that can act as phytoanticipins are phenylpropanoids, terpenoids, cyanogenic glucosides, and fatty acid derivatives (Dixon, 2001; Piasecka et al., 2015).

In addition to the failure of a putative pathogen to recognize a host-plant because of the lack of specific plant-derived signals, the above described phenomenon's reason that the most interactions between plants and pathogenic microorganism do not lead to an infection, which is generally described as nonhost resistance (Thordal-Christensen, 2003; Fig. 1.1).

1.2 Inducible defense mechanisms

If a pathogen succeeds to overcome constitutive defense layers, plants can recognize pathogens and induce a broad range of defense responses. The recognition of pathogen occurs thereby via MAMPs, PAMPs, DAMPs, or via the detection of effectors which are in particular secreted by microbial pathogens to their host to suppress host immunity (Thordal-Christensen, 2003; Jones and Dangl, 2006; Lotze et al., 2007; Spoel and Dong, 2012). Therefore, PAMP triggered immunity (PTI) and effector triggered immunity (ETI) can be discriminated (Jones and Dangl, 2006).

1.2.1 PAMP-triggered immunity

PAMPs are recognized by pattern recognition receptors (PRR) in mammals and plants (Zipfel, 2008; Boller and He, 2009; Kawai and Akira, 2010). In plants, PRRs are localized at plasma membranes. Intensively studied bacterial PAMPs are flg22, lipopolysaccharides (LPS), and the elongation factor Tu (EF-Tu). In plants, flg22, a highly conserved peptide sequence in the N-terminus of bacterial flagellin, which is a major protein constituent of the flagellum, is recognized by the PRR FLAGELLIN SENSING 2 (FLS2) (Felix et al., 1999). The recognition of flg22 via the receptor-like protein kinase FLS2 triggers a broad range of defense responses in *Arabidopsis* and other plants, including an oxidative burst and changes in the plant metabolome, resulting in increased resistance against bacterial pathogens (Felix et al., 1999; Zipfel et al., 2004; Mishina and Zeier, 2007; Návarová et al., 2012). For a successful activation of flg22-inducible immunity, FLS2 needs to form a dimer-complex with BAK1, a receptor kinase which is also involved in brassinosteroid signaling (Chinchilla et al., 2007, Sun et al., 2013). As well as flg22, EF-Tu and LPS are highly conserved bacterial patterns. LPS are glycolipids in the outer membrane of gram-negative bacteria and EF-Tu is a highly abundant protein involved in translation mechanisms in bacteria. Whereas the PRR for LPS in plants is not identified yet, the PRR for EF-Tu is known. A highly conserved peptide sequence of bacterial EF-Tu (elf18) is recognized by the EF-TU RECEPTOR (EFR), another receptor-like protein kinase. In the same way as for FLS2, signaling activity of EFR is dependent on functional BAK1 (Zipfel, 2008; Monaghan and Zipfel, 2012). Beside to those bacterial PAMPs, plants can recognize chitin and xylanase from fungi, heptaglucan from oomycotes, or damaged plant-cell wall-derived oligogalacturonides (DAMPs) to initiate defense responses (Monaghan and Zipfel, 2012).

1.2.2 Effector-triggered immunity

To overcome PTI, microbial pathogens can secrete effectors to their host to interfere with PTI-associated defense signaling. To secrete effectors into their host, bacteria have fixed a so called type III secretion system (TTSS) during evolution to colonize their respective host organisms (Büttner and He, 2009). If the secreted effectors successfully suppress PTI, the pathogen can colonize its host, which is then called effector-triggered susceptibility or a compatible interaction between the bacterial pathogen and its host (Jones and Dangl, 2006). However, in adaptation to their pathogens, plants have developed also specific mechanisms to recognize those effectors directly or indirectly by so-called resistance-proteins. This concept of plant resistance is described as gene-for-gene resistance and is realized when an avirulence-gene of an adapted pathogen is suitable to a resistance-gene of the host (Flor, 1971). If a product of an avirulence gene is recognized by a plant, the plant responds with a fast activation of defense responses, which suppress pathogen proliferation by triggering a programmed cell death in the infected area. This process is called the hypersensitive response (HR) (Mur et al., 2008). The interaction between an avirulent bacterial pathogen and a host plant is described as an incompatible interaction. Bacterial pathogens can secrete a large number of effectors to plants, which have several targets within the plant cell, but the recognition of only one of them is often sufficient to trigger a defense response (Jones and Dangl, 2006; Cunnac et al., 2009; Lewis et al., 2015). A well-studied effector-protein in the interaction of the hemibiotrophic bacterial plant-pathogen *Pseudomonas syringae* and *Arabidopsis thaliana* is AvrRpm1. The *P. syringae* avirulence gene *Rpm1* is recognized by the *Arabidopsis* resistance-gene *RPM1/RPS3* (Bisgrove et al., 1994). In uninfected *Arabidopsis* plants RPM1 forms a complex with RIN4 (RPM1 INTERACTING PROTEIN 4) to affirm that defense signaling is not activated (Axtell and Staskawicz, 2003). Upon recognition of bacterial effectors by resistance proteins of the plants, RIN4 gets phosphorylated and RPM1-mediated signaling is activated (Liu et al., 2011a). In addition to effectors which target plant signaling pathways, bacterial pathogens also secrete toxins to plants which trigger necrosis and chlorosis and are therefore harmful for plants (Bender et al., 1999). Out of those, coronatine (COR) is of special interest. COR secreted by bacterial pathogens into a plant cell mimics jasmonate-isoleucine (JA-Ile), the bioactive form of jasmonic acid (JA). JA-Ile and COR are both recognized by the *Arabidopsis* receptor *CORONATINE INSENSITIVE1* (COI1) and thereby activate JA signaling. JA-signaling negatively regulates the biosynthesis of salicylic acid (SA) which is indispensable for plant defense against biotrophic and

hemibiotrophic bacterial pathogens, suggesting that bacteria can modulate plant metabolism to suppress immunity (Katsir et al., 2008; Koo et al., 2009; Pieterse et al., 2012; Wasternack and Hause, 2013). Consistent with the above described roles for effectors and the TTSS, *P. syringae*-mutant strains, which lack specific effectors or the TTSS, lose their ability to successfully infect Arabidopsis or fail to induce specific defense responses in Arabidopsis (Adio et al., 2011; Torres Zabala et al., 2015).

One of the earliest immune responses in the incompatible interaction between bacterial pathogens and plants is a rapid production of reactive oxygen species (ROS), also described as oxidative burst (Lamb and Dixon, 1997). Upon infection with an avirulent bacterial pathogen or treatment with flg22 in Arabidopsis several ROS are produced, including superoxide (O_2^-), hydroxyl radical ($\cdot OH$), and hydrogen peroxide (H_2O_2) (Lamb and Dixon; 1997; Torres et al., 2002, Farmer and Davoine, 2007). The generation of ROS upon infection can directly harm the invading pathogen, lead to a reinforcement of the plant cell wall, contribute to the accumulation of defense-related metabolites such as SA, and is an essential signal for HR establishment (Lamb and Dixon; 1997). In Arabidopsis, the *RESPIRATORY BURST OXIDASE HOMOLOGUE D* (*RBOHD*) is required for the extracellular accumulation of H_2O_2 . An Arabidopsis *rbohD* knock-out mutant plant is therefore impaired in the oxidative burst and HR upon inoculation with avirulent bacterial pathogens (Torres et al., 2002),

However, the signaling pathways of PTI and ETI in plants overlap to a certain amount because several defense responses and signals are activated in both PTI and ETI, as described in the following.

1.2.3 Systemic acquired resistance

Plant immune responses are not restricted to the site of infection. A local infection of Arabidopsis plants with an avirulent or virulent bacterial pathogen, as well as the local recognition of PAMPs, leads to an increased resistance of the whole plant foliage against a broad spectrum of pathogens. This phenomenon is described as systemic acquired resistance (SAR) (Mishina and Zeier, 2007; Fu and Dong, 2013). Thereby in Arabidopsis SAR is established in the compatible and incompatible interaction with bacterial pathogens, but although ETI triggered ROS signaling contributes to SA generation which is crucial for a full SAR response, SAR establishment is independent of leaf tissue necrosis and HR (Mishina and Zeier, 2007). SAR is regulated by the immune regulatory metabolites pipecolic acid (Pip) and salicylic acid (SA). Thereby Pip orchestrates SAR via SA-dependent and SA-

independent pathways (Vlot et al., 2009; Návarová et al., 2012; Bernsdorff et al., 2016). A detailed introduction for SAR is given in chapter 6.

1.2.4 Primary and secondary metabolism in plant defense

Plants in general produce over 100.000 low-molecular-mass metabolites which are nonessential for the basic developmental processes of plants and are therefore described as secondary metabolites (Dixon, 2001). Plants respond to invading pathogens with the accumulation of primary and secondary metabolites with a broad structural diversity. Thereby some metabolites possess a direct antimicrobial activity, weather some plant metabolites act as signals, controlling the expression of defense-related gens and contributing to plant initiate immunity by regulatory means. Several examples for the role of primary and secondary metabolites in inducible plant immunity are addressed in the following.

1.2.4.1 Phytohormones in plant defense

Plant growth and development are regulated by phytohormones, which represent signal-active, low-molecular-weight natural products that are produced by all plants. Plant hormones also take main regulatory roles in plant defense signaling.

1.2.4.2 Salicylic acid (SA)

The best/studied plant hormone in the interaction between microorganisms and plants is salicylic acid (SA). In plants two pathways have been proposed for the biosynthesis of SA. In the first Phe is converted via PHENYLALANINE AMMONIUM LYASE (PAL) to cinnamate which is further converted to SA. In the second described biosynthetic pathway SA is produced from chorismate, which is converted to isochorismate via ISOCHORISMATE SYNTHASE 1 (ICS1). By an elimination of pyruvate from isochorismate via ISOCHORISMATE PYROVATE LYASE (IPL) in the next biosynthetic step SA is produced (Chen et al., 2009). However, for SA-accumulation in Arabidopsis upon pathogen infection the biosynthetic pathway via ICS1 is activated and the pathway via PAL is dispensable (Wildermuth et al., 2001). In plants, SA can be converted into a glycosidic bound form (SAG). SAG is transported to the vacuole where it functions as an inactive storage form of SA, which can be converted back to free SA (Vlot et al., 2009). Moreover, SA can be conjugated to amino acids. It was reported that free SA in Arabidopsis, can be conjugated to aspartate which forms salicyloyl-aspartate (SA-Asp). Although exogenous applied SA-Asp

increases *PR1* gene expression in *Arabidopsis*, the role of SA-amino acid conjugates in plant defense is not fully understood yet (Chen et al., 2013).

Upon infection by bacterial pathogens in *Arabidopsis*, transcript levels of *ICS1* are highly increased and a strong accumulation of SA can be observed. Thereby the accumulation of SA is not only restricted to the site of bacterial infection but also takes place in distal leaf tissue. SA biosynthesis is positively regulated by the gene-product of *PHYTOALEXIN-DEFICIENT 4* (*PAD4*), SA needs downstream signaling via *NONEXPRESSOR OF PATHOGENESIS-RELATED GENES 1* (*NPR1*) and SA accumulation contributes to PTI, ETI and SAR (Gaffney et al., 1993; Nawrath and Métraux, 1999; Wildermuth et al., 2001; Vlot et al., 2009, Fu and Dong, 2013). In plant defense the generation of several *PATHOGENESIS RELATED* (*PR*) proteins is regulated by SA. *PR*-proteins are small proteins, which when expressed upon a pathogen inoculation, can reduce diseases of the host, probably caused by the fact that some of those *PR*-proteins harm the pathogen directly. However, although the target of several *PR*-proteins is not known yet, some of them could be identified as chitinases or as compounds which are toxic for microorganisms, for example defensins and thionins (van Loon et al., 2006a). *Arabidopsis* mutant plants which are impaired in biosynthesis, accumulation, or downstream signaling of SA are highly impaired in the pathogen-triggered expression of *PR*-proteins and in PTI and ETI signaling. They also exhibit a highly increased susceptibility to bacterial pathogens, and are attenuated in SAR establishment (Gaffney et al., 1993; Nawrath and Métraux, 1999; Wildermuth et al., 2001; Vlot et al., 2009; Bernsdorff et al., 2016). Furthermore, exogenously applied SA or constitutive activated SA signaling in mutant plants can increase the expression of *PR*-genes and increase resistance against bacterial pathogens (Bowling et al., 1997; Vlot et al., 2009; Stahl et al., 2016). Beyond to plant defense, SA is also implicated in several other physiological processes, such as the induction of flowering, vegetative growth, respiration, photosynthesis, and senescence. Furthermore, SA is involved in response to several abiotic stressors including osmotic stress, heat, heavy metal toxicity, and drought (Rivas-San Vicente and Plasencia, 2011).

1.2.4.3 Jasmonic acid (JA), abscisic acid (ABA), and ethylene

Jasmonic acid is produced by plants from linolenic acid, which is derived from plastid and plasma membranes, and is described for roles in flower and seed development, in response to abiotic stressors, in senescence, and in primary and secondary metabolism. Moreover, JA is the major regulator of plant defense against

necrotrophic pathogens and insect herbivores (Wasternack and Hause, 2013). The bioactive form of JA is a conjugate of JA and the branched-chain amino acid Ile (jasmonate-isoleucine; JA-Ile). In the induction of JA-related defense responses COI1 forms complexes with *JASMONATE ZIM-DOMAIN* (JAZ) proteins which can bind JA-Ile and this process is indispensable for the induction of JA controlled defense responses (Xie et al., 1998; Katsir et al., 2008; Wasternack and Hause, 2013). Although JA is not directly involved in defense responses against *P. syringae*, it accumulates in *Arabidopsis* leaves which are inoculated with virulent and avirulent *P. syringae* (Gruner et al., 2007; Mishina and Zeier, 2007; Gruner et al., 2013). Furthermore, JA is relevant for plant resistance against *P. syringae*, caused by the regulation of SA and JA in an antagonistic manner (see 1.2.4.4).

Stomata on plant leaves are natural surface openings which can be used by pathogens to enter their host (Zeng et al., 2010). A rapid plant defense-response upon recognition of bacterial pathogens via PAMPs is the closure of stomata (Melotto et al., 2006). Stomatal closure in plants is controlled by abscisic acid (ABA) a plant hormone which is synthesized from carotenoids (Nambara and Marion-Poll, 2005). Consistent with that, *Arabidopsis* mutant plants defective in ABA-signaling are impaired in pathogen-inducible closure of stomata. Plant pathogenic bacteria try to suppress stomata closure via the virulence factor coronatine as a strategy of pathogenesis (Melotto et al., 2006). However, although the closure of stomata is one of the fastest responses upon recognition of bacterial pathogens (1 h post inoculation), the strongest accumulation of ABA in *P. syringae*-infected *Arabidopsis* can be observed 48 h post inoculation (hpi) (Gruner et al., 2013).

As well as JA, the gaseous plant hormone ethylene is described mainly in the defense against necrotrophic pathogens (van Loon et al., 2006b). Ethylene is synthesized from adenosyl-methionine, described to induce fruit ripening, and is described to be generated in plants in response to several abiotic and biotic stressors (Bleecker and Kende, 2000). In the incompatible interaction between plants and necrotrophic pathogens, a strong ethylene burst can be observed and *Arabidopsis* mutant plants impaired in ethylene-signaling exhibit increased susceptibility to obligatory necrotrophic plant pathogens including *Botrytis cinerea*, *Chalara elegans*, *Fusarium oxysporum*, and *Xanthomonas Campestris* (van Loon et al., 2006b). Moreover, ethylene is involved in PTI-signaling. In *Arabidopsis*, the knock-out of ETHYLENE-INSENSITIVE 2 (EIN2), which represents a main receptor of ethylene in *Arabidopsis*, decreases the sensitivity to elf18 and flg22 (Tintor et al., 2013). Thereby

especially EFR-activity requires ethylene-signaling by the potentiation of SA-related signaling, which is caused by the repression of JA-biosynthesis via ethylene (Tintor et al., 2013). Ethylene-signaling is furthermore involved in signaling processes involved in the induction of induced systemic resistance (ISR). ISR describes a phenomenon in which particular root-associated growth-promoting bacteria confer broad-spectrum systemic resistance to above-grown plant parts (Pieterse et al., 2014). Arabidopsis plants express ISR upon root-colonization by the bacterium *Pseudomonas fluorescens* WCS417 (*Psm* WCS417). Arabidopsis mutant plants insensitive to ethylene in the roots but not in the leaves (*eir1-1*) fail to express ISR in the above grown part of the plants upon root-colonization by *Psm* WCS417. This demonstrates that ethylene signaling is required for ISR establishment at the site of ISR-induction (Knoester et al., 1999; van Loon et al., 2006b; Pieterse et al., 2014).

1.2.4.4 Phytohormone cross-talk in plant defense

The signaling pathways of plant hormones are interconnected and underlie a complex regulatory network (Glazebrook, 2001; Pieterse et al., 2012). A profoundly studied crosstalk between phytohormones is the antagonistic effect of JA- and SA-signaling. The exogenous application of SA leads to a suppression of the expression of genes involved in JA-biosynthesis and JA-signaling (Peña-Cortés et al., 1993; Doares et al., 1995; Spoel et al., 2003; Gruner et al., 2013). The SA-inducible suppression of JA-signaling requires SA downstream signaling via NPR1. Arabidopsis *npr1* mutant plants fail to suppress JA-responsive genes upon exogenous application of SA (Spoel et al., 2003). For the activation of SA-responsive defense signaling, NPR1 has to interact with TGA transcription factors in the nucleus (Dong, 2004). Interestingly, the localization of NPR1 to the nucleus is not necessary for the SA-triggered suppression of JA-signaling, which indicates that the SA-mediated downregulation of the JA response is a consequence of a function of NPR1 in the cytosol (Spoel et al., 2003; Koornneef and Pieterse, 2008). Other important regulators in the crosstalk between SA and JA are WRKY transcription factors, the glutaredoxin GRX480, and *MAP KINASE 4* (MPK4) (Koornneef and Pieterse, 2008; Pieterse et al., 2012). In Arabidopsis, MPK4 acts as a negative regulator of SA signaling which therefore positively regulates JA responses (Petersen et al., 2000). Recently, it was shown that the Arabidopsis MYC transcription factors are targets for the hormone crosstalk between SA and JA. In Arabidopsis, oviposition by the butterfly *Pieris brassicae* triggers the activation of SA-signaling. This activation suppresses JA-signaling which is needed for plant defense against the feeding larvae which emerge from the eggs (Bruessow et al., 2010). The

recognition of insect eggs strongly diminishes the protein levels of MYC2, MYC3, and MYC4 which are basic helix-loop-helix transcription factors that control jasmonate-related defense responses (Schmiesing et al., 2016).

Arabidopsis MYC2 expression is also regulated in an ABA-dependent manner, indicating that ABA can influence JA-signaling. Moreover, exogenous application of ABA can increase or suppress the expression of several JA-responsive and ethylene-responsive genes, suggesting that ABA can influence JA-signaling positively as well as negatively (Robert-Seilaniantz et al., 2011). JA and ethylene are regulated in an antagonistic way and therefore ABA also exhibits an influence on ethylene signaling (Robert-Seilaniantz et al., 2011; Kazan and Lyons, 2014). Consistent with that, ABA-signaling affects plant pathogen interactions in different ways, depending on the lifestyle of the pathogen. ABA-signaling negatively influences the resistance of Arabidopsis against the necrotrophic fungus *Fusarium oxysporum*, but contributes positively to resistance-signaling against biotrophic bacterial pathogens (Anderson et al., 2004; Thaler and Bostock, 2004). In contrast, it could be shown that *Pseudomonas syringae* DC3000 triggered ABA-signaling antagonizes some SA-mediated defense responses, including the increased expression of PAMP-inducible SA-dependent genes (de Torres Zabala et al., 2009). Moreover, it could be shown that ABA and SA antagonistically control the endogenous level of NPR1, which is the main SA receptor in Arabidopsis. ABA promotes the degradation of NPR1 via the *CULLIN 3* (CUL3) – based ligase, whereupon SA protects NPR1 prior the ABA-mediated degradation. Thereby the temporal patterns and the strength of ABA and SA accumulation are crucial for the regulation of NPR1 degradation (Ding et al., 2016).

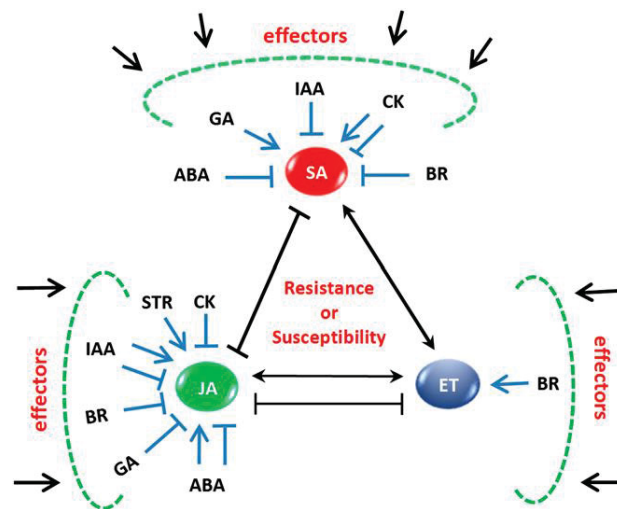


Figure 1.2 **Plant hormone crosstalk in plant defense signaling.**

The plant hormones SA, JA, and ethylene (ET) are the main regulatory phytohormones in plant immunity. Furthermore, the plant hormones ABA, auxin (IAA), cytokinin (CK), brassinosteroid (BR), gibberellic acid (GA), and strigolactones (STR) regulate plant defense responses, either directly or by the regulation of the primary defense hormones. Pathogens modulate this regulatory network via their effectors which induces resistance or susceptibility.

Figure from: Kazan and Lyons, 2014.

Figure from: Kazan and Lyons, 2014.

In *Arabidopsis*, about half of the genes which are induced in response to ethylene are also induced in response to JA, suggesting that some defense responses are regulated synergistically by JA and ethylene (Xu et al., 1994). An extensively examined example for such a response is the expression of *Arabidopsis PLANT DEFENSIN 1.2 (PDF1.2)*. *PDF1.2* is required to produce a defensin in response to the pathogenic fungi *Alternaria brassicicola*, which possess antifungal activity. The expression of *PDF1.2* in response to *A. brassicicola* is dependent on both ethylene and JA signaling (Xu et al., 1994; Penninckx et al. 1996; Kunkel and Brooks, 2002). Moreover, ethylene and JA can act antagonistically to regulate defense responses. Although the molecular mechanisms behind this antagonism are not fully elucidated yet, it was shown that the transcription factor MYC2, a regulator of JA signaling, can interact with the transcription factor ETHYLENE-INSENSITIVE 3 (EIN3), which is required for ethylene signaling. MYC2 can interact with EIN3 to suppress the transcriptional activity of EIN3 which represses ET-signaling and EIN3 can interact with MYC2 to suppress the expression of several JA-regulated defense genes (Song et al., 2014). Furthermore, some data suggests that SA- and ethylene-signaling can influence each other. For example, although the expression of *PR* genes in *Arabidopsis* is not dependent on ethylene signaling the SA-mediated expression of *PR1* is potentiated upon ethylene exposure (Lawton et al., 1994). In contrast, the same study showed also, that basal *PR1* levels are increased in *ein2* mutant plants, which suggests that ethylene signaling could repress some SA-dependent defense responses (Lawton et al., 1994; Kunkel and Brooks, 2002). A schematic scheme for the signaling interactions of phytohormones which regulate plant immunity is depicted in Fig. 1.2. Interestingly, several of those signaling pathways are hijacked by pathogens via their effectors to modulate plant hormone regulation. That can induce resistance or susceptibility, like the above described example of bacterial derived coronatine shows (Kazan and Lyons, 2014).

1.2.4.5 Pipecolic acid (Pip)

Pipecolic acid is a non-protein amino acid derived from the Asp-derived amino acid Lys, which is produced by several plant species under diseased conditions (Pálfi and Dézsi et al., 1968; Návarová et al., 2012; Zeier, 2013). In the last years it could be shown that Pip is produced by *Arabidopsis* in compatible and incompatible interactions with bacterial pathogens and upon egg deposition of the butterfly *Pieris brassica* (Návarová et al., 2012; Hilfiker et al., 2014; Bernsdorff et al., 2016), by tobacco *Nicotiana tabacum* cv Xanthi plants in response to bacterial pathogens (Vogel-

Adghough et al., 2013), upon infection by the pathogenic fungus *Fusarium virguliforme* and aphid-infestation in soybean (Klein et al., 2015; Abeysekara et al., 2016), and by rice upon infection by the pathogenic fungus *Rhizoctonia solani* (Suharti et al. 2016). In *Arabidopsis*, Pip is the main regulator of SAR and orchestrates SAR via SA-dependent and SA-independent pathways. SA acts downstream of Pip and *FLAVIN-DEPENDENT MONOOXYGENASE1* (FMO1) in defense-signal-amplification and is necessary for a complete and strong SAR response. Notably, Pip-deficient and Pip-insensitive *ald1* and *fmo1* mutants are completely SAR-deficient and don't show systemic defense responses upon local *P. syringae* inoculation. Furthermore, Pip accumulation during SAR mediates the defense priming response that is associated with SAR establishment. Priming is described as a status in which a plant can react more quickly and vigorously to a subsequent pathogen infection (Návarová et al., 2012; Bernsdorff et al., 2016). A more detailed introduction for Pip and its role in SAR establishment is given in chapter 6.

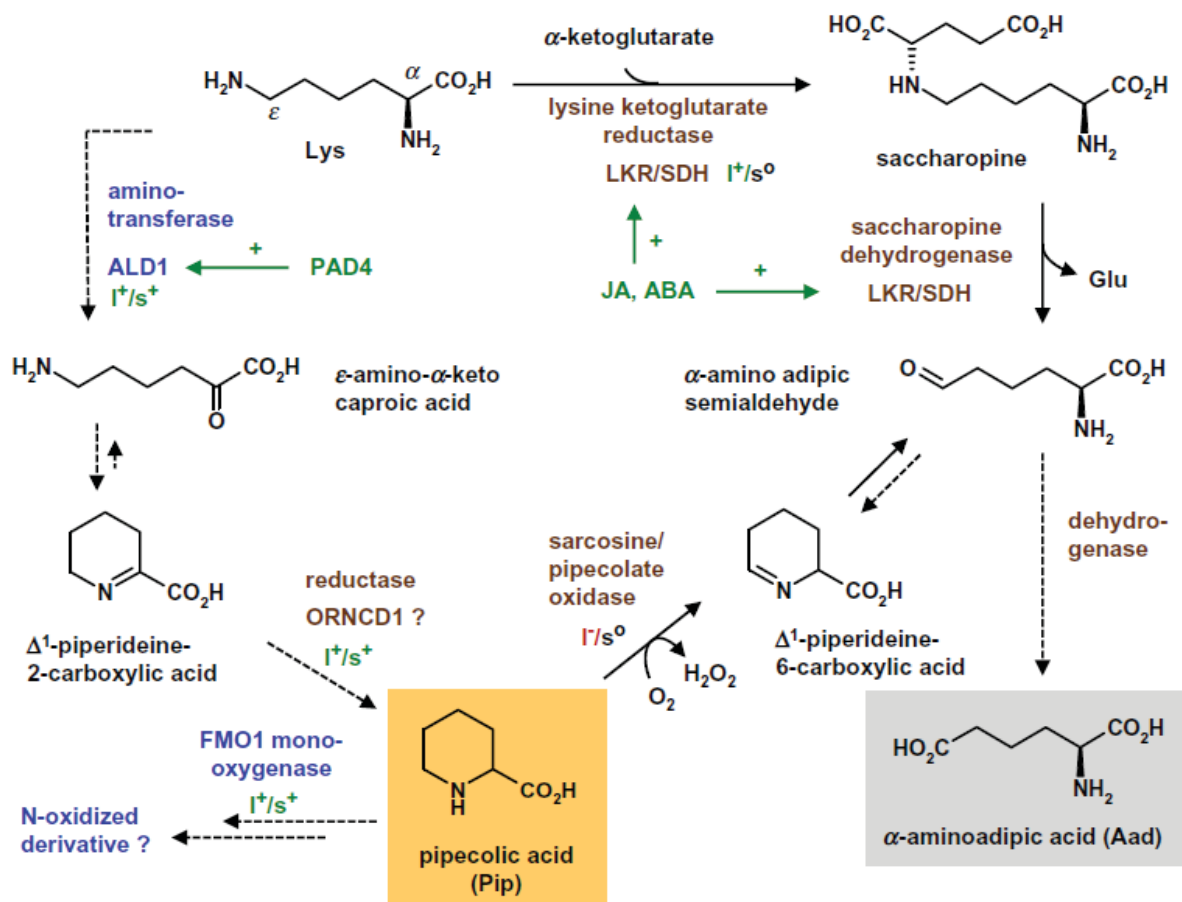


Figure 3.1 Possible scheme for the metabolism of the Lys catabolites Pip and Aad following pathogen attack.

Figure from: Zeier, 2013.

Pip is derived from Lys, but the exact biochemical pathway of Pip production via AGD2-LIKE DEFENSE RESPONSE PROTEIN 1 (ALD1) remains to be elucidated. However, *Arabidopsis ald1* mutant plants fail to accumulate Pip upon *P. syringae* inoculation (Návarová et al., 2012). It is proposed, that the conversion of Lys into Pip proceeds via ϵ -amino- α -keto caproic acid and Δ^1 -piperidine-2-carboxylic acid (P2C) (Fig. 1.3; Zeier, 2013). That involves the loss of the α -amino group of Lys and the introduction of the ϵ -nitrogen into Pip.

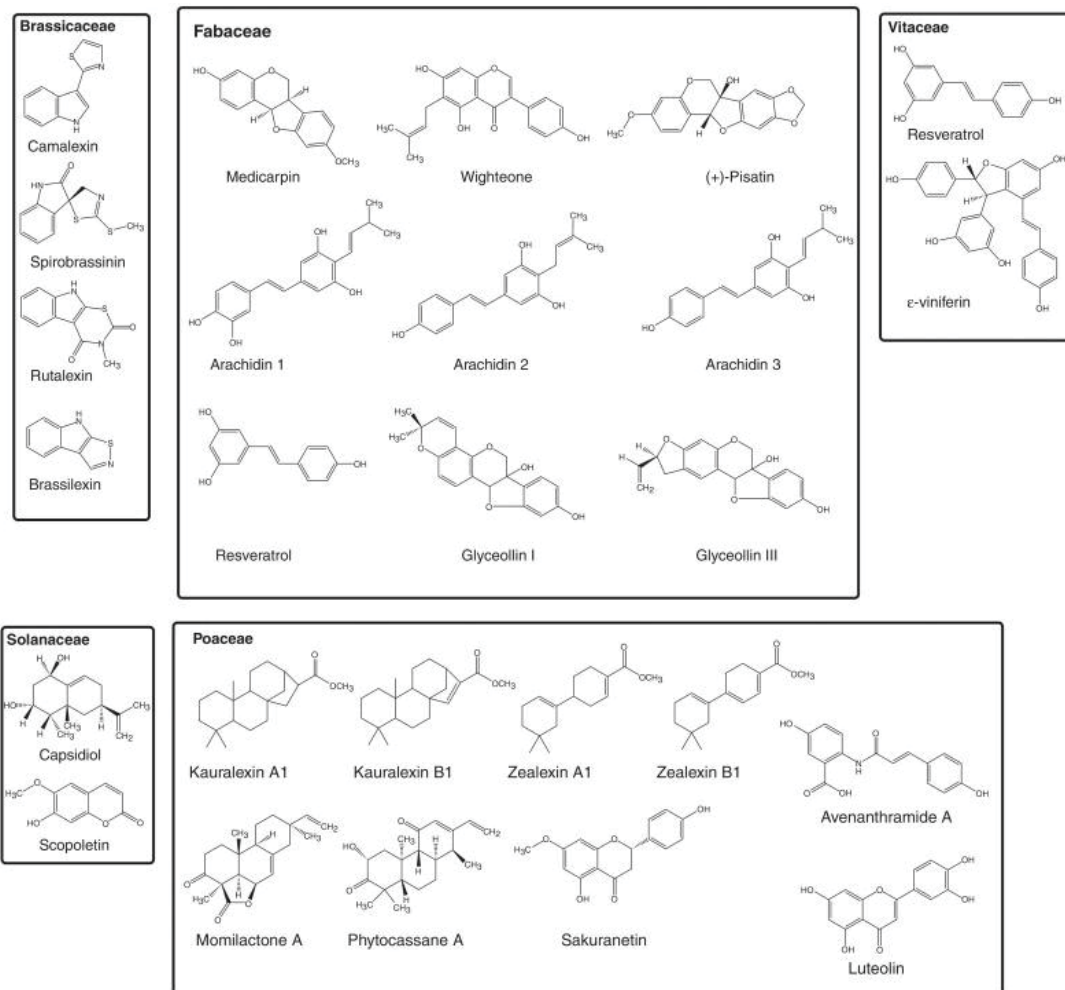
Beside to Pip, the endogenous production of several other amino acids is increased upon *P. syringae*-inoculation. Out of those amino acids α -amino adipic acid (Aad) is produced in the highest fold change between $MgCl_2$ and *P. syringae* treated leaves (Návarová et al., 2012). Aad is, as well as Pip, a Lys catabolite. Until now, the exact biosynthetic pathway of Aad in *Arabidopsis* is not fully elucidated and it is suggested that Lys and/or Pip can serve as a precursor for Aad (Zeier, 2013). Via the saccharopine pathway Lys can be converted to α -amino adipic semialdehyde by the LYSINE KETOGLUTARATE REDUCTASE (LKR) and the SACCHAROPINE DEHYDROGENASE (SDH). α -amino adipic semialdehyde serves as a precursor for Aad (Fig 1.3; Galili et al., 2001; Zeier, 2013). In the second proposed pathway, Pip can serve as precursor for Aad. Thereby, *Arabidopsis* SACROSINE / PIPECOLATE OXIDASE (SOX) reduces Pip to Δ^1 -piperidine-6-carboxylic acid (P6C) which can be further metabolized to Aad via hitherto not classified enzymes (Fig. 1.3; Goyer et al., 2004; Zeier et al., 2013). However, the fact that *ald1* mutant, which is impaired in Pip biosynthesis (Návarová et al., 2012), is not impaired in *P. syringae*-triggered Aad accumulation indicate that the main source in *Arabidopsis* for Aad generation is Lys via the LKR/SDH pathway and not Pip (Návarová et al., 2012).

1.2.4.6 Phytoalexins

Besides phytoanticipins, which possess antimicrobial properties and are constitutively generated by plants, plants produce several metabolites de novo upon recognition of an invading pathogen that have antimicrobial properties. Those metabolites are designated as phytoalexins (VanEtten et al., 1994). In this context, a phytoanticipin can also act as a phytoalexin when it is generated constitutively within a plant, but generated de novo in an increased amount upon infection by a plant pathogen (VanEtten et al., 1994; Dixon, 2001). The accumulation of phytoalexins in response to pathogens is reported in several plant species (Fig. 1.4; Ahuja et al., 2012). Upon biotic stress, members of the Fabaceae family produce phytoalexins

Introduction

belonging mainly to the substance class of isoflavones, including glyceollins, pisatin, resveratrol, and arachidins. Most of them are reported to accumulate upon infection by necrotrophic fungal pathogens but the production of some can also be observed upon MeJA treatment (Ahuja et al., 2012). The phytoalexins in Vitaceae mainly belong to the stilbene family. They are derived from resveratrol which can be metabolized to methylated derivatives or oligomers such as viniferin. Although resveratrol itself possesses an antifungal activity, the fungicide toxicity of some of the methylated derivatives and oligomers is higher compared to resveratrol. The accumulation of those stilbene phytoalexins is also inducible by JA and MeJA (Ahuja et al., 2012).



TRENDS in Plant Science

Figure 1.4 Structures of selected phytoalexins which are produced by members of the plant families Brassicaceae, Fabaceae, Vitaceae, Solanaceae, and Poaceae.

Figure from: Ahuja et al., 2012.

In the crop plants tobacco and pepper, which belong to the family of Solanaceae, the main phytoalexin which is produced upon infection by pathogenic fungi is capsidiol. Capsidiol is a sesquiterpene that negatively influences the growth

and germination of several fungi (Ahuja et al., 2012). A further phytoalexin in tobacco is scopoletin (Fig. 1.4), which accumulates upon infection by the pathogenic fungus *Botrytis cinerea*. Scopoletin is a methyl-coumarin derived from the aromatic amino acid phenylalanine (Phe). It accumulates in the *B. cinerea*-resistant tobacco cultivar *N. tabacum* cv. Petit Havana, but not in the *B. cinerea*-susceptible cultivar *N. tabacum* cv. Xanthi. This suggests that scopoletin accumulation contributes to the resistance of *N. tabacum* cv. Petit Havana against *B. cinerea*. Consistent with that, scopoletin inhibits the germination of *B. cinerea*-spores, whereupon the mycelium growth of *B. cinerea* is just slightly inhibited by scopoletin (El Oirdi et al., 2010). Moreover, it could be shown that scopoletin and its glycosidic bound form scopolin accumulate in tobacco cultivars *N. tabacum* cv. Samsun and *N. sylvestris* upon treatment with a purified glycoprotein from the plant pathogenic oomycete *Phytophthora megasperma* (Costet et al., 2002).

In cruciferous plants (Brassicaceae) over 40 phytoalexins are known, including brassisins, rutalexin, and camalexin. The phytoalexins from cruciferous plants represent indole alkaloids which are derived from the aromatic amino acid Trp and most of them contain a sulfur atom derived from cysteine (Fig. 1.4; Pedras et al., 2011; Ahuja et al., 2012). The best studied phytoalexin in Brassicaceae is camalexin in the model plant *Arabidopsis thaliana*. Camalexin biosynthesis in *Arabidopsis* is induced by a large variety of plant pathogens, such as bacteria, fungi, and oomycetes (Glawischnig, 2007). Also recognition on site of the plant of PAMPs and toxins can lead to an accumulation of camalexin in *Arabidopsis* (Tsuji et al., 1993). Moreover, abiotic stressors, such as treatment with heavy metal ions and UV-B irradiation can trigger camalexin accumulation (Van Breusegem et al., 2008). However, not all pathogens which trigger camalexin accumulation in the case of infection are susceptible to camalexin. Camalexin deficient mutant plants (*PHYTOALEXIN DEFICIENT 3*; *pad3*) do not show increased susceptibility against the bacterial pathogen *P. syringae* (Glazebrook and Ausubel, 1994). This is possibly caused by the fact that camalexin harms *P. syringae* at a concentration of 500 mg/ml which is probably not reached in situ (Rogers et al., 1996). In turn *Arabidopsis pad3* mutant plants are more susceptible against the necrotrophic fungal pathogens *Alternaria brassicicola* and *Leptosphaeria maculans* (Thomma et al., 1999). Furthermore, camalexin in *Arabidopsis* contributes in combination with indolic glucosinolates to the resistance towards the plant pathogenic oomycete *Phytophthora brassicae* (Schlaeppli et al., 2010). Further information about the biosynthesis of camalexin and other Trp-derived indolic metabolites is given in chapter 5.

Recently a novel Trp-derived metabolite which acts as a phytoalexin, 4-hydroxy-3-carbonyl nitrile, could be identified (Rajniak et al., 2015). As well as camalexin, 4-hydroxy-3-carbonyl nitrile is synthesized from Trp via indole-3-acetaldoxim (IAOx). For 4-hydroxy-3-carbonyl nitrile biosynthesis IAOx is converted to indole-3-carbonyl nitrile via the FLAVIN-DEPENDENT OXIDOREDUCTASE 1 (FOX1). In the next biosynthetic pathway step, 4-hydroxy-3-carbonyl nitrile is generated out of indole-3-carbonyl nitrile via hydroxylation and the introduction of the hydroxyl group is realized by the cytochrome P450 monooxygenase 82C2 (CYP82C2). In Arabidopsis, transcript levels of *CYP82C2* are highly increased under a variety of pathogen treatment conditions, including treatment with flg22 and *P. syringae* inoculation (Rajniak et al., 2015). Consistent with the above described role for CYP82C2, an accumulation of 4-hydroxy-3-carbonyl nitrile can be observed in Arabidopsis plants which are infected with an avirulent *P. syringae*-strain (*P. syringae* pv. *tomato* DC3000 *avrRpm1* (*Psta*)), and *cyp82c2* mutant plants fail to accumulate 4-hydroxy-3-carbonyl nitrile upon *Psta*-infection. Moreover, *cyp82c2* and camalexin deficient *pad3* mutant plants exhibit a highly increased susceptibility to the virulent *P. syringae* pv. *tomato* DC3000 (*Pst*) when the plants are surface-inoculated (Rajniak et al., 2015). Contrary to, that pressure-inoculated camalexin-deficient *pad3* plants do not show an increased susceptibility against virulent *P. syringae* (Glazebrook and Ausubel, 1994). However, in wild-type plants which were pre-infiltrated with camalexin, indole-3-carbonyl nitrile, or 4-hydroxy-3-carbonyl nitrile 24 h before the surface-inoculation with *Pst* just the pre-treatment with 4-hydroxy-3-carbonyl nitrile could increase resistance against *Pst*, whereupon pre-treatments with camalexin or indole-3-carbonyl nitrile had no effect. The generation of 4-hydroxy-3-carbonyl nitrile not only seems to contribute to plant resistance against bacterial pathogens. Arabidopsis *cyp82c2* mutant plants exhibit increased susceptibility to the fungal necrotrophic pathogens *Alternaria brassicicola* and *Botrytis cinerea*, but not to the obligate biotroph fungal pathogen *Golovinomyces orontii*. Furthermore, purified indole-3-carbonyl and 4-hydroxy-3-carbonyl nitrile have a growth inhibitory effect on *Alternaria brassicicola* and *Botrytis cinerea*, in the same amplitude like camalexin (Rajniak et al., 2015).

1.2.4.7 Oxylipins

Oxylipins are lipophilic metabolites which are mainly derived by the oxidation of the polyunsaturated fatty acids linolenic acid (18:3), linoleic acid (18:2), and rosinic acid (16:3). The desaturation of fatty acids in Arabidopsis is catalyzed by the FATTY ACID DESATURASES (FAD) 3, 7 and 8 and the triple mutant *fad3 fad7 fad8* lacks

both, tri-unsaturated fatty acids and JA (McConn et al., 1997). The first step in the biosynthesis of oxylipins is the generation of fatty acid hydroperoxides, which can take place by enzymatic or chemical formation (Mueller and Berger, 2009; Mosblech et al., 2009). The non-enzymatic generation of oxylipins is catalyzed by radicals and ROS. The best-studied oxylipin in plant-defense is JA. Besides JA, the generation of several other oxylipins is reported in plants in response to wounding and different biotic and abiotic stressors. In *Arabidopsis* plants inoculated with virulent and avirulent strains of the bacterial plant pathogen *P. syringae* the accumulation of the enzymatically formed oxylipins JA and 12-oxophytodienoic acid (OPDA) has been reported. Furthermore, the enzymatically formed unsaturated C18 fatty acids linoleic acid and linolenic acid accumulate in *P. syringae*-inoculated *Arabidopsis* leaves (Yaeno et al., 2004). Additionally, it was reported that several non-enzymatically formed oxylipins accumulate in *Arabidopsis* in response to *P. syringae*-infection, including hydroxy fatty acids (HO-FA) and F₁-phytoprostanes (PPF₁), (Grun et al., 2007). Thereby the endogenous levels of HO-FA, PPF₁, JA, and OPDA rise in early stages of the interaction with the avirulent strain and in late stages of the interaction with both, the virulent and the avirulent strain. This indicates that effector-triggered ROS signaling contributes to the early accumulation of oxylipins in response to bacterial pathogens. However, it still remains to be clarified which specific ROS initiate especially non-enzymatically generation of oxylipins (Grun et al., 2007). A further membrane derived metabolite, which is described to accumulate in *Arabidopsis* in response to infections by bacterial pathogens, is the sphingolipid phytosphingosine (Peer et al., 2010). Sphingolipids are essential components of membranes in all eukaryotes organisms and are reported for a regulatory role in programmed cell death reactions in plants (Worrall, 2003). The infection of *Arabidopsis* plants with virulent and avirulent *P. syringae* triggers a fast accumulation of free phytosphingosine. Thereby the infection with the avirulent strain leads to a long-lasting accumulation of phytosphingosine, whereupon the infection with virulent *P. syringae* triggers a fast accumulation of phytosphingosine but the levels return to basal levels at 5 hpi. The HR, which is a form of programmed cell death, is only observed in the interaction of *Arabidopsis* with avirulent *P. syringae* but not in the interaction with virulent *P. syringae*. The long-lasting higher levels of phytosphingosine in *Arabidopsis* in the incompatible interaction could therefore indicate a positive role of phytosphingosine in the regulation of HR (Peer et al., 2010). However, oxylipins in general are reported for a high signaling activity in plants. In tomato, tobacco, and *Arabidopsis* cell cultures which are treated with phytoprostanes and isoprostanes, the activation of defense responses is reported. This includes the

accumulation of phytoalexins, an increased activity of MAP kinases, and increased transcript levels of genes that are related to plant defense (Thoma et al., 2003; Loeffler et al., 2005; Farmer and Davoine, 2007). Notably, in *Arabidopsis*, the induction by phytoprostanes and OPDA of a certain amount of genes is dependent on the TGA transcription factors TGA2, TGA5, and TGA6. This observation makes TGA transcription factors a possible downstream signaling component of oxylipins (Mueller et al., 2008). Moreover, malondialdehyde (MDA) is reported to activate defense signaling in *Arabidopsis* (Weber et al., 2004). MDA is a product from the oxidation of polyunsaturated fatty acids. In *Arabidopsis* plants which are treated with volatile MDA a strong increase of transcript levels of genes which are described for defense-signaling is reported (Weber et al., 2004). It is also speculated that oxylipin metabolism could be functional for SAR establishment. The polyunsaturated fatty acid linolenic acid serves as a precursor for azelaic acid (AZA), (Zoeller et al., 2012). AZA has been suggested as an essential compound and a long-distance signal in SAR establishment (Jung et al., 2009; Dempsey and Klessig, 2012; Cecchini et al., 2015b).

A further process in the interaction of *P. syringae* and *Arabidopsis* which is controlled by jasmonate signaling is the elicitation of the volatile sesquiterpenoid (E,E)-4,8,12-trimethyl-1,3,7,11-tridecatetraene (TMTT) (Attaran et al., 2008). *Arabidopsis* plants elicit TMTT production upon inoculation with virulent and avirulent *P. syringae* between 10 – 48 hpi. Beside to *P. syringae* inoculation, the infiltration of copper sulfate triggers the production of TMTT, which is also a treatment that activates JA biosynthesis. The *P. syringae*-inducible generation of TMTT is highly dependent on functional oxylipin-signaling, because mutant plants which are impaired in JA biosynthesis fail to elicit TMTT upon *P. syringe*-infection. Moreover, mutant plants impaired in downstream JA-signaling show a reduced production of TMTT upon *P. syringae* infection. However, the production of TMTT in *Arabidopsis* upon *P. syringae*-infection seems to be a by-product of activated JA-signaling, rather than a defense response which contributes to *Arabidopsis* resistance against bacterial pathogens. In *Arabidopsis*, TMTT is synthesized via the *TERPENE SYNTHASE GENE 4* (*TPS4*). The *Arabidopsis* knock-out mutant *tps4* fail to elicit TMTT upon *P. syringae* infection, copper sulfate infiltration, or fungal elicitor treatment, but doesn't exhibit increased susceptibility to *P. syringae* or an attenuated SAR-response (Attaran et al., 2008; Herde et al., 2008).

1.2.4.8 Stigmasterol

A further metabolite pathway which is activated in *Arabidopsis* upon *P. syringae*-infection is the conversion from β -sitosterol to stigmasterol (Griebel and Zeier, 2010). Sterols constitute essential membrane compounds of all eukaryotic organisms which influence the fluidity and the permeability of phospholipid bilayers (Schaller, 2003). In *Arabidopsis* the most abundant sterol in membranes is β -sitosterol (Schaeffer et al., 2001). Stigmasterol is synthesized from β -sitosterol via C22 desaturation of β -sitosterol and this desaturation is processed by the cytochrome P450 monooxygenase 710A1 (CYP710A1). The transcript levels of *CYP710A1* are increased in *Arabidopsis* upon infection with virulent and avirulent *P. syringae* (Zimmermann et al., 2004; Griebel and Zeier, 2010). Consistently, an accumulation of stigmasterol can be observed in *Arabidopsis* plants inoculated with virulent and avirulent *P. syringae*-strains (Griebel and Zeier, 2010). The formation of stigmasterol is thereby independent of SA-, JA-, and ethylene-signaling, but can also be triggered by perception of the bacterial PAMPs flg22 and LPS or by the production of ROS. Interestingly, *cyp710A1* knock-out plants which fail to convert β -sitosterol to stigmasterol, exhibit increased resistance against virulent and avirulent *P. syringae*. That indicates that *P. syringae* promotes plant disease susceptibility via the stimulation of sterol C22 desaturation in leaves, which increases the stigmasterol to β -sitosterol ratio in plant membranes (Griebel and Zeier, 2010).

1.3 The model pathosystem *Arabidopsis thaliana* and *Pseudomonas syringae*

Arabidopsis thaliana L. Heynh (thale cress) is a species in the family Brassicaceae. It is an annual dicot which is in general established as model organism in plant research. *Arabidopsis* has a short life cycle and the genome is sequenced. The genome consists of approximately 30.000 genes that are located on 5 chromosomes and a large collection of knock-out mutants is available. *Pseudomonas syringae* is a gram-negative bacterium and several pathovars (pv.) can infect different plant species. In this study, we used the hemibiotrophic strain *Pseudomonas syringae* pv. *maculicola* ES4326 (*Psm*), which is able to infect *Arabidopsis*. In addition we used the avirulent *Psm avrRpm1* strain, which expresses the *avrRpm1* avirulence gene (Bisgrove et al., 1994). The use of *Psm* and *Psm avrRpm1* allow investigating effects of PTI and ETI in the model pathosystem *Arabidopsis thaliana* and *Pseudomonas syringae*.

1.4 Aims and form of the thesis

As described above, *Arabidopsis* plants respond to inoculation with the hemibiotrophic bacterial pathogen *Psm* with changes in primary and secondary metabolism and the produced metabolites have a broad structural diversity. Those metabolites include the phenolic SA (Vlot et al., 2009), proteinogenic and non-protein amino acids (Adio et al., 2011; Návarová et al., 2012), Trp-derived indolics (Glazebrook and Ausubel, 1994; Rajniak et al., 2015; Stahl et al., 2016), volatile terpenoids (Attaran et al., 2008), oxylipins (Grun et al., 2007; Gruner et al., 2013), stigmasterol (Griebel and Zeier, 2010), and others (Chaouch et al., 2012; Piasecka et al., 2015). My doctoral research project aimed on the identification of novel metabolites pathways which are activated in *Arabidopsis* upon infection by *P. syringae*. Furthermore, it aimed to functional investigate these metabolite pathways in plant immunity, as well as to identify regulatory principles underlying these pathogen-inducible metabolic pathways. A further focus was led on the role of Pip in the establishment of SAR. To this end, experiments were conducted to clarify if Pip can be metabolized to other metabolites, which could take a functional role in plant immunity, and if Pip could take a functional role in SAR-establishment as a long-distance signal. The different identified and investigated metabolic pathways are described here in individual chapters. They involve tocopherols, N-acylated amino acids, the methyl-coumarin scopoletin, Trp-derived indolics, and the Lys catabolite Pip. Each chapter consists of a specific introduction, a results-section, and a separated discussion. Chapter 5 “Indolic compounds in systemic acquired resistance” was previously published in Stahl et al. (2016). Author contributions for this project can be found under “Author contributions Chapter 5” (page 210). Methods, references, and supplemental material for all chapters are summarized at the end of the thesis.

2 Tocopherols in Arabidopsis basal resistance

2.1 Abstract

Tocopherols are lipid-soluble antioxidants with vitamin E activity that are synthesized exclusively by photosynthetic organisms and occur in plastids of higher plants. The four known tocopherols, α -, β -, γ - and δ -tocopherol, differ in number and position of methyl groups on their chromanol head group. In *Arabidopsis thaliana* leaves α -tocopherol constitutes the main tocopherol form, whereas seeds predominantly contain γ -tocopherol. We realized that inoculation of Arabidopsis leaves with virulent or avirulent *Pseudomonas syringae* strains induces increased expression of several genes involved in early steps of tocopherol biosynthesis. Subsequent metabolite analyses revealed that *P. syringae* inoculation triggers a strong accumulation of β -tocopherol and quantitatively moderate production of γ - and δ -tocopherol in leaves, whereas α -tocopherol levels essentially remain constant. Analyses of Arabidopsis lines impaired in classical defense pathways showed that pathogen-induced tocopherol accumulation is virtually independent of salicylic acid-, pipelicolic acid-, jasmonic acid-, or abscisic acid/signaling. However, external supply with reactive oxygen species or the flg22 peptide proved sufficient to elevate β -tocopherol levels in leaves. The tocopherol content and composition of biosynthetic pathway mutants greatly differed from those of the wild-type in non-inoculated and inoculated leaves. Notably, *vte2* which is fully impaired in basal and pathogen-induced tocopherol generation but not in the accumulation of other defense related metabolites exhibits increased susceptibility towards virulent *P. syringae*. This is accompanied by increased levels of lipid peroxidation after *P. syringae* infection in this mutant. The lack of tri-unsaturated fatty acids in a *vte2-1 fad3-2 fad7-2 fad8* quadruple mutant prevents increased lipid peroxidation in the *vte2* background and restores pathogen resistance to wild-type levels. Our results therefore suggest that basal levels and induced production of tocopherols contribute to Arabidopsis basal resistance against *Pseudomonas syringae* by preventing oxidative damage of lipids.

One sentence summary: Tocopherol biosynthesis is regulated upon *P. syringae*-infection and tocopherols contribute to Arabidopsis basal resistance by protecting tri-unsaturated fatty acids prior non-enzymatic lipid peroxidation.

2.2 Introduction

The multilayered plant immune system includes constitutive and inducible defense responses and is accompanied with the endogenous production of metabolites with a broad structural diversity. In *Arabidopsis thaliana* leaves inoculated with the hemibiotrophic bacterial pathogen *Pseudomonas syringae* the accumulation of several metabolites is described. The chorismate-derived phenolic metabolite salicylic acid (SA) is produced in high quantities in Arabidopsis leaves upon *P. syringae* infection and has been described to contribute to resistance against many biotrophic and hemibiotrophic pathogens. Thereby the generation of SA via *ISOCHORISMATE SYNTHASE1* (ICS1) is not only restricted to the site of bacterial inoculation (“local leaves”), but takes also place in leaf tissue distal to that (“systemic leaves”) (Nawrath and Métraux, 1999; Wildermuth et al., 2001; Vlot et al., 2009). The accumulation of SA in response to bacterial pathogens is closely associated with the establishment of systemic acquired resistance (SAR) (Gaffney et al., 1993), which describes a form of inducible plant innate immunity of the whole plant foliage, conferring a long-lasting protection against a broad spectrum of pathogenic microorganisms, triggered by a first recognition of a pathogen (Fu and Dong, 2013). Furthermore, the lysine catabolite piperolic acid (Pip) has been described as a crucial mediator of plant resistance and SAR. In Arabidopsis inoculated with *P. syringae*, Pip accumulates in local infected leaves, in leaf tissue distal to that and in petiole exudates from inoculated leaves. An Arabidopsis mutant with an impaired biosynthesis of Pip (*ald1*) shows decreased resistance against *P. syringae* and is lacking the ability to establish SAR. Exogenous treatment with Pip complements these resistance defects and further increases pathogen resistance against *P. syringae* of wild-type plants (Návarová et al., 2012). The establishment of SAR is tightly associated with defense priming, which describes a status in which plants are able to mobilize more quickly and vigorously defense responses after a pathogen attack. Defense priming in Arabidopsis SAR is controlled by Pip via SA-dependent and SA-independent pathways (Návarová et al., 2012; Bernsdorff et al., 2016). Pip is also indispensable for induction of SAR in Arabidopsis after oviposition by *Pieris brassica* (Hilfiker et al., 2014). Notably, Pip furthermore accumulates in leaves of tobacco (*Nicotiana tabacum* cv Xanthi) plants inoculated with *Pseudomonas syringae* pv *tabaci* (*Pstb*) and exogenous applied Pip increases resistance of tobacco plants against *P. syringae* cultivars by priming salicylic acid and nicotine accumulation in tobacco (Vogel-Adghough et al., 2013). Moreover, in Arabidopsis the indolic phytoalexin camalexin and other Trp-derived compounds accumulate in response to pathogen infections. Indolic metabolites, derived from the

aromatic amino acid Trp, are plant natural products that play a crucial role in the defense of cruciferous plants against their natural enemies, such as herbivores or pathogenic fungi (Schlaeppli et al., 2008; 2010; Bednarek et al., 2009; Bednarek, 2012). Recently, it was shown that in Arabidopsis upon *P. syringae*-infection in addition to camalexin over 20 other indolic metabolites are generated, such as indole-3-carboxylic acid (ICA) or indol-3-methylamine (I3A). Interestingly, the activation of indole-metabolism was thereby not only restricted to the site of bacterial attack and some branches of the indole pathway were also activated in systemic leaves, resulting in an accumulation of I3A, ICA, and indole-3-carbaldehyde (ICC) in those leaves (Stahl et al., 2016). Other examples for metabolites which accumulate in Arabidopsis in response to invading bacterial pathogens are the unsaturated sterol stigmasterol and several oxylipins (Griebel and Zeier 2010, Grun et al., 2007).

Here we show that the biosynthesis of tocopherols is strongly activated upon *P. syringae* infection in Arabidopsis. Tocopherols and tocotrienols are lipid soluble antioxidants which are together described under the term tocochromanols. They are exclusively synthesized by photosynthetic organisms such as plants, algae, and cyanobacteria but are essential for human diet and are therefore in this context also described by the term vitamin E (Schneider, 2005). Tocochromanols are composed of a chromanol head group and a lipophilic side chain. This lipophilic side chain is 3-fold unsaturated in tocotrienols and saturated in tocopherols. Tocopherols are synthesized by all photosynthetic organisms and are more abundant in vascular plants than in evolutionary early photosynthetic organisms, whereupon tocotrienols can only be found in specific plant groups and accumulate in higher amounts in seeds and fruits (Esteban et al., 2009; Falk and Munné-Bosch, 2010). The four known tocopherols, α -, β -, γ - and δ -tocopherol, differ in number and position of methyl groups on their chromanol head group (Fig. 2.1). In plants homogentisic acid, which is generated from the shikimate pathway-driven aromatic amino acid tyrosine, serves as a precursor for the chromanol head group of tocopherols and subsequent methylation steps generate the four different tocopherol forms. The lipophilic side chain of tocopherols is derived from phytyl-diphosphate, which is attached via the homogentisate phytyltransferase (VTE2) to homogentisic acid (for review see DellaPenna and Pogson, 2006). The therefore needed phytyl-diphosphate can be either derived from de novo generation from geranylgeranyl-diphosphate or from the degradation of chlorophyll. Chlorophyll degradation produces phytol, which is phosphorylated by the phytyl-phosphate kinases VTE5 and VTE6 to phytyl-diphosphate (Valentin et al., 2006; vom Dorp et al., 2015). An overview of tocopherol biosynthesis is given in Fig. 2.1. The endogenous

concentrations of the different tocopherol forms vary between different plant tissues. Seeds predominantly contain tocotrienols and γ -tocopherol, whereas α -tocopherol constitutes the main tocopherol form in chloroplast membranes in leaves of higher plants (Grusak and DellaPenna, 1999; Cahoon et al., 2003; Havaux et al., 2003). In general, tocopherols are described as important antioxidants which protect polyunsaturated lipids from oxidative damage or can chemically scavenge various reactive oxygen species (ROS). For instance, they have important protection functions in seeds and in chloroplast membranes (Maeda and DellaPenna, 2007; Dörmann, 2007; Falk and Munné-Bosch, 2010). A tocopherol deficient Arabidopsis mutant (*vte2*) is impaired in seed germination because of increased non-enzymatic lipid oxidation in mutant seedlings and furthermore non-enzymatic lipid peroxidation is also increased in this mutant under combination of high-light and nonfreezing cold stress (Sattler et al., 2004; 2006; Havaux et al., 2006). Interestingly, increased lipid peroxidation in *vte2* seedlings during germination is accompanied by a transcriptional reprogramming similar to transcriptional reprogramming observed after biotic stresses such as *Botrytis*- or *P. syringae*-infection. In consequence, an accumulation of camalexin without any pathogen contact can be observed in *vte2* seedlings, indicating a signaling activity of oxidized polyunsaturated lipids in plant immunity (Sattler et al., 2006). Moreover, tocopherols are described for functions in several abiotic stress responses, in flowering, in the regulation of photo-assimilate export, and in response to salt stress (Falk and Munné-Bosch, 2010; Ellouzi et al., 2013) and elevated tocopherol levels in plants are described under high-light conditions, under temperature stress, under drought, and in response to copper (Munné-Bosch et al., 1999; Collakova and DellaPenna, 2003; Bergmüller et al., 2003; Ledford et al., 2004; Luis et al., 2006).

Here we demonstrate that tocopherol biosynthesis in Arabidopsis is also activated upon a biotic stimulus. Transcriptional reprogramming of tocopherol biosynthesis upon *P. syringae* infection triggers a strong accumulation of β -tocopherol and quantitatively moderate production of γ - and δ -tocopherol in leaves, whereas α -tocopherol levels essentially remain constant. Furthermore, we provide a plausible model of how basal and pathogen-triggered tocopherol generation contributes to Arabidopsis basal resistance against *P. syringae* by protecting tri-unsaturated fatty acids from oxidation.

2.3 Results

2.3.1 Tocopherol biosynthesis in Arabidopsis is induced upon *Pseudomonas syringae* inoculation

A local infection of Arabidopsis leaves with several cultivars of the hemibiotrophic bacterial pathogen *Pseudomonas syringae* leads to a transcriptional reprogramming of the plant at the site of bacterial inoculation and in systemic, non-inoculated leaf tissue (Gruner et al., 2013; Torres Zabala et al., 2015; Lewis et al., 2015; Bernsdorff et al., 2016). Comparative genome-wide microarray analyses of Col-0 leaves inoculated with the compatible (virulent) *Pseudomonas syringae* pv. *maculicola* ES4326 (*Psm*) strain or the avirulent strain *Pseudomonas syringae* pv. *tomato* DC3000 *avrRpm1* (*Pst avrRpm1*) and control MgCl₂-infiltrated leaves suggested that the expression of genes involved in tocopherol biosynthesis is changed in local infected leaf tissue. The expression of three genes involved in tocopherol biosynthesis, *TAT7*, *HPPD*, and *VTE2*, was increased in leaves inoculated with *Pst avrRpm1* 24 hours post inoculation (hpi) and in leaves inoculated with *Psm* at 24 and 32 hpi. Moreover, transcript levels of *VTE3* were decreased in leaves inoculated with both strains at both time-points compared to MgCl₂ infiltrated leaves (Table S1).

We confirmed changes in the expression of tocopherol biosynthesis genes by measurement of transcript levels by quantitative real-time PCR in leaves inoculated with *Psm* or the avirulent *Psm avrRpm1* strain, expressing the *avrRpm1* avirulence gene (Bisgrove et al., 1994), in comparison to MgCl₂-infiltrated leaves at 48 hpi. Transcript levels of *TAT7*, *HPPD*, and *VTE2* were increased in leaves inoculated with virulent *Psm* or avirulent *Psm avrRpm1*, whereas *VTE3* transcripts were decreased after inoculations at 48 hpi (Fig. 2.2). Expression levels of *VTE1* and *VTE4* did not show a clear tendency for up or down regulation after *Psm* or *Psm avrRpm1* inoculation at the investigated time points (Fig 2.2; Table S1). Overall, the qPCR analysis confirmed the microarray data. In leaf tissue distal to the sites of bacterial inoculations transcript levels of genes involved in tocopherol biosynthesis did not change after infection of local leaves compared to plants which were infiltrated with MgCl₂ (data not shown).

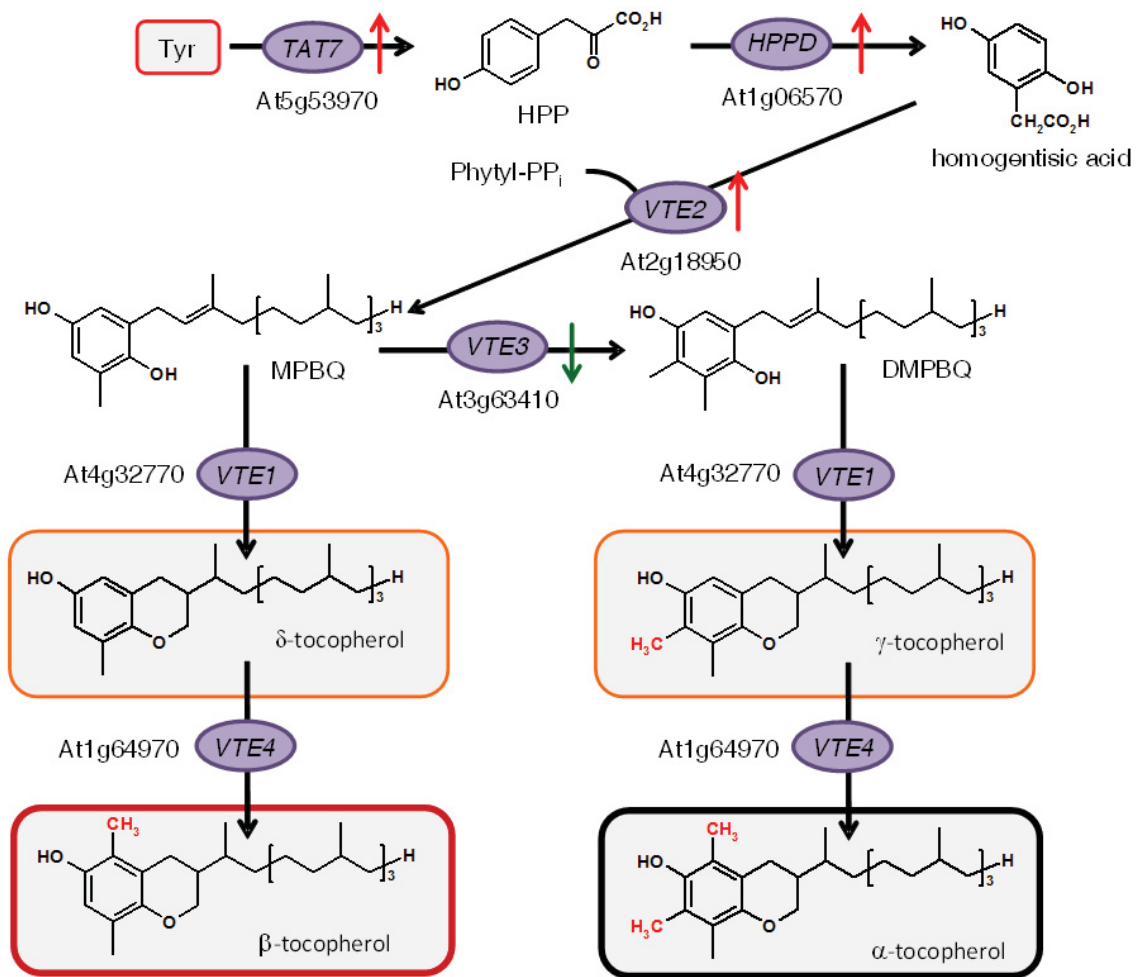


Figure 2.1 **Scheme of tocopherol-biosynthesis in *Arabidopsis* and changes in tocopherol-biosynthesis upon *P. syringae* infection.**

Red arrows indicate increased transcript levels upon *P. syringae* infection. Green arrow indicates decreased levels of VTE3 upon *P. syringae* infection. Metabolites in red rimmed boxes accumulate to high amounts upon *P. syringae* infection. Metabolites in orange rimmed boxes accumulate to moderate amounts upon *P. syringae* infection. α-tocopherol levels, rimmed in black, do not change upon *P. syringae* infection.

TAT7 = tyrosine amino transferase, **HPPD** = p-hydroxyphenylpyruvate dioxygenase, **VTE1** = tocopherol cyclase, **VTE2** = homogentisate phytoltransferase, **VTE3** = MPBQ methyltransferase, **VTE4** = γ-tocopherol methyltransferase, **Tyr** = tyrosine, **HPP** = p-hydroxyphenylpyruvate, **MPBQ** = methyl-6-phytyl-1,4-benzoquinone, **DMPBQ** = 2,3-dimethyl-6-phytyl-1,4-benzoquinone.

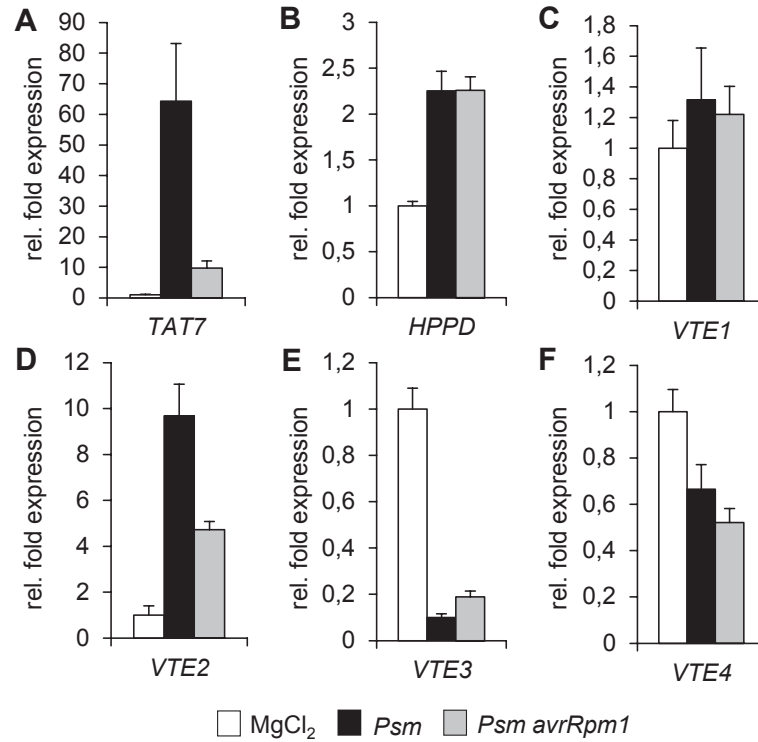


Figure 2.2 Inoculation of Arabidopsis leaves with *Psm* and *Psm avrRpm1* triggers a transcriptional reprogramming of genes involved in tocopherol biosynthesis.

Relative expression of (A) *TAT7*, (B) *HPPD*, (C) *VTE1*, (D) *VTE2*, (E) *VTE3*, and (F) *VTE4* upon *Psm*- and *Psm avrRpm1*-inoculation (48 hpi). Expression was normalized to the respective MgCl₂ control expression level. Asterisks denote statistically differences between MgCl₂-infiltration and *Psm*- or *Psm avrRpm1*-inoculation. ***P < 0.001, **P < 0.01, and *P < 0.05 (two tailed *t* test).

To investigate if transcriptional regulation of tocopherol biosynthesis after *P. syringae* inoculation would result in an accumulation of tocopherols, we conducted GS/MS-based comparative metabolite profiling experiments with inoculated leaf tissue and control-infiltrated (MgCl₂) leaves within a time-course analysis. We thereby quantified the four known tocopherols (Fig. 2.1) 8, 24, and 48 hpi at the inoculation site and in distal, systemic leaves at 48 hpi and compared them to the temporal accumulation of free SA. The endogenous α -tocopherol levels, which constitute the main tocopherol form in Arabidopsis leaves, remained at constantly high levels (approx. 20 μ g⁻¹ FW) in MgCl₂-treated and *P. syringae*-inoculated leaves at all investigated time points at inoculation sites and also in distal leaf tissue (Fig. 2.3A). The three forms β -, γ -, and δ -tocopherol accumulated at 48 hpi in *Psm*- and *Psm avrRpm1*-inoculated leaves but not in distal, non-inoculated tissue (Fig. 2.3B-D). Most prominently, endogenous levels of β -tocopherol increased at inoculation sites up to concentrations of approximately 13 μ g⁻¹ FW.

In response to microbial pathogen attack, SA biosynthesis is triggered by effector-triggered and PAMP-triggered immune signaling pathways in Arabidopsis leaves. SA accumulation contributes to plant resistance against many biotrophic and hemibiotrophic pathogens (Wildermuth et al., 2001; Vlot et al., 2009). We next compared pathogen triggered tocopherol accumulation to temporal SA accumulation. At 8 hpi, the *Psm avrRpm1*-triggered SA accumulation was stronger than *Psm*-triggered accumulation, showing that effector-triggered immune signaling contributes to early SA accumulation (Fig. 2.3E). A similar accumulation pattern could not be observed for pathogen-triggered tocopherol accumulation. *Psm* and *Psm avrRpm1*-triggered accumulation of β -, γ -, and δ -tocopherol could only be observed 48 hpi at inoculation sites. This indicates that both effector-triggered and PAMP-triggered immune signaling exhibits influence on pathogen-triggered tocopherol accumulation at late stages in the interaction of *P. syringae* and Arabidopsis. Furthermore, this indicates that early recognition of *P. syringae*-derived effectors has no influence on tocopherol generation in Arabidopsis.

Perception of PAMPs and ROS can trigger defense responses in Arabidopsis (Lamb and Dixon, 1997; Jones and Dangl, 2006; Mishina and Zeier, 2007; Griebel and Zeier, 2010). To investigate if PAMP or ROS perception is sufficient to trigger tocopherol generation, we infiltrated plants with 100 nM of flg22, an elicitor-active peptide of the bacterial flagellum (Gómez-Gómez et al., 1999), and with an enzyme/substrate mix of 0.5 mM xanthine and 0.5 U ml⁻¹ xanthine oxidase, which causes a continuous production of O₂⁻ (Delledonne et al., 1998). Notably, a moderate but significant β -tocopherol accumulation was triggered by exogenous application of flg22 and O₂⁻, whereas endogenous α -tocopherol levels were not affected in response to both treatments (Fig. 2.4).

This data so far indicated that the transcript levels of genes coding for enzymes of early steps of tocopherol biosynthesis, *TAT7*, *HPPD*, and *VTE2*, were increased in later stages of *P. syringae* infection in Arabidopsis (Fig. 2.2; for overview see Fig. 2.1). Previous experiments showed that also the aromatic amino acid tyrosine, which serves as a precursor for the chromanol head-group of tocopherols, is accumulating in *Psm*-inoculated leaves (Návarová et al., 2012). The consequence of the transcriptional reprogramming of tocopherol biosynthesis upon *P. syringae* infection is a strong accumulation of β -tocopherol and quantitatively moderate production of γ -, and δ -tocopherol, whereas α -tocopherol levels are not changed in response to bacterial inoculation (Fig. 2.3; Fig. 2.1). The observed decrease in *VTE3* transcript levels upon

inoculation is consistent with the specific accumulation patterns found for the different tocopherols because attenuation of the VTE3-mediated methylation reaction will direct the pathway towards β -tocopherol production (Fig. 2.1).

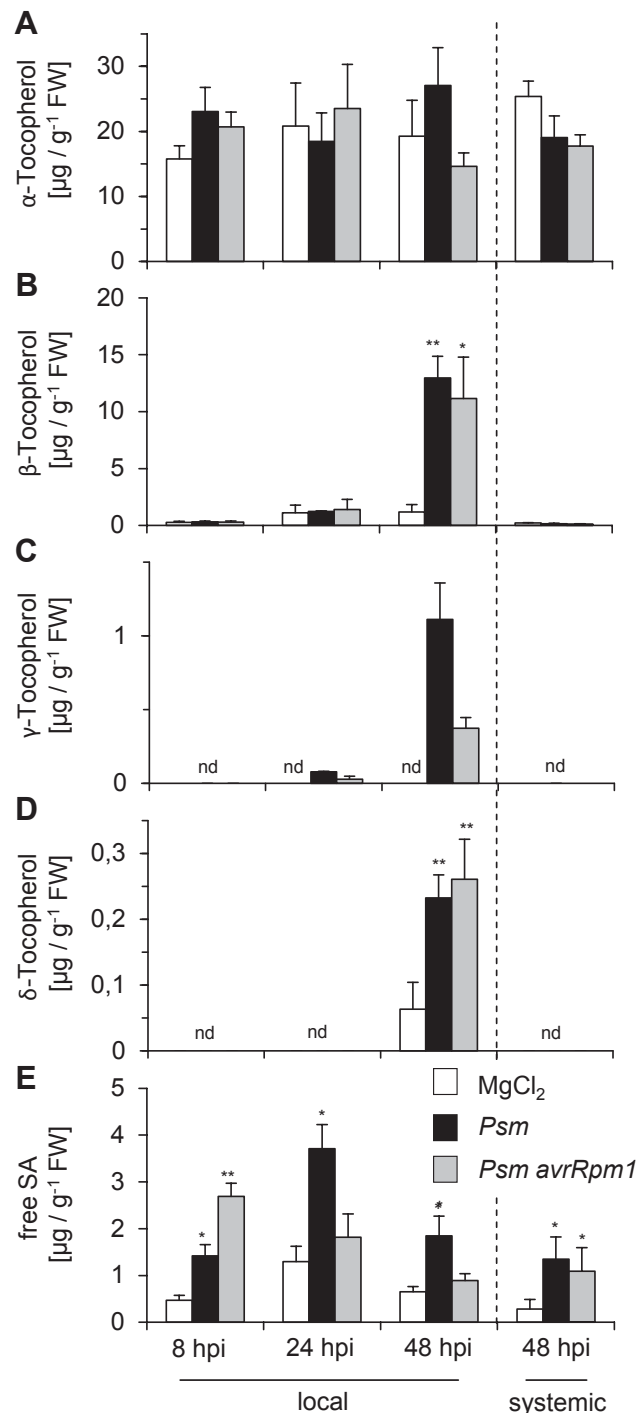


Figure 2.3 Temporal accumulation of tocopherols upon *Psm*- and *Psm avrRpm1*-inoculation.

Endogenous levels of (A) α -tocopherol, (B) β -tocopherol, (C) γ -tocopherol, (D) δ -tocopherol, and (E) free SA upon *Psm*- and *Psm avrRpm1*-inoculation at infection-sites 8, 24, and 48 hpi and 48 hpi in leaves distal to the site of infiltration. Asterisks denote statistically differences between MgCl_2 -infiltration and *Psm*- or *Psm avrRpm1*-inoculation. *** $P < 0.001$, ** $P < 0.01$, and * $P < 0.05$ (two tailed t test). nd = not detected

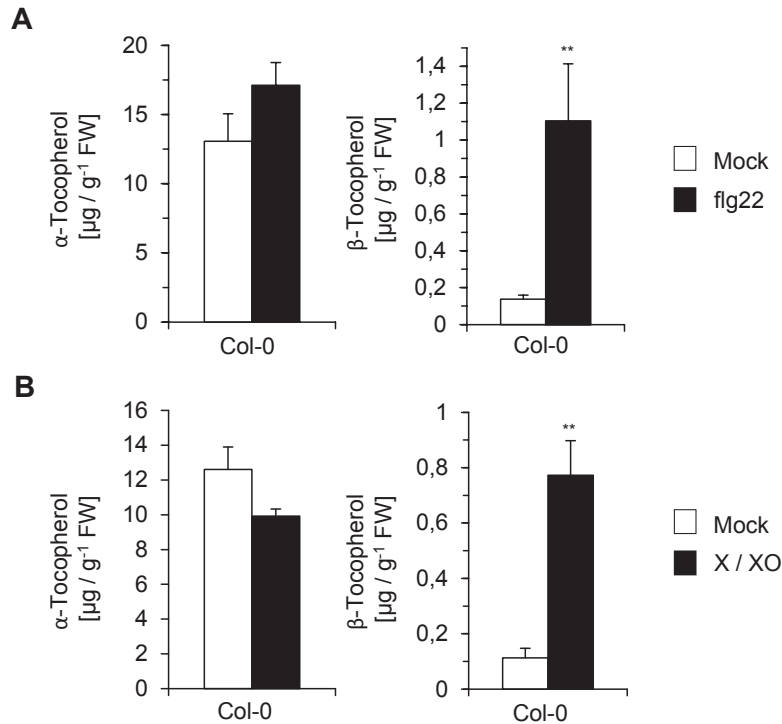


Figure 2.4 **Exogenous application of superoxide and flg22 is sufficient to trigger a moderate β-tocopherol accumulation**

(A) Endogenous levels of α-tocopherol and β-tocopherol in leaves infiltrated with 100 nM of flg22 and control-infiltrated leaves, 48 h post infiltration. Control infiltration (Mock) has been conducted with water. Asterisks denote statistically differences between Mock-infiltration and flg22-infiltration. ***P < 0.001, **P < 0.01, and *P < 0.05 (two tailed *t* test).

(B) Endogenous levels of α-tocopherol and β-tocopherol in leaves infiltrated with an enzyme/substrate mix of 0.5 mM xanthine and 0.5 U ml⁻¹ xanthine oxidase (X / XO), which is leading to a continuously production of O₂⁻, and control-infiltrated leaves, 48 h post infiltration. Control infiltration (Mock) has been conducted with a mix of 0.5 mM xanthine and the reaction buffer without the enzyme. Asterisks denote statistically differences between Mock-infiltration and X / XO-infiltration. ***P < 0.001, **P < 0.01, and *P < 0.05 (two tailed *t* test).

2.3.2 Pathogen-triggered tocopherol generation is independent of classical stress inducible signaling molecules SA, JA, ABA, ethylene, Pip and extracellular H₂O₂

The endogenous production of secondary metabolites, which is part of the multilayered plant immune system, underlies a complex regulatory network (Glazebrook, 2001; Pieterse et al., 2012). To investigate whether pathogen-triggered tocopherol accumulation underlies the control of classical defense signaling pathways in Arabidopsis we measured tocopherol levels in well-characterized defense mutants for β-tocopherol, the most prominently accumulating tocopherol. Pathogen-triggered β-tocopherol accumulation after inoculations with *Psm* and *Psm avrRpm1* was wild-type-

like in the ethylene signaling mutant *etr1* (Bleecker et al., 1988), the jasmonate (JA) biosynthesis mutant *dde2* (von Malek et al., 2002), the SA biosynthesis mutant *sid2* (Wildermuth et al., 2001), the abscisic acid (ABA) biosynthesis mutant *aba2-1* (Léon-Kloosterziel et al., 1996), the coronatine insensitive JA signaling mutant *coi1* (Xie et al., 1998), and in the Pip biosynthesis mutant *ald1* (Návarová et al., 2012) (Fig. 2.5). Notably, the Arabidopsis *cpr5-2* mutant, which exhibits increased pathogen resistance because of constitutively activated defense signaling and constitutive ROS production in leaves (Bowling et al., 1997; Maeto et al., 2006), contains increased endogenous β -tocopherol levels in MgCl₂-infiltrated leaves without any pathogen contact (Fig. 2.5). However, pathogen-triggered β -tocopherol accumulation was also wild-type-like in the *rbohD* mutant which is impaired in the *P. syringae*-inducible extracellular accumulation of hydrogen peroxide (H₂O₂) (Torres et al., 2002), indicating that only certain ROS exhibits an effect on tocopherol biosynthesis (Fig. 2.5).

2.3.3 The *vte2-2* mutant exhibits increased susceptibility against *Psm* and is fully impaired in basal and pathogen-triggered Tocopherol accumulation but not in the accumulation of other defense-related metabolites

To investigate the functional relevance of basal and pathogen-triggered tocopherol generation for Arabidopsis resistance against bacterial pathogens, we determined the multiplication of *Psm* three days post inoculation in leaves of previously described mutants impaired in different steps of tocopherol biosynthesis (Fig. 2.6). The *vitamin E deficient* mutant (*vte*) *1* is deficient in tocopherol cyclase activity, which impairs tocopherol biosynthesis but is leading to an accumulation of the redox-active intermediate 2,3-dimethyl-6-phytyl-1,4-benzoquinone (DMPBQ) (Porfirova et al., 2002; Sattler et al., 2003; for overview of tocopherol biosynthetic pathway see Fig. 2.1). *vte2-2* is impaired in homogentisate phytyl transferase activity and is deficient in tocopherol generation and in the generation of the intermediate DMPBQ (Havaux et al., 2005). The MPBQ methyltransferase VTE3 catalysis a key methylation step in tocopherol and plastoquinone biosynthesis, therefore homozygous Arabidopsis *vte3* mutants are not viable (Cheng et al., 2003) and experiments had to be conducted with heterozygous *vte3* mutant plants. A further key methylation reaction step in tocopherol biosynthesis is catalyzed by the γ -tocopherol methyltransferase VTE4 (Bergmüller et al., 2003). Out of the tyrosine aminotransferase (TAT) protein family the TAT7 is involved in tocopherol biosynthesis in Arabidopsis and corresponding *tat7* mutants show reduced endogenous tocopherols levels compared to Col-0 (Riewe et al., 2012).

Tocopherols in Arabidopsis basal resistance

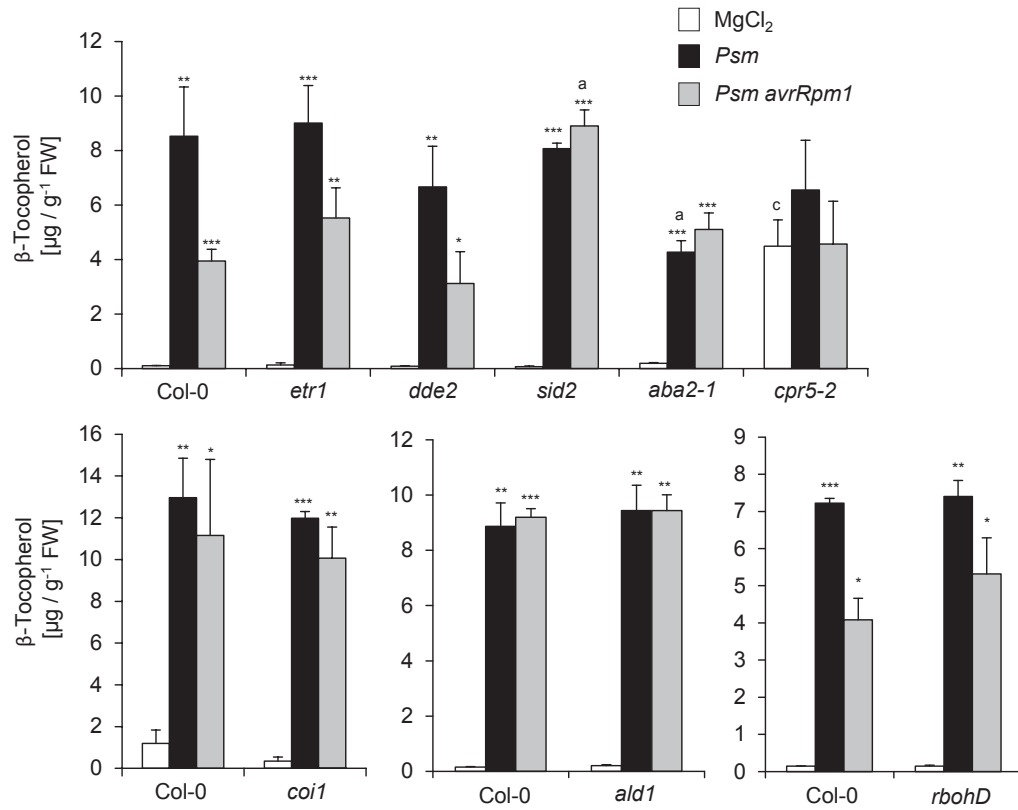


Figure 2.5 Pathogen-triggered generation of β -tocopherol is virtually independent of ethylene-, jasmonic acid-, salicylic acid-, abscisic acid-, pipecolic acid-signaling and extracellular H₂O₂.

Endogenous levels of β -tocopherol in several Arabidopsis mutants impaired in different defense signaling pathways at 48 hpi upon *Psm*- and *Psm avrRpm1*-inoculation. Asterisks denote statistically differences between MgCl₂-infiltration and *Psm*- or *Psm avrRpm1*-inoculation. ***P < 0.001, **P < 0.01, and *P < 0.05. Letters denote statistically differences between the same treatment of Col-0 and the respective mutant. ^cP < 0.001, ^bP < 0.01, and ^aP < 0.05 (two tailed *t* test).

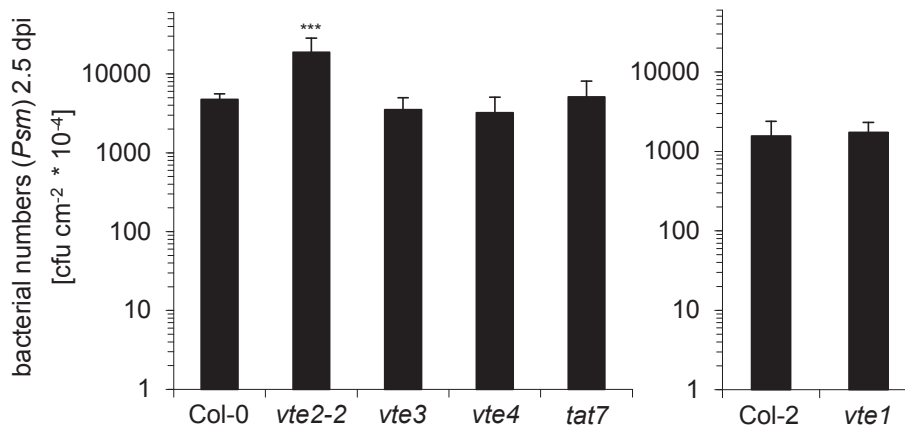


Figure 2.6 The *vte2-2* mutant exhibits increased susceptibility against *Psm*.

Bacterial numbers of compatible *Psm* (applied in titers of OD₆₀₀ 0.001) in several mutants with described defects in tocopherol biosynthesis three days after inoculation. Bacterial numbers are means from 12 parallel samples, each consisting of three leaf disks. Asterisks denote statistically differences between Col-0 or Col-2 and the respective mutant. ***P < 0.001, **P < 0.01, and *P < 0.05 (two tailed *t* test).

The bacterial proliferation rates were wild-type-like in *vte1*, heterozygote *vte3*, *vte4*, and *tat7* mutant plants but significantly increased by approximately four times in *vte2-2* mutant plants compared to Col-0 (Fig. 2.6). The relative increase in bacterial growth was also visible in the phenotype of inoculated leaves. Leaves of *vte2-2* plants showed stronger disease symptoms 2.5 days post *Psm* inoculation than leaves of Col-0, *vte3*, *vte4*, and *tat7*, including stronger yellowing leaves and necrosis (Fig. S1). Notably, the *vte2-2* mutant, which exhibited an increased susceptibility to *Psm*, was the only investigated mutant which was fully impaired in basal and pathogen triggered tocopherol generation. We measured endogenous tocopherol levels in leaves of Col-0 and *vte2-2* plants after $MgCl_2$, *Psm*, and *Psm avrRpm1* infiltrations at 48 hpi. Pathogen inoculations led to a strong accumulation of β -tocopherol and quantitatively moderate production of γ -, and δ -tocopherol, whereas α -tocopherol level remained constant in Col-0, whereas in *vte2-2* only traces of each tocopherol type could be detected after all treatments (Fig. 2.7A-D). Comparison of total tocopherol contents of all investigated genotypes showed that used lines *vte4*, *vte1*, *tat7*, and heterozygote *vte3* still can generate tocopherol amounts, also those amounts were significantly decreased compared to Col-0 (Fig. S2). Furthermore, due to the function of VTE1, VTE3, and VTE4 in tocopherol biosynthesis corresponding mutants presumably still synthesize the redox-active intermediates MPBQ and/or DMPBQ (Dörmann, 2007; Fig. 2.1). To investigate if the susceptibility-phenotype of *vte2-2* (Fig. 2.6) is a consequence to the lack of basal and pathogen-triggered tocopherol accumulation (Fig. 2.7) and not to other possible impaired defense signaling pathways in the mutant, we measured endogenous levels of defense-related metabolites SA, camalexin, and stigmaterol in leaves of Col-0 and *vte2-2* plants after inoculations.

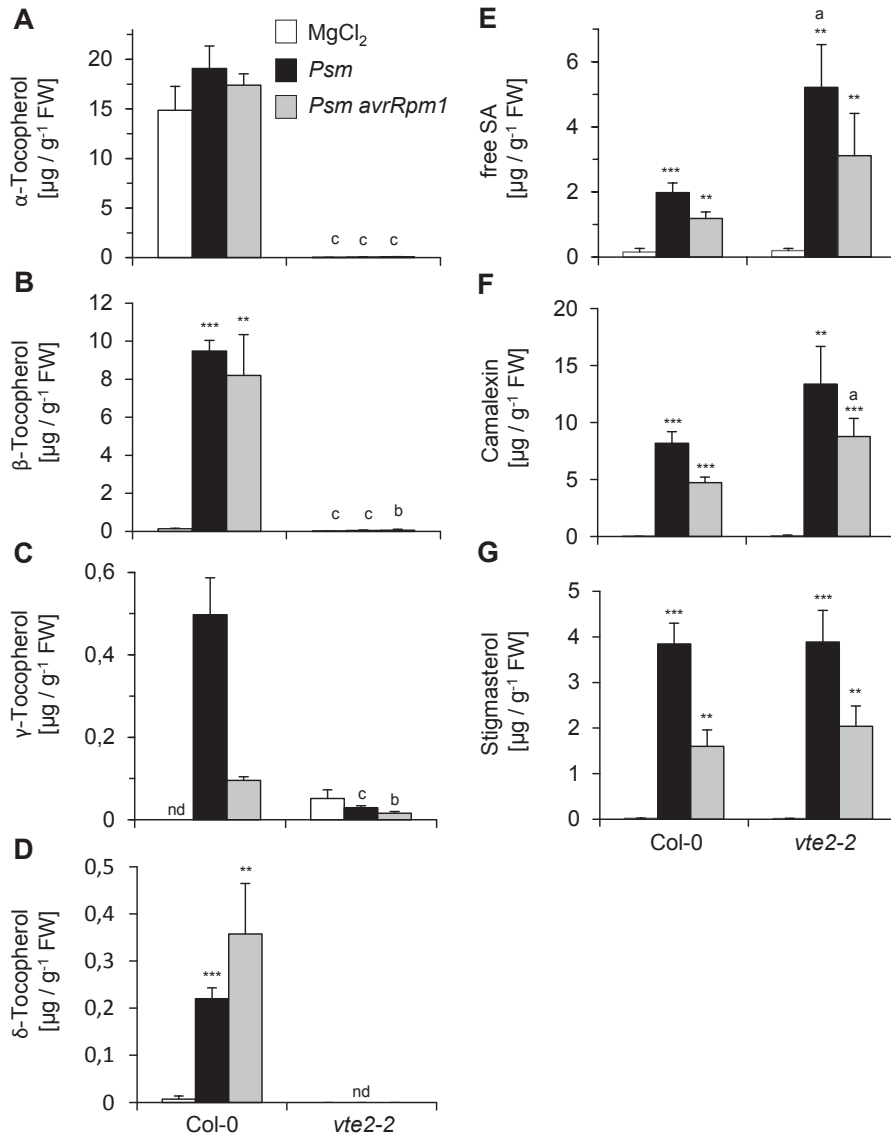


Figure 2.7 The *vte2-2* mutant is fully impaired in basal and pathogen-triggered tocopherol generation but not in the accumulation of other defense-related metabolites.

Endogenous levels of (A) α-tocopherol, (B) β-tocopherol, (C) γ-tocopherol, (D) δ-tocopherol, (E) free SA, (F) camalexin, and (G) stigmaterol in leaves infiltrated with MgCl₂, *Psm*, or *Psm avrRpm1* at 48 hpi in Col-0 and *vte2-2*. Asterisks denote statistically differences between MgCl₂-infiltration and *Psm*- or *Psm avrRpm1*-inoculation. ***P < 0.001, **P < 0.01, and *P < 0.05. Letters denote statistically differences between the same treatment of Col-0 and *vte2-2*. ^cP < 0.001, ^bP < 0.01, and ^aP < 0.05 (two tailed *t* test). nd = not detected.

The accumulation of the phenolic metabolite SA contributes to resistance against *Psm* and many other different biotrophic and hemibiotrophic pathogens in plants (Nawrath and Métraux, 1999; Vlot et al., 2009) and the *Psm*-triggered conversion of β-sitosterol to stigmasterol via the cytochrome P450 monooxygenase (CYP) 710A1 leads to an increased plant disease susceptibility to *Psm* in Arabidopsis (Griebel and Zeier, 2010). Furthermore, indole biosynthesis via CYP79B2 and

CYP79B3 is highly activated in Arabidopsis after *Psm* inoculation and one of the most dominantly accumulating Trp-derived indolics is camalexin (Stahl et al., 2016). Moreover, *vte2-1* seedlings exhibit increased endogenous camalexin levels 3 and 6 days after germination (Sattler et al., 2006). SA and camalexin accumulated in Col-0 and *vte2-2* leaves 48 hours post inoculations with *Psm* and *Psm avrRpm1* (Fig. 2.7E-F). Thereby, by trend the pathogen-triggered accumulations of SA and camalexin were higher in *vte2-2* compared to Col-0, probably due to the higher bacterial proliferation rates and the thereby increased pathogen-trigger in the mutant (Fig. 2.6). Increased camalexin levels without any pathogen contact in adult *vte2-2* mutant plants could not be observed (Fig. 2.7F) and the pathogen induced conversion of β -sitosterol to stigmasterol was wild-type-like in *vte2-2* (Fig. 2.7G). To investigate whether basal and pathogen-triggered tocopherol generation also takes a functional role in SAR establishment, we infiltrated leaves of Col-0 and *vte2-2* plants with *Psm* to induce SAR in the whole plant foliage or with 10 mM MgCl₂ as a control. 48 h later both sets of plants were inoculated with *Psm* in leaves distal to the site of first infiltrations and 2.5 days later bacterial numbers in those leaves were determined. Bacterial multiplications were decreased in both genotypes after a first inoculation with *Psm* compared to control-infiltrated plants, indicating that tocopherol generation is not necessary for SAR establishment (Fig. S3). Thereby the bacterial numbers in *vte2-2* were significantly increased after both treatments compared to Col-0. In SAR-positive *vte2-2* plants bacteria could proliferate to similarly amounts like in control-infiltrated Col-0 plants, suggesting that basal and pathogen-triggered tocopherol generation is also of functional relevance for pathogen-resistance in the case of SAR establishment.

2.3.4 The *vte2-2* mutant exhibits an increased amount of non-enzymatic lipid peroxidation in leaves after *Psm* inoculation

Several studies have established that tocopherols are of functional relevance in the protection of polyunsaturated fatty acids (PUFAs) towards oxidative damage (Schneider, 2005). Experiments including *vte2* mutants demonstrated that tocopherols control lipid peroxidation in Arabidopsis in early developmental stages (Sattler et al., 2004; 2006). A secondary end product of oxidized PUFAs is malondialdehyde (MDA) (Weber et al., 2004). Tocopherol deficient *vte2* mutants exhibit increased accumulation of MDA under combination of non-freezing cold- and high-light-stress and during germination (Havaux et al., 2006; Sattler et al., 2006). Furthermore, experiments with *vte2* seedlings indicated that non-enzymatic lipid peroxidation takes a role in the regulation of Arabidopsis defense-responses against pathogens (Sattler et al., 2006).

We therefore measured non-enzymatic lipid peroxidation in Col-0 and *vte2-2* after inoculations with *Psm* and *Psm avrRpm1* via quantification of MDA. In Col-0, MDA amounts were significantly increased 48 hpi in leaves inoculated with *Psm* and *Psm avrRpm1* compared to MgCl₂-infiltrated leaves (Fig. 2.8). Thereby the amount of MDA was approximately 2.5 times higher in *Psm*-inoculated leaf tissue than in MgCl₂-infiltrated leaves. In the *vte2-2* mutant, non-enzymatic lipid peroxidation was also significantly increased after bacterial inoculations. Remarkably, inoculation with virulent *Psm* but not avirulent *Psm avrRpm1* induced significantly higher MDA accumulation in *vte2-2* than in the Col-0 wild-type. Therefore, increased non-enzymatic lipid peroxidation in *vte2-2* in response to *Psm* attack correlates with decreased basal resistance against this pathogen (Fig. 2.6; Fig. 2.8). Because of the observation that MgCl₂-infiltrated *vte2-2* leaves exhibits moderate but significantly increased levels of MDA in MgCl₂-infiltrated leaves compared to Col-0, we included measurement of MDA in untreated leaves in our experiments. Untreated adult *vte2-2* leaves showed no difference in non-enzymatic lipid peroxidation compared to Col-0, indicating that also the mechanical stimulus of the MgCl₂-infiltration leads to a small increase of non-enzymatic lipid peroxidation in *vte2-2*, and that tocopherols in the wild-type protect PUFAs against oxidative damage (Fig. 2.8).

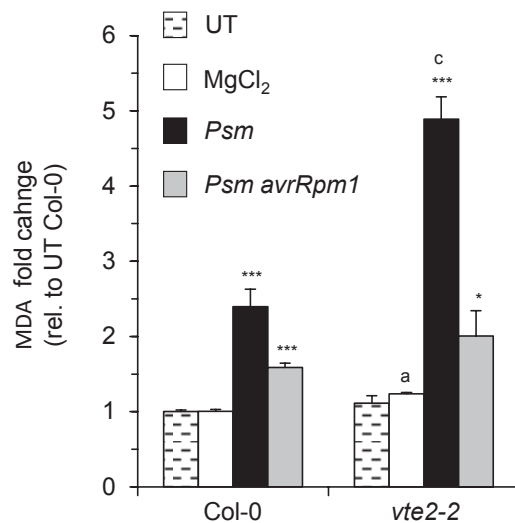


Figure 2.8 **The *vte2-2* mutant exhibits increased nonenzymatic lipid peroxidation upon *Psm*-inoculation.**

MDA was determined, as a marker for nonenzymatic lipid peroxidation, in untreated leaves (UT), in leaves infiltrated with 10 mM MgCl₂, and in leaves inoculated with *Psm*- or *Psm avrRpm1*, at 48 hpi, in Col-0 and in *vte2-2*. MDA levels were normalized to the level measured in untreated Col-0 levels. Asterisks denote statistically differences between untreated leaves and MgCl₂-infiltrated leaves or statistically differences between MgCl₂-infiltration and *Psm*- or *Psm avrRpm1*-inoculation. ***P < 0.001, **P < 0.01, and *P < 0.05. Letters denote statistically differences between the same treatment of Col-0 and *vte2-2*. ^cP < 0.001, ^bP < 0.01, and ^aP < 0.05 (two tailed *t* test).

2.3.5 Reduced non-enzymatic lipid peroxidation in the *vte2* background abolishes the *vte2* susceptibility phenotype

To investigate if the increased susceptibility of *vte2-2* against *Psm* is a consequence of the increased non-enzymatic lipid peroxidation after *Psm*-inoculation in the mutant (Fig. 2.6, Fig. 2.8), we integrated the quadruple mutant *fad3-2 fad7-2 fad8 vte2-1* in our experiments. The fatty acid desaturases (FAD) 3, 7, and 8 catalyze the generation of tri-unsaturated fatty acids in Arabidopsis and the corresponding triple mutant exhibits decreased levels of tri-unsaturated fatty acids and MDA compared to the wild-type (McConn and Browse, 1996; Weber et al., 2004). In *fad3-2 fad7-2 fad8 vte2-1*, genetically removed tri-unsaturated fatty acids abolish *vte2*-specific phenotypes in the *vte2* background, such as impaired seedling development and increased MDA levels in seedlings (Mène-Saffrané et al., 2007). Because the quadruple mutant was generated in the *vte2-1* background (Mène-Saffrané et al., 2007), we also integrated the *vte2-1* single mutant to our experiments. As for *vte2-2*, non-enzymatic lipid peroxidation was increased to significantly higher levels in *Psm*-inoculated leaf tissue of *vte2-1* than in the wild-type at 48 hpi (Fig. 2.9A). By contrast, non-enzymatic lipid peroxidation was wild-type-like in two independent *fad3-2 fad7-2 fad8 vte2-1* quadruple mutant lines in *Psm*-inoculated leaves and thereby significantly decreased compared to *Psm*-inoculated leaves (Fig. 2.9A). This suggests that the decreased amounts of tri-unsaturated fatty acids in the quadruple mutant leads to decreased non-enzymatic lipid peroxidation after *Psm* inoculation. In untreated leaves of the *fad3-2 fad7-2 fad8 vte2-1* lines, levels of MDA were significantly decreased compared to Col-0, whereas MDA levels after $MgCl_2$ infiltration were wild-type-like in the two lines (Fig. 2.9A). As well as the *vte2-2*-mutation, the *vte2-1*-mutation results in lack of basal and pathogen-triggered tocopherol generation (Fig. S4A-D). That gave us the opportunity to test if increased levels of non-enzymatic lipid peroxidation after *Psm* inoculation in the *vte2* mutants is functionally relevant for the increased susceptibility phenotype of the *vte2* mutants. We therefore compared bacterial proliferation rates of *Psm* in Col-0, *vte2-1*, *vte2-2*, and the two quadruple lines 2.5 days after inoculation. Compared to Col-0, bacterial numbers were significantly increased in the two single mutant lines *vte2-1* and *vte2-2* (Fig. 2.9B). Like the amount of MDA in *Psm*-inoculated leaves (Fig. 2.9A), the bacterial proliferation rates were wild-type-like in *fad3-2 fad7-2 fad8 vte2-1* mutant lines and significantly decreased compared to the *vte2-1* single mutant (Fig. 2.9B). It was previously shown that *fad3* and *fad7fad8* mutants are more susceptible to avirulent *P. syringae* strains (Yaeno et al., 2004). In combination with the here shown results, this suggests that basal levels and induced production of tocopherols contribute to

Arabidopsis basal resistance against *Psm*, by preventing oxidative damage of tri-unsaturated fatty acids.

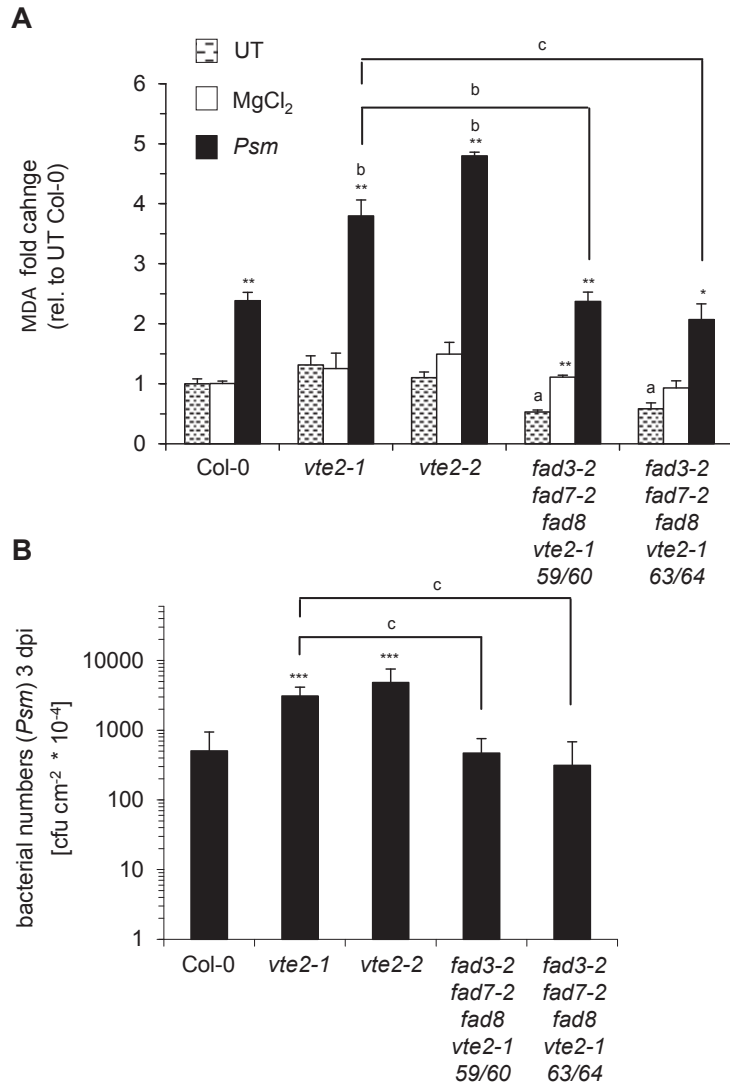


Figure 2.9 **Reduced nonenzymatic lipid peroxidation in the *vte2* background complements the *vte2* susceptibility phenotype.**

(A) MDA was determined, as a marker for nonenzymatic lipid peroxidation, in untreated leaves (UT), in leaves infiltrated with 10 mM MgCl₂, and in leaves inoculated with *Psm* at 48 hpi in *Col-0*, *vte2-1*, *vte2-2*, and in to lines of the quadruple mutant *fad3-2 fad7-2 fad8 vte2-1*. Asterisks denote statistically differences between untreated leaves and MgCl₂-infiltrated leaves or statistically differences between MgCl₂-infiltration and *Psm*-inoculation. ***P < 0.001, **P < 0.01, and *P < 0.05. Letters denote statistically differences between the same treatment of *Col-0* and the respective mutant or the statistically differences between the same treatment of *vte2-1* and the respective quadruple mutant. °P < 0.001, °bP < 0.01, and °aP < 0.05 (two tailed *t* test).

(B) Bacterial numbers of compatible *Psm* (applied in titers of OD₆₀₀ 0.001) in *Col-0*, *vte2-1*, *vte2-2*, and in to lines of the quadruple mutant *fad3-2 fad7-2 fad8 vte2-1*. Bacterial numbers are means from 10 parallel samples, each consisting of three leaf disks. Asterisks denote statistically different between *Col-0* and the respective mutants. ***P < 0.001, **P < 0.01, and *P < 0.05. Letters denote statistically differences between *vte2-1* and the respective quadruple mutant. °P < 0.001, °bP < 0.01, and °aP < 0.05 (two tailed *t* test).

2.4 Discussion

Tocopherols and tocotrienols, which are collectively described as tocochromanols, are exclusively synthesized by photosynthetic organisms but are essential for human diet. Therefore, most studies regarding the biological function of tocochromanols have been conducted in mammalian systems and their functional roles in plants are not fully understood yet (Schneider, 2005; DellaPenna and Pogson, 2006; Maeda and DellaPenna, 2007; Dörmann, 2007; Falk and Munné-Bosch, 2010). Beside the established and suggested roles of tocopherols in plants in response to several abiotic stressors, in relationship to flowering and seed germination, and in the regulation of photo-assimilate export, our study reveals a novel pathogen-inducible regulation of tocopherol biosynthesis and a novel functional role of tocopherols in Arabidopsis basal resistance against virulent *P. syringae*. Our study further suggests that tocopherols prevent oxidative damage of tri-unsaturated fatty acids after *P. syringae*-infection which is associated with enhanced disease resistance.

2.4.1 The transcriptional reprogramming of tocopherol biosynthesis upon *P. syringae* infection leads to a strong accumulation of β -tocopherol in Arabidopsis

Out of the group of tocochromanols, tocopherols are synthesized by all photosynthetic organisms and accumulate to higher amounts in vascular plants than in early photosynthetic organisms, whereas tocotrienols are only present in specific plant groups and are generally found in seeds and fruits of angiosperms (Esteban et al., 2009; Falk and Munné-Bosch, 2010). Tocopherol biosynthesis has been previously described to be regulated upon perception of different abiotic stresses. Endogenous tocopherol levels in several photosynthetic organisms were increased under high-light conditions (Collakova and DellaPenna, 2003; Ledford et al., 2004), under temperature stress (Bergmüller et al., 2003), under drought (Munné-Bosch et al., 1999), and in response to copper (Luis et al., 2006). Here we could demonstrate that tocopherol biosynthesis is also regulated upon a biotic stress exposure. Transcript levels of *TAT7*, *HPPD*, and *VTE2*, which catalyze early steps of tocopherol biosynthesis, were highly increased in *Psm*- and *Psm avrRpm1*-inoculated Arabidopsis leaves 48 hpi, whereas *VTE3* transcripts were highly decreased after both inoculations (Fig. 2.2; Table S1). This distinct transcriptional regulation of tocopherol biosynthesis upon *P. syringae* infection is leading to an activation of the tocopherol biosynthetic pathway towards the generation of β -tocopherol (Fig. 2.1). As a consequence, a strong accumulation of β -

tocopherol could be observed at 48 hpi, whereas γ -, and δ -tocopherol only accumulated to quantitatively moderate amounts and α -tocopherol levels remained essentially constant. The pathogen-triggered tocopherol accumulation was restricted to the site of bacterial inoculation and could not be observed in distal leaf tissue (Fig. 2.3A-D; Fig. 2.10). Comparison of *Psm*- and *Psm avRpm1*-triggered tocopherol generation with temporal accumulation patterns of free SA showed that both effector-triggered and PAMP-triggered immune signaling contribute to pathogen-triggered tocopherol accumulation at late stages in the interaction between *P. syringae* and Arabidopsis (Fig. 2.3). Consistent with this finding, a quantitatively moderate but significant accumulation of β -tocopherol could also be observed at 48 hpi after leaf-infiltration with bacterial peptide flg22 (Fig. 2.4A; Fig. 2.10). flg22 is a highly conserved 22 amino acid peptide sequence from the bacterial flagellum and recognition of flg22 via the FLS2 and BAK1 receptors is sufficient to trigger defense responses such as production of ROS or the accumulation of defense-related metabolites such as SA and Pip (Gómez-Gómez et al., 1999; Chinchilla et al., 2007; Mishina and Zeier, 2007; Návarová et al., 2012). Plant derived ROS in general, are described to play an important role in defense signaling against several pathogens (Lamb and Dixon, 1997; Baxter et al., 2014). Exogenous application of an enzyme/substrate mixture of 0.5 mM xanthine and 0.5 U ml⁻¹ xanthine oxidase, which results in continuous production of O₂⁻ (Delledonne et al., 1998), also leads to an quantitatively moderate generation of β -tocopherol. This indicates that, as part of effector-triggered and PAMP-triggered immune signaling also ROS signaling is involved in pathogen-triggered tocopherol accumulation (Fig. 2.4B; Fig. 2.10). Consistent with this finding, the Arabidopsis mutant *cpr5-2*, which is described for increased pathogen resistance because of constitutively activated defense signaling and constitutive ROS production in leaves (Bowling et al., 1997; Maeto et al., 2006), exhibits increased endogenous β -tocopherol levels in mock-treated leaves in the absence of a pathogen contact (Fig. 2.5). However, Arabidopsis mutant *rbohD*, which is impaired in the extracellular accumulation of hydrogen peroxide (H₂O₂) via *RESPIRATORY BURST OXIDASE HOMOLOGUE D* (RBOHD) also described as oxidative burst (Torres et al., 2002), was not impaired in pathogen-triggered in tocopherol generation, indicating that RBOHD-independent ROS sources contribute to pathogen-triggered tocopherol generation (Fig. 2.5). Notably, recent findings indicate that production of ROS in different plant cellular compartments have divergent effects and functions in plants and especially chloroplast derived H₂O₂ contributes to phytoalexin and stigmaterol production (Sewelam et al., 2014).

Until now it is not fully understood if the different forms of tocopherols (Fig. 2.1) adopt divergent functional roles in plants (Falk and Munné-Bosch, 2010). In the present study, we could show that the infiltration of *P. syringae*, flg22, and O₂⁻ into Arabidopsis leaves leads to a distinct accumulation of β-tocopherol whereupon α-tocopherol levels remain constant (Fig. 2.3; Fig. 2.4; Fig. 2.5; Fig. 2.7; Fig. 2.10; Fig. S4). Due to its chemical structure α-tocopherol has been described as the tocopherol-form with the highest antioxidant activity (Schneider, 2005). To most efficiently protect from damage by pathogen-inducible lipid peroxidation (Fig. 2.8), it might thus be expected that plants respond with α-tocopherol generation and not with an activation of β-tocopherol biosynthesis. However, besides to its role as lipid-soluble antioxidant, α-tocopherol is described as an important constituent of bio membranes which is involved in stabilizing membrane structures. This could explain elevated basal α-tocopherols levels compared to the other tocopherol forms (Wang and Quinn, 2000). Furthermore, the study of model membranes mimicking the lipid composition of plant chloroplast membranes showed that α-tocopherol has highest effects on membrane stability at concentration close to the concentrations which are reached *in vivo* in chloroplast membranes (Hincha, 2008). Therefore, it is likely that tocopherol levels in chloroplast membranes are precisely regulated and it would be maybe wrong to assume that the higher the tocopherol levels in a plant are the better the plant is protected (Falk and Munné-Bosch, 2010). Here, we cannot finally clarify the question why especially β-tocopherol biosynthesis is distinctly up-regulated. But due to model membrane studies of Hincha (2008), basal α-tocopherol levels might be already in an ideal concentration in chloroplast-membranes and higher levels could decrease membrane stability and would be hence harmful for the plant. Therefore, the plant could respond to the higher oxidative pressure after *P. syringae*-infection with the accumulation of β-tocopherol as an alternative to α-tocopherol (Fig. 2.1; Fig. 2.3).

2.4.2 Pathogen-triggered tocopherol generation is independent from classical phytohormone defense-signaling

The endogenous production of phytohormones in response to several pathogens is an integral part of the complex regulatory network underlying plant immunity (Glazebrook, 2001; Pieterse et al., 2012). Moreover, distinct plant defense responses underlie the control of phytohormone-mediated defense signaling. For example, specific branches of *Psm*-activated indole metabolism in Arabidopsis are positively influenced by exogenous application of Pip and SA. Consistent with that, the endogenous *Psm*-induced accumulation of several indolics is decreased in mutant

plants impaired in SA biosynthesis (Stahl et al., 2016). Jasmonate has been previously implicated in the induction of TAT and tocopherol biosynthesis after UV-treatment (Sandorf and Holländer-Czytko, 2002). We therefore measured if tocopherol accumulation after *P. syringae*-infection is controlled by phytohormone signaling. Here, we could demonstrate that *P. syringae*-triggered generation of β -tocopherol proceeds independently of SA-, JA-, ABA-, ethylene-, and Pip-related defense signaling because well-characterized biosynthetic and signaling mutants in these pathways show wild-type-like in *P. syringae*-inducible β -tocopherol accumulation (Fig. 2.5; Fig. 2.10).

2.4.3 Constitutive and pathogen-induced tocopherols contribute to Arabidopsis basal resistance to *Psm* and protect tri-unsaturated fatty acids from non-enzymatic lipid peroxidation during infection

Our study shows that *P. syringae* inoculation triggers an increased generation of MDA (Fig. 2.8; Fig. 2.9; Fig. 2.10), a end product of oxidized tri-unsaturated fatty acids (Weber et al., 2004). MDA levels in plants are increased under conditions with ROS overproduction and oxidation products in plants are described to have effective biological activities (Farmer and Davoine, 2007). In general, tocopherols are described to protect plant PUFAs under those conditions from oxidative damage and tocopherol-deficient mutants show increased lipid peroxidation and MDA levels under abiotic stress conditions and during seed germination (Sattler et al., 2004; 2006; Havaux et al., 2005; 2006; Mène-Saffrané et al., 2007). Here we could demonstrate that tocopherols also protect PUFAs in Arabidopsis from increased oxidative damage after *P. syringae* infection because *vte2* mutant plants, which were fully impaired in basal and pathogen-triggered tocopherol generation (Fig. 2.7; Fig. S4), exhibit increased MDA levels after *Psm*-inoculations compared to wild-type plants (Fig. 2.8; Fig. 2.9). Increased nonenzymatic lipid peroxidation in *vte2* seedlings during germination has been described to reprogram gene expression, with an activation of genes related with biotic stress responses. This transcriptional reprogramming is associated with tissue damage and an activation of camalexin biosynthesis, indicating that non-enzymatic lipid peroxidation products have a signaling activity in plant-pathogen interactions and protection from lipid peroxidation takes a functional role in pathogenies (Sattler et al., 2006). Elevated levels of MDA and camalexin compared to the wild-type like in *vte2* seedlings could not be observed in adult untreated *vte2* plants (Fig. 2.7; Fig. 2.8; Fig. 2.9). Notably, there was a trend to a higher pathogen-triggered camalexin accumulation in the *vte2-2* mutant than in the wild-type (Fig. 2.7F). That could be reasoned by higher bacterial multiplication rates in this mutant (Fig 2.6) or underlining the signaling effect of

lipid peroxidation on camalexin biosynthesis, because pathogen induced accumulation of MDA was higher in this mutant compared to the wildtype (Fig. 2.8; Fig. 2.9). However, the two investigated mutant lines *vte2-1* and *vte2-2*, which were fully impaired in basal and pathogen-triggered tocopherol generation (Fig. 2.7; Fig. S4), both exhibit increased non-enzymatic lipid peroxidation upon *Psm*-infection (Fig. 2.8; Fig. 2.9) and increased susceptibility against *Psm* (Fig. 2.6; Fig. 2.9; Fig. S1). Notably, the increased susceptibility against *Psm* could just be observed in mutants defective in the homogentisate phytyl transferase gene *VTE2* and not in the other investigated tocopherol biosynthesis mutants *tat7*, *vte1*, *vte3* (heterozygote), and *vte4* (Fig. 2.6; Fig. S1). That could be reasoned by that those two mutants were fully impaired in basal and pathogen-triggered tocopherol generation (Fig. 2.7; Fig. S4) and the other mutants are still able to synthesis tocopherol amounts, although those amounts were significantly decreased compared to Col-0 (Fig. S2). Furthermore, the mutants *vte1*, *vte3*, and *vte4* are predicted to still synthesize, due to their function in tocopherol biosynthesis, the redox-active intermediates MPBQ and/or DMPBQ (Dörmann, 2007; Fig. 2.1). Several findings indicate that the pathway intermediates MPBQ and/or DMPBQ are able to restore tocopherol functions in plants. For example, *vte2*-specific phenotypes under stress-conditions und during germination, such as MDA generation and camalexin production in the absence of pathogens, cannot be observed in *vte1* mutants because they still can generate the redox-active pathway intermediate DMPBQ (Porfirova et al., 2002; Sattler et al., 2003; 2004; 2006). Thus, the complete absence of tocopherols (Fig 2.7; Fig. S4) and their reported inability to synthesize benzoquinone intermediates distinguish *vte2* plants from *vte1*, *vte3*, and *vte4*. We suggest that both factors are from functional relevance why increased susceptibility to *Psm* was exclusively observed in *vte2* mutants.

SAR is a form of inducible plant innate immunity realized in the whole plant foliage and confers long-lasting protection against a broad spectrum of pathogenic microorganisms. It is triggered by a first recognition of a pathogen and its establishment in systemic tissue is dependent by pipecolic acid (Pip)- and salicylic acid (SA)-controlled pathways (Gaffney et al., 1993; Návarová et al., 2012; Fu and Dong, 2013; Shah and Zeier, 2013, Bernsdorff et al., 2016). Here we could demonstrate that tocopherol generation is not necessary for SAR establishment because bacterial numbers were decreased in Col-0 and *vte2-2* in plants which were first inoculated with *Psm* compared to plants which were first infiltrated with MgCl₂ (Fig. S3). However, bacteria could still proliferate in SAR-induced *vte2-2* plants to the same extent than in un-induced wild-type plants, suggesting that tocopherols contribute to Arabidopsis

basal and acquired resistance. The establishment of SAR is closely connected with defense priming of gene expression and metabolite pathways (Návarová et al., 2012; Bernsdorff et al., 2016). Priming describes a status in which plants are able to mobilize more quickly and vigorously defense responses after pathogen attack and defense priming in Arabidopsis-SAR is controlled by Pip via SA-dependent and SA-independent pathways (Návarová et al., 2012; Bernsdorff et al., 2016). Therefore, for future experiments it would be interesting to clarify the question if protection from non-enzymatic lipid peroxidation via tocopherols is under the control of defense priming, which was not investigated in this study.

To proof the hypothesis, that the increased susceptibility of the *vte2* mutants (Fig. 2.6; Fig. 2.9) is a consequence of the increased non-enzymatic lipid peroxidation after *Psm*-infection (Fig. 2.8; Fig. 2.9), we included the quadruple mutant *fad3-2 fad7-2 fad8 vte2-1* in our experiments. The quadruple mutant *fad3-2 fad7-2 fad8 vte2-1* lacks both, tri-unsaturated fatty acids, which are the most susceptible fatty acids for non-enzymatic lipid peroxidation and the major source for MDA generation in Arabidopsis (Weber et al., 2004), and tocopherols. The inability of the quadruple mutant to produce tri-unsaturated fatty acids in the *vte2* background abolishes several observed *vte2* phenotypes, such as impaired seed germination and increased non-enzymatic lipid peroxidation during germination (Mène-Saffrané et al., 2007). Our findings indicate that pathogen-triggered non-enzymatic lipid peroxidation is decreased in the quadruple mutants compared to the *vte2-1* single mutants and reduces MDA generation to wild-type-levels (Fig. 2.9A). Moreover, the increased susceptibility phenotype of *vte2* mutants was lost in the *fad3-2 fad7-2 fad8 vte2-1* quadruple mutant lines. Bacterial numbers in the quadruple mutants were significantly decreased compared to the *vte2-1* single mutant and were thereby, as well as the MDA levels, wild-type-like (Fig. 2.9B). The fatty acid desaturases FAD3, FAD7, and FAD8 catalyzing the generation of tri-unsaturated fatty acids in Arabidopsis and therefore the quadruple mutants are impaired in generation of α -linolenic acid, the precursor for the biosynthesis of JA in Arabidopsis (Mène-Saffrané et al., 2007; Maeda et al., 2008; Wasternack and Hause, 2013). JA and SA are described to be regulated in an antagonistic way and hence the lack of JA might lead to an increased biosynthesis of the immune regulator SA (Pieterse et al., 2012; Wasternack and Hause, 2013). Because increased endogenous generated and exogenous applied SA contributes to plant resistance against bacterial pathogens (Nawrath and Métraux, 1999; Wildermuth et al., 2001; Vlot et al., 2009; Stahl et al., 2016), we measured endogenous levels of free and glycosidic bound SA in quadruple mutants in untreated, $MgCl_2$ -infiltrated, and *Psm*-inoculated leaves (Fig.

S4E-G). Indeed, endogenous levels of SA were increased in JA-deficient quadruple mutants in untreated and MgCl₂-infiltrated leaves compared to Col-0, whereas total SA levels after *Psm* inoculation were only slightly increased in one of the two used quadruple mutants (Fig. S4G). Compared to untreated, an increased endogenous generation of SA could be observed in MgCl₂-infiltrated leaves, indicating that, as well as the increased MDA generation in *vte2-2* in MgCl₂-infiltrated leaves (Fig. 2.8), the mechanical stimulus exerted by MgCl₂-infiltration might lead to an activation of defense responses to a certain degree.

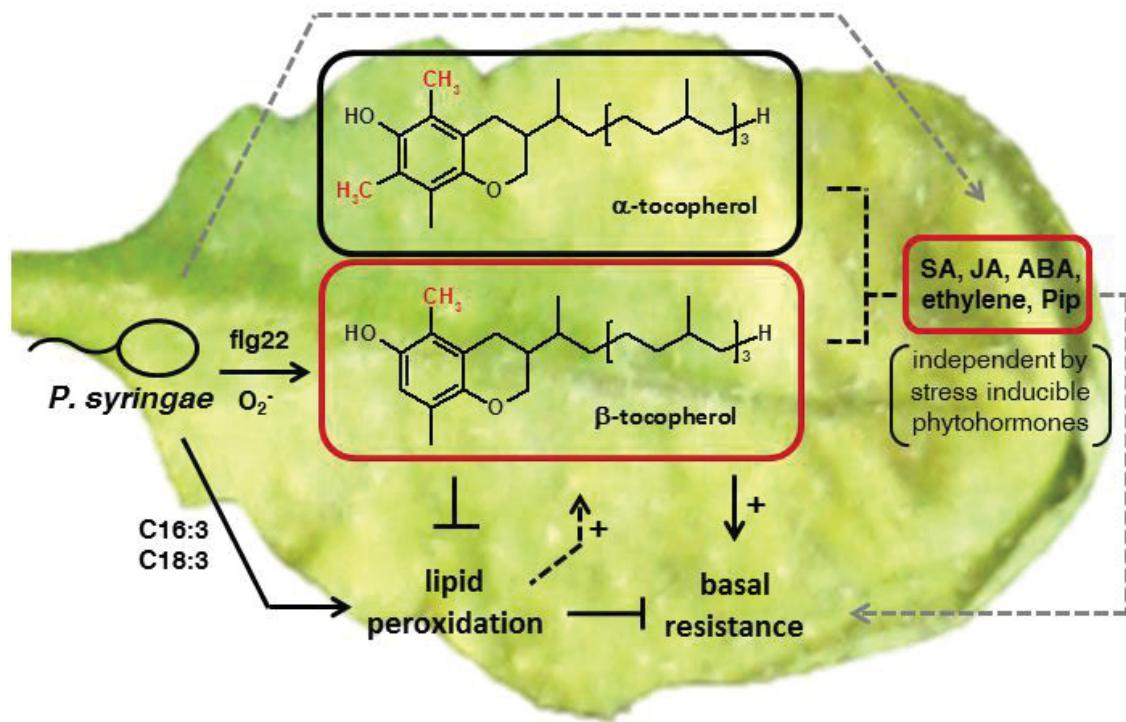


Figure 2.10 **Proposed model for the role of tocopherols in Arabidopsis basal resistance against *Psm*.**

Infection of *P. syringae* triggers strong generation of β -tocopherol, whereas α -tocopherol levels essentially remain constant, which is virtually independent from classical stress inducible phytohormones such as SA, JA, ABA, ethylene, and Pip. *P. syringae*-infection also leads to increased nonenzymatic lipid peroxidation of tri-unsaturated fatty acids, which is decreasing Arabidopsis basal resistance. Constitutive α - and pathogen-triggered β -tocopherol protect tri-unsaturated fatty acids from increased oxidation during pathogen infection and contribute to basal resistance against *Psm*. Furthermore, we cannot exclude that increased lipid peroxidation after *P. syringae*-infection might exhibit an influence on tocopherol biosynthesis.

It was shown previously that the knock-out of *FAD3*, *FAD7*, or *FAD8* results in decreased levels of tri-unsaturated fatty acids and JA but not increases resistance against *P. syringae*. Rather the knock-out of those genes results in an increased susceptibility of mutant plants. Arabidopsis *fad3* and *fad7fad8* mutant plants exhibit

increased susceptibility against avirulent *P. syringae* strains (*Pst* DC3000 *avrRpm1* and *Pst* DC3000 *avrRpt2*) and show a wild-type-like resistance against virulent *P. syringae* (*Pst* DC3000) (Yaeno et al., 2004). Anyway, we cannot exclude that the elevated basal SA levels in *fad3-2 fad7-2 fad8 vte2-1* mutants, compared to *vte2-1*, contribute to the increased resistance in the quadruple mutants. However, the data of this study indicates a role for basal and pathogen-triggered tocopherol generation in Arabidopsis resistance against bacterial pathogens and can deliver a plausible model for this (Fig. 2.10). In this model, effector-triggered and PAMP-triggered immune signaling results in a transcriptional reprogramming of tocopherol biosynthesis leading to an accumulation of especially β -tocopherol at later stages of the infection process, whereas α -tocopherol levels remain constant. This tocopherol accumulation is achieved independently from the SA-, JA-, ABA-, ethylene-, and Pip-signaling pathways. Furthermore, the infection of *P. syringae* leads to increased non-enzymatic lipid peroxidation in Arabidopsis leaves and the constitutively high α - as well as the strongly induced β -tocopherol levels counteract this oxidative lipid damage. Importantly, the high amounts of constitutive and inducible tocopherols after inoculation are associated with increased basal resistance to *P. syringae* infection. Experiments with quadruple mutants unable to produce both tocopherols and trienoic acids indicate that protective function of tocopherols towards lipid peroxidation and their resistance-enhancing function might be casually related, although further experiments have to confirm this hypothesis. Because oxidation products in plants are described to have powerful signaling activities (Farmer and Davoine, 2007), it might be that also increased lipid peroxidation after *P. syringae* infection could exhibit a signaling effect on tocopherol biosynthesis, such as on camalexin biosynthesis during seed germination (Sattler et al., 2006). Also this hypothesis would have to be proven in future studies.

3 Amino acid metabolism in plant defense

3.1 Introduction

Arabidopsis plants respond to an infection by the hemibiotrophic bacterial pathogen *P. syringae* rapidly with changes in primary and secondary metabolism and the produced metabolites have a broad structural diversity (this study; Griebel and Zeier, 2010; Návarová et al., 2012; Chaouch et al., 2012; Stahl et al., 2016). Beside to numerous secondary metabolites, also several free amino acids accumulate in *P. syringae*-infected Arabidopsis leaf tissue, such as the branched-chain amino acids Val, Leu, and Ile or the aromatic amino acids Phe, Tyr, and Trp (Ward et al., 2010; Návarová et al., 2012; Zeier, 2013). These amino acids can either serve as precursors for the immune regulatory metabolite pipecolic acid (Pip) (Návarová et al., 2012), for other secondary metabolites with an antimicrobial activity such as Trp-derived indolics (Stahl et al., 2016; chapter 5), or can have a direct influence on inducible immune responses. For example, the oxidation of the non-polar amino acid Pro contributes to the ROS burst which is triggered by avirulent bacterial pathogens and described as the hypersensitive response (HR). Pro accumulate in Arabidopsis leaves infected with avirulent *P. syringae* strains which trigger the HR but not in leaves which are infected with virulent *P. syringae* strains (Fabro et al., 2004; Návarová et al., 2012). Pro dehydrogenases (ProDH) are reported to be involved in the oxidation of free Pro in Arabidopsis (Deuschle et al., 2004). Transcript levels of several ProDH are increased in Arabidopsis leaves infected with avirulent *P. syringae* and mutant plants with silenced ProDH exhibits attenuated oxidative burst (Cecchini et al., 2011). Consistent with this, exogenous applied Pro triggers in Arabidopsis a generation of ROS, an accumulation of SA, and HR-like controlled cell death (Deuschle et al., 2004; Chen et al., 2011).

Besides amino acids which are used for proteins plants produce numerous of non-protein amino acids and several of them are described for a role in plant immunity against different pathogens (Huang et al., 2011; Zeier, 2013). One of the best studied non-protein amino acids in plant-insect-interactions is L-canavanine which is a major nitrogen storage compound in the seeds of several leguminous plants (Rosenthal, 2001). L-Canavanine has a toxic impact on several different organisms including plant-pathogens such as bacteria, fungi, and insects but also on other organisms like yeast, mammals, algae, and several higher plants (Rosenthal, 2001; Nakajima et al., 2001; Huang et al., 2011). Previous studies have reported that in the interaction of

Arabidopsis and the bacterial pathogen *P. syringae*, several non-protein amino acids are produced, such as Pip, α -aminoadipic acid (Aad), γ -aminobutyric acid GABA, and N^δ-acetyl-ornithine (Návarová et al., 2012; Adio et al., 2011). Thereby N^δ-acetyl-ornithine is not only produced in Arabidopsis upon infection by *P. syringae* but also upon infestation by the larvae of *Plutella xylostella* and *Pieris rapae* or infestation by the aphid *Myzus persicae* (Adio et al., 2011). However, experiments with artificial diets and the use of knock-out mutants which are impaired in the generation of N^δ-acetyl-ornithine suggest that N^δ-acetyl-ornithine accumulation just negatively influence progeny of phloem-sap sucking aphids but not of *P. syringae* or the larvae of *Plutella xylostella* and *Pieris rapae* (Adio et al., 2011). The non-protein amino acid which accumulates to the highest amounts in *P. syringae*-infected Arabidopsis leaves is the Lys catabolite Pip (Návarová et al., 2012). The accumulation of Pip is not only restricted to the site of bacterial infection. Pip also accumulates in leaves distal to the inoculation site and is enriched in petiole exudates collected from from *P. syringae*-infected leaves (Návarová et al., 2012). Pip functions in Arabidopsis as the main regulator of plant systemic acquired resistance (SAR) and orchestrates SAR via SA-dependent and -independent pathways (Návarová et al., 2012; Bernsdorff et al., 2016; a detailed introduction for Pip in SAR can be found in chapter 6). Furthermore, several non-protein amino acids are described for activity role in defense priming. Defense priming is designated as a status in which plants are able to react more quickly and vigorously to a pathogen attack (Conrath et al., 2015; Bernsdorff et al., 2016). Thereby the primed state in plant can be induced by a first infection of a pathogen in distal leaves (SAR-associated priming) or by the exogenous application of priming-active compounds. Pip plays an important regulatory role in defense priming. Exogenous applied Pip via the root systems primes Arabidopsis plants for a quick and vigorous defense response and can partial compensate SAR deficiency of *ald1* mutant plants which are impaired in Pip biosynthesis (Návarová et al., 2012; Bernsdorff et al., 2016). Moreover, Pip-deficient *ald1* and Pip-insensitive *fmo1* fail to induce SAR-associated priming, which indicates that Pip is in addition to its role as the main regulator of SAR also a main regulator of defense priming which is accompanied with SAR (Návarová et al., 2012; Bernsdorff et al., 2016). Besides Pip, several other metabolites with a broad structural diversity are reported in the induction of priming in several plant species against different pathogens, including the amino acids Met, GABA, and BABA (Balmer et al., 2015; Conrath et al., 2015).

3.2 Results

An infection of *Arabidopsis* leaves by the bacterial pathogen *P. syringae* triggers a massive change in the *Arabidopsis* leaf metabolome. Metabolites with a broad structural diversity, small benzoic acids such as SA, phytosterols, tocopherols, Trp-derived indolics, and others accumulate in infected leaves (this study; Vlot et al., 2009; Griebel and Zeier, 2010; Chaouch et al., 2012; Stahl et al., 2016). Furthermore, also a drastic change in the endogenous levels of free amino acids is reported in *Psm*-infected leaves (Návarová et al., 2012). Beside to the amino acids which are used for proteins, several non-protein amino acids are produced in *Arabidopsis* leaves which are infected with *Psm* including Pip, Aad, GABA, and N^δ-acetyl-ornithine (Návarová et al., 2012; Adio et al., 2011). In addition, we show here that several acylated forms of free amino acids accumulate in *Arabidopsis* leaves upon *Psm*-infection.

3.2.1 Accumulation of acetylated and formylated amino acids upon *Psm*-infection

To identify potential novel metabolites which accumulate in *Arabidopsis* upon *Pseudomonas syringae* pv. *maculicola* ES4326 (*Psm*) infection, we conducted comparative metabolite profiling experiments with leaf-extracts from MgCl₂-infiltrated and *Psm*-infiltrated leaves via GC/MS-analysis. By comparative analyses of individual ion chromatograms we observed several substances that accumulated in extracts of *Psm*-inoculated Col-0 leaves compared to MgCl₂-infiltrated leaves. Comparison of the mass spectra with a NIST mass-spectral library (Wiley275) revealed similarities among these substances to N-acetylated and N-formylated amino acids. We compared mass spectra and retention times of those substances with those of commercial available and chemically synthesized authentic standards and could identify nine N-formylated and N-acetylated amino acids (Fig. 3.1). In particular these include N-formyl-Leu, N-acetyl-Leu, N-formyl-Ile, N-acetyl-Ile, N-acetyl-Val, N-acetyl-Pro, N-acetyl-Phe, N-acetyl-Trp, and a formylated version of the non-protein amino acid pipecolic acid (N-formyl-Pip). Detailed information for mass spectra, chemical structure, and retention time of these metabolites are given in Fig. S5 and table S7. All of these metabolites accumulated significantly in extracts of *Psm*-inoculated Col-0 leaves (Fig. 3.1). The pathogen triggered accumulation of these N-acylated amino acids was mostly pronounced 48 hpi and restricted to the inoculation site as depicted in Fig. 1, whereas their levels in distal leaves have not been affected by local *Psm*-inoculation. As an example, the temporal patterns of the *P. syringae*-induced accumulation of N-formyl-Leu are depicted in Fig. 3.2. Temporal accumulation patterns for the other N-acylated

amino acids are depicted in Fig. S6. To investigate if ETI could contribute to the accumulation of those metabolites in early stages after *P. syringae* infection, we determined levels of the detected acylated amino acids also upon inoculation of *Arabidopsis* with the avirulent *Psm avrRpm1* strain which is expressing the *avrRpm1* avirulence gene (Bisgrove et al., 1994). Upon inoculation with *Psm avrRpm1*, only a moderate increase of acylated amino acids could be observed. As for the compatible interaction, the strongest effect could be observed at 48 hpi (Fig. 3.2; Fig. S6).

Metabolite	Col-0_48 hpi_local leaves		ratio <i>P</i> / <i>M</i>	[ng / g FW]
	MgCl ₂ [ng / g FW]	<i>Psm</i>		
N-alpha-acetyl-L-valine ¹	5.3 ± 0.8	28.6 ± 3.4	5.4 ***	0 - 10
N-acetyl-L-leucine ¹	15.4 ± 6.4	60.1 ± 6.7	3.9 **	10 - 50
N-acetyl-L-isoleucine ¹	5.5 ± 0.5	48.7 ± 5.6	8.8 ***	50 - 150
N-formyl-L-leucine ¹	29.4 ± 13.9	370.6 ± 41.8	12.6 ***	150 - 300
N-formyl-isoleucine ²	33.9 ± 5.4	276.3 ± 138.5	8.2 *	300 - 500
N-acetyl-L-proline ¹	95.7 ± 33.3	736.3 ± 60.9	7.7 ***	500 - 1000
N-acetyl-L-phenylalanine ¹	24.9 ± 4.8	233.5 ± 42.5	9.4 **	1000 - 2500
N-formyl-Pip ²	43.2 ± 16.0	544.3 ± 188.7	12.6 *	> 2500
N-acetyl-DL-tryptophane ¹	15.3 ± 7.2	227.1 ± 44.2	14.8 **	

Figure 3.1 **Changes in endogenous levels of identified N-acylated amino acids in *Arabidopsis* (Col-0) after inoculation with *Psm* at the infection-site.**

¹ Identified by commercial available authentic standards (Sigma Aldrich®).

² Identified by chemical synthesized authentic standards (synthesized by Michael Hartmann according to the protocol published previously by West et al. (2011)).

Mean values for the endogenous levels of the identified acylated amino acids are given in [ng / g FW]. Ratio *P* / *M* means the fold-change between the *Psm*-inoculated and the MgCl₂-infiltrated leaves. Leaves for the extraction were harvested 48 h after the inoculation. Asterisks denote statistically differences between *Psm* (*P*) and MgCl₂ (*M*) samples (two tailed *t*-test; ****P* < 0.001, ***P* < 0.01 and **P* < 0.05).

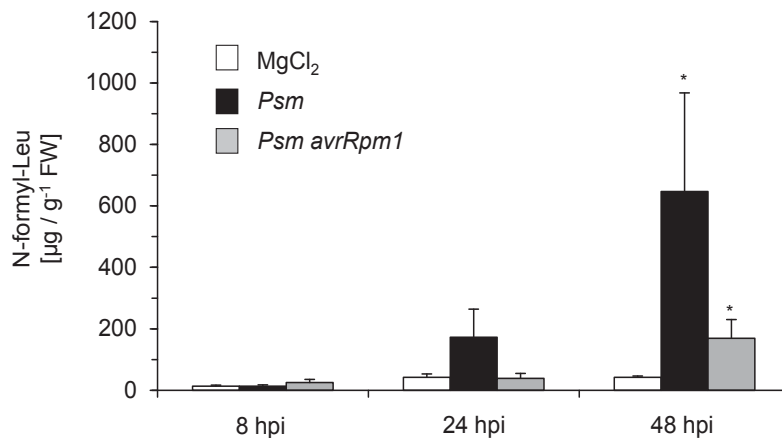


Figure 3.2 Temporal accumulation of N-formyl-Leu upon *Psm*- and *Psm avrRpm1*-inoculation.

Endogenous levels of N-formyl-Leu upon *Psm*- and *Psm avrRpm1*-inoculation at infection-sites 8, 24, and 48 hpi. Mean values for the endogenous levels of N-formyl-Leu are given in [ng / g FW]. Asterisks denote statistically differences between MgCl₂-infiltration and *Psm*- or *Psm avrRpm1*-inoculation. ***P < 0.001, **P < 0.01, and *P < 0.05 (two tailed t test).

3.2.2 The *P. syringae*-induced accumulation of the identified acylated amino acids is influenced by stress-inducible phytohormone pathways and is activated by constitutive defense signaling

To investigate if the pathogen induced generation of the identified acylated amino acids is controlled by classical phytohormone defense signaling pathways, we determined the levels of those in well characterized phytohormone mutants at sites of *Psm*- and *Psm avrRpm1*-inoculation (Fig. 3.3; Fig. 3.4; Fig. S7 – Fig. S9). In the ethylene signaling mutant *etr1* (Bleecker et al., 1988) endogenous levels of all nine acylated amino acids were decreased in *Psm*- and *Psm avrRpm1*-inoculated leaves compared to inoculated Col-0 leaves. Furthermore, the fold-changes of endogenous levels of those metabolites upon *P. syringae* inoculation were significantly lower in *etr1* than in Col-0 (Fig. 3.3; Fig. 3.4A). The accumulation of acylated amino acids was partly but not fully dependent on ethylene signaling because a slight induction could be measured in *etr1* (Fig. 3.3; Fig. 3.4A). In the jasmonate (JA) biosynthesis mutant *dde2* (von Malek et al., 2002) a similar strong tendency could not be observed. However, the *Psm*-triggered accumulation of four specific compounds, N-formyl-Leu, N-formyl-Ile, N-acetyl-Pro, and N-formyl-Pip, was markedly decreased compared to inoculated Col-0 plants. This tendency could not be observed for the other here-described acylated amino acids (Fig. 3.3; Fig. 3.4B). Moreover, pathogen-triggered accumulation of the nine acyl-derivatives was wild-type like in SA biosynthesis mutant *sid2* (Wildermuth et al., 2001) (Fig. 3.3; Fig. S7). The *P.syringae*-inducible accumulation of the identified

acylated amino acids was also independent on Pip-signaling, because Pip-deficient *ald1* and Pip-insensitive *fmo1* mutant plants were not impaired the *Psm*-inducible generation of these acyl-derivatives (Fig. 3.3; Fig. S9). We also measured the *Psm*- and *Psm avrRpm1*-triggered accumulation of the here described metabolites in three mutants impaired in abscisic acid (ABA) biosynthesis and signaling (Fig. 3.3; Fig. S8). The generation of the nine acylated amino acids was wild-type-like in *aba2-1*, which is fully impaired in ABA biosynthesis (Léon-Kloosterziel et al., 1996), and in the ABA signaling mutant *abi1* (Arend et al., 2009) (Fig. S8A; Fig. S8C). This result suggests that accumulation is independent of ABA-signaling. However, the Arabidopsis mutant *nced3*, which is impaired in 9-cis-epoxycarotenoid dioxygenase activity and contains decreased ABA levels (Iuchi et al., 2001), exhibited increased levels of the nine acylated amino acids in MgCl₂-infiltrated leaves compared to Col-0 (Fig. S8B). Interestingly, in the *cpr5-2* mutant, in which defense signaling is constitutively activated (Bowling et al., 1997; Maeto et al., 2006), endogenous levels of all here described metabolites were significantly increased in MgCl₂-infiltrated leaves compared to Col-0 (Fig. 3.3; Fig. 3.4C).

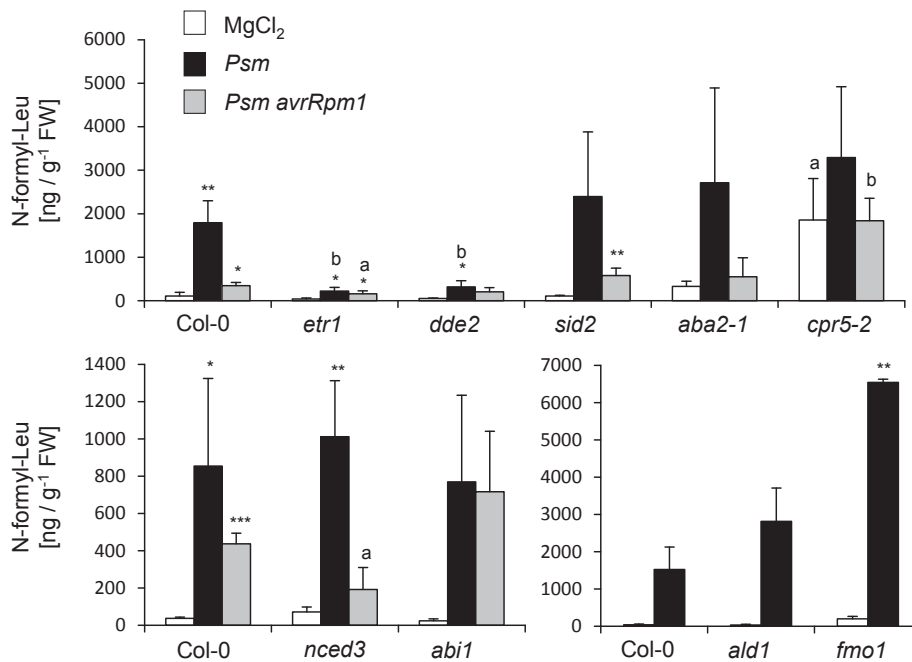


Figure 3.3 Pathogen-triggered generation of N-formyl-Leu in different phytohormone-biosynthesis and –signaling mutants.

Exemplary for the *P. syringae* triggered accumulation of acylated amino acids the endogenous levels N-formyl-Leu in several Arabidopsis mutants impaired in different defense signaling pathways at 48 hpi upon *Psm*- and *Psm avrRpm1*-inoculation are depicted. Asterisks denote statistically differences between MgCl₂-infiltration and *Psm*- or *Psm avrRpm1*-inoculation. ***P < 0.001, **P < 0.01, and *P < 0.05. Letters denote statistically differences between the same treatment of Col-0 and the respective mutant. ^cP < 0.001, ^bP < 0.01, and ^aP < 0.05 (two tailed *t* test).

Amino acid metabolism in plant defense

Metabolite	Col-0_48 hpi local leaves					etr1_48 hpi_ local leaves				
	MgCl ₂ [ng / g FW]	<i>Psm</i> [ng / g FW]	ratio P / M	<i>Psm avrRpm1</i> [ng / g FW]	ratio Avr / M	MgCl ₂ [ng / g FW]	<i>Psm</i> [ng / g FW]	ratio P / M	<i>Psm avrRpm1</i> [ng / g FW]	ratio Avr / M
N-acetyl-Val	37.6 ± 16.1	119.0 ± 34.7	3.2 *	90.8 ± 19.6	2.4 *	27.3 ± 5.7	36.9 ± 7.1 a	1,4	33.6 ± 7.5 b	1,2
N-acetyl-Leu	46.8 ± 17.2	88.6 ± 16.2	1.9 *	28.8 ± 3.4	0,6	21.1 ± 10.7	39.2 ± 8.5 b	1,9	40.1 ± 20.4	1,9
N-acetyl-Ile	46.5 ± 28.8	101.8 ± 28.9	2,2	64.0 ± 16.1	1,4	22.2 ± 7.9	45.8 ± 6.7 a	2.1 *	46.2 ± 12.4	2,1
N-formyl-Leu	106.8 ± 88.1	1793.9 ± 506.1	16.8 **	348.3 ± 74.1	3.3 *	43.0 ± 19.7	223.9 ± 82.0 b	5.2 *	162.2 ± 66.2 a	3.8 *
N-formyl-Ile	133.5 ± 108.7	1469.6 ± 357.2	11.0 **	270.2 ± 40.1	2	54.7 ± 17.1	176.5 ± 58.0 b	3.2 *	110.6 ± 28.5 b	2
N-acetyl-Pro	659.2 ± 203.7	5215.8 ± 214.8	7.9 ***	2548.1 ± 848.1	3.9 *	562.2 ± 96.9	3204.8 ± 59.1 c	5.6 ***	1886.3 ± 774.5	3.4 *
N-acetyl-Phe	10.7 ± 3.9	50.9 ± 11.4	4.8 **	18.8 ± 9.6	1,8	6.1 ± 4.4	16.0 ± 2.9 b	2.6 *	10.7 ± 5.7	1,8
N-formyl-Pip	117.5 ± 72.6	1051.5 ± 273.6	8.9 **	208.0 ± 49.7	1,8	41.8 ± 6.0	133.4 ± 54.2 b	3.2 *	91.2 ± 27.8	2.2 *
N-acetyl-Trp	32.6 ± 13.9	291.8 ± 148.9	8.9 *	115.5 ± 71.0	3,5	44.5 ± 25.1	75.5 ± 25.1	1,7	78.1 ± 16.2	1,7
scopoletine	5.5 ± 4.0	39.2 ± 14.7	7.1 *	31.7 ± 7.3	5.8 **	7.2 ± 6.4	43.0 ± 10.0	6.0 **	30.8 ± 7.0	4.3 *

Metabolite	Col-0_48 hpi local leaves					dde2_48 hpi_ local leaves				
	MgCl ₂ [ng / g FW]	<i>Psm</i> [ng / g FW]	ratio P / M	<i>Psm avrRpm1</i> [ng / g FW]	ratio Avr / M	MgCl ₂ [ng / g FW]	<i>Psm</i> [ng / g FW]	ratio P / M	<i>Psm avrRpm1</i> [ng / g FW]	ratio Avr / M
N-acetyl-Val	37.6 ± 16.1	119.0 ± 34.7	3.2 *	90.8 ± 19.6	2.4 *	46.3 ± 40.5	161.2 ± 77.9	3,5	117.5 ± 119.7	2,5
N-acetyl-Leu	46.8 ± 17.2	88.6 ± 16.2	1.9 *	28.8 ± 3.4	0,6	33.2 ± 18.6	60.0 ± 10.5	1,8	43.5 ± 12.6	1,3
N-acetyl-Ile	46.5 ± 28.8	101.8 ± 28.9	2,2	64.0 ± 16.1	1,4	28.1 ± 10.8	69.5 ± 24.6	2,5	44.3 ± 15.0	1,6
N-formyl-Leu	106.8 ± 88.1	1793.9 ± 506.1	16.8 **	348.3 ± 74.1	3.3 *	53.3 ± 9.3	317.4 ± 143.4 b	6.0 *	203.9 ± 99.8	4,5
N-formyl-Ile	133.5 ± 108.7	1469.6 ± 357.2	11.0 **	270.2 ± 40.1	2	44.9 ± 7.4	341.3 ± 141.1 b	7.6 *	188.8 ± 78.0	4.2 *
N-acetyl-Pro	659.2 ± 203.7	5215.8 ± 214.8	7.9 ***	2548.1 ± 848.1	3.9 *	662.4 ± 194.7	3393.4 ± 311.8 b	5.1 ***	1663.9 ± 288.1	2.5 **
N-acetyl-Phe	10.7 ± 3.9	50.9 ± 11.4	4.8 **	18.8 ± 9.6	1,8	6.5 ± 2.7	64.1 ± 33.7	9.9 *	56.2 ± 69.7	8,6
N-formyl-Pip	117.5 ± 72.6	1051.5 ± 273.6	8.9 **	208.0 ± 49.7	1,8	47.5 ± 5.0	291.7 ± 64.5 b	6.1 **	158.0 ± 57.3	3.3 *
N-acetyl-Trp	32.6 ± 13.9	291.8 ± 148.9	8.9 *	115.5 ± 71.0	3,5	81.4 ± 28.1	357.5 ± 139.6	4.4 *	471.4 ± 603.2	5,8
scopoletine	5.5 ± 4.0	39.2 ± 14.7	7.1 *	31.7 ± 7.3	5.8 **	8.7 ± 1.4	539.4 ± 326.6	62.0	186.4 ± 202.0	21,4

Metabolite	Col-0_48 hpi local leaves					cpr5-2_48 hpi_ local leaves					ratio cpr5-2 / Col-0
	MgCl ₂ [ng / g FW]	<i>Psm</i> [ng / g FW]	ratio P / M	<i>Psm avrRpm1</i> [ng / g FW]	ratio Avr / M	MgCl ₂ [ng / g FW]	<i>Psm</i> [ng / g FW]	ratio P / M	<i>Psm avrRpm1</i> [ng / g FW]	ratio Avr / M	
N-acetyl-Val	37.6 ± 16.1	119.0 ± 34.7	3.2 *	90.8 ± 19.6	2.4 *	106.5 ± 13.5 b	85.9 ± 27.5	0,8	98.4 ± 24.4	0,9	2.8 **
N-acetyl-Leu	46.8 ± 17.2	88.6 ± 16.2	1.9 *	28.8 ± 3.4	0,6	112.2 ± 22.1 a	104.6 ± 32.7	0,9	95.8 ± 40.6 a	0,9	2.4 *
N-acetyl-Ile	46.5 ± 28.8	101.8 ± 28.9	2,2	64.0 ± 16.1	1,4	182.5 ± 14.6 b	153.0 ± 50.3	0,8	150.6 ± 97.0	0,8	3.9 **
N-formyl-Leu	106.8 ± 88.1	1793.9 ± 506.1	16.8 **	348.3 ± 74.1	3.3 *	1858.9 ± 952.9 a	3292.6 ± 1626.0	1,6	1840.1 ± 513.0 b	1	17.4 *
N-formyl-Ile	133.5 ± 108.7	1469.6 ± 357.2	11.0 **	270.2 ± 40.1	2	1671.8 ± 694.1 a	2656.4 ± 1268.5	1,6	1504.9 ± 408.6 b	0,9	12.5 *
N-acetyl-Pro	659.2 ± 203.7	5215.8 ± 214.8	7.9 ***	2548.1 ± 848.1	3.9 *	3349.8 ± 691.2 b	3491.5 ± 1570.0	1	3214.5 ± 1136.7	1	5.1 **
N-acetyl-Phe	10.7 ± 3.9	50.9 ± 11.4	4.8 **	18.8 ± 9.6	1,8	26.4 ± 5.7 a	48.9 ± 14.0	1,9	30.2 ± 6.6	1,1	2.5 *
N-formyl-Pip	117.5 ± 72.6	1051.5 ± 273.6	8.9 **	208.0 ± 49.7	1,8	760.2 ± 108.1 b	1652.8 ± 276.1	2.2 **	881.6 ± 81.3 c	1,2	6.5 **
N-acetyl-Trp	32.6 ± 13.9	291.8 ± 148.9	8.9 *	115.5 ± 71.0	3,5	374.9 ± 118.7 b	759.5 ± 35.6 b	2.0 **	507.5 ± 76.9 b	1,4	11.5 **
scopoletine	5.5 ± 4.0	39.2 ± 14.7	7.1 *	31.7 ± 7.3	5.8 **	111.1 ± 9.1 c	94.5 ± 24.8 a	0,9	103.7 ± 47.0	0,9	20.2 ***

[ng / g FW]							
0 - 10	10 - 50	50 - 150	150 - 300	300 - 500	500 - 1000	1000 - 2500	> 2500

Figure 3.4 Accumulation of the identified acylated amino acids in *etr1*, *dde2*, and *cpr5-2* after inoculation with *Psm* and *Psm avrRpm1*.

Accumulation of the identified acylated amino acids in the ethylene-signaling mutant *etr1* (A), the JA-biosynthesis mutant *dde2* (B), and in *cpr5-2* (C) after inoculation with *Psm* and *Psm avrRpm1*. Mean Values for the endogenous levels of the identified metabolites are given in [ng / g FW]. Leaves for the extraction were harvested 48 h after the inoculation. Ratio P / M means the fold-change between *Psm*-inoculated and MgCl₂-infiltrated leaves. Ratio Avr / M means the fold-change between *Psm avrRpm1*-inoculated and MgCl₂-infiltrated leaves. Ratio M *cpr5-2* / Col-0 means the fold-change between MgCl₂-infiltrated leaves of *cpr5-2* and Col-0. Asterisks denote statistically differences between *Psm* (P), *Psm avrRpm1* (Avr) and MgCl₂ (M) samples (two tailed *t*-test; ***P < 0.001, **P < 0.01 and *P < 0.05). Letters denote statistically differences between the same treatment of Col-0 and the respective mutant (^c P < 0.001, ^b P < 0.01, and ^a P < 0.05; two tailed *t* test).

3.2.3 Investigating the role of amino acid acylation in inducible plant immunity

Next we were interested in the question if the identified nine N-acetylated and N-formylated amino acids have an influence on *Arabidopsis* basal resistance. Therefore we functionally characterized different candidate genes that were up-regulated in *Arabidopsis* leaves following *P. syringae* inoculation according to microarray data (Table S2). The chosen candidate genes all encode for enzymes and proteins with reported or putative functions in amino acid metabolism.

The *Arabidopsis* N-acetyltransferase 1 (ATF1) is described as an acyl-CoA N-acyltransferases (NAT) superfamily protein which is involved in acetylation reactions of α -amino groups from amino acids (Hwang et al., 2009). Furthermore, it was shown that *ATF1* transcript levels are increased in *Arabidopsis* upon cabbage leaf curl virus infection (Ascencio-Ibáñez et al., 2008). The *Arabidopsis* gene *DARK INDUCIBLE 4 (DIN4)* encodes for a branched chain amino acid α -keto acid dehydrogenase which is involved in the degradation of branched chain amino acids (Binder, 2010). The *Arabidopsis* ISOVALERYL-COA-DEHYDROGENASE 1 (IVD1) is reported to function in branched chain amino acid catabolism (Binder, 2010; Peng et al., 2015). *UGT79B5* encodes for a UDP-glucosyl transferases superfamily protein with a hitherto unknown function. This gene is downregulated in response to auxin overproduction in *Arabidopsis* (Morant et al., 2014). The *Arabidopsis* protein N-ACETYLTRANSFERASE ACTIVITY 1 (NATA1) was described to function in the biosynthesis in N^δ-acetyl-ornithine. Moreover, endogenous levels of N^δ-acetyl-ornithine are increased in leaves which are infected with *Psm* (Adio et al., 2011).

To test if those enzymes are involved in the generation of the nine identified acylated amino acids, we measured pathogen-triggered accumulation of those in knock-out mutants for the above described genes in *Psm*-infected leaves at 48 hpi (Fig. S10; Fig. S11). Information for the investigated knock-out lines and for the identification of homozygous T-DNA insertion lines is given under 7.1, in Table S4, and Fig. S19. However, the accumulation of the here-described metabolites was not impaired in *atf1*, *ugt79b5*, *nata1-1*, *din4-a*, *din4-c*, *ivd1-a*, and *ivd1-b* mutant plants. Moreover, in some of the investigated mutants some of the nine amino acid derivatives accumulate to higher amounts compared to Col-0. For example, endogenous levels of N-formly-Pip in MgCl₂- and *Psm*-treated leaves of *ivd-b* mutant plants were 3 to 4 times higher than in Col-0 wild-type plants (Fig. S11B). We therefore compared the accumulation of the

nine non-protein amino acids with the pathogen induced accumulation of SA. Notably, in cases where basal and *Psm*-triggered endogenous levels of the non-protein amino acids were increased in mutant plants compared to Col-0, SA levels were also increased (Fig. S10; Fig. S11). This indicates that the increased accumulation of several of the acylated amino acids is due to a stronger activation of defense-signaling in some of the mutants and weakens a putative regulatory role of the chosen candidate genes in the *Psm*-triggered generation of the here described N-acetylated and N-formylated amino acids.

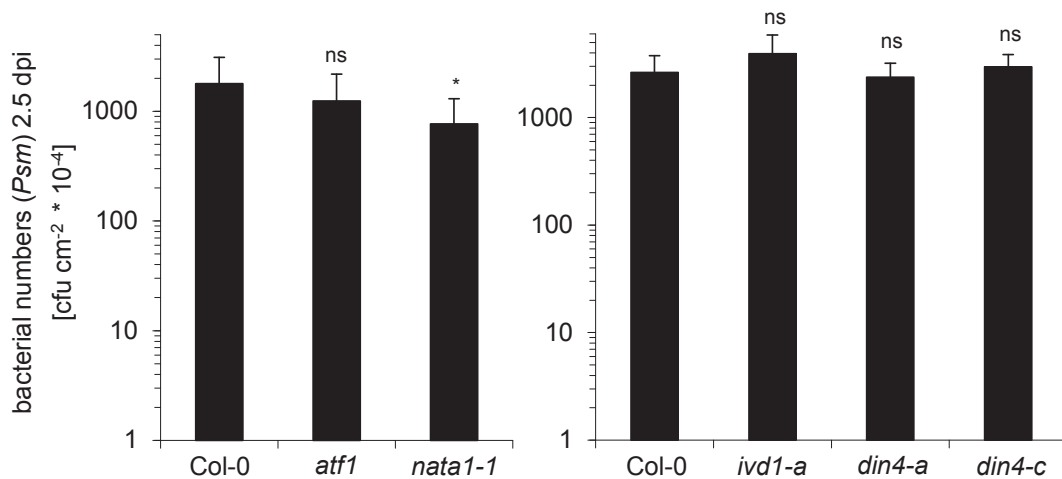


Figure 3.5 **Basal resistance of *atf1*, *nata1*, *ivd1-a*, *din4-a*, and *din4-c* mutant plants against *Psm*.**

Bacterial numbers of compatible *Psm* (applied in titers of OD600 0.001) in *atf1*, *nata1*, *ivd1-a*, *din4-a*, and *din4-c* mutants plants. Bacterial numbers were determined 2.5 d after the inoculation. Bacterial numbers are means from 12 parallel samples, each consisting of three leaf disks. Asterisks denote statistically differences between Col-0 and the respective mutant. ***P < 0.001, **P < 0.01, and *P < 0.05 (two tailed t test); ns = not significant.

Although the investigated mutants did not fail to accumulate the nine identified non-protein amino acids, increased transcript levels of the corresponding genes upon *Psm*-inoculation (Table S2) suggested that those could play a role in Arabidopsis immunity against bacterial pathogens. We therefore determined the multiplication of *Psm* 2.5 days post inoculation in leaves of *atf1*, *nata1-1*, *ivd1-a*, *din4-a*, and *din4-c* mutant plants and compared them to those in Col-0. None of the investigated mutants showed significant differences in basal resistance to the wild-type except *nata1* (Fig. 3.5). The *nata1-1* mutant exhibited decreased susceptibility to *Psm* infection, consistent with previously described increased basal resistance of *nata1-1* mutant plants against *P. syringae* DC3000 (Adio et al., 2011). We also measured the ability to establish systemic acquired resistance (SAR) in *atf1*, *ugt79b5*, *nata1*, *ivd1-a*, *din4-a*, and *din4-c*

mutant plants. To induce SAR in the whole plant foliage three local leaves were infiltrated with *Psm* and as a control, the same amount of plants was infiltrated with 10 mM MgCl₂. 48 h later all plants were infiltrated with *Psm* in leaves distal to the site of first infiltration and 2.5 days later bacterial numbers were determined in those leaves (Fig. S12). In all investigated mutants, the bacterial numbers were decreased after a first inoculation with *Psm* compared to control-infiltrated plants in the same way like in Col-0 wild-type plants, indicating that those genes have no functional role in SAR-establishment.

3.3 Discussion

3.3.1 Identification of nine N-acetylated and N-formylated amino acids which accumulate in Arabidopsis leaves in response to a *Psm*-infection

Arabidopsis plants produce upon *Psm*-infection metabolites with a broad structural diversity. Here we could demonstrate that beside to previously described *Psm*-induced changes of free proteinogenic and non-protein amino acids, also several acylated amino acids are produced in Arabidopsis. It was previously reported that the non-protein amino acids Pip, Aad, GABA, and N^δ-acetyl-ornithine accumulate in *Psm*-infected Arabidopsis plants (Návarová et al., 2012; Adio et al., 2011). We could show that N-terminal-formylated and N-terminal-acetylated forms of the branched-chain amino acid Leu (N-formyl-Leu, N-acetyl-Leu) and Ile (N-formyl-Ile, N-acetyl-Ile), an N-acetylated form of the aliphatic branched-chain amino acid Val (N-acetyl-Val), a N-formylated form of the Lys catabolite Pip, and N-acetylated forms of the aromatic amino acids Phe (N-acetyl-Phe) and Trp (N-acetyl-Trp) accumulate in Arabidopsis leaves which are inoculated with *Psm* at 48 hpi (Fig. 3.1). Interestingly, the non-acetylated and non-formylated forms of Leu, Ile, Val, Pip, Phe, and Trp also accumulate in Arabidopsis leaves upon *Psm*-infection (Návarová et al., 2012). Therefore, it is possible that the biosynthesis of the here described acetylated and formylated amino acids upon *Psm*-infection are favored by the increased levels of precursor-forms of those amino-acids. In contrast to that, N-acetyl-Pro accumulated to the highest amounts out of the nine identified non-protein amino-acids (Fig. 3.1; Fig. 3.4 Fig. S6 – Fig. S11), albeit endogenous levels of Pro do not change in Arabidopsis upon *Psm*-infection (Návarová et al., 2012). This could indicate that acetylation and formylation of free amino acids in Arabidopsis are activated upon *Psm*-infection and are not just a passive consequence to the higher levels of free amino acids in *Psm*-infected leaves. Accordingly, increased

levels of exogenous fed heavy isotopic labeled Pip (D_9 -Pip) are transformed to N-formyl-Pip in leaves which are inoculated with D_9 -Pip and *Psm* compared to leaves which were just fed with D_9 -Pip (the role of Pip as a precursor for N-formyl-Pip is discussed in detail in chapter 6).

3.3.2 Regulation of *Psm*-inducible accumulation of the nine identified acylated amino acids

The regulatory processes for metabolism of N-acetylated and N-formylated amino acids under different environmental conditions are rarely elucidated until now (Binder, 2010). Several genes which are involved in the degradation of the branched chain amino-acids Val, Leu, and Ile show increased transcript levels in darkness and under carbohydrate starvation (Schuster and Binder, 2005; Binder, 2010). Moreover, *Arabidopsis* mutants impaired in IVD1-activity exhibit accelerated senescence under cultivation conditions with extended darkness (Araujo et al., 2010). It was also reported that in addition to *Psm*-infection, infestation by *Plutella xylostella*, *Pieris rapae*, or aphids, a strong accumulation of N^{δ} -acetyl-ornithine in *Arabidopsis* can be triggered by exogenous treatment with MeJA. Moreover, the coronatine insensitive JA signaling mutant *coi1* fails to accumulate N^{δ} -acetyl-ornithine upon MeJA-treatment. A moderate accumulation of N^{δ} -acetyl-ornithine could also be observed upon exogenous treatment with ABA, whereupon exogenous applied SA had no effect on N^{δ} -acetyl-ornithine generation (Adio et al., 2011). To investigate if the accumulation of the here described nine N-acetylated and N-formylated amino acids is influenced by classical stress-inducible phytohormones, we determined *Psm*-induced levels of those metabolites in *Arabidopsis* mutants which are impaired in ethylene-, JA-, SA-, Pip-, and ABA-signaling (Fig. 3.3; Fig. 3.4; Fig. S7 - Fig. S9).

Interestingly, in the ethylene-signaling and JA- biosynthesis mutants *etr1* and *dde2* (Bleecker et al., 1988; von Malek et al., 2002) the accumulation of several of the here described acetylated and formylated amino acids was decreased compared to Col-0 (Fig. 3.3; Fig. 3.4A-B). The accumulation of all nine acylated amino acids was significantly decreased in *etr1* (Fig. 3.3; 3.4A). The *Psm*-triggered accumulation of four specific acyl-derivatives, N-formyl-Leu, N-formyl-Ile, N-acetyl-Pro, and N-formyl-Pip, was markedly decreased in *dde2* compared to *Psm*-inoculated Col-0 plants (Fig. 3.3; Fig. 3.4B). That indicates that ethylene- and JA-signaling could positively influence *Psm*-triggered generation of those acylated amino acids. To test this hypothesis it would be interesting for future studies to investigate if the accumulation of those nine

acylated amino acids is inducible by exogenous treatment with ethylene and JA. SA-, Pip-, and ABA-signaling seem not to influence *Psm*-inducible accumulation of the here described acetylated and formylated amino acids because the *Psm*-triggered accumulation of those was wild-type-like in *sid2*, *ald1*, *fmo1*, *aba2-1*, and *abi1* mutant plants (Fig. 3.3; Fig. S7 - Fig. S9). Furthermore, we determined the endogenous levels of the nine identified acylated amino acids in the *cpr5-2* mutant which is described for constitutive activated defense signaling and ROS overproduction (Bowling et al., 1997; Maeto et al., 2006). Thereby we could measure that all nine formylated and acetylated amino acids accumulate without pathogen contact in *cpr5-2* mutant plants (Fig. 3.4C), which suggests that pathogen inducible defense-signaling contributes to the generation of those metabolites and that the acetylation and formylation of those amino acids could not just be a passive process due to the higher endogenous levels of those amino acids upon *Psm*-inoculation. Interestingly, in *cpr5* also the expression of JA- and ethylene-responsive genes, such as *PDF1.2*, is constitutively increased, indicating that in addition to SA-pathway also JA- and ethylene-pathways are activated in this mutant (Clarke et al., 2001). That underlines a putative role of ethylene- and JA-signaling in the acylation of free amino acids in plant immunity. The increased levels of the nine acylated amino acids in *cpr5-2* could furthermore indicate that also ROS signaling contributes to the generation of N-acetylated and N-formylated amino acids.

3.3.3 Investigations for a putative role of N-acetylated and N-formylated amino acids in Arabidopsis inducible immunity against *Psm*

A general approach in Arabidopsis to test whether the pathogen-triggered activation of a metabolite-pathway contributes to plant resistance against the pathogen is the use of mutant plants with a specific knock-out in a gene involved in this metabolic-pathway. We searched for genes with reported functions in amino acid metabolism and which vary in transcript levels upon *Psm*-infection (Table S2). We determined endogenous levels of the identified N-acetylated and N-formylated amino acids upon *Psm*-infection in knock-out mutants for *ATF1*, *UGT97B5*, *NATA1-1*, *DIN4*, and *IVD1* (Fig. S10; Fig. S11). None of the investigated mutants was impaired in the *Psm*-induced accumulation of the nine identified acylated amino acids suggesting that *ATF1*, *UGT97B5*, *NATA1-1*, *DIN4*, and *IVD1* are not involved in the generation of the here described N-acetylated and N-formylated amino acids. Unfortunately, therefore we could not test if the generation of those metabolites contributes to Arabidopsis basal resistance. However, because transcript levels of these genes are enriched in *Psm*-infected leaf tissue, we tested if the knock-out of those genes affects Arabidopsis

resistance against *Psm*. Out of *atf1*, *nata1-1*, *ivd1-a*, *din4-a*, and, *din4-c* mutant plants only *nata1-1* exhibited a significant difference in basal resistance against *Psm* (Fig. 3.5). Thereby basal resistance of *nata1-1* mutant plants was significantly increased compared to Col-0 as described previously by Adio et al. (2011). This is probably caused by that plant susceptibility to bacterial pathogens, induced by coronatine, needs functional NATA1, which is indispensable for N^δ-acetyl-ornithine biosynthesis (Adio et al. 2011; Geng et al. 2012, Zeier, 2013). The tendency for increased basal resistance of *nata1-1* against *Psm* could also be observed in plants used for a SAR-assay which were first infiltrated with MgCl₂, but the difference here was not significant (Fig. S12).

Here we could not clarify the question if the identified N-acetylated and N-formylated amino acids N-acetyl-Val, N-acetyl-Leu, N-acetyl-Ile, N-formyl-Leu, N-formyl-Ile, N-acetyl-Pro, N-acetyl-Phe, N-formyl-Pip, and N-acetyl-Trp which accumulate in *Psm*-infected leaves contribute to Arabidopsis resistance against bacterial pathogens. It is reported that N^δ-acetyl-ornithine in Arabidopsis is produced upon *Psm*-infection, *Plutella xylostella*-attack, *Pieris rapae*-attack, aphid-infestation (*Myzus persicae*) (Adio et al., 2011). However, N^δ-acetyl-ornithine accumulation in Arabidopsis just negatively influences the growth of *Myzus persicae* but not the performance of *Psm*, *Plutella xylostella*, and *Pieris rapae* on the plants. Accordingly, an artificial diet containing N^δ-acetyl-ornithine reduces progeny production of *Myzus persicae* but the growth of *Psm* in a medium containing N^δ-acetyl-ornithine is not negatively affected (Adio et al., 2011). Amino acids can also be conjugated to other metabolites such as indole-3-acetic acid (IAA), JA, or SA and those conjugates can be relevant for plant immunity (Zeier, 2013). A recently described amino acid conjugate is N-acyl-homoserine lactone which exogenously applied primes Arabidopsis plants for cell wall reinforcement and induces resistance against bacterial pathogens in a SA-dependent manner (Schenk et al., 2014). For future studies it would be interesting to investigate if the here described nine acylated amino acids have an antimicrobial activity, can exogenously applied influence Arabidopsis basal resistance against plant-pathogens, are compounds which can activate defense priming in Arabidopsis, and if those can be conjugated to other metabolites to form conjugates with a functional relevance for plant immunity.

However, to fully elucidate the role of the here described N-acetylated and N-formylated amino acids in plant immunity, the biosynthetic pathways of those need to be clarified to generate knock-out mutants which are impaired in the accumulation specific N-acetylated and N-formylated amino acids. Interesting candidates for this

would be members of the Gcn5-related N-acetyltransferase (GNAT) gene family. In plants several GNATs, such as NATA1, are known and each exhibits remarkable specificity for acetyl donors and acceptors (Dyda et al., 2000). In Plants the biosynthesis of arginine from glutamate involves the acetylation of glutamate, catalyzed by N-acetylglutamate synthase (NAGS) (Kalamaki et al., 2009). In Arabidopsis two proteins (NAGS1 and NAGS2) are known that catalyze this reaction and it would be interesting to investigate if similar proteins are also involved in the *P. syringae*-inducible generation of the here described acylated amino acids. Another group of acyltransferases in plants is the BAHD acyltransferases family. The BAHD acyltransferases constitute a large family of acyl CoA-utilizing enzymes which are found in several plant species and are involved in the generation of epicuticular waxes, small volatile esters, modified anthocyanins, phytoanticipins, and phytoalexins (D'Auria, 2006). The products formed by members of the BAHD acyltransferases family are structural divers, which makes them promising candidates that could also be involved in the generation of the here described acylated amino acids. Here we just identified N-acyl-derivatives. For future studies it would be interesting to investigate if also S- or O-acylation reactions are involved in the de novo production of metabolites upon *P. syringae*-infection.

4 Scopoletin in Arabidopsis initiate immunity

4.1 Introduction

Scopoletin is a methyl-coumarin derived from the aromatic amino acid Phe, which is found frequently in the plant kingdom and which was first described for an effect on root growth via indole-3-acetic acid (IAA; auxin) (Andreae, 1952) (for chemical structure of scopoletin see Fig. 4.1). In several different plant species, different possible pathways for the biosynthesis of scopoletin have been reported (Gnonlonfin et al., 2012). In Arabidopsis scopoletin is synthesized via *ortho*-hydroxylation of feruloyl-CoA, which is catalyzed by the 2-oxoglutarate-dependent dioxygenase FERULOYL COA ORTHO-HYDROXYLASE 1 (F6'H1) (Kai et al., 2008). Scopoletin and other coumarins are described as phytoalexins with antimicrobial properties in several plant species (Tal and Robeson, 1986, Lay and Anderson, 2005; Kai et al., 2006; Sun et al., 2014). For example, scopoletin is produced by the rubber tree *Hevea brasiliensis* upon infection with the pathogenic fungi *Microcyclus ulei* (P. Henn.) and inhibits conidium germination and germ tube elongation of this fungus (Garcia et al., 1995). Scopoletin accumulates in the *B. cinerea*-resistant tobacco cultivar *N. tabacum* cv. Petit Havana, but not in the *B. cinerea*-susceptible cultivar *N. tabacum* cv. Xanthi. This suggests that scopoletin accumulation contributes to the resistance of *N. tabacum* cv. Petit Havana against *B. cinerea*. Consistent with that, scopoletin inhibits the germination of *B. cinerea*-spores, whereupon the mycelium growth of *B. cinerea* is just slightly inhibited by scopoletin (El Oirdi et al., 2010). Moreover, it could be shown that scopoletin and its glycosidic bound form scopolin accumulate in tobacco cultivars *N. tabacum* cv. Samsun and *N. sylvestris* upon treatment with a purified glycoprotein from the plant pathogenic oomycete *Phytophthora megasperma* (Costet et al., 2002). It was also shown that scopoletin accumulate in *Nicotiana tabacum* L. *Samsun NN* upon tobacco mosaic virus (TMV) infection. Scopoletin accumulates in this case at the TMV inoculation areas and is responsible for the fluorescence emission of HR-spots (Chaerle et al., 2007). Furthermore, it was shown that scopoletin and the glycosidic bound form scopolin are produced in Arabidopsis leaves upon infection with virulent and avirulent *Pseudomonas syringae* pv. *tomato* (*Pst*). The *Pst*-induced generation of scopoletin is thereby regulated by *RESPIRATORY BURST OXIDASE HOMOLOGUE* (RBOH) *D* and *F*, indicating that *P. syringae* induced scopoletin accumulation is regulated by reactive oxygen species (ROS) (Chaouch et al., 2012).

Beside to biological stressors such as fungi, bacteria, viruses, or microbial derived elicitors also abiotic stressors such as wounding or exogenous chemical

treatment with SA, methyl jasmonate (MeJA), kinetin, or IAA can induce the formation of scopoletin in various plant species (Gnonlonfin et al., 2012). In addition to that, coumarins and especially scopoletin are reported for an important role in iron (Fe) uptake from alkaline substrates in Arabidopsis (Schmid et al., 2014). Iron is highly abundant in most substrates, but its low solubility in soils restricts Fe uptake by plants. Under low iron availability plants acidify their rhizosphere and, by reducing ferric to ferrous, iron can be acquired. Under iron-deficiency stress scopoletin is the most prominent coumarin in root exudates, but failed to reduce ferric to ferrous. However, an Arabidopsis mutant which is impaired in the biosynthesis of scopoletin and other coumarins via F6'H1 (*fb'h1*), exhibits high iron-deficiency induced chlorosis and several exogenously applied coumarins can complement this mutant phenotype. The data indicates that root released coumarins take an important role in iron-acquisition mechanisms in plants (Schmid et al., 2014). Interestingly, recent studies showed that similar signaling pathways to limited iron availability are also activated during induced systemic resistance (ISR) (Zamioudis et al., 2014; 2015). ISR describes a phenomenon in which selected root associated growth promoting bacteria contribute to systemic resistance of the above grown part of the plant against a broad spectrum of pathogens (Pieterse et al., 2014). Beneficial rhizosphere bacteria such as the root colonizing bacterium *Pseudomonas fluorescens* WCS417 stimulate an iron-deficiency response in Arabidopsis roots, suggesting that beneficial rhizobacteria stimulate systemic immunity and mechanisms involved in iron uptake (Zamioudis et al., 2014; 2015). However, a functional link between iron-deficiency-signaling and ISR-signaling has not been reported yet.

Here we demonstrate that scopoletin biosynthesis is activated in Arabidopsis upon infection with the hemibiotrophic bacterial pathogen *Pseudomonas syringae* pv. *maculicola* ES4326 (*Psm*) in compatible and incompatible interactions. Furthermore, we show that coumarin metabolism moderately contributes to Arabidopsis basal resistance against *P. syringae*.

4.2 Results

4.2.1 Scopoletin biosynthesis is activated in Arabidopsis upon *Psm*-infection

Infection of Arabidopsis leaves with *Psm* leads to a strong transcriptional reprogramming at the infection-site and in distal leaf tissue (Gruner et al., 2013; Bernsdorff et al., 2016). We determined transcript levels of *F6'H1*, which is indispensable for scopoletin generation in Arabidopsis (Kai et al., 2008), by quantitative real-time PCR in leaves inoculated with *Psm* or the avirulent *Psm avrRpm1* strain expressing the *avrRpm1* avirulence gene (Bisgrove et al., 1994) in comparison to MgCl₂-infiltrated leaves at 48 hpi. Transcript levels of *F6'H1* were increased in leaves inoculated with *Psm* and *Psm avrRpm1* at 48 hpi (Fig. 4.1A). Consistent with accumulation of the scopoletin precursor Phe upon *Psm*-infection (Návarová et al., 2012) and increased *F6'H1* transcript levels, an accumulation of scopoletin could be observed in *Psm*- and *Psm avrRpm1*-inoculated leaves (Fig. 4.1B). Thereby scopoletin accumulated in *Psm*- and *Psm avrRpm1*-inoculated Col-0 leaves at 24 and 48 hpi, indicating that effector-triggered and PAMP-triggered immune signaling contributes to scopoletin generation. Scopoletin accumulation was restricted to the inoculation site, because its levels were not increased in untreated, systemic leaves in response to bacterial inoculation. Furthermore, *f6'h1* mutant plants failed to accumulate scopoletin upon *P. syringae*-infection (Fig. 4.1B). Scopoletin is reported to be highly abundant in roots and is described to be released by Arabidopsis roots in response to limited iron availability (Gnonlonfin et al., 2012; Schmid et al., 2014). We therefore measured endogenous scopoletin levels in roots (Fig. 4.1C). Scopoletin levels in roots were highly decreased in *f6'h1* mutant plants. Moreover, scopoletin levels in roots of Col-0 plants which were infiltrated with MgCl₂ were in a similar range to leaves inoculated with *Psm* (Fig. 4.1C). We also checked if leaf-inoculation influences scopoletin levels in roots, but endogenous scopoletin levels in roots did not change after leaf-inoculation with *Psm* compared to plants which were infiltrated with MgCl₂ (data not shown).

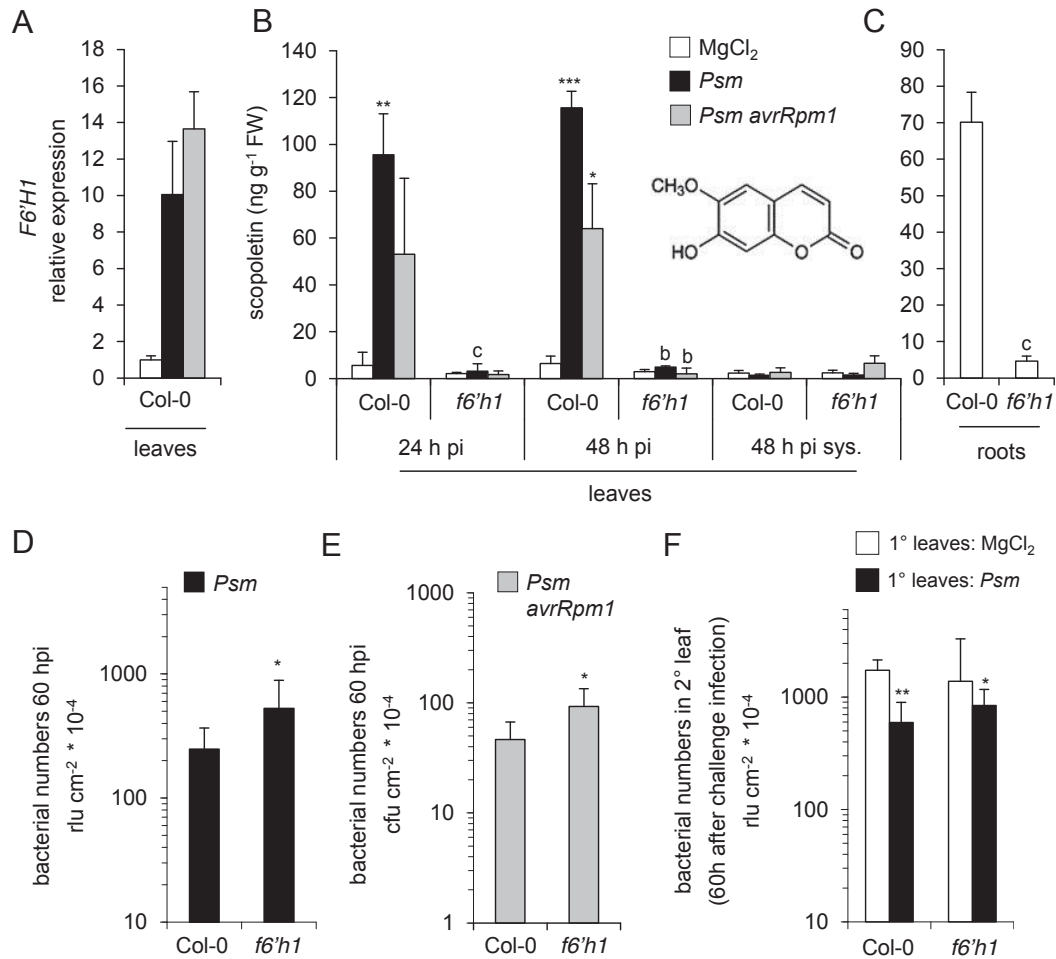


Figure 4.1 **Scopoletin biosynthesis is activated upon *P. syringae*-infection and coumarin metabolism contributes to Arabidopsis basal resistance against *P. syringae*.**

(A) Transcript levels of *F6'H1* in Col-0 leaves inoculated with *Psm* and *Psm avrRpm1* at 48 hpi.

(B) Accumulation of scopoletin in Col-0 and *f6'h1* mutant plants. Scopoletin levels were determined in local inoculated leaves at 24 and 48 hpi and in systemic non-inoculated leaves at 48 hpi. Control plants were infiltrated with a 10 mM MgCl₂ solution.

(C) Scopoletin levels in roots of Col-0 and *f6'h1* mutant plants. Roots of plants were used which were infiltrated with 10 mM MgCl₂.

(D) (E) Bacterial numbers of compatible *Psm* and *Psm avrRpm1* (applied in titers of OD₆₀₀ 0.001) in Col-0 and scopoletin deficient *f6'h1* mutant plants. Bacterial numbers were determined 2.5 d after the inoculation. Bacterial numbers are means from 6 parallel samples, each consisting of three leaf disks.

(F) SAR assay with Col-0 and *f6'h1* mutant plants. Local leaves were infiltrated with either 10 mM MgCl₂ or, to induce SAR, with *Psm* (applied in titers of OD₆₀₀ 0.005). Two days later three leaves, distal to the site of first infiltration, per plant were infiltrated with *Psm* (applied in titers of OD₆₀₀ 0.001). Bacterial numbers in those leaves were determined 60 h post second infiltration. Bacterial numbers are means from 6 parallel samples, each consisting of three leaf disks.

Asterisks denote statistically significant differences between MgCl₂- and *P. syringae*-infiltrated plants of one genotype at one time-point ***P < 0.001, **P < 0.01, and *P < 0.05. Letters denote statistically differences between the same treatment of Col-0 and *f6'h1* at one time-point. cP < 0.001, bP < 0.01, and aP < 0.05 (two tailed t test).

4.2.2 Coumarin metabolism moderately contributes to Arabidopsis basal resistance against *P. syringae*

The impaired *P. syringae*-triggered scopoletin accumulation in the *f6'h1* mutant gave us the opportunity to directly test if scopoletin accumulation is from functional relevance for Arabidopsis basal resistance to *P. syringae*. We therefore determined the multiplication of *Psm* and *Psm avrRpm1* three days post inoculation in leaves of Col-0 and *f6'h1* mutant plants (Fig. 4.1D; Fig. 4.1E). The *f6'h1* mutant plants exhibits an increased susceptibility against *Psm* and *Psm avrRpm1* compared to Col-0 plants. Thereby the increased susceptibility phenotype of *f6'h1* mutant plants was more pronounced in plants inoculated with *Psm avrRpm1* compared to plants inoculated with *Psm* (Fig. 4.1D; Fig. 4.1E). We also checked if pathogen-triggered scopoletin generation takes a functional role in SAR establishment (Fig. 4.1F). Therefore we infiltrated leaves of Col-0 and *f6'h1* mutant plants with *Psm* to induce SAR in the whole plant foliage or with 10 mM MgCl₂ as a control. Two days later both sets of plants were inoculated with *Psm* in leaves distal to the site of first infiltrations and 2.5 days later bacterial numbers in those leaves were determined. Bacterial numbers were decreased in both genotypes after a first inoculation with *Psm* compared to control-infiltrated plants, indicating that scopoletin accumulation is not necessary for SAR establishment (Fig. 4.1F).

4.3 Discussion

Here we could demonstrate that scopoletin biosynthesis via 2-oxoglutarate-dependent dioxygenase F6'H1 is activated in Arabidopsis upon *P. syringae*-infection. Thereby this activation is restricted to the site of infection and takes place in compatible (*Psm*) and incompatible (*Psm avrRpm1*) *P. syringae* Arabidopsis interactions (Fig. 4.1A; Fig. 4.1B). Moreover, it was previously reported that also scopoletin precursor Phe is accumulating in *Psm*-inoculated Arabidopsis leaves (Návarová et al., 2012). It was previously described that scopoletin is produced by various plant species in response to several biotic stressors such as fungi, bacteria, viruses, or microbial derived elicitors (Gnonlonfin et al., 2012). Furthermore, it was reported that in Arabidopsis scopoletin and the glycosidic bound form scopolin are generated in leaves inoculated with virulent and avirulent *Pst* (Chaouch et al., 2012). Mutant plants deficient in H₂O₂-signaling via RBOHD exhibit an increased scopoletin accumulation upon *Pst*-infection. Moreover, the catalase-deficient mutant *cat2*, which is described for constitutively activated photo-respiratory oxidative stress responses (Queval, et al 2007), also exhibited increased scopoletin levels without any pathogen contact and this

effect was even more pronounced in a *cat2 rbohD* double mutant (Chaouch et al., 2012). Together these results indicate that *P. syringae*-triggered scopoletin accumulation is regulated via ROS-signaling. The Arabidopsis mutant *cpr5-2* is described for constitutively activated defense signaling and constitutive ROS production in leaves (Bowling et al., 1997; Maeto et al., 2006). Consistent with observation of Chaouch et al. (2012), that *cat2* mutant plants accumulate scopoletin without any pathogen contact, also *cpr5-2* mutant plants exhibit highly increased scopoletin levels in MgCl₂-infiltrated plants compared to Col-0 (Fig. 4.2). This observation underpins a possible regulatory role of ROS in pathogen-triggered scopoletin accumulation.

Beside to biological stressors, in several plant species enhanced scopoletin generation was reported in response to abiotic stressors such as wounding or exogenous chemical treatment with SA, MeJA, kinetin, or IAA (Gnonlonfin et al., 2012). However, in Arabidopsis exogenous treatment with synthetic IAA induce scopoletin and scopolin accumulation, whereupon exogenous treatments with SA and MeJA had no effect on endogenous scopoletin levels (Kai et al., 2006). Anyway, we checked *Psm*-triggered scopoletin accumulation in SA-deficient and JA-deficient Arabidopsis mutants *sid2* and *dde2* (Fig. 4.2). Interestingly, the endogenous scopoletin levels did not differ in MgCl₂-infiltrated leaves between investigated mutants and Col-0 wild-type plants, but in *Psm*- and *Psm avrRpm1*-inoculated leaves of *sid2* and *dde2* mutant plants scopoletin accumulated to higher amounts than in Col-0 leaves after the same inoculations (Fig. 4.2). This could indicate that *P. syringae*-induced scopoletin accumulation in Arabidopsis could be inhibited by the defense-signaling phytohormones SA and JA, which would have to be proven in future studies. In contrast to the observation that *P. syringae*-triggered scopoletin accumulation is increased in JA-deficient Arabidopsis mutants, for scopoletin accumulation in response to an infection of the necrotrophic fungus *Aternaria alternata* in tobacco plants functional JA-signaling is indispensable (Sun et al., 2014). Thereby downstream of JA the transcription factor *MYC2* is required which is described as a master regulator of several JA responses (Sun et al., 2014). Recently *MYC2* was reported as an important target for SA/JA-crosstalk in plant defense responses in Arabidopsis (Schmiesing et al., 2016). Therefore it would be interesting for future studies to investigate the role of SA and JA in *P. syringae*-inducible scopoletin accumulation.

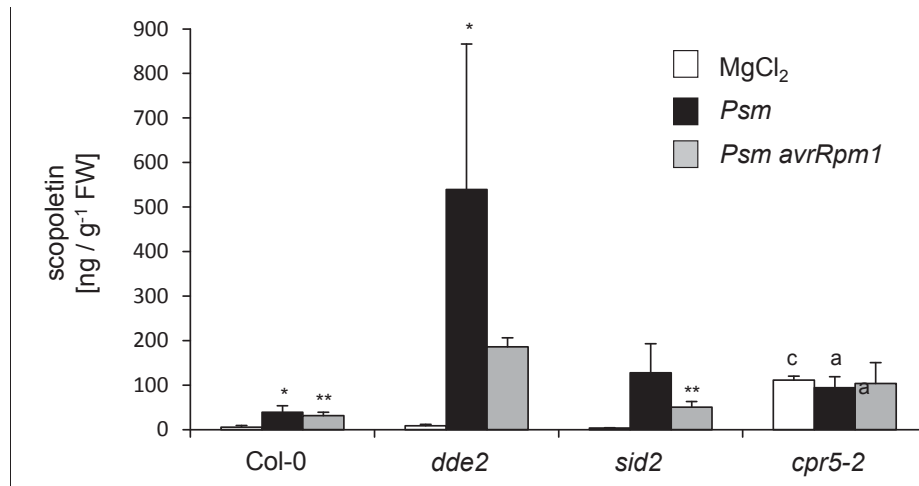


Figure 4.2 **Pathogen-triggered generation of scopoletin in mutants impaired in defence signaling pathways.**

Endogenous levels of scopoletin in several Arabidopsis mutants (*dde2*, *sid2*, *cpr5-2*) impaired in different defense signaling pathways at 48 hpi upon *Psm*- and *Psm avrRpm1*-inoculation. Asterisks denote statistically differences between MgCl₂-infiltration and *Psm*- or *Psm avrRpm1*-inoculation. ***P < 0.001, **P < 0.01, and *P < 0.05. Letters denote statistically differences between the same treatment of Col-0 and the respective mutant. ^cP < 0.001, ^bP < 0.01, and ^aP < 0.05 (two tailed t test).

It was also demonstrated here that Arabidopsis mutant plants which are impaired in scopoletin biosynthesis via 2-oxoglutarate-dependent dioxygenase F6'H1 exhibit a moderate increased susceptibility against *Psm* and *Psm avrRpm1* (Fig. 4.1D; Fig. 4.1E). Here we just quantified scopoletin in *P. syringae*-inoculated leaves, but *f6'h1* mutants are also described to be impaired in the generation of other coumarins such as esculetin (Schmid et al., 2014). We therefore cannot specify if the decreased basal resistance of *f6'h1* is reasoned by the lack of scopoletin or by the lack of other coumarins. An antimicrobial property for scopoletin was described against the pathogenic fungus *Microcyclus ulei*. Conidium germination and germ tube elongation of this fungus are inhibited by scopoletin (Garcia et al., 1995). Moreover, a test of the antibacterial activity of over 40 coumarins on several different gram-positive and gram-negative bacteria indicates that coumarins can have antibacterial properties (de Souza et al., 2005). Thereby the presence of an OH group at position 7 on the benzopyran core structure of coumarins seems to be required for this antibacterial activity (de Souza et al., 2005). However, an antibacterial activity of scopoletin and other coumarins on *P. syringae* has not been demonstrated yet and remains to be elucidated, but activated scopoletin biosynthesis upon *P. syringae*-infection and decreased basal resistance against *P. syringae* of *f6'h1* mutant plants suggest that coumarin metabolism could contribute to Arabidopsis basal resistance. Observations that scopoletin is produced de novo upon *P. syringae*-inoculation in Arabidopsis (Fig.

4.1; Chaouch et al., 2012), increased *P. syringae* susceptibility of *f6'h1* (Fig. 4.1), and that scopoletin exhibits antimicrobial activity on several pathogenic fungi (Garcia et al., 1995; Gnonlonfin et al., 2012) make scopoletin a promising candidate for a phytoalexin in Arabidopsis. Therefore, it remains also to be elucidated in future studies if scopoletin generation contributes to Arabidopsis resistance against pathogenic fungi and oomycetes.

Furthermore, coumarins and especially scopoletin are described for a role in iron uptake from alkaline substrates and *f6'h1* mutant plants are highly stressed under limited iron availability (Schmid et al., 2014). Similar signaling pathways to limited iron availability are also activated during ISR-induction (Zamioudis et al., 2014; 2015). Therefore it would be interesting for future studies to investigate if coumarins and scopoletin have in addition to low Fe stress and basal resistance also a function in ISR establishment.

5 Indolic compounds in systemic acquired resistance

Regulatory and functional aspects of indolic metabolism in plant systemic acquired resistance¹

5.1 Abstract

Tryptophan-derived, indolic metabolites possess diverse functions in Arabidopsis innate immunity to microbial pathogen infection. Here, we investigate the functional role and regulatory characteristics of indolic metabolism in Arabidopsis systemic acquired resistance (SAR) triggered by the bacterial pathogen *Pseudomonas syringae*. Indolic metabolism is broadly activated in both *P. syringae*-inoculated and distant, non-inoculated leaves. At inoculation sites, camalexin, indol-3-ylmethylamine (I3A), and indole-3-carboxylic acid (ICA) are the major accumulating compounds. Camalexin accumulation is positively affected by *MYB122*, and the cytochrome P450 genes *CYP81F1* and *CYP81F2*. Local I3A production, by contrast, occurs via indole glucosinolate breakdown by *PEN2*-dependent and independent pathways. Moreover, exogenous application of the defense hormone salicylic acid stimulates I3A generation at the expense of its precursor indol-3-ylmethylglucosinolate (I3M), and the SAR regulator pipelicolic acid primes plants for enhanced *P. syringae*-induced activation of distinct branches of indolic metabolism. In uninfected systemic tissue, the metabolic response is more specific and associated with enhanced levels of the indolics I3A, ICA, and indole-3-carbaldehyde (ICC). Systemic indole accumulation fully depends on functional *CYP79B2/3*, *PEN2*, and *MYB34/51/122*, and requires functional SAR signaling. Genetic analyses suggest that systemically elevated indoles are dispensable for SAR and associated systemic increases of salicylic acid. However, soil-grown but not hydroponically -cultivated *cyp79b2/3* and *pen2* plants, both defective in indolic secondary metabolism, exhibit pre-induced immunity, which abrogates their intrinsic ability to induce SAR.

¹ This chapter was published previously under Stahl et al. (2016). Author contributions for the article are listed under "Author contributions Chapter 5" (page 210).

5.2 Introduction

The immune system of plants is based on a multi-layered arsenal of constitutive and inducible defense strategies. (Thordal-Christensen et al., 2003). These involve the action of low molecular weight plant metabolites at different functional levels. Phytoanthicipins are pre-existing plant natural products with antimicrobial activity that can act as resistance determinants of plant species to insufficiently adapted pathogenic microbes (Bednarek and Osbourn, 2009). For instance, antifungal triterpene saponins such as avenacin protect oat plants against root infection by varieties of the fungal pathogen *Gaeumannomyces graminis* that lack saponin-deglycosylating enzymes (Papadopoulou et al., 1999). Phytoalexins, by contrast, are antimicrobial low molecular weight secondary metabolites only produced in the course of a plant-pathogen interaction. The antifungal sorghum deoxyanthocyanidins apigeninidin and luteolinidin, which focally accumulate in response to attempted infection by the fungus *Colletotrichum graminicola* in attacked leaf cells, are classical examples for phytoalexins (Snyder and Nicholson, 1990).

Some plant metabolites act as defensive signals, coordinating the expression of defense-related genes and promoting plant pathogen resistance by regulatory means. The phenolic salicylic acid (SA) is produced from chorismate in response to attack by many microbes and confers disease resistance to many biotrophic and hemibiotrophic pathogens (Nawrath and Métraux, 1999; Wildermuth et al., 2001; Vlot et al., 2009). The biosynthesis of SA is a central part of the inducible defense repertoire of plants that is activated after the perception of common microbial structures, so-called pathogen-associated molecular patterns (PAMPs), or after the recognition of effectors highly specific to particular pathogen isolates (Spoel and Dong, 2012). In contrast to effector-triggered immunity (ETI) that culminates in a localized cell death reaction at sites of pathogen ingress, PAMP-triggered immunity (PTI) is weaker and usually not efficient enough to entirely prohibit infection by adapted pathogens (Jones and Dangl, 2006).

PTI or plant basal resistance can be augmented by biotic and abiotic environmental cues (Singh et al., 2014). A well-known response of plants to biotic stress is systemic acquired resistance (SAR) (Shah and Zeier, 2013; Fu and Dong, 2013). SAR develops after a localized microbial leaf inoculation and provides broad-spectrum resistance to subsequent infection in the whole foliage. SA is an important regulatory metabolite in the SAR process. In *Arabidopsis thaliana*, proper SAR activation requires pathogen-induced, ISOCHORISMATE SYNTHASE1 (ICS1)-mediated SA accumulation (Nawrath and Métraux, 1999; Wildermuth et al., 2001).

Another central SAR regulatory metabolite is the non-protein amino acid pipecolic acid (Pip) (Návarová et al., 2012). In *Arabidopsis* plants attacked by the bacterial pathogen *Pseudomonas syringae*, Pip and SA accumulate both in inoculated leaves and systemically in leaf tissue distant from initial inoculation. Pip is synthesized from Lys upon pathogen attack by AGD2-LIKE DEFENSE RESPONSE PROTEIN 1 (ALD1) and enhances plant resistance via FLAVIN-DEPENDENT MONOOXYGENASE 1 (FMO1) (Návarová et al., 2012; Zeier, 2013). Both *ALD1* and *FMO1* are indispensable for SAR (Song et al., 2004; Mishina and Zeier, 2006; Návarová et al., 2012). During SAR, elevated Pip levels prime plants for enhanced and effective defense activation upon subsequent pathogen challenge (Návarová et al., 2012; Vogel-Adghough et al., 2013; Bernsdorff et al., 2016).

The significance of Pip in SAR exemplifies that amino acid-related metabolic pathways accomplish integral tasks in the plant immune system (Zeier, 2013). Tryptophan (Trp) catabolism constitutes another important metabolic branch in plant immunity that produces defense-relevant indolic compounds. Trp-derived indolics are particularly prominent in *Arabidopsis* and other cruciferous plants (Bednarek et al., 2011). The entry reaction into indolic secondary metabolism in *Arabidopsis* is catalysed by the two cytochrome P450 enzymes CYP79B2 and CYP79B3, which convert Trp into indole-3-acetaldoxime (IAOx) (Zhao et al., 2002). From IAOx, several branches of indolic metabolism diverge, leading to the formation of indole glucosinolates, the phytoalexin camalexin, and a series of other low molecular weight indolics including indole-3-carboxylic acid (ICA) and the phytohormone indole-3-acetic acid (Glawischnig, 2007; Bender and Celenza, 2009; Sonderby et al., 2010; Bednarek, 2012).

Indol-3-ylmethylglucosinolate (I3M) constitutes the major indole glucosinolate in *Arabidopsis* rosette leaves (Brown et al., 2003). Members of the cytochrome P450 subfamily CYP81F are able to hydroxylate I3M and thereby catalyse the first step in the formation of less-prominently occurring 4- and 1-methoxylated I3M derivatives (Pfalz et al., 2011). Indole glucosinolates can be degraded enzymatically or non-enzymatically to different breakdown products. I3M hydrolysis, for instance, can lead to the formation of indole-3-acetonitrile (IAN) and indole-3-carbinol (I3C) (Kim et al., 2008). Moreover, fungal attack causes conversion of I3M to indol-3-ylmethylamine (I3A) in a *PENETRATION2* (*PEN2*)-dependent manner (Bednarek et al., 2009). *PEN2* encodes an atypical myrosinase that has been initially identified as a critical determinant of *Arabidopsis* penetration resistance to non-adapted powdery mildew pathogens (Lipka et al., 2005; Bednarek et al., 2009). It is now established that the indole

glucosinolate/PEN2-myrosinase system constitutes an important early defense layer that restricts invasion of Arabidopsis by different non-adapted and adapted fungal and oomycete pathogens (Sanchez-Vallet et al., 2010; Schlaeppi et al., 2010; Consonni et al., 2010; Bednarek, 2012; Hiruma et al., 2013). The biosynthesis of indolic glucosinolates is distinctly regulated by the three MYB-type transcription factors MYB34, MYB51 and MYB122 (Frerigmann and Gigolashvili, 2014).

Another branch of indolic metabolism results in the formation of camalexin, the most prominent phytoalexin in Arabidopsis (Glawischnig, 2007). Camalexin accumulates to high levels in Arabidopsis leaves inoculated with hemibiotrophic *P. syringae* bacteria or necrotrophic fungi such as *Alternaria brassicola* or *Botrytis cinerea* and exhibits *in vitro* antimicrobial activity (Kliebenstein et al., 2005; Schuhegger et al., 2007). SAR-induced plants are primed for enhanced camalexin biosynthesis through Pip accumulation (Návarová et al., 2012). The *phytoalexin-deficient3 (pad3)* mutant is defective in camalexin biosynthesis and exhibits increased susceptibility to *A. brassicola* and *B. cinerea* but not to *P. syringae* infection, indicating that camalexin protects against the former two but not against the latter pathogen (Thomma et al., 1999; Ferrari et al., 2007). The sequential action of indole glucosinolates and camalexin restricts colonisation of Arabidopsis by the hemibiotrophic oomycete *Phytophthora brassicae* (Schlaeppi et al., 2010). The two cytochrome P450 enzymes CYP71A13 and CYP71B15 (alias PAD3) participate in camalexin biosynthesis. *In vitro* biochemical studies indicate that CYP71A13 acts in an earlier step of camalexin biosynthesis and converts IAOx to IAN (Nafisi et al., 2007). PAD3 catalyzes the two final biosynthetic steps from Cys-IAN to camalexin (Schuhegger et al., 2006; Böttcher et al., 2009).

In addition to camalexin, indole-3-carbaldehyde (ICC), ICA and ICA-derivatives are formed in response to pathogen infection or abiotic stress in Arabidopsis roots and leaves (Hagemeier et al., 2001; Bednarek et al., 2005; Böttcher et al., 2009; Iven et al., 2012; Gamir et al., 2012). Besides accumulating in free or glycosylated form, ICA is esterified to cell wall components in pathogen-inoculated tissue (Tan et al., 2004; Forcat et al., 2010). Recently, a model for the biosynthesis of ICC and ICA derivatives, involving ARABIDOPSIS ALDEHYDE OXIDASE1 (AAO1) and CYP71B6, was presented (Böttcher et al., 2014).

In the present work, we investigate the significance and regulatory characteristics of indolic metabolism during the Arabidopsis SAR response. We show that *P. syringae*-induced SAR is accompanied by a strong and broad activation of

indolic metabolism in inoculated leaves and in uninfected, systemic leaves. The local metabolic response includes strong accumulation of camalexin, I3A, and ICA, and enhanced production of about 20 other GC/MS-detectable indolic compounds. Metabolite analyses of indole pathway mutants suggest that besides *CYP71A13* and *PAD3*, the cytochrome P450 *CYP81F1* and *CYP81F2*, and the MYB transcription factor *MYB122* positively regulate camalexin production. Moreover, mutational defects of *CYP71A13*, *CYP81F1* and *CYP81F2* cause metabolic imbalances that result in over-accumulation of IAN, I3A, and ICA upon bacterial inoculation. Local I3A production proceeds via *PEN2*-dependent and independent metabolic pathways, and I3A generation from I3M is stimulated by exogenous SA. Similar to camalexin accumulation (Návarová et al., 2012), the pathogen-induced biosynthesis of I3A and ICA is primed by pre-treatment of plants with Pip. In leaves distant from inoculation, the *P. syringae*-induced activation of indolic metabolism results in the accumulation of I3A, ICA, and ICC, indicating that SAR establishment equips plants with increased levels of defense-relevant indolics throughout the foliage. However, mutant analyses argue against a direct functional role for these indolics in general SAR activation. Notably, mutational defects of *CYP79B2/3* and *PEN2*, which weakens pre-invasion immune layers, can lead to a pre-activation of post-invasion defenses in soil-grown plants that increases plant basal resistance and results in an apparent loss of SAR inducibility.

5.3 Results

5.3.1 SAR establishment in Arabidopsis is associated with a strong activation of indolic metabolism

A localized leaf inoculation with avirulent or virulent strains of the bacterial pathogen *Pseudomonas syringae* induces systemic acquired resistance in the foliage of Arabidopsis plants (Shah and Zeier, 2013). Two days after inoculation of lower (1°) leaves with the compatible *P. syringae* pv. *maculicola* ES4326 (*Psm*) strain, SAR fully develops in non-treated upper (2°) leaves. This is associated with significant accumulation of the two SAR regulatory metabolites SA and Pip, and with a massive transcriptional reprogramming in 2° leaves (Návarová et al., 2012; Gruner et al., 2013; Bernsdorff et al., 2016). To investigate a possible role of indolic metabolism in the establishment of SAR, we performed comparative GC/MS-based metabolite analyses of 1° treated leaves and non-treated 2° leaves two days after *Psm* inoculation or mock-control treatment in Arabidopsis wild-type and selected mutant lines.

Indolic compounds in systemic acquired resistance

Table 1. Indolic metabolite accumulation in *P. syringae* pv. *maculicola* (*Psm*)-inoculated leaves of soil-cultivated Arabidopsis Col-0 plants, as determined by comparative, GC/MS based analyses of leaf extracts from wild-type Col-0 and the *cyp79b2/3* mutant impaired in Trp catabolism.

#	RT (min)	m/z	compound		abundance	Col-0	Col-0	79b2/3	79b2/3
						mock	<i>Psm</i>	mock	<i>Psm</i>
						(mean ± SD)			
1	11.6	<u>86</u> , 59	n. i.		++	1.0 ± 0.2	17.9** ± 5.1	1.2 ± 0.4	3.5* ± 1.5
2	13.7	<u>117</u> , 90, 89	Indole ²	<u>C</u>	++	1.0 ± 0.2	15.8** ± 4.1	0.7 ± 0.1	0.5 ± 0.2
3	15.3	<u>131</u> , <u>130</u>	Indole-3-carbinol (I3C) ¹	<u>J</u>	+	1.0 ± 0.1	2.3* ± 0.4	0.2 ± 0.1	0.2 ± 0.02
4	16.4	162, 144, <u>102</u>	n. i.		+	1.0 ± 0.5	31.9*** ± 0.9	0.4 ± 0.1	3.2* ± 0.9
5	17.0	<u>132</u>	n. i.		++	1.0 ± 0.4	5.1** ± 1.1	0.3 ± 0.1	0.3 ± 0.1
6	20.8	161, <u>130</u>	Indole-3-ethanole (Tryptophol) ²	<u>K</u>	+	1.0 ± 0.4	5.5*** ± 0.1	n. d.	n. d.
7	21.4	189, <u>158</u>	n. i. (MS similar to 2-Methyl-indole-3-carboxylic acid ³)		+	1.0 ± 0.2	22.6*** ± 1.5	n. d.	n. d.
8	21.45	<u>155</u> , 130	Indole-3-acetonitrile (IAN) ²	<u>H</u>	++	1.0 ± 0.3	1.5 ± 0.1	0.06 ± 0.01	0.06 ± 0.02
9	21.5	<u>145</u> , <u>144</u> , 116	Indole-3-carbaldehyde (ICC) ¹	<u>E</u>	++	1.0 ± 0.4	7.2** ± 1.7	0.4 ± 0.1	0.6 ± 0.2
10	21.6	<u>142</u> , 115, 88	Indole-3-carbonitrile (ICN) ²	<u>G</u>	++	1.0 ± 0.6	26.8*** ± 3.7	1.1 ± 0.3	1.8 ± 0.6
11	22.1	175, <u>144</u> , 116	Indole-3-carboxylic acid (ICA) ¹	<u>D</u>	+++	1.0 ± 0.6	75.1*** ± 5.4	1.4 ± 0.4	1.6 ± 0.5
12	22.8	184, <u>158</u>	n. i.		+	1.0 ± 0.4	33.8** ± 8.1	n. d.	n. d.
13	23.7	<u>184</u> , 155, <u>129</u>	n. i.		+	1.0 ± 0.4	93.5** ± 21.3	n. d.	n. d.
14	24.0	<u>186</u> , <u>171</u> , 143	4-Methoxy-indole-3-acetonitrile ²	<u>I</u>	++	1.0 ± 0.1	1.9* ± 0.4	0.10 ± 0.01	0.11 ± 0.06
15	24.3	170, <u>144</u> , 116	n. i.		+++	1.0 ± 0.1	68.4** ± 16.1	0.7 ± 0.2	0.7 ± 0.3
16	24.4	<u>161</u> , <u>160</u> , 104	n. i. (MS similar to 5-Hydroxy-indole-3-carbaldehyde ³)		+	1.0 ± 0.3	10.1*** ± 0.7	0.24 ± 0.11	0.26 ± 0.05
17	25.0	174, <u>130</u>	n. i.		++	1.0 ± 0.2	88.6** ± 18.9	0.7 ± 0.2	1.7 ± 0.5
18	26.0	191, <u>160</u> , 132	n. i. (MS similar to 5-Methoxy-tryptophol ³)		+	1.0 ± 0.4	46.3*** ± 6.8	0.7 ± 0.4	0.8 ± 0.3
19	26.4	<u>200</u> , 142, 115	Camalexin ¹	<u>B</u>	++++	1.0 ± 0.6	75.1*** ± 5.4	1.4 ± 0.4	1.6 ± 0.5
20	29.5	<u>271</u> , <u>229</u> , 201	n. i.		+	1.0 ± 0.2	43.0*** ± 4.1	0.6 ± 0.2	1.1 ± 0.6
21	29.7	260, <u>201</u> , 142	n. i.		+	1.0 ± 0.2	99.7** ± 22.2	1.0 ± 0.3	0.7 ± 0.2
22	31.1	<u>189</u>	n. i.		++	1.0 ± 0.2	121.9** ± 33.8	1.2 ± 0.4	13.1* ± 5.7
	32.6	<u>412</u> , 351, <u>255</u>	Stigmasterol		+++	1.0 ± 0.1	138.8*** ± 20.5	2.0 ± 0.5	95.5*** ± 8.7

Table-legend is given on the next page.

Legend for table 1:

Leaves of the Col-0 wild-type and *cyp79b2/3* were inoculated with *Psm* or infiltrated with a $MgCl_2$ -solution (mock-treatment), and harvested at 48 hpi for metabolite analyses. Analyses included leaf extraction, work-up, methylation of potentially existing free carboxylic groups in analytes, and GC/MS-based separation and detection. Comparison of individual ion chromatograms (*m/z* between 50 and 300) identified 22 peaks that significantly accumulated in extracts of *Psm*-inoculated Col-0 leaves but not in *cyp79b2/3*, and thus represent putative indolics. Many substances unrelated to the indole pathway significantly accumulated in both Col-0 and *cyp79b2/3* upon *Psm* inoculation (stigmasterol is listed in the bottom line as an example). Retention times (RT) and typical masses (*m/z*) in the mass spectra (MS) of the substance peaks are given.

Peak areas were related to the fresh weight of leaf samples and the area of the *m/z* 130 ion of the internal standard indole-3-propionic acid (IPA). Means and standard deviations (SD) from the resulting values were calculated and expressed relative to the mean value of the Col-0 mock-sample. The depicted values are based on at least three replicate samples per treatment and genotype. Asterisks denote statistically significant differences between $MgCl_2$ - and *Psm*-treatments of each genotype (****P* < 0.001, ***P* < 0.01, **P* < 0.05; two tailed *t* test). Plus signs indicate the range of the peak area values for the Col-0-*Psm* samples and thus yield estimates for the absolute amounts of accumulating substances in leaves (++++: very strong accumulation, mean peak area > $2 \cdot 10^8$; +++: strong, $2 \cdot 10^7$ - $2 \cdot 10^8$; ++: medium, $2 \cdot 10^6$ - $2 \cdot 10^7$; +: weak, < $2 \cdot 10^6$).

Substance identification was performed on basis of:

¹: comparison of RT and MS with those of authentic substances or

²: matching the MS with spectra of the NIST library.

³: MS of substance peaks showed similar but not identical mass spectra to the given compounds (n. i.: substance not identified).

The precursor amino acid for indolic secondary metabolites, Trp (A) (Fig. 5.1), significantly accumulates in *Psm*-inoculated leaves of wild-type Col-0 plants (Fig. 5.2; Návarová et al., 2012). A *cyp79b2 cyp79b3* (*cyp79b2/3*) double knockout mutant is blocked in the production of Trp-derived metabolites such as indole glucosinolates and camalexin (Glawischnig et al., 2004; Böttcher et al., 2009; Bednarek et al., 2009). By GC/MS-profiling, we comparatively analysed metabolic changes in wild-type Col-0 and *cyp79b2/3* in *Psm* treated 1° leaves compared to mock-treated control leaves. Based on comparative analyses of individual ion chromatograms (*m/z* between 50 and 300), we identified 22 substances that significantly accumulated in extracts of *Psm*-inoculated Col-0 leaves but not in leaves of *cyp79b2/3*, suggesting that these compounds represent Trp-derived metabolites (Table 1). By comparison of their mass spectra and retention times with those of authentic standards, and by matching of mass spectra with spectra from the NIST library, we were able to identify 9 of these 22 substances. All of them represent 3-substituted indole derivatives (Table 1, Fig. 5.1).

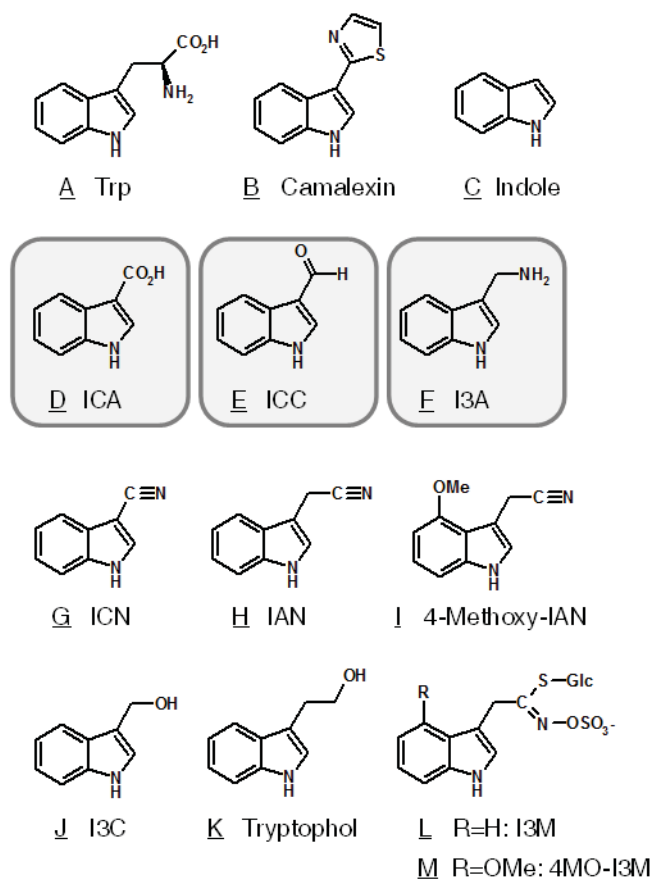


Figure 5.1 Chemical structure of selected indolics.

(A) Tryptophan (Trp), **(B)** camalexin, **(C)** indole, **(D)** indole-3-carboxylic acid (ICA), **(E)** indole-3-carbaldehyde (ICC), **(F)** indole-3-ylmethylamine (I3A), **(G)** indole-3-carbonitrile (ICN), **(H)** indole-3-acetonitrile (IAN), **(I)** 4-Methoxy-IAN, **(J)** indole-3-carbinol (I3C); **(K)** tryptophol; **(L)** indole-3-ylmethylglucosinolate (I3M), **(M)** 4-Methoxy-I3M. The three indolics accumulating systemically in plants when leaf-inoculated with *P. syringae* are highlighted in grey.

As expected, the indolic phytoalexin camalexin (B) prominently accumulated in *Psm* inoculated (1°) leaves of Col-0 at 48 hours post inoculation (hpi) (Table 1, Figs. 5.1 and 5.2). Moreover, ICA (D) and, as deduced from its similar mass spectrum, a substance structurally related to ICA (substance #15 in Table 1), were substantially produced in *Psm*-inoculated Col-0 leaves (Table 1, Figs. 5.1 and 5.2). Albeit accumulating to lower absolute levels than ICA, the levels of ICC (E), indole-3-carbonitrile (ICN, G), and indole (C) were also significantly increased at sites of bacterial attack (Table 1, Figs. 5.1 and 5.2). A comparatively weak but statistically significant enrichment was found for three other compounds, 4-methoxy-indole-3-acetonitrile (I), I3C (J), and tryptophol (K). Further, IAN (H) was present in extracts of Col-0 plants but hardly detectable in extracts of *cyp79b2/3*. IAN levels, however, were not significantly influenced by bacterial attack (Table 1). 12 of the 20 pathogen-induced substances that were designated as indolics by the GC/MS-based profiling analyses

could not be structurally identified. However, the mass spectra of 3 of these compounds exhibited close similarity to the spectra of 2-methyl-ICA, 5-hydroxy-ICC, and 5-methoxy-tryptophole (Table 1). Although the unidentified compounds only accumulated to comparatively low absolute levels in Col-0, virtually all of these substances showed a marked relative enrichment in extracts from *Psm*-inoculated compared to extracts from control leaves.

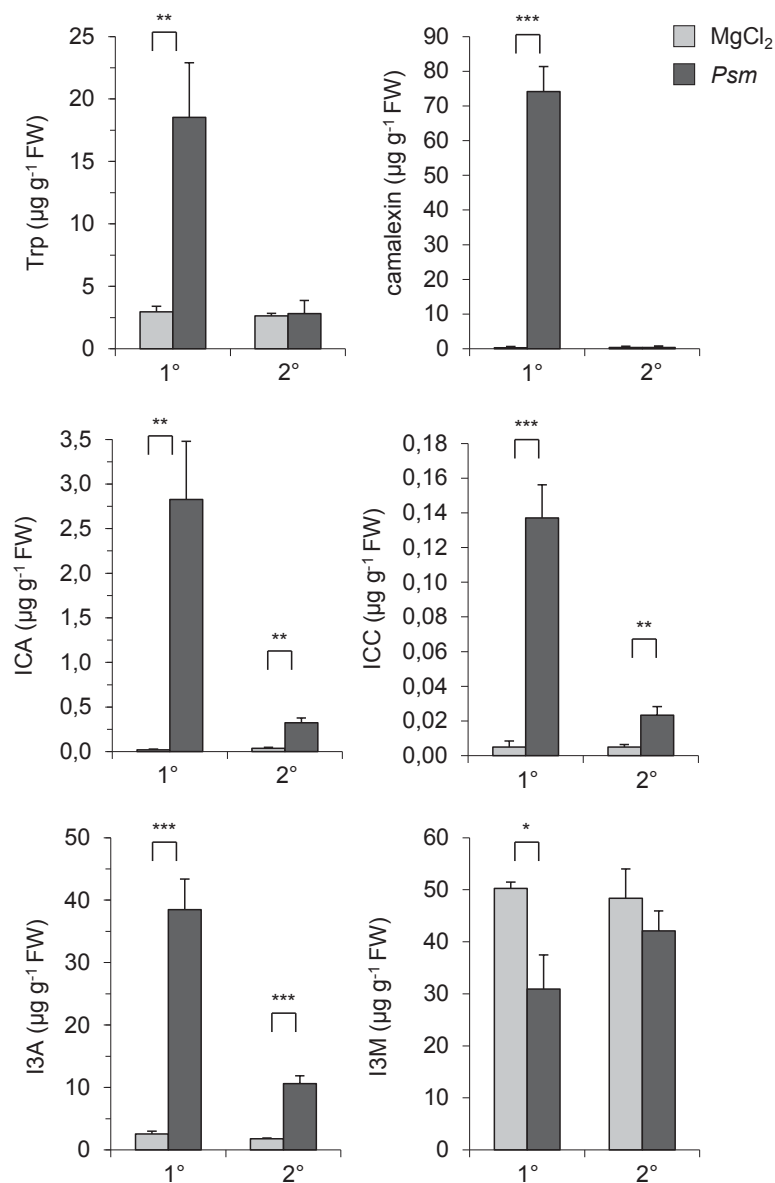


Figure 5.2 Indole accumulation in *P. syringae*-inoculated (1°) and in non-inoculated, systemic leaf tissue (2°) of *Arabidopsis* Col-0 plants.

Levels of Trp, camalexin, ICA, ICC, I3A, and I3M in leaves of soil-cultivated Col-0 plants inoculated with *P. syringae* pv. *maculicola* (*Psm*) or infiltrated with a 10 mM MgCl₂ mock-control solution, are given in µg g⁻¹ leaf fresh weight (FW). 1°: inoculated/treated leaves. 2°: leaves distal to inoculation/treatment. Leaf samples were harvested at 48 hours post inoculation (hpi). Data represent the mean ± SD of at least three replicate samples. Asterisks denote statistically significant differences between MgCl₂- and *Psm*-treatments (***P < 0.001, **P < 0.01, *P < 0.05; two tailed *t* test).

In *Arabidopsis* leaves inoculated with non-adapted powdery mildew fungi, the indolic amine I3A (Fig. 5.1, substance F) accumulates at fungal inoculation sites. I3A is a hydrolysis product of I3M (Fig. 5.1, substance L), the main indole glucosinolate in accession Col-0 (Brown et al., 2003; Bednarek et al., 2009). Due to their hydrophilic nature, I3M and I3A are not analyzable by the GC/MS-based analytical method applied for the above-described indolics. We therefore applied targeted, HPLC-based analysis to determine whether the leaf levels of I3A and I3M would be altered upon bacterial inoculation. Strikingly, *Psm* treatment of plants triggered a very strong increase of I3A levels in inoculated leaves, which came quantitatively close to the induced levels of camalexin at 48 hpi (Fig. 5.2). Concomitantly, the levels of I3M significantly decreased in leaves inoculated with *Psm*, consistent with a conversion of I3M into I3A upon bacterial attack (Fig. 5.2).

Our data so far indicate that indolic metabolism is strongly activated in *Psm*-inoculated, 1° leaves in the course of SAR establishment. The accumulating indolics share this feature with various structurally unrelated metabolites, such as branched-chain and aromatic amino acids, Lys, Pip, α -amino adipic acid, free and glycosylated SA, jasmonic acid, unsaturated fatty acids, abscisic acid, the C16-homoterpene (E,E)-4,8,12-trimethyl-1,3,7,11-tridecatetraene (TMTT), and the phytosterol stigmasterol (Mishina and Zeier, 2007; Attaran et al., 2008; Griebel and Zeier, 2010; Návarová et al., 2012; Gruner et al., 2013). Compared to these massive and broad metabolic alterations at bacterial inoculation sites, metabolic changes in distal, non-infected (2°) *Arabidopsis* leaves upon SAR induction by *Psm* are rare and have only been described for the critical SAR regulators Pip and SA, but not for the other above-enumerated substances (Návarová et al., 2012). Importantly, from the 23 indolic substances determined to locally accumulate upon *Psm*-inoculation (Table 1, Fig. 5.2), 3 compounds were found to significantly increase in distal, 2° leaf tissue at 48 hpi: I3A, ICA, and ICC (Fig. 5.2). On the basis of their systemic accumulation in the foliage upon SAR activation, we hypothesized that I3A, ICA, and ICC could be functionally relevant in the SAR process.

5.3.2 Temporal patterns of indolic metabolite accumulation in inoculated leaves

We next examined the temporal accumulation patterns of the most prominently generated indolics at inoculation sites, camalexin, I3A, and ICA, and compared them to SA accumulation in leaves inoculated with the compatible (virulent) *Psm* strain and the

avirulent *Psm avrRpm1* strain expressing the *avrRpm1* avirulence gene (Bisgrove et al., 1994). Leaf samples were thereby analyzed at 6, 10, 24, and 48 hpi (Fig. 5.3). Between 6 and 24 hpi, the *Psm avrRpm1*-triggered accumulation of the examined indolics was stronger than the *Psm* induced accumulation, indicating that effector-triggered immune signaling exhibits a strong influence on early indolic metabolite accumulation. At 48 hpi, the indolics accumulated to highest levels in leaves inoculated with *Psm*, suggesting significant contributions of PAMP-triggered immune signaling for the activation of Trp catabolism at later stages of the compatible Arabidopsis-*P. syringae* interaction (Fig. 5.3). Moreover, ICA and I3A exhibited a similar accumulation pattern than SA during early interaction stages and started to accumulate before camalexin levels increased (Fig. 5.3).

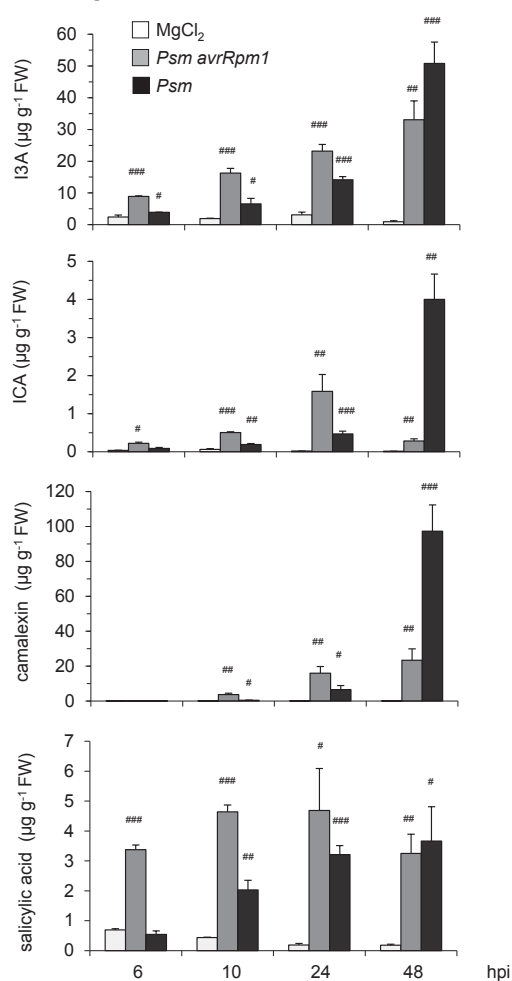


Figure 5.3 Time course of indole accumulation in Col-0.

Time course of I3A, ICA, camalexin, and salicylic acid (SA) accumulation in leaves of soil-cultivated Col-0 plants inoculated with compatible *Psm* or hypersensitive response-inducing *Psm avrRpm1*. Endogenous levels of metabolites were determined in inoculated leaves at 6, 10, 24 and 48 hpi. Data represent the mean \pm SD of at least three replicate samples. Hash symbols denote statistically significant differences between the MgCl₂ control treatment and the *Psm* or *Psm avrRpm1* inoculation at each time point (###P < 0.001, ##P < 0.01, #P < 0.05; two tailed *t* test).

5.3.3 Biosynthetic and regulatory aspects of indolic metabolism at sites of bacterial inoculation

Besides CYP79B2/3, several other proteins involved in the biosynthesis and the regulation of indolic metabolism have been characterized (Bednarek et al., 2009; Bender and Celenza, 2009; Sonderby et al., 2010; Böttcher et al., 2014). Previous microarray analyses indicate that several of the genes involved in the indolic pathway are up-regulated upon *Psm*-inoculation (Table S1; Wang et al., 2008; Gruner et al., 2013). To get further insights into biosynthetic and regulatory aspects of *P. syringae*-induced indolic metabolism, we compared the accumulation pattern of Trp, I3A, ICA, ICC, and camalexin in *Psm*-inoculated leaves at 48 hpi in wild-type Col-0 and selected mutant lines with defined gene defects in Trp-derived metabolism (Figs. 5.4 and 5.5). Notably, in *cyp79b2/3*, Trp levels were elevated under basal conditions and over-produced after pathogen infection, whereas, as outlined before (Table 1), the Trp-derived indolics were absent or only faintly produced in this mutant (Fig. 5.4). The blockage of the first step of Trp catabolism in *cyp79b2/3* therefore results in an over-accumulation of Trp, the precursor amino acid of indolic metabolism, after *P. syringae* infection.

The peroxisome-associated glycosyl hydrolase PENETRATION2 (PEN2) contributes to non-host resistance of Arabidopsis to non-adapted fungal and adapted oomycete pathogens (Lipka et al., 2005; Bednarek et al., 2009; Schlaeppi et al., 2010; Sanchez-Vallet et al., 2010). I3A accumulation in Arabidopsis triggered by powdery mildew fungi is fully dependent on functional PEN2 (Bednarek et al. 2009), and we thus analyzed *P. syringae* triggered indolic metabolite accumulation in the *pen2-2* (*pen2*) knockout mutant. I3A accumulation in *Psm*-inoculated leaves was markedly lower than in the wild-type, though a significant increase after bacterial inoculation was still detected in *pen2*. In addition, *Psm* inoculated *pen2* leaves also exhibited attenuated accumulation of ICA, ICC, and camalexin, and did not show pathogen-induced decreases of I3M (Fig. 5.4; Fig. S13).

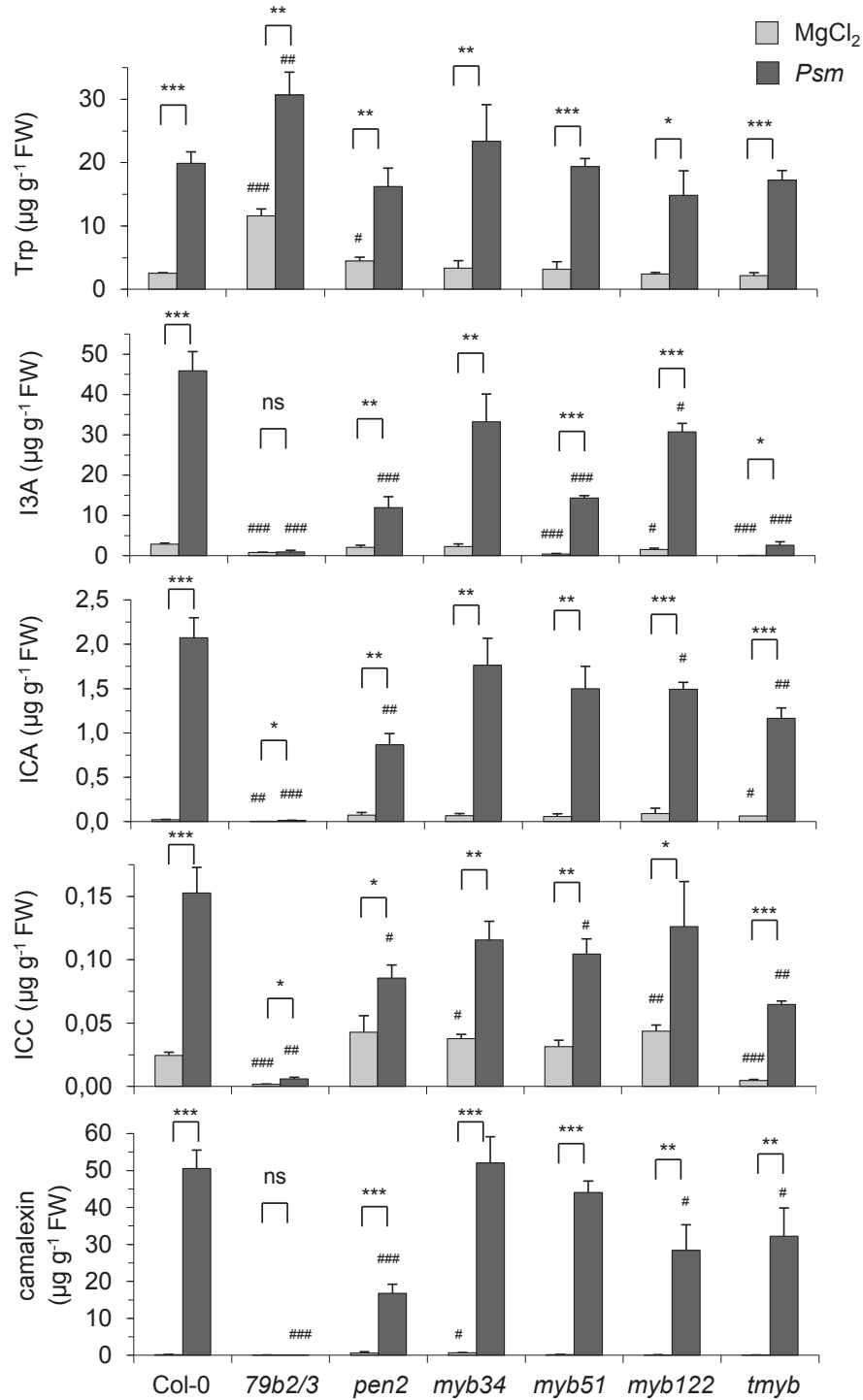


Figure 5.4 *P. syringae*-inducible indole accumulation in mutants impaired in indolic metabolism at the site of inoculation.

Accumulation of Trp, I3A, ICA, ICC, and camalexin in Col-0, *cyp79b2/b3*, *pen2*, *myb34*, *myb51*, *myb122* and *myb34/51/122* (*tmyb*) in *Psm*-inoculated leaves of soil-cultivated plants. Endogenous levels of metabolites were determined at 48 hpi. Data represent the mean \pm SD of at least three replicate samples. Asterisks denote statistically significant differences between MgCl₂ and *Psm* treatment in one genotype (***) $P < 0.001$, ** $P < 0.01$, * $P < 0.05$; two tailed *t* test). Hash symbols denote statistically significant differences between the same treatment of Col-0 and the corresponding mutant (### $P < 0.001$, ## $P < 0.01$, # $P < 0.05$; two tailed *t* test).

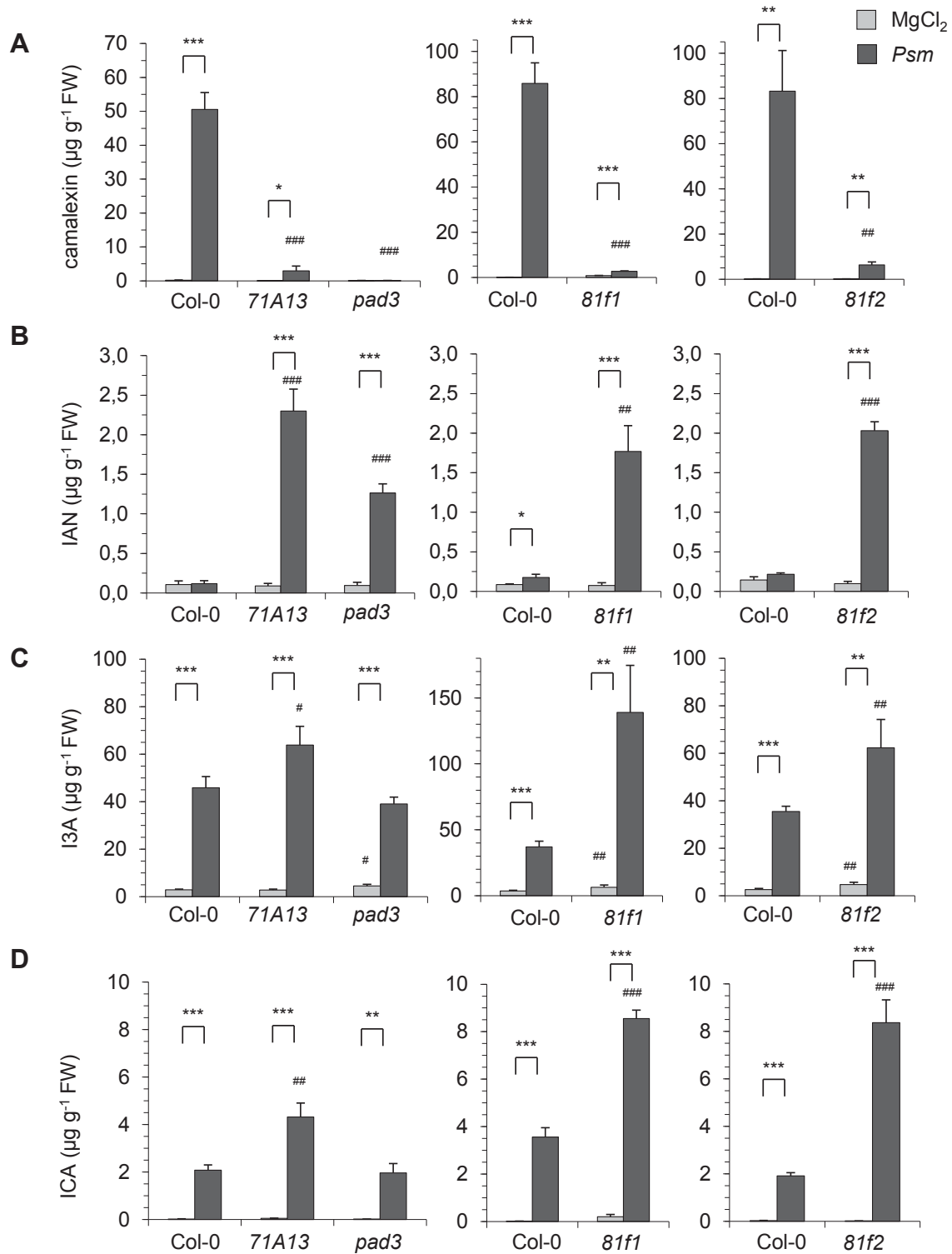


Figure 5.5 *P. syringae*-inducible indole accumulation in mutant plants affected in camalexin production.

Levels of (A) camalexin, (B) IAN, (C) I3A, and (D) ICA in *Psm*-inoculated and MgCl₂-infiltrated leaves of soil-cultivated Col-0, *cyp71A13*, *pad3*, *cyp81f1*, and *cyp81f2* plants at 48 hpi. Results from three independent biological experiments with Col-0 plants and different mutant combinations are depicted. Data represent the mean ± SD of at least three replicate samples. Compare legend to Fig. 5.4 for further details.

The biosynthesis of indole glucosinolates is regulated by the three MYB-type transcription factors MYB34, MYB51, and MYB122 (Malitsky et al., 2008; Gigolashvili et al., 2009). Whereas MYB51 and MYB122 are up-regulated in *Psm*-inoculated leaves, the expression of MYB34 is reduced upon bacterial inoculation (Table S3). Consistent with the function of the three MYB regulators in indole glucosinolate production, a *myb34 myb51 myb122* triple knockout mutant (*tmyb*) showed strongly reduced basal I3M levels and greatly diminished accumulation of indole glucosinolate-derived I3A in *Psm*-inoculated leaves (Fig. 5.4; Fig. S13). Further, the *Psm*-triggered generation of ICA, ICC, and camalexin was reduced in *tmyb* plants, albeit not to the same extent as I3A production. A similar trend was observed for a *myb51 myb122* double mutant (Fig. S14A). Analyses of single MYB knockout mutants indicated that *MYB51* provides the strongest contribution to *Psm*-induced I3A generation, whereas *MYB122* most pronouncedly affects camalexin biosynthesis (Fig. 5.4). This suggests distinct regulation of different branches of indolic metabolism in *P. syringae*-inoculated leaves. From the overall patterns of metabolite accumulation in the different mutant plants, it appears that ICA and ICC production is closely coordinated, and that the biosynthesis of ICA (ICC), I3A, and camalexin involve distinctive regulatory mechanisms (Fig. 5.4).

We next examined how defects in camalexin biosynthesis would affect the generation of different indolics in *Psm*-inoculated leaves. The camalexin biosynthesis genes *CYP71A13* and *PAD3* (alias *CYP71B15*) are strongly up-regulated in *Psm*-inoculated leaves (Table S3; Zhou et al., 1999; Nafisi et al., 2007). Whereas *PAD3* was shown to catalyze the final steps in camalexin biosynthesis (Schuhegger et al., 2006; Böttcher et al., 2009), biochemical characterization of recombinant *CYP71A13* suggests that it is involved in an earlier step in which IAOx is converted to IAN (Nafisi et al., 2007). Consistent with the function of *CYP71A13* and *PAD3* in camalexin biosynthesis, camalexin accumulation was low or completely absent in *Psm*-inoculated leaves of *cyp71A13-1* (*cyp71A13*) and *pad3-1* (*pad3*) mutant plants, respectively (Fig. 5.5A). In both mutants, this was accompanied with a strong over-accumulation of IAN, a camalexin pathway intermediate that did not or only slightly accumulate in the wild-type (Fig. 5.5B). This finding is consistent with the reported function of *PAD3* downstream of IAN generation (Böttcher et al., 2009), as blockage of a particular metabolic pathway can result in precursor accumulation. However, since *CYP71A13* is reported to catalyze IAOx to IAN conversion (Nafisi et al., 2007), over-accumulation of IAN in *cyp71A13* knockout plants is not readily comprehensible with the currently proposed schemes for camalexin biosynthesis (Geu-Flores et al., 2011; Su et al.,

2011). Moreover, the *cyp71A13* but not *pad3* mutant plants also exhibited *Psm*-induced over-accumulation of I3A and ICA (Fig. 5.5C, D).

Another gene strongly up-regulated in *Psm*-inoculated leaves is *CYP81F1*, one out of four CYP81F gene family members. Transcript levels of the other three members are only slightly (*CYP81F2*) or not (*CYP81F3* and *CYP81F4*) affected by *Psm* inoculation (Table S3). Transient expression assays in *Nicotiana benthamiana* using individual CYP81F isoforms indicate that all four members are capable of hydroxylating I3M to 1- and/or 4-hydroxyindole glucosinolates, which are subsequently methylated in planta (Pfalz et al., 2011). Consistently, Bednarek and colleagues have shown that *CYP81F2* is essential for the powdery mildew-induced accumulation of 4-methoxyindol-3-ylmethylglucosinolate (Bednarek et al., 2009). Surprisingly, both a *cyp81f1* and a *cyp81f2* knockout line showed strongly reduced accumulation of camalexin in *Psm*-inoculated leaves (Fig. 5.5A). Moreover, as in *cyp71A13*, the reduced camalexin production was associated with a marked over accumulation of IAN, I3A, and ICA in both *cyp81f1* and *cyp81f2* (Fig. 5.5B-D). Further, opposing to Col-0 and *pad3*, bacterial attack did not result in decreased levels of the indole glucosinolate I3M in *cyp81f1*, *cyp81f2*, and *cyp71A13* (Fig. S13). Therefore, defects in the two *CYP81F* isoforms and in *CYP71A13* have severe impact on the accumulation of metabolites originating from different branches of indolic metabolism.

The immune regulator salicylic acid is synthesized in *P. syringae*-inoculated *Arabidopsis* leaves and coordinates the activation of different defense pathways (Vlot et al., 2009). We investigated the impact of exogenously supplied SA on the induction of indolic metabolism, both alone and in combination with a *Psm* challenge (Fig. 5.6A). For this purpose, leaves of Col-0 plants were infiltrated with 0.5 mM SA, and 4 hours later, the same leaves were infiltrated with mock-solution, a *Psm* suspension, or not treated again. Leaf samples were harvested at 10, 24, and 48 h after the second treatment. SA treatment alone was sufficient to trigger about 5-fold increases in the levels of I3A, and this was apparent for all the time points under investigation and accompanied with decreases in the levels of the precursor glucosinolate I3M (Fig. 5.6A). Moreover, a *Psm* challenge following SA pretreatment resulted in significantly stronger increases of I3A than *Psm* challenge alone at 10 hpi. This effect was levelled out at later time points after bacterial challenge (Fig. 5.6A). Camalexin levels were also increased by exogenous SA alone, although this effect was quantitatively small and only observable late after SA application (from day 1 after treatment onwards). In addition, an SA pre-treatment did not augment the *Psm*-induced camalexin

accumulation (Fig. 5.6A). Exogenous SA had also no significant effect on basal and *Psm* induced ICA levels until 24 h after bacterial inoculation (Fig. S15). However, the *Psm* triggered accumulation of ICA, I3A, and camalexin was lower in SA-pretreated plants at the latest time point after inoculation (48 hpi; Fig. 5.6A, Fig. S15). This might be related with the strong resistance increase induced by exogenous SA and a consequential significant attenuation of bacterial growth at later infection stages (Fig. S16D), resulting in a considerable lower pathogen stimulus during later stages of the bacterial challenge.

The previous analysis revealed a remarkable effect of the defense hormone SA on indolic metabolism – it promotes I3A generation at the expense of its precursor I3M (Fig. 5.6A). Pipecolic acid, another immune and SAR regulatory metabolite, also affects the indole pathway, since it is able to prime Arabidopsis plants for enhanced camalexin accumulation (Návarová et al., 2012). Interestingly, pre-treatments of plants with Pip also resulted in a significantly stronger *Psm*-induced generation of I3A and ICA in leaves (Fig. 5.6B). The primed *Psm*-induced generation of I3A in the presence of elevated Pip was not associated with a stronger pathogen-triggered decrease of I3M, indicating that Pip stimulates I3A generation by general pathway activation rather than by specifically promoting I3M to I3A conversion (Fig. 5.6B). Pip treatment without subsequent pathogen challenge had no marked effect on I3A or ICA levels (Fig. 5.6B). Together, these analyses and our previous findings indicate that Pip primes the *P. syringae*-induced activation of several distinct branches of indolic metabolism in Arabidopsis (Fig. 5.6B; Návarová et al., 2012).

Indolic compounds in systemic acquired resistance

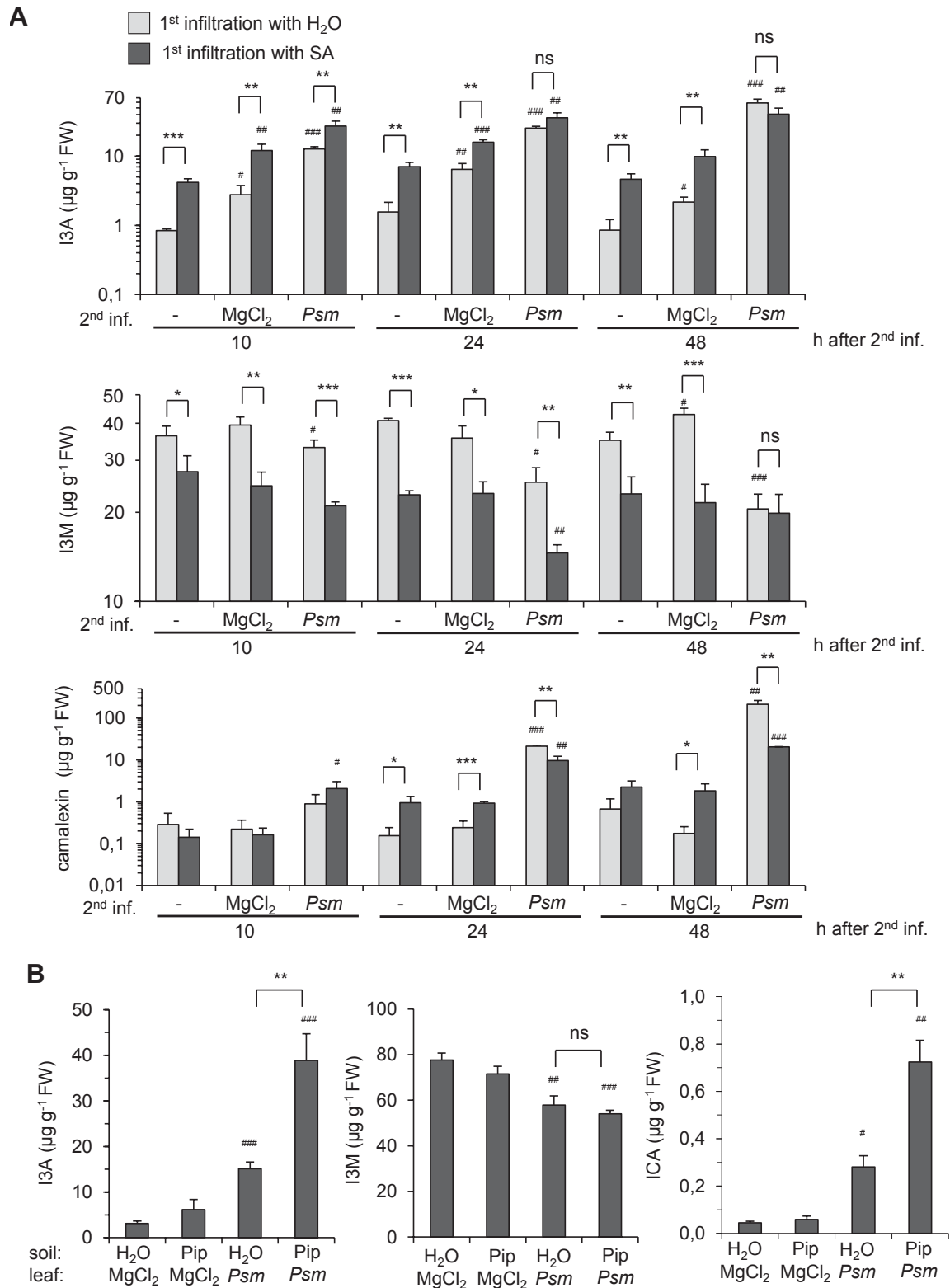


Figure 5.6 Impact of exogenous salicylic acid and pipercolic acid treatments on basal and inducible levels of indolics in leaves of Col-0 plants.

Figure-legend is given on the next page.

Legend for figure 5.6:

(A) Exogenous SA increases the basal and *Psm*-inducible levels of I3A at the expense of I3M. Please note the logarithmic scaling of the y-axes.

Three leaves of soil-grown Col-0 plants were first infiltrated with H₂O (light bars) or 0.5 mM SA solution (dark bars) (1st infiltration/inf.). 4 hours later, the same leaves were subject to a second infiltration (2nd inf.) with a 10 mM MgCl₂ (mock) solution or a suspension of *Psm*. For a third batch of plants, leaves were kept untreated (-) after the first infiltration. The leaves were harvested at the indicated times after the second treatment. Data represent the mean ± SD of three biological replicate leaf samples from different plants. Asterisks denote statistically significant differences between the respective H₂O and SA treatments (***P < 0.001, **P < 0.01, *P < 0.05, ns: no significant differences; two tailed *t* test). Hash symbols above a *Psm*-sample indicate whether statistically significant differences exist between the secondarily mock- or *Psm*-treated samples that received the same first treatment. Analogously, hash symbols above a MgCl₂-sample indicate whether statistically significant differences exist between the secondarily mock-treated and the untreated (-) samples (####P < 0.001, ###P < 0.01, #P < 0.05; two tailed *t* test).

(B) Exogenous Pip primes plants for enhanced *Psm*-triggered I3A and ICA accumulation.

Soil-grown Col-0 plants were supplied with 10 ml of 1 mM Pip (corresponding to a dose of 10 µmol) or with 10 ml of H₂O (control treatment) via the root system. Leaves were challenge-inoculated with *Psm* or mock-infiltrated with 10 mM MgCl₂ one day later. Metabolite levels in leaves were determined 10 h after the challenge treatment. Values represent the mean ± SD of three biological replicates from different plants. Asterisks indicate whether statistically significant differences exist between the H₂O/*Psm*-samples and the Pip/*Psm*-samples (***P < 0.001, **P < 0.01, *P < 0.05, ns: no significant differences; two tailed *t* test). Hash symbols indicate whether statistically significant differences exist between a given sample and the respective H₂O/mock-control samples (####P < 0.001, ###P < 0.01, #P < 0.05; two tailed *t* test).

5.3.4 Systemic accumulation of I3A, ICA, and ICC is dependent on *CYP79B2/3*, *PEN2*, *MYB34/51* and requires functional SAR signaling

We next examined the genetic components required for the specific accumulation of I3A, ICA, and ICC in systemic, non-inoculated leaf tissue upon SAR induction. Unlike wild-type plants, *cyp79b2/3*, *pen2*, and *tmyb* mutant plants completely lacked the accumulation of I3A, ICA, and ICC in 2° leaves upon 1° leaf-inoculation (Fig. 5.7). In addition, systemic accumulation of the three indolics was reduced in *myb34* and *myb51* single mutant and in *myb51 myb122* double mutant plants, whereas *cyp71A13* and *myb122* showed wild-type-like accumulation patterns (Fig. 5.7; Fig. S14B). Thus, the systemic accumulation of indolic metabolites in Arabidopsis fully depends on functional CYP79B2/3, PEN2, and on the combined action of the three myb factors, in particular MYB34 and MYB51. A notable difference between local and systemic accumulation of indole derivatives relies in the fact that they accumulate in a partially PEN2-independent manner in 1° leaves, whereas they fully require PEN2 to

accumulate in 2° leaves.

We then addressed the question as to whether the systemic accumulation of I3A, ICA, and ICC would be functionally relevant for the SAR response. To tackle this issue, we first examined whether the systemic increase of indolics would be associated with the ability of plants to induce SAR. Two indispensable SAR players are Arabidopsis ALD1 and FMO1, which are required for the biosynthesis and signal transduction of the SAR regulator pipecolic acid, respectively (Návarová et al., 2012). In SAR-defective *ald1* and *fmo1* mutants (Song et al., 2004; Mishina and Zeier, 2006; Bernsdorff et al., 2016), the systemic accumulation of the indolics was fully absent (Fig. 5.8A). In contrast, I3A, ICA, and ICC accumulated in inoculated leaves of *ald1* and *fmo1* to at least the same levels than in inoculated Col-0 leaves (Fig. 5.8B), indicating that Pip signaling is required for the systemic but not the local production of the indolics.

Two other important SAR components are ICS1/SID2, which is necessary for the pathogen-induced accumulation of SA (Nawrath and Métraux, 1999; Wildermuth et al., 2001), and NON-EXPRESSION OF PATHOGENESIS-RELATED GENES1 (NPR1), a transcriptional co-activator that acts downstream of SA and has been identified as a bona fide SA receptor (Wu et al., 2012; Fu and Dong, 2013). Although SA-deficient *sid2-1* (*sid2*) mutants are strongly impaired in their ability to induce SAR, recent experiments in our laboratory indicate that a modest residual SAR response takes place in *Psm*-inoculated *sid2* (Bernsdorff et al., 2016). Consistent with this, the *Psm*-induced systemic accumulation of I3A, ICA, and ICC was markedly reduced but not fully absent in *sid2* (Fig. 5.8A). Moreover, *npr1-2* (*npr1*) mutant plants, which suffer from a total loss of *Psm*-triggered SAR (Mishina and Zeier, 2006; Attaran et al., 2009; Návarová et al., 2012), completely fail to accumulate indolic compounds in 2° leaf tissue (Fig. 5.8A). In *Psm*-inoculated *sid2* and *npr1* leaves, by contrast, the accumulation of ICA and ICC was not impaired. However, a small but significant reduction of I3A accumulation was detected in both *sid2* and *npr1* (Fig. 5.8B), confirming our conclusions from SA feeding experiments that SA positively regulates *Psm* induced I3A generation (Fig. 5.8B). Together, the compromised accumulation of I3A, ICA, and ICC in distal leaves of *ald1*, *fmo1*, *sid2*, and *npr1* indicates that systemic activation of indolic metabolism after *Psm* inoculation requires functional SAR signaling.

Indolic compounds in systemic acquired resistance

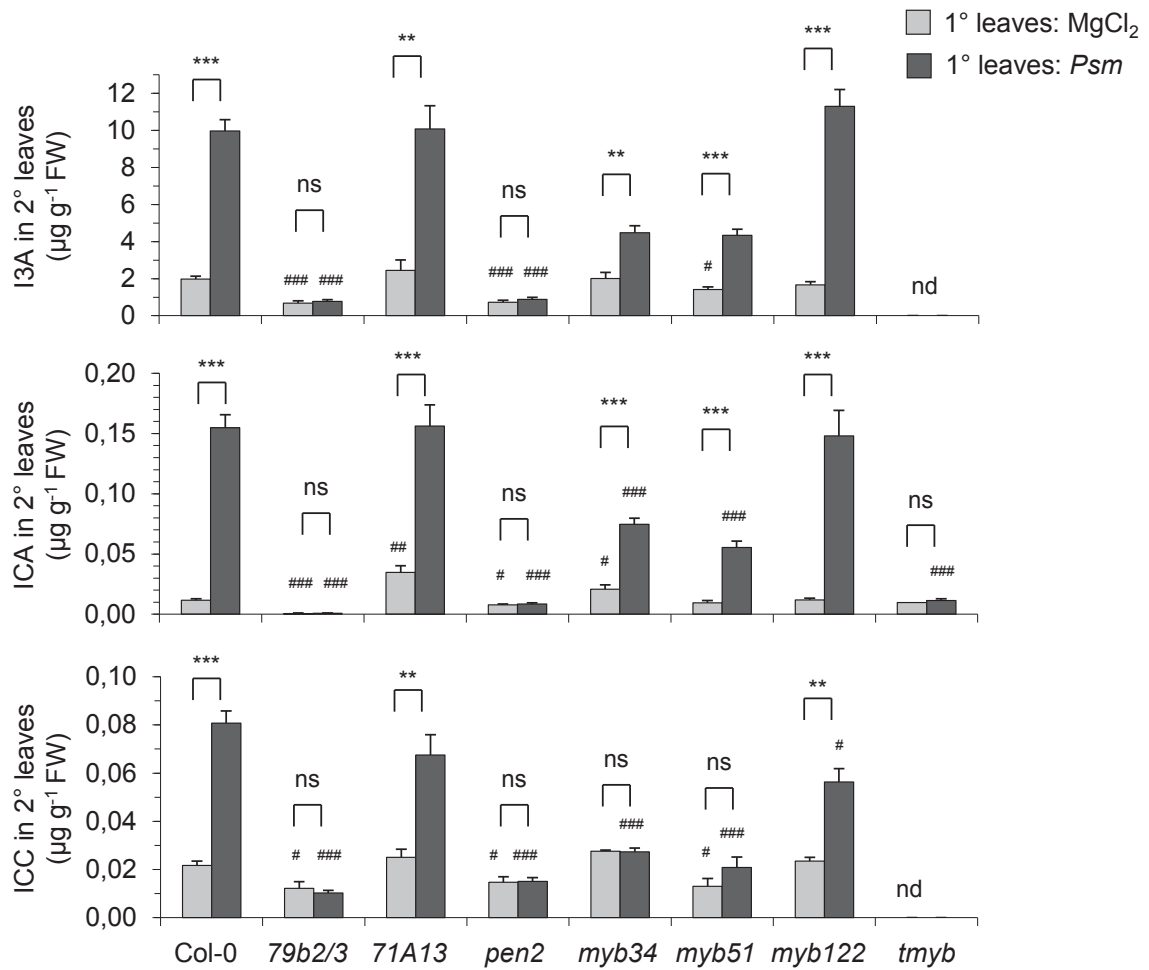


Figure 5.7 *P. syringae*-inducible indole accumulation in mutants impaired in indolic metabolism in leaves distal from the inoculation site.

Levels of I3A, ICA, and ICC in Col-0, *cyp79b2/b3*, *cyp71A13*, *pen2*, *myb34*, *myb51*, *myb122*, and *myb34/51/122* (*tmyb*) in upper (2°) leaves after *Psm*-inoculation or MgCl₂-infiltration of lower (1°) leaves. Metabolite levels were determined at 48 hpi. Data represent the mean ± SD of at least three replicate samples. Asterisks denote statistically significant differences between MgCl₂ and *Psm* treatment in one genotype (***P < 0.001, **P < 0.01, *P < 0.05, ns: no significant differences; two tailed *t* test). Hash symbols denote statistically differences between the same treatment of Col-0 and the corresponding mutant (####P < 0.001, ###P < 0.01, #P < 0.05; two tailed *t* test).

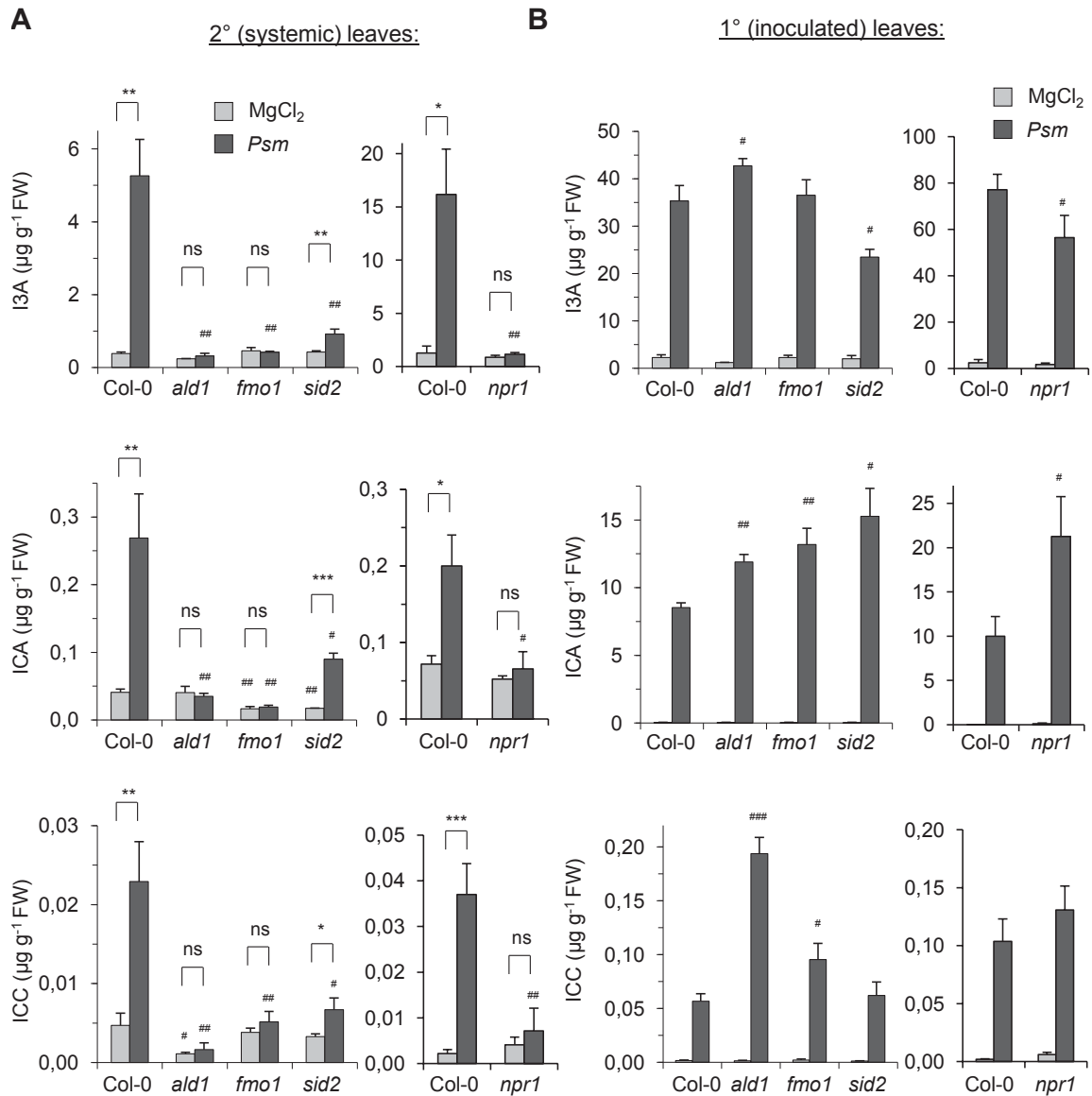


Figure 5.8 Levels of indolic metabolites in leaves of SAR-deficient mutant plants following *P.syringae* inoculation.

Levels of I3A, ICA and ICC in soil-grown Col-0, Pip-deficient *ald1*, *fmo1*, SA-deficient *sid2*, and *npr1* in (A) 2° leaves distal to the inoculation site and (B) in 1°, *Psm*-inoculated leaves. Levels of metabolites were determined at 48 hpi. A MgCl₂-infiltration of 1° leaves served as the mock-control treatment. Data represent the mean ± SD of at least three replicate samples. Two independent experiments, one comprising Col-0, *ald1*, *fmo1*, and *sid2*, and one involving Col-0 and *npr1*, are shown. Compare legend to Fig. 5.4 for further details.

5.3.5 Pre-induced immunity of soil-grown *cyp79b2/3* and *pen2* plants mask their intrinsic ability for SAR establishment

The absence of *Psm*-induced systemic accumulation of I3A, ICA, and ICC in *cyp79b2/3*, *pen2* and *tmyb* mutant plants allowed us to directly test their functional relevance in the SAR process. Therefore, we inoculated soil-grown plants with *Psm* in lower 1° leaves to induce SAR or performed a control treatment by infiltrating 10 mM MgCl₂. 48 h later, upper 2° leaves of both induced and control plants were challenge-inoculated with *Psm*, and bacterial growth in 2° leaves was assessed three days after the challenge inoculation (Mishina and Zeier, 2007). Wild-type Col-0 plants showed a strong and highly reproducible SAR response, as bacterial multiplication in challenge-inoculated 2° leaves was generally attenuated by 20- to 50-fold as a consequence of the 1°-*Psm*-treatment (Fig. 5.9A). The situation for *cyp79b2/3* and *pen2* plants was different, because mock-treated plants of these mutants generally exhibited a higher resistance than mock-control plants from the wild-type. The 1° *Psm*-treatment in these lines either failed to induce a significant SAR response or only had a comparatively weak resistance-inducing effect. A typical experimental outcome is shown in Fig. 5.9A, although the amount of pre-induced resistance in *cyp79b2/3* and *pen2* as well as the degree of the apparently weakened SAR effect in these mutants showed some variation between experiments. We then compared basal resistance to *Psm* on naïve, not previously treated Col-0, *cyp79b2/3*, and *pen2* plants and confirmed the elevated resistance phenotype of soil-grown *cyp79b2/3* and *pen2* (Fig. 5.9B).

Because of the varying degree of pre-induced resistance in *cyp79b2/3* and *pen2*, we reasoned that variations of resistance-inducing environmental cues during plant growth rather than direct regulatory effects of indolic metabolites might underlie the observed SAR attenuation. When plants were grown in hydroponic culture rather than in soil, the differences in basal resistance between Col-0, *cyp79b2/3*, and *pen2* were virtually absent (Fig. 5.9B). Notably, the strongly diminished induction of growth-related resistance in hydroponically cultivated *cyp79b2/3* and *pen2* plants was associated with the ability to establish a strong and reproducible SAR response in these mutants (Fig. 5.9A). This difference between soil- and hydroponically grown plants also got apparent when basal and systemically induced levels of SA were determined. Soil-grown control plants of *cyp79b2/3* and *pen2* contained elevated basal SA levels compared to soil grown wild-type plants (Fig. 5.9C). They also failed to increase SA levels in 2° leaves upon 1° leaf-inoculation, a characteristic SAR response that is stably observed in wild-type Col-0 plants (Fig. 5.9C). In contrast to soil-grown

plants, hydroponically cultivated *cyp79b2/3* and *pen2* plants exhibited small or no elevated basal levels of SA, respectively, and systemic SA levels increased to similar levels than in the wild-type upon SAR induction by *Psm* (Fig. 5.9C). This again indicates that cultivation-dependent resistance induction of *cyp79b2/3* and *pen2* plants alleviate their ability to systemically respond to bacterial inoculation.

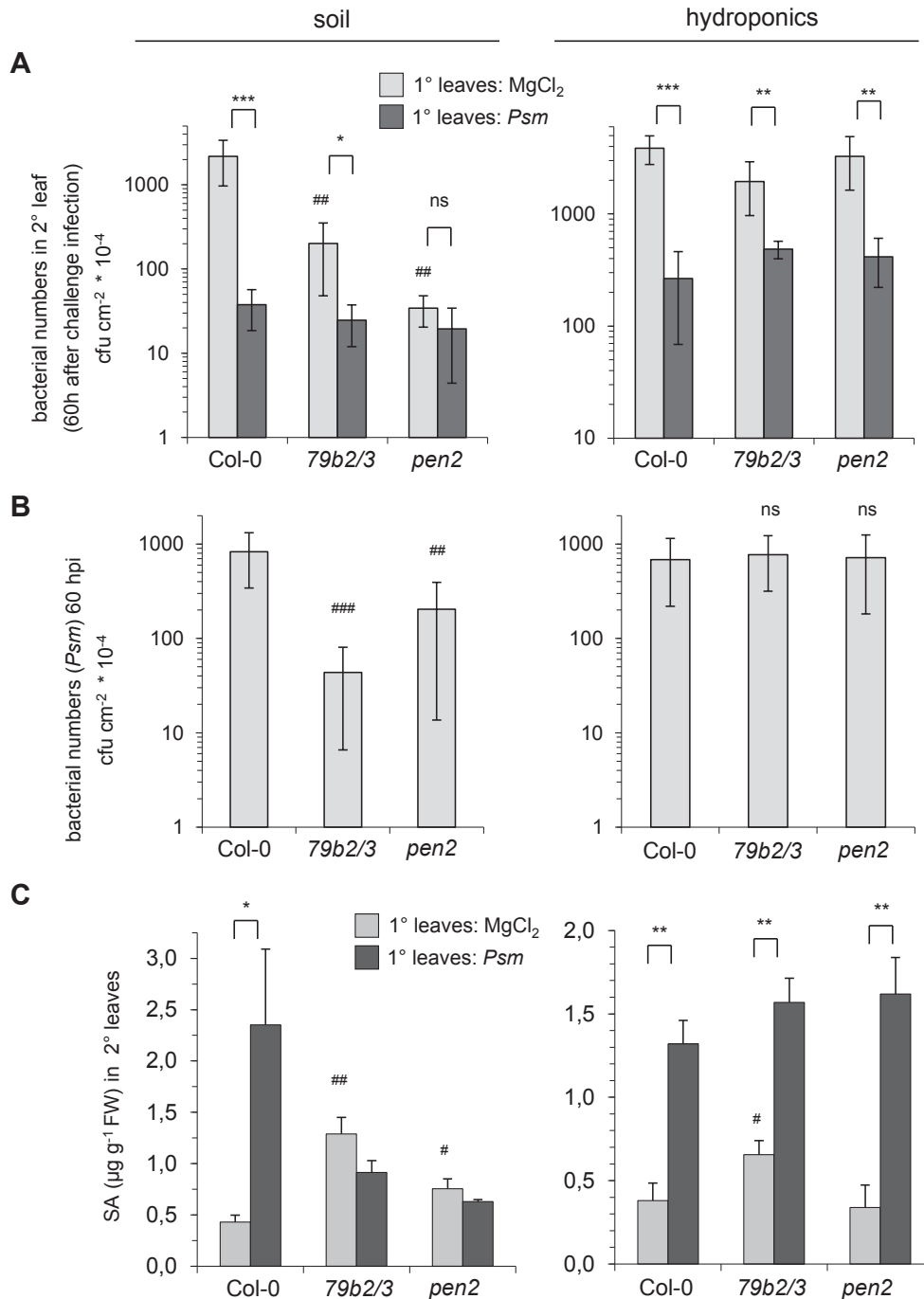


Figure 5.9 Pre-induced immunity of soil-grown *cyp79b2/3* and *pen2* plants dampens *P. syringae*-triggered SAR.

Figure-legend is given on the next page.

Legend Figure 5.9:

(A) SAR assays using soil-grown (left) and hydroponically-cultivated (right) Col-0, *cyp79b2/b3* and *pen2* plants. Lower (1°) leaves were infiltrated with either 10 mM MgCl₂ or inoculated with *Psm* to induce SAR. Two days later, three upper (2°) leaves were challenge-infected with *Psm*. Bacterial growth in upper leaves was determined 60 h post 2° leaf-inoculation. Data represent the mean ± SD of at least seven replicate samples. Asterisks denote statistically significant differences between *Psm*-pre-treated and mock-control samples (***P < 0.001, **P < 0.01, *P < 0.05, ns: not significant; two tailed *t* test). Hash symbols denote statistically significant differences between the same treatment of Col-0 and the corresponding mutant within one cultivation system (####P < 0.001, ###P < 0.01, #P < 0.05; two tailed *t* test).

(B) Basal resistance assay in Col-0, *cyp79b2/b3* and *pen2* with soil-grown plants and plants cultivated in a hydroponic system. Full-grown leaves of naïve plants were inoculated with *Psm*, and bacterial growth was assessed 60 h later. Data represent the mean ± SD of at least seven replicate samples. See (A) for further details.

(C) Levels of SA in distal, 2° leaves upon *Psm*-inoculation of 1° leaves of soil- and hydroponically-cultivated Col-0, *cyp79b2/b3* and *pen2* plants at 48 hpi. MgCl₂-infiltration of 1° leaves served as the mock-control treatment. Data represent the mean ± SD of at least three replicate samples. Details as described in the legend to Fig. 5.7.

Similar to *cyp79b2/3* and *pen2*, *tmyb* mutant plants lacked the systemic elevation of I3A, ICA, and ICC upon *Psm* inoculation, and *myb34*, *myb51*, and *myb51myb122* showed a markedly attenuated but not fully compromised accumulation of the indolics (Fig. 5.7; Fig. S14B). Compared to the wild-type, soil-grown *myb34*, *myb51*, *myb51 myb 122*, and *tmyb* plants also exhibited a moderately elevated basal resistance to *Psm*, but this resistance phenotype was markedly less pronounced than the strong phenotype of soil-grown *cyp79b2/3* and *pen2* (Fig. 5.10). Moreover, all the *myb* mutants were able to increase resistance of 2° leaves to *Psm* in response to a 1° bacterial inoculation to the same extent as Col-0 plants, indicating normal SAR induction in these lines (Fig. 5.10). SAR establishment in the *myb* lines was also associated with a significant increase of SA levels in 2° leaves (Fig. S17). These findings and the overall SAR data on *cyp79b2/3* and *pen2* indicate that the systemic elevation of I3A, ICA, and ICC observed upon bacterial attack are not crucial for the establishment of SAR in Arabidopsis.

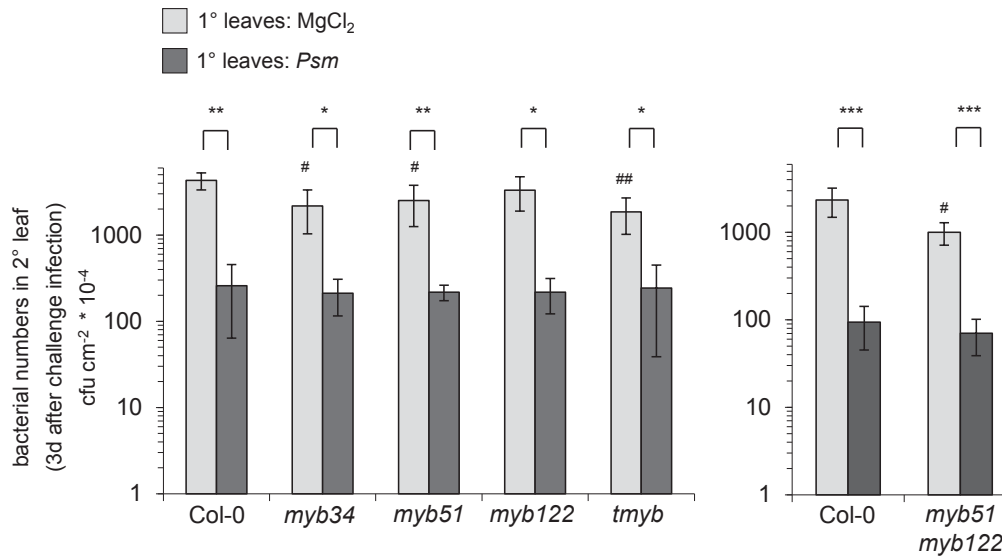


Figure 5.10 **Soil-grown *myb34*, *myb51*, *myb122*, *myb51 myb122*, and *tmyb* plants display normal SAR.**

SAR assay with soil grown Col-0, *myb34*, *myb51*, *myb122*, *myb51 myb122*, and *myb34/51/122* (*tmyb*) plants, as described in the legend of Fig. 5.9A.

5.3.6 Exogenous application of indole-3-carboxylic acid does not lead to a major resistance increase to *Psm* infection

We have shown previously that exogenous feeding of Arabidopsis or tobacco plants with physiological doses (10 μ mol) of the SAR regulator Pip, which systemically accumulates in the plant, substantially increases basal resistance to *P. syringae* (Návarová et al., 2012; Vogel-Adghough et al., 2013; Bernsdorff et al., 2016). Analogously, we investigated whether exogenous application of ICA, one of the systemically accumulating indolics that is commercially available, would elevate resistance of Arabidopsis plants to *Psm* infection. For that, we applied 10 μ mol of exogenous ICA to pots of individual Arabidopsis plants and challenge-inoculated leaves one day later with *Psm* (Návarová et al., 2012). In one out of several independent experiments, ICA slightly increased resistance of plants to a subsequent *Psm* challenge in a significant manner, but this increase was low when directly compared to resistance induction by exogenous Pip (Fig. S16A). In the remaining experiments, exogenous ICA failed to induce resistance of Col-0 plants to *Psm* in a statistically significant manner (Fig. S16B, C). In addition to Col-0, we also employed plants with defects in SAR and/or basal resistance in this assay (Fig. S16C). The mutants included knockout lines of the two key immune regulatory genes *PHYTOALEXIN-DEFICIENT4* (*PAD4*) and *NPR1* (Feys et al., 2001; Fu and Dong, 2013). Both *pad4-1* (*pad4*) and *npr1* knockout lines exhibited significantly decreased

basal resistance to *Psm* than Col-0 plants, and ICA treatment resulted in a small but significant resistance increase in these mutants which corresponded to a two-fold reduction of bacterial growth at 3 dpi (Fig. S16C). In addition to soil feeding, we also syringe-infiltrated leaves of Col-0 plants with 0.5 mM ICA or SA solutions, challenged-inoculated the same leaves 4 h later with *Psm*, and scored bacterial growth three days later. Whereas SA pre-treatment strongly induced resistance to *Psm*, ICA pre-treatment had no effect (Fig. S16D). Together, the ICA feeding experiments support above-described genetic studies which indicate that ICA is not a critical regulator of SAR and basal immunity to *Psm*. However, ICA seems to moderately contribute to *Psm* resistance if major immune signaling pathways are dysfunctional.

5.4 Discussion

Trp catabolism in Arabidopsis proceeds via the cytochrome P450s CYP79B2 and CYP79B3 and diverges into different metabolic branches, leading to the synthesis of indole glucosinolates and their breakdown products, camalexin biosynthesis, and the formation of a series of other low molecular weight indolics such as ICA (Fig. 5.11A; Glawischnig, 2007; Bender and Celenza, 2009; Sonderby et al., 2010; Bednarek, 2012). Previous studies have demonstrated crucial roles of Trp-derived indolics in Arabidopsis immunity against herbivores and a diverse range of microbial pathogens (Glawischnig, 2007; Kim et al., 2008; Bednarek, 2012). In this study, we show that Trp-derived metabolism is broadly activated in Arabidopsis after inoculation with the hemibiotrophic, SAR-inducing bacterial pathogen *Pseudomonas syringae* pv. *maculicola*, both at sites of bacterial attack (Fig. 5.11A) and in leaves distant from inoculation. Using Arabidopsis lines defective in defined biochemical or regulatory steps of Trp-derived secondary metabolism, we have investigated regulatory aspects of *P. syringae*-induced indolic metabolism and its functional significance for SAR.

5.4.1 Activation and regulatory aspects of Trp-derived metabolism in *P. syringae*-inoculated leaves

The induction of indolic metabolism in *Psm*-inoculated Col-0 leaves involves, besides a massive production of the phytoalexin camalexin (Tsuji et al., 1992; Glazebrook and Ausubel, 1994; Zhao and Last, 1996), a similarly strong accumulation of the indole glucosinolate breakdown product I3A, markedly enhanced production of ICA, ICC, ICN, I3C, tryptophol, and indole, and the formation of several other, not yet entirely identified indolics (Fig. 5.1; Fig. 5.11A). These metabolites are not or only in traces detectable in the *cyp79b2/3* double mutant (Table 1; Figs. 5.2, 5.4, 5.11A).

Enhanced de novo synthesis of the precursor amino acid Trp is an integral part of the *P. syringae*-induced activation of indolic metabolism in Arabidopsis (Fig. 5.2; Hagemeyer et al., 2001; Návarová et al., 2012). The blockage of the first step of Trp catabolism in *cyp79b2/3* results in an over-accumulation of the pathway precursor Trp in leaves under basal conditions and after *P. syringae* infection (Figs. 5.4, 5.11A).

Our study approves that camalexin accumulation is restricted to the sites of bacterial attack and does not extend to distal leaves (Fig. 5.2; Gruner et al., 2013). During the first hours after *P. syringae* inoculation, camalexin production lags behind the synthesis of I3A, ICA, or the phenolic SA in naïve plants (Fig. 5.3). After SAR establishment, however, plants are primed for a faster induction of camalexin biosynthesis if pathogen challenge occurs again (Návarová et al., 2012). Priming of camalexin biosynthesis requires the accumulation of the SAR regulator Pip, and a feasible mechanism includes partial pre-activation of the biosynthetic pathway at the level of transcription, since *CYP71A13* and *PAD3* but not *CYP79B2/3* are up-regulated systemically in SAR-induced plants (Návarová et al., 2012; Gruner et al., 2013; Table S3). Remarkably, feeding of plants with Pip not only primes plants for enhanced camalexin accumulation (Návarová et al., 2012) but also for a stronger production of two other major *P. syringae*-induced indolics, I3A and ICA (Fig. 5.6B). Therefore, Pip is able to prime the activation of several distinct branches of inducible indolic metabolism in Arabidopsis (Fig. 5.11A).

Although camalexin heavily accumulates upon bacterial attack in Arabidopsis leaves, bacterial growth assays with camalexin-deficient *pad3* demonstrate that the phytoalexin is dispensable for the full expression of basal immunity to *P. syringae* (Glazebrook and Ausubel, 1994). By contrast, camalexin is a direct resistance determinant of Arabidopsis to the necrotrophic fungi *Alternaria brassicicola*, *Botrytis cinerea*, and *Leptosphaeria maculans*, as well as to the oomycete pathogen *Phytophthora brassicae* (Thomma et al., 1999; Bohman et al., 2004; Ferrari et al., 2007; Schlaeppi et al., 2010). In line with previous studies (Zhou et al., 1999; Glawischnig et al., 2004; Nafisi et al., 2007), our data show that *P. syringae*-induced camalexin accumulation proceeds via the biosynthetic genes *CYP79B2/3*, *CYP71A13* and *PAD3* (Fig. 5.4; Fig. 5.5A; Fig. 5.11A). Further, our mutant analyses indicate that *MYB122* positively regulates *P. syringae*-induced camalexin accumulation (Fig. 5.4). *MYB122* was recently assigned an accessory role in the regulation of indolic glucosinolate biosynthesis, with *MYB34* and *MYB51* possessing a more dominant regulatory role in this pathway (Frerigmann and Gigolashvili, 2014; Fig. S13).

Moreover, MYB122 was shown to positively influence UV light-induced camalexin accumulation (Frerigmann et al., 2015). Thus, several transcription factor genes, including *WRKY33* (Mao et al., 2011), *ANAC042* (Saga et al., 2012), and *MYB122* (this study; Frerigmann et al., 2015) appear to be involved in the regulation of camalexin biosynthesis.

Similar to the biosynthetic mutant *cyp71A13*, both *cyp81f1* and *cyp81f2* display strongly reduced *P. syringae*-induced camalexin accumulation (Fig. 5.5A). When heterologously expressed in metabolically engineered *Nicotiana benthamiana* plants, Arabidopsis CYP81F1 and CYP81F2 have the biochemical capacity to 1- and 4-hydroxylate I3M, which is required for the formation of the methoxylated I3M derivatives 1- and 4-methoxy-I3M (1- and 4-MeO-I3M), respectively (Pfalz et al., 2011). Whereas *cyp81f2* shows reduced 4-MeO-I3M levels, corroborating a role for CYP81F2 in I3M methoxylation, *cyp81f1* shows a glucosinolate profile indistinguishable from the wild-type (Pfalz et al., 2011). Notably, the *cyp81F1* and *cyp81F2* mutants share also other metabolic peculiarities with *cyp71A13* (Fig. 5.5; Fig. 5.11A). Mutational defects in *CYP71A13*, *CYP81F1* and *CYP81F2* all result in a marked over-accumulation of I3A and ICA upon *Psm* inoculation (Fig. 5.5C, D). In addition, the levels of the indole glucosinolate I3M, which decrease in *Psm*-inoculated Col-0 leaves, rise in *cyp81F1*, *cyp81F2*, and *cyp71A13* upon bacterial attack (Fig. S13). And finally, IAN, an I3M hydrolysis product whose levels are virtually not enhanced by *Psm* attack in the wild-type (Kim et al., 2008; Fig. 5.5B), strongly accumulates in *Psm*-inoculated *cyp71A13*, *cyp81F1*, and *cyp81F2* (Fig. 5.5B). It is feasible that in *cyp81F1* and *cyp81F2*, impaired conversion of I3M into methoxylated forms redirects its catabolism towards hydrolytic breakdown and thus hyper-accumulation of substances such as I3A and IAN (Fig. 5.11A). This could in turn explain ICA over-production, since a biochemical pathway from IAN to ICA exists (Böttcher et al., 2014). By contrast, the strong camalexin-deficient phenotype of *cyp81F1* and *cyp81F2* cannot be readily explained by this supposed redirection of indolic metabolism on the basis of the currently discussed biosynthetic scheme, because over-accumulation of the pathway intermediate IAN should rather favour camalexin production (Fig. 5.11A). Similarly, over-accumulation of IAN in *cyp71A13* is unexpected, because recombinant CYP71A13 is able to convert IAOx into IAN (Nafisi et al., 2007), and a defect in the monooxygenase *in planta* is thus expected to result in IAN shortage. Potentially, blockage of the direct IAOx to IAN conversion step in *cyp71A13* redirects the metabolic flow towards indole glucosinolate formation, resulting in increased I3M production and subsequent I3M to IAN hydrolysis (Fig. 5.11A; Fig. S13). Compared to *cyp71A13*, *cyp81F1*, and *cyp81F2*, the

disturbances of indolic metabolism are more constrained in *pad3*, which is impaired in the final step of camalexin biosynthesis (Schuhegger et al., 2006). Here, the blockage of *Psm*-induced camalexin accumulation results in IAN over-production but does not affect I3A and ICA formation or the degradation of I3M after bacterial inoculation (Fig. 5.5; Fig. 5.11A; Fig. S13).

Besides camalexin biosynthesis, indole glucosinolate breakdown leading to I3A accumulation is a major part of indolic metabolism in *P. syringae*-inoculated Col-0 leaves (Fig. 5.2). I3A accumulation in Arabidopsis is so far documented to occur upon fungal and oomycete but not upon bacterial attack, for instance after leaf inoculation with the non-adapted powdery mildew *Blumeria graminis* f.sp. *hordei*, *P. brassicae*, *Plectosphaerella cucumerina*, and *Colletotrichum gloeosporioides* (Bednarek et al., 2009; Sanchez-Vallet et al., 2010; Schlaeppli et al., 2010; Hiruma et al., 2013). The determined levels of I3A accumulating in these interactions were between 1 and 10 nmol⁻¹ fresh weight (FW). In *P. syringae*-infected leaves, I3A accumulated to about 50 mg g⁻¹ FW at 48 hpi (Fig. 5.3), which, on a molar basis, corresponds to 340 nmol g⁻¹ FW. Therefore, the absolute levels of I3A produced in *P. syringae*-inoculated leaves exceed those previously quantified for fungal inoculations by one to two orders of magnitude.

Our study reveals a positive regulatory role of the defense hormone SA on I3A production. First, the *P. syringae*-induced levels of I3A are significantly lower in SA-deficient *sid2* and in SA downstream signaling-defective *npr1* than in the wild-type (Fig 5.8). Second, exogenous application of SA is sufficient to trigger I3A elevations with concomitant decreases of the precursor glucosinolate I3M (Fig. 5.6A). Third, induced I3A accumulation early after *P. syringae* inoculation is stronger in SA-pre-treated than in non-pre-treated plants (Fig. 5.6A). The generation of I3A after fungal attack fully depends on the atypical myrosinase PEN2 (Bednarek et al., 2009; Sanchez-Vallet et al., 2010). Although the production of I3A does not fully correlate with penetration resistance of Arabidopsis against non-adapted powdery mildews if different mutant lines are considered, genetic evidence indicates that indole glucosinolate degradation via PEN2 is a critical determinant of Arabidopsis preinvasion resistance to fungal and oomycete pathogens (Bednarek et al., 2009; Sanchez-Vallet et al., 2010; Schlaeppli et al., 2010; Hiruma et al., 2013). I3A accumulation in *P. syringae*-inoculated *pen2* leaves is markedly reduced but not fully abrogated (Fig. 5.4). This suggests that *P. syringae*-induced I3A is formed via PEN2-dependent and PEN2-independent pathways (Fig. 5.11A). Microarray data suggest that *PEN2* is not upregulated by SA after exogenous

treatment or *P. syringae* inoculation in Col-0 leaves (Thibaud-Nissen et al., 2006; Wang et al., 2008; Gruner et al., 2013). Taking the above SA regulatory role in I3A production into account, it is possible that another, SA-inducible β -glucosidase contributes to the PEN2-independent pathway of I3A formation from I3M (Fig. 5.11A).

I3A formation is also markedly impaired in *myb51* and *myb51 myb122*. Moreover, the *tmyb* triple knockout line fails to produce I3A in both control and Psm-inoculated plants (Fig. 5.4). Therefore, MYB51, alone and in combination with MYB34 and MYB122, has a major regulatory impact on *P. syringae*-induced I3A biosynthesis (Fig. 5.11A). This coincides with the regulatory role of MYB34 and MYB51 in the biosynthesis of the precursor glucosinolate I3M (Frerigmann and Gigolashvili, 2014; Fig. S13). Even though I3A accumulates to high levels in leaves of wild-type plants during the bacterial interaction, the I3A-depleted *pen2*, *cyp79b2/3*, and *tmyb* lines are not impaired in basal resistance to Psm (Fig. 5.9B), indicating that indole glucosinolate breakdown is not a critical determinant for basal immunity to compatible *P. syringae* bacteria.

The Trp-derived carboxylic acid ICA is an additional indolic compound that accumulates to levels of more than 1 mg g⁻¹ FW in Psm-inoculated Arabidopsis leaves at 48 hpi, which is quantitatively lower than camalexin or I3A production but in the range of induced SA levels (Fig. 5.3 and 5.4). A biochemical pathway involved in the AgNO₃-induced formation of ICA and glycosylated ICA derivatives has been established recently. IAN is thereby converted into the indolic aldehyde ICC by CYP71B6, and ICC is in turn oxidized to ICA by the aldehyde oxidase AAO1 (Böttcher et al., 2014). ICC is also synthesized upon *P. syringae* inoculation in leaves, albeit to lower amounts than ICA (Fig. 5.4). ICA, ICC, and hydroxylated and glycosylated derivatives thereof are formed in response to infection by different pathogens or abiotic stress in Arabidopsis roots and leaves (Hagemeyer et al., 2001; Bednarek et al., 2005; Böttcher et al., 2009; Gamir et al., 2012). Hydrolysis and chemical analyses of pathogen-treated leaf or root tissue indicate that a portion of the accumulating ICA, along with several benzoic acid and cinnamic acid derivatives, becomes esterified to cell walls upon pathogen inoculation (Tan et al., 2004; Forcat et al., 2010). From these studies, it is not yet clear whether free or bound ICA or ICC contribute to plant pathogen resistance. Our findings show that ICA and ICC formation in *P. syringae*-inoculated leaves depends on *cyp79b2/3* and is attenuated in *pen2* and *tmyb* (Fig. 5.4). Moreover, a recent study reports that the accumulation of ICA and ICA glucosides in Arabidopsis upon treatment with the bacterial PAMP flagellin is attenuated in *pen2* and

tmyb mutants (Frerigmann et al., 2016). This suggests that the hydrolysis of indole glucosinolates contributes to ICA and ICC production upon bacterial inoculation (Fig. 5.11A). Since the *cyp79b2/3*, *pen2*, or *tmyb* mutants do not exhibit defects in basal resistance to *Psm* (Fig. 5.9 and 5.10), it is unlikely that ICA or ICC represent major resistance determinants against compatible *P. syringae* infection. Our exogenous feeding assays indicate that the resistance-enhancing capacity of ICA in wild-type Col-0 plants is small to non-existent (Fig. S.16). However, a modest contribution of ICA to Arabidopsis resistance might exist if major resistance signaling components such as PAD4 or NPR1 are dysfunctional (Fig. S16C).

5.4.2 Systemic indole accumulation and its functional relevance for SAR

Notably, our results show that indolic metabolism is activated systemically when plants experience a locally restricted leaf inoculation with *P. syringae*. The metabolic response in leaves distant from the site of bacterial attack is quantitatively milder than the local response and specifically involves the accumulation of I3A, ICA, and ICC (Fig. 5.2). Thus, the three indoles share the relatively rare feature to systemically accumulate in the plant upon a localized bacterial inoculation with the SAR-regulatory metabolites Pip and SA (Návarová et al., 2012; Zeier, 2013). Among them, I3A is produced to highest levels in the distal leaf tissue, reaching values of about 10 mg g⁻¹ FW upon inoculation (Figs. 5.2 and 5.7). The absolute I3A levels after SAR activation are therefore in a similar range than the levels of Pip and higher than those of SA (Návarová et al., 2012).

The regulatory principles of *P. syringae*-induced I3A, ICA, and ICC formation differ in locally inoculated and in systemic tissue. First, systemic but not local indole accumulation requires the Pip and SA biosynthetic genes *ALD1* and *ICS1* (alias *SID2*) as well as intact *FMO1* and *NPR1* (Fig. 5.8). Therefore, functional SAR signaling, which involves Pip and SA accumulation, is required for the systemic but not local accumulation of I3A, ICA, and ICC. Second, the systemic production of I3A, ICA, and ICC is totally absent in the *pen2* and *tmyb* mutant lines, whereas their local accumulation is not fully compromised (Figs 5.4 and 5.7). This indicates that MYB34/51/122-regulated biosynthesis of indole glucosinolates and their PEN2-mediated breakdown are obligatory for the *P. syringae*-induced accumulation of I3A, ICA, and ICC in systemic leaf tissue (Fig. 5.7 and Fig. S13; Bednarek et al., 2009; Frerigmann and Gigolashvili, 2014). The ability of the *ald1*, *fmo1*, *sid2*, and *npr1* lines

of local indole production and their failure of systemic indole elevation also indicate that I3A, ICA, and ICC are synthesized de novo in distal tissue in context with SAR establishment rather than by long-distance transport from locally infected to uninfected, systemic leaves.

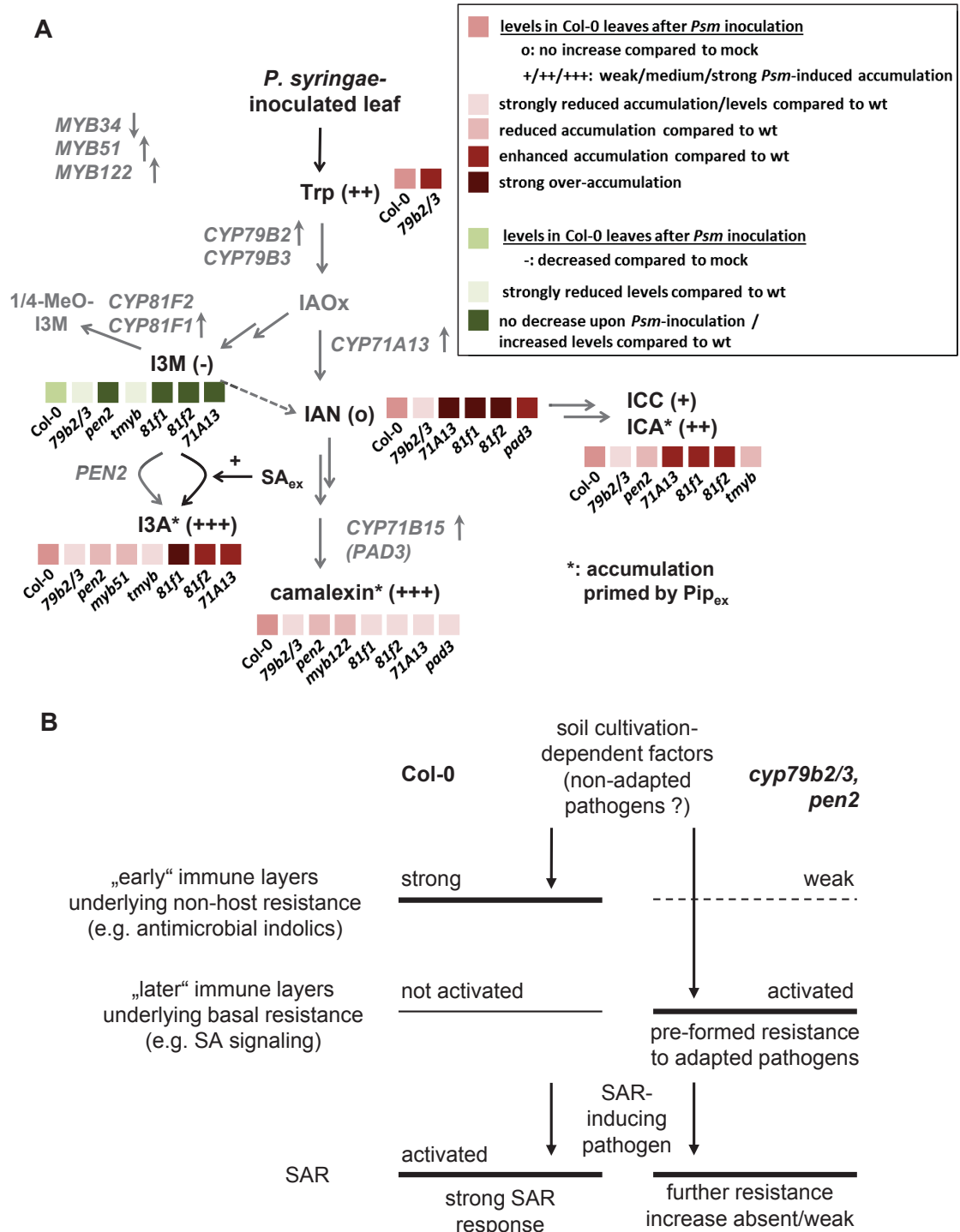


Figure 5.11 Regulation of induced indolic metabolism in *P. syringae*-inoculated leaves, and possible consequences of dysfunctional, indole-related early immune layers on basal resistance and SAR.

Figure-legend is given on the next page.

Legend Figure 5.11:

(A) Simplified scheme of Trp-derived indolic metabolism in Arabidopsis and its activation in *P. syringae*-inoculated leaves. The general pathway is depicted in grey. Small up (down) arrows symbolize gene up- (down-) regulation upon bacterial inoculation (see Table S3). Metabolites determined in leaf extracts in this study are illustrated in black. The number of plus signs in brackets symbolises the quantity of *Psm*-induced indole accumulation in inoculated Col-0 leaves (see legend). The coloured squares next to or below the assessed metabolites symbolise the levels of these metabolites compared to wild-type Col-0 in *Psm*-inoculated leaves of mutant plants (see legend for details). Only mutants with accumulation patterns markedly differing from the wild-type are depicted for a particular metabolite (abbreviations: *79b2/3* = *cyp79b2/3*, *71A13* = *cyp71A13*, *81f1* = *cyp81f1*, *81f2* = *cyp81f2*). The levels of indoles in leaves of mutant plants reflect the influences of the functional genes on (*Psm*-induced) indolic metabolism. Note that, besides the biosynthetic pathway genes *CYP79B2/3*, *CYP71A13* and *PAD3*, *CYP81F1*, *CYP81F2*, and *MYB122* positively regulate camalexin production. Functional *CYP71A13*, *CYP81F1*, and *CYP81F2* negatively affect I3A, IAN, ICA, and ICC levels. I3A formation is positively regulated by *PEN2*, *MYB51*, and *MYB34*, and a *PEN2*-independent mode for I3A production exists. ICA and ICC formation is also stimulated by the action of *PEN2*. Trp catabolism is incapacitated if *CYP79B2* and *CYP79B3* are defective, leading to Trp over-accumulation. Exogenous SA stimulates I3M to I3A conversion. Exogenous Pip primes plants for enhanced *Psm*-triggered accumulation of I3A, camalexin, and ICA.

(B) Soil cultivation-dependent pre-induced immunity in *cyp79b2/3* and *pen2* masks *P. syringae*-triggered SAR. In the Col-0 wild-type, early pre-invasion immune layers, involving indole glucosinolate hydrolysis products such as I3A, are intact. Post-invasion, inducible immune layers are not activated. These naïve plants are able to induce a strong SAR response upon *P. syringae* attack of leaves. In *cyp79b2/3* and *pen2*, indole metabolism and early immune layers are weakened, and a soil cultivation-dependent factor induces enhanced basal resistance and SA accumulation. In these non-naïve plants with pre-induced immunity, a further resistance increase by SAR-inducing *P. syringae* is low or absent.

After recognizing the systemic activation of indolic metabolism in *P. syringae*-inoculated Arabidopsis plants, a major aim of the current study was to test whether the systemically accumulating indoles would be functionally relevant for SAR. A previous finding that exogenous 3-acetyl-3-hydroxyoxindole, an oxidized indole derivative isolated from extracts of the Assam Indigo plant *Strobilanthes cusia*, activates the SA pathway and a SAR-like response in tobacco further pointed to this possibility (Li et al., 2008). Since *tmyb*, *pen2*, and *cyp79b2/3* failed to systemically elevate I3A, ICA, and ICC, and *myb34*, *myb51*, and *myb51 myb122* had a significantly weaker systemic response than the wild-type (Fig. 5.7 and Fig. S14B), we were directly able to test this hypothesis. Bacterial growth assays with *P. syringae* as the inducing and the challenging pathogen demonstrated, however, that the systemic accumulation of the indolics is not a decisive event for SAR establishment. First, soil-grown *tmyb* triple and *myb* single and double mutants were able to systemically enhance resistance to 2° bacterial challenge when inoculated in 1° leaves with *Psm* (Fig. 5.10). Along with this, an inducing leaf inoculation also resulted in significantly elevated levels of SA in distal

leaves of *tmyb* and *myb* single and double mutant plants (Fig. S17). Second, the *cyp79b2/3* and *pen2* mutants were able to induce a wild-type-like SAR response when grown in hydroponic culture, and this was again associated with an increase of SA in distal leaves upon *Psm* inoculation of 1° leaves (Fig 5.9A and 5.9C). The activation of SAR toward *P. syringae* and the associated activation of the SA pathway are therefore independent of the systemic accumulation of indolics.

Our data thus indicate that increased systemic de novo production of I3A, ICA, and ICC is a consequence rather than the cause of SAR activation, for which Pip and SA are the essential, signaling active metabolites (Nawrath and Métraux, 1999; Návarová et al., 2012; Bernsdorff et al., 2016; Fig 5.8A). However, although the elevated levels of indolics during SAR do not contribute to resistance induction toward the bacterial hemibiotroph *P. syringae*, they might well increase defense readiness against other pathogen types, because indole glucosinate breakdown products such as I3A are discussed as antifungal compounds providing direct protection against non-adapted and adapted fungal or oomycete pathogens (Bednarek et al., 2009; Consonni et al., 2010; Sanchez-Vallet et al., 2010; Schlaeppli et al., 2010; Bednarek, 2012; Hiruma et al., 2013). The well-established SAR assay system that uses Arabidopsis and *P. syringae* as the inducing and the challenging pathogen is predominantly employed in the current SAR research to study the mechanisms of SAR activation (Shah and Zeier, 2013). However, this system does not yield information about the broadness of resistance activation in SAR. To investigate the broad-spectrum character of SAR (Sticher et al., 1997) and the contributions of individual defense pathways in the protection against a particular pathogen, assays with different types of challenging pathogens should be developed in the future and combined with mutant analyses.

5.4.3 Cultivation-dependent pre-induced immunity in *cyp79b2/3* and *pen2* dampens *P. syringae*-triggered SAR

To varying degrees between individual experiments, soil-grown *cyp79b2/3* and *pen2* plants exhibited enhanced basal resistance and contained elevated SA levels, tendencies that were absent or only marginally observed in hydroponically cultivated plants (Fig. 5.9B and 5.9C). This suggests that soil cultivation-dependent factors pre-activate inducible immune responses such as the SA pathway in *cyp79b2/3* and *pen2* but not in the wild-type (Fig. 5.11B). Since CYP79B2/3 and PEN2 are essential components of pre-invasion immunity that underlie non-host resistance (Lipka et al.,

2005; Bednarek et al., 2009; Schlaeppli et al., 2010), defects in early immune layers seem to entail the activation of later layers, i.e. inducible defense responses, under certain growth conditions. Consistently, constitutively activated SA defenses were also observed for mutants defective in *PEN1* and *PEN3*, encoding a syntaxin and an ATP binding cassette transporter, respectively, which constitute other critical elements of Arabidopsis pre-penetration resistance to fungal ingress (Collins et al., 2003; Stein et al., 2006; Zhang et al., 2007). A speculative scenario is that soil-inhabiting microbes failing to overcome pre-invasion immune layers in the wild-type can pass these early obstacles in *cyp79b2/3* and *pen2* and, as a consequence, continuously elicit inducible, post-invasion responses in the course of plant growth. Plants thereby lose their naive character and increase resistance to adapted pathogens (Fig. 5.11B). This “pre-formed” immunity then apparently alleviates a further strong resistance enhancement upon inoculation with a SAR-inducing pathogen, which is observed in the naive wildtype (Fig. 5.11B). The SAR-positive phenotype of hydroponically grown, not pre-induced *cyp79b2/3* and *pen2* plants indicate their intrinsic ability to induce SAR. Interestingly, loss of *PEN1*, *PEN2*, *PEN3*, and *CYP79B2/3* attenuates the hypersensitive cell death response triggered by *P. syringae* effectors (Johansson et al., 2014), indicating that inducible immune responses other than SAR are affected if early plant immune layers are dysfunctional.

6 Metabolism and transport of Pip in Arabidopsis SAR

6.1 Abstract

Systemic acquired resistance (SAR) is a long lasting form of inducible plant immunity. SAR protects the entire foliage against a broad spectrum of pathogens and is triggered by a first inoculation or recognition of a pathogen in a locally defined leaf. The capability of SAR establishment in plants is dependent on pipercolic acid (Pip) and salicylic acid (SA) signaling pathways. Pip act as the main regulator of SAR and orchestrates SAR establishment via SA-dependent and –independent pathways. SA acts downstream of Pip and FLAVIN-DEPENDENT MONOOXYGENASE1 (FMO1) in defense-signal-amplification and is necessary for a complete and strong SAR response. Notably, Pip-deficient and Pip-insensitive *ald1* and *fmo1* mutants are completely SAR-deficient and don't show systemic defense responses upon local *P. syringae* inoculation. Here we investigated whether Pip can serve as a precursor for new potential defense related metabolites and investigated a potential role for Pip as a long-distance signal in SAR establishment. We therefore fed deuterium-labeled Pip into distinct leaves in combination with an infection with the hemibiotrophic bacterial pathogen *Pseudomonas syringae* pv. *maculicola* ES4326 (*Psm*). We show that exogenous fed Pip at the inoculation site can be metabolized to N-formyl-Pip and partially also to α -aminoadipic acid (Aad). Moreover, Pip can serve as a precursor for two until now not identified FMO1-generated metabolites. Furthermore, the exogenous fed Pip could be detected also in leaves distal to the site of application. However, this transport was not increased in plants which were in addition to Pip-infiltration also infected with *Psm*. Interestingly, Pip-deficient *ald1* mutant plants co-infiltrated with Pip and *Psm* could activate SAR systemic defense responses to a certain extent, whereas local Pip- or *Psm*-infiltration alone was not sufficient to trigger any systemic response in *ald1* mutant plants. Consistent with the previously described role of FMO1 in SAR downstream of Pip, the co-infiltration of Pip and *Psm* could, although partially complementing the SAR-defect of *ald1*, not restore SAR in *fmo1* mutant plants.

6.2 Introduction

Systemic acquired resistance (SAR) is a long lasting form of inducible plant immunity. SAR protects the entire foliage against a broad spectrum of pathogens and is triggered by a first inoculation or recognition of a pathogen in a locally defined leaf (Fu and Dong, 2013). Arabidopsis SAR in systemic leaf tissue (2°) can be activated by treatment of local leaves (1°) with compatible virulent and incompatible avirulent bacterial pathogens as well as by treatment with several PAMPs and insect eggs (Mishina and Zeier, 2007; Hilfiker et al., 2014). The establishment of SAR is accompanied by a strong transcriptional reprogramming in locally inoculated leaves and in leaf tissue distal to the site of inoculation (Gruner et al., 2013; Bernsdorff et al., 2016). Moreover, SAR establishment in response to bacterial pathogens is also accompanied by the accumulation of metabolites with a broad structural diversity at the infection-site, including amino acids, small benzoic acids, phytosterols, tocopherols, Trp-derived indolics, and others (this study; Griebel and Zeier, 2010; Chaouch et al., 2012; Návarová et al., 2012; Stahl et al., 2016). The accumulation of metabolites in systemic leaves is more specific. Only several metabolites are described to accumulate in leaves distal to the inoculation site in SAR-activated plants: The phenolic salicylic acid (SA) and its glucoside SAG (Vlot et al., 2009), the non-protein coding amino acid pipercolic acid (Pip) (Návarová et al., 2012), and the three Trp-derived indolic metabolites indol-3-ylmethylamine (I3A), indole-3-carboxylic acid (ICA), and indole-3-carbaldehyde (ICC) (Stahl et al., 2016). Whereas the systemic accumulation of the three indolic metabolites I3A, ICA, and ICC is dispensable for SAR-establishment (Stahl et al., 2016; Chapter 5), the systemic accumulations of SA and Pip are of utmost relevance for SAR establishment.

The generation of SA via ISOCHORISMATE SYNTHASE1 (ICS1) takes place in local infected leaves and in leaf tissue distal to that. Furthermore, the accumulation of SA in response to bacterial pathogens is closely related to SAR establishment and mutant plants deficient in SA biosynthesis exhibits highly increased basal susceptibility and highly decreased SAR (Gaffney et al., 1993; Nawrath and Métraux, 1999; Wildermuth et al., 2001; Vlot et al., 2009; Attaran et al., 2009). It is also well established that the positive regulation of SA biosynthesis by PHYTOALEXIN-DEFICIENT4 (PAD4), as well as SA downstream signaling via NONEXPRESSOR OF PATHOGENESIS-RELATED GENES (NPR1), contributes to PAMP-triggered immunity, effector-triggered immunity and SAR (Durrant and Dong, 2004; Vlot et al., 2009; Fu and Dong, 2013). However, recently it was shown that on the transcriptional

level not all systemic defense responses which contribute to SAR are abolished in SA-deficient *sid2* mutant plants. A local infection with the hemibiotrophic pathogen *Pseudomonas syringae* pv. *maculicola* ES4326 (*Psm*) triggers a strong transcriptional reprogramming in leaf tissue distal to the infection-site in Arabidopsis. Those regulated genes can be discriminated in downregulated (SAR-) and upregulated (SAR+) genes (Bernsdorff et al., 2016). Interestingly, a part of the SAR+ and SAR- genes is still regulated in SA-deficient *sid2* mutant plants, whereas other systemic processes which are accompanied with SAR establishment, such as the decrease in photosynthetic rate, are dependent on functional SA biosynthesis (Bernsdorff et al., 2016). Consistent with partial SAR activation on the transcriptional level, *sid2* mutant plants are able to activate a highly decreased but significant SAR upon *Psm*-infection. Therefore, defense-signaling pathways which contribute to SAR can be separated in SA-dependent and -independent pathways (Bernsdorff et al., 2016).

An outstanding functional role in SAR establishment is described for the Lys catabolite Pip (Fig. 1.3), a non-protein coding amino acid (Návarová et al., 2012). Pip is produced by several plants within the angiosperms (Morrison, 1953; Zacharius et al., 1954; Návarová et al., 2012). It was reported already 1968 by Pálfi and Dézsi that Pip is produced by several plant species under diseased conditions. Moreover, Pip is described as a neurotransmitter in rat brains (Charles, 1986). In Arabidopsis, Pip is produced via AGD2-LIKE DEFENSE RESPONSE PROTEIN 1 (*ALD1*) (Návarová et al., 2012; Zeier, 2013). The aminotransferase *ALD1* is described to exhibit a strong substrate specificity for Lys (Song et al., 2004a), and it could be shown that *ALD1* transcripts are increased in locally inoculated and systemic non-infected leaves during SAR establishment. Moreover, *ALD1* is indispensable for SAR establishment in Arabidopsis (Song et al., 2004b). Accordingly, it was shown that upon *Psm*-infection, Arabidopsis plants accumulate Pip at the inoculation sites, in leaves distal to the site bacterial inoculation, and in petiole-exudates collected from inoculated leaves (Návarová et al., 2012). Moreover, an *ald1* knock-out mutant is defective in Pip biosynthesis and fully impaired in any systemic defense response (Návarová et al., 2012; Bernsdorff et al., 2016). Exogenous applied Pip via the root-system can partial complement the susceptibility-phenotype of *ald1* mutant plants and furthermore also increase pathogen resistance of Col-0 wild-type plants (Návarová et al., 2012). The effect that exogenous applied Pip increases plant resistance against *P. syringae* could also be observed in *Nicotiana tabacum* cv Xanthi plants. Furthermore, exogenously applied Pip primes tobacco plants for a quicker and more vigorous activation of SA- and nicotine-biosynthesis after infection with *P. syringae* pv. *tabaci* (Vogel-Adghough et

al., 2013). Recently it could also be shown that Pip is also indispensable for SAR activation after oviposition by *Pieris brassicae* (Hilfiker et al., 2014). Moreover, several recent studies report that Pip is produced in response to several different plant pathogens, such as *Fusarium virguliforme*, *Rhizoctonia solani*, *P. syringae*, or aphids, in several different plant species such as soybean, tobacco, or rice (Vogel-Adghough et al., 2013, Klein et al., 2015; Abeysekara et al., 2016; Suharti et al. 2016). This indicates that Pip as a metabolite relevant for defense signaling is highly conserved within the plant kingdom. Pip has also been identified as a mediator of defense-priming associated with SAR (Návarová et al., 2012; Bernsdorff et al., 2016). Priming describes a status, induced by a first stress or an exogenous applied compound, in which a plant is able to react more quickly and vigorously to subsequent stressors (Conrath, 2011). In contrast to SA-deficient *sid2* mutant plants which activate SAR to a certain extent, Pip-deficient *ald1* mutant plants and Pip- and SA-deficient *sid2 ald1* double mutant plants fail to activate any systemic defense response after a local pathogen infection, indicating that Pip orchestrate SAR via SA-dependent and -independent pathways (Bernsdorff et al., 2016).

All hitherto studied defense responses that are orchestrated by Pip, such as SAR, defense priming, and Pip-mediated resistance, are dependent on functional *FLAVIN-DEPENDENT MONOOXYGENASE1 (FMO1)* (Návarová et al., 2012; Hilfiker et al., 2014; Bernsdorff et al., 2016). FMO1 was described before Pip as a crucial component in SAR establishment, and *FMO1* transcripts are increased in local and systemic leaves after local inoculation with compatible virulent and incompatible avirulent bacterial pathogens as well as by treatment with several PAMPs (Mishina and Zeier, 2006; 2007; Návarová et al., 2012). The observation that exogenous application of Pip can partial complement resistance deficiency of *ald1* but not of *fmo1* mutant plants contributed to a current working model in which FMO1 is placed downstream of Pip in SAR establishment (Návarová et al., 2012; Bernsdorff et al., 2016).

However, the SAR-signal transition from local infected leaves to systemic non-inoculated leaf tissue is not clarified yet. Several different metabolites have been suggested to take a role in this context, including dehydroabietinal (DA), azelaic acid (AZA), the methyl ester of SA (MeSA), glycerol-3-phosphate (G3P), and Pip, but until now, unequivocal evidence for a function of any of these compounds as SAR long-distance signals has not been demonstrated (Shah and Zeier, 2013). Here, we investigated a potential role of Pip as a long-distance signal in SAR establishment by exogenously feeding Pip via the leaf. Thereby, the use of deuterium labeled Pip gave

us the opportunity to investigate the mobility of Pip within a plant and the metabolism of Pip after *Psm*-inoculation.

6.3 Results

Exogenous application of Pip via the root-system increases resistance of *Arabidopsis thaliana* and *Nicotiana tabacum* against several *P. syringae* cultivars (Návarová et al., 2012; Vogel-Adghough et al., 2013). This experimental approach allows investigating the role of Pip in plant immunity in the whole above ground grown plant tissue, but reveals no information for the role of Pip as a long-distance signal in the establishment of SAR. To establish SAR schematically, three steps can be formally distinguished: (I) After pathogen recognition at the inoculation site SAR-inducing signals have to be formed, (II) SAR-signals have to be transmitted to leaves distal to the site of infection, and (III) in those systemic leaves it is necessary that mobile signals are detected and forwarded to induce the formation of a systemic immune response.

To investigate a potential role of Pip as a long-distance signal in the establishment of SAR, we infiltrated Pip in leaves instead of feeding Pip via the root-system, although it was shown previously that infiltration of Pip into leaves not increases resistance against *Psm* of those leaves (Návarová et al., 2012). That is probably caused by, that infiltrated Pip stays in the apoplastic space of leaves due to a lack of efficient uptake of Pip via the plasma membrane into the cell interior (Návarová et al., 2012). If Pip is applied via the root, it presumably reaches the cytoplasm because amino acid uptake via the root and transport to the above grown parts of the plant is a natural process (Perchlik et al., 2014). Notably, the Pip concentrations reached in leaves after feeding Pip via the root are in the same range as the levels reached in distal leaves of SAR-activated plants (Návarová et al., 2012).

We infiltrated three local leaves (1°) per plant with 10 mM MgCl₂, *Psm* suspension (OD₆₀₀ 0.005), Pip solution (1 mM), or a co-infiltration with *Psm* (OD₆₀₀ 0.005) and Pip solution (1 mM) (for overview of experimental setup see: Fig. 6.1A). This approach allowed us to investigate the effects of Pip alone and Pip in combination with a *Psm*-stimulus at the infection-site (1°; local leaves) and in leaves distal to the infection site (2°; systemic leaves). For investigation of the mobility of Pip inside a plant, the function of Pip as a long-distance signal in the establishment of SAR, and the metabolism of Pip in plant immunity the experiments have been conducted with deuterium labeled Pip (D₉-Pip).

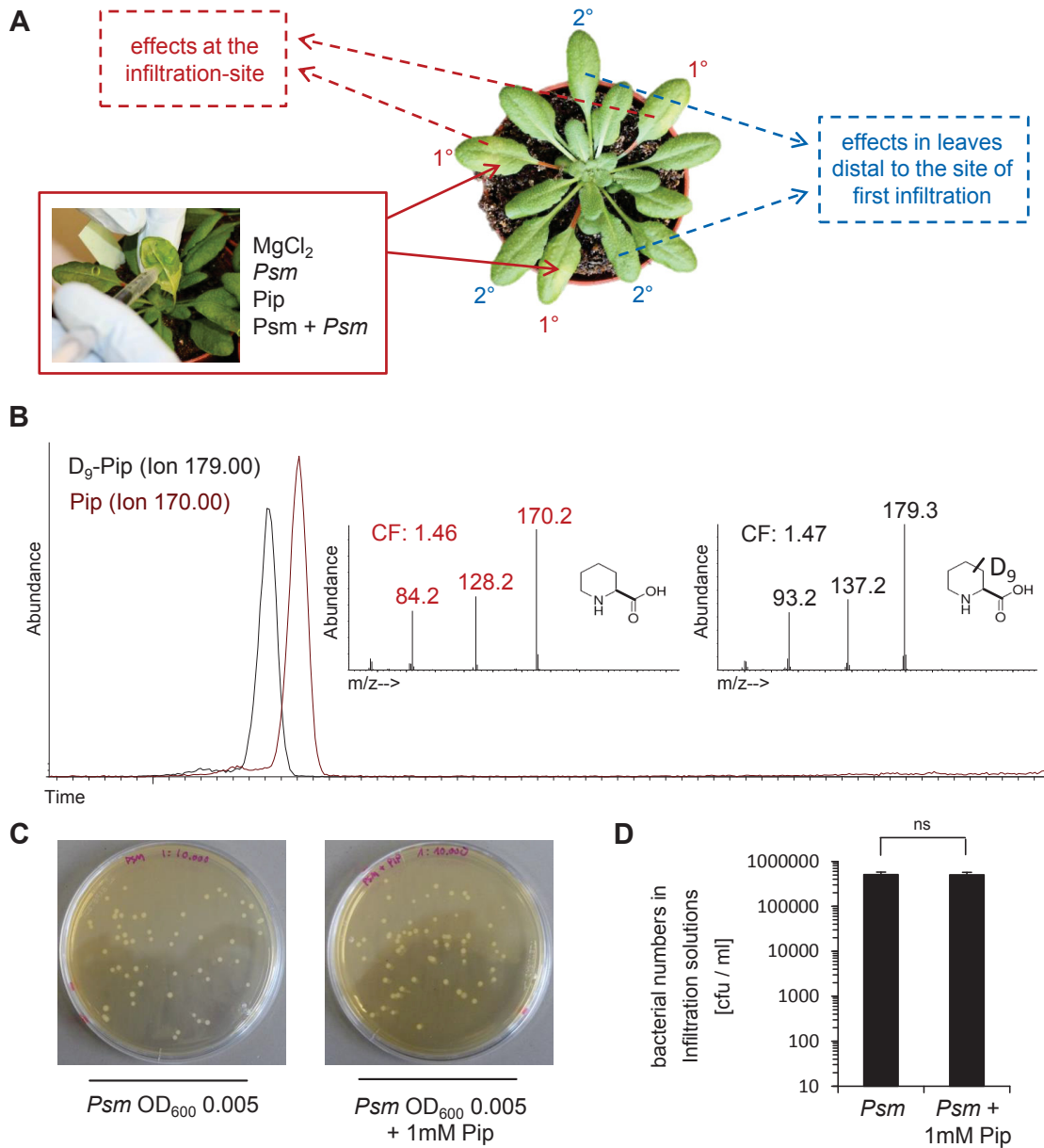


Figure 6.1 **Experimental setup for Pip and D₉-pip feeding via the leaf.**

(A) The feeding of Pip via the leaf allow to investigate effects and metabolism of Pip at the infection-site, as well as transport and the effects to/in systemic not-infiltrated leaves.

(B) Single-ion-chromatograms obtained from authentic standards of Pip [*m/z* 170] and D₉-Pip [*m/z* 179] and mass-spectra for both standards. Mass-spectra were recorded in the in the electron ionization mode. CF's are generated correction factors for Pip and D₉-Pip corresponding to the internal standard norvaline which was used for quantification.

(C) (D) Experiment to test if 1 mM Pip in the solution for the Pip + *Psm* co-infiltration harms *Psm* directly. Aliquots of *Psm* and Pip + *Psm* solutions were diluted 1: 10.000 and plated five times. **(D)** Cfu / ml for the infiltration-solutions were calculated.

Unlabeled Pip and D₉-Pip could, due to their retention times and their mass spectra, be discriminated by GC/MS-analysis (Fig. 6.1B). To test if 1 mM Pip in the solution for the Pip + *Psm* co-infiltration harms *Psm* directly we plated aliquots of *Psm*- and Pip + *Psm*-solutions and determined bacterial numbers on those plates. Thereby, Pip had no negative effect on viability of *Psm* at the infiltration time and same amount of bacteria were applied into the leaves (Fig. 6.1C and D).

6.3.1 A co-infiltration of Pip and *Psm* leads to a partial SAR response in *ald1* but not in *fmo1*

A key step of the biosynthesis of Pip in Arabidopsis is catalyzed by the Lys aminotransferase ALD1, which is suggested to catalyze the generation of ϵ -amino- α -keto caproic acid out of Lys (Fig. 1.3; Zeier, 2013). Recent data indicates that *ALD1* is localized in the chloroplast (Cecchini et al., 2015a; Friederike Bernsdorff and Jürgen Zeier, personal communication). The infiltration of Pip from the abaxial side of the leaf probably fled the apoplastic space with Pip, but Pip will probably reach the chloroplast where it is synthesized naturally or the cytoplasm.

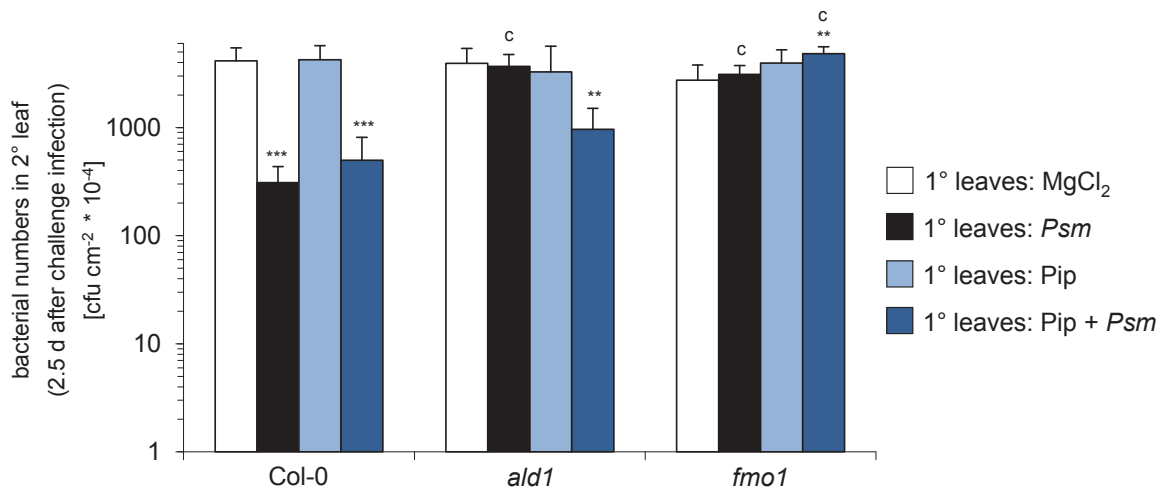


Figure 6.2 A co-infiltration of Pip + *Psm* partial complements SAR deficiency of *ald1* in a FMO1-dependent manner

SAR assay in Col-0, *ald1*, and *fmo1*. Local leaves were infiltrated with either 10 mM MgCl₂, to induce SAR with *Psm* (applied in titers of OD₆₀₀ 0.005), with Pip (1 mM), or with a mixture of Pip + *Psm* (OD₆₀₀ 0.005 and 1 mM, respectively). Two days later three leaves, distal to the site of first infiltration, per plant were infiltrated with *Psm* (applied in titers of OD₆₀₀ 0.001). Bacterial numbers in those leaves were determined 60 h post second infiltration. Bacterial numbers are means from 6 parallel samples, each consisting of three leaf disks. Asterisks denote statistically significant differences between first MgCl₂- and *Psm*, Pip, or Pip + *Psm* infiltrated plants of one genotype ***P < 0.001, **P < 0.01, and *P < 0.05. Letters denote statistically differences between the same treatment of Col-0 and the respectively mutant. ^cP < 0.001, ^bP < 0.01, and ^aP < 0.05 (two tailed *t* test).

We therefore wanted to test whether the experimental setup is artificial or is from biological relevance and tested the establishment of SAR after the different infiltrations (Fig. 6.2). Bacterial multiplication rates were decreased in systemic leaves of Col-0 plants which were first infiltrated in local leaves with *Psm* compared to those plants which were first infiltrated with $MgCl_2$. This effect was absent in *ald1* and *fmo1* mutant plants as described previously (Návarová et al., 2012). The infiltration of Pip alone to local leaves was thereby not sufficient to trigger a SAR response in systemic leaves in one of the investigated genotypes. In the Col-0 wild-type the SAR effect after the co-infiltration of Pip and *Psm* was comparable to the effect which was observed after the *Psm*-inoculation. Interestingly, a marked SAR response could be observed in *ald1* after the co-infiltration but not in *fmo1* (Fig. 6.2). The decrease in bacterial multiplication rates after the co-infiltration in *ald1* was significant compared to $MgCl_2$ -treated *ald1* plants but not as high as in *Psm*-inoculated Col-0 plants and is therefore in the following described as “partial SAR”. The observed partial SAR response in *ald1* after the Pip + *Psm* co-infiltration indicated that although the infiltration of Pip in the apoplastic area is artificial, SAR signaling pathways are activated by this treatment. The observation that *fmo1* mutants fail to establish SAR after the co-infiltration underlines the role of functional FMO1 downstream of Pip in SAR (Návarová et al., 2012; Bernsdorff et al., 2016).

6.3.2 Upon *P. syringae*-infection, Pip can be metabolized via FMO1-dependent and –independent pathways at the inoculation-site

FMO1 is described to be an essential component of biological induced SAR and acts downstream of Pip in the induction of SAR, in Pip-inducible resistance, and in Pip-mediated defense priming (Mishina and Zeier, 2006; Návarová et al., 2012; Bernsdorff et al., 2016). Moreover, an increased expression of *FMO1* in systemic leaf tissue can be observed 2 days after inoculation of local leaves with several *P. syringae* cultivars and PAMPs (Mishina and Zeier, 2007). Here we could furthermore demonstrate that SAR induction after a co-infiltration with Pip and *Psm* is impaired in *fmo1* mutant plants (Fig. 6.2). To investigate if Pip can be further metabolized at the infection-site, we conducted comparative metabolite profiling experiments with plants with $MgCl_2$, *Psm*, D_9 -Pip, or D_9 -Pip + *Psm*. In infiltrated leaf tissue, Pip and D_9 -could be discriminated and quantified (for mass spectra of Pip and D_9 -Pip see Fig. S6.1B). Unlabeled Pip accumulated in leaves inoculated with *Psm* and after the co-infiltration of D_9 -Pip + *Psm* in the wild-type and in *fmo1*, whereas *ald1* mutant plants failed to accumulate Pip as described previously by Návarová et al. (2012) (Fig. 6.3A). The infiltration of D_9 -Pip

alone was not sufficient to trigger endogenous Pip generation at the infiltration site. D₉-Pip could only be detected in plants which were infiltrated with D₉-Pip and the measured levels were in a similar range after both D₉-Pip treatments in all investigated genotypes (Fig. 6.3B).

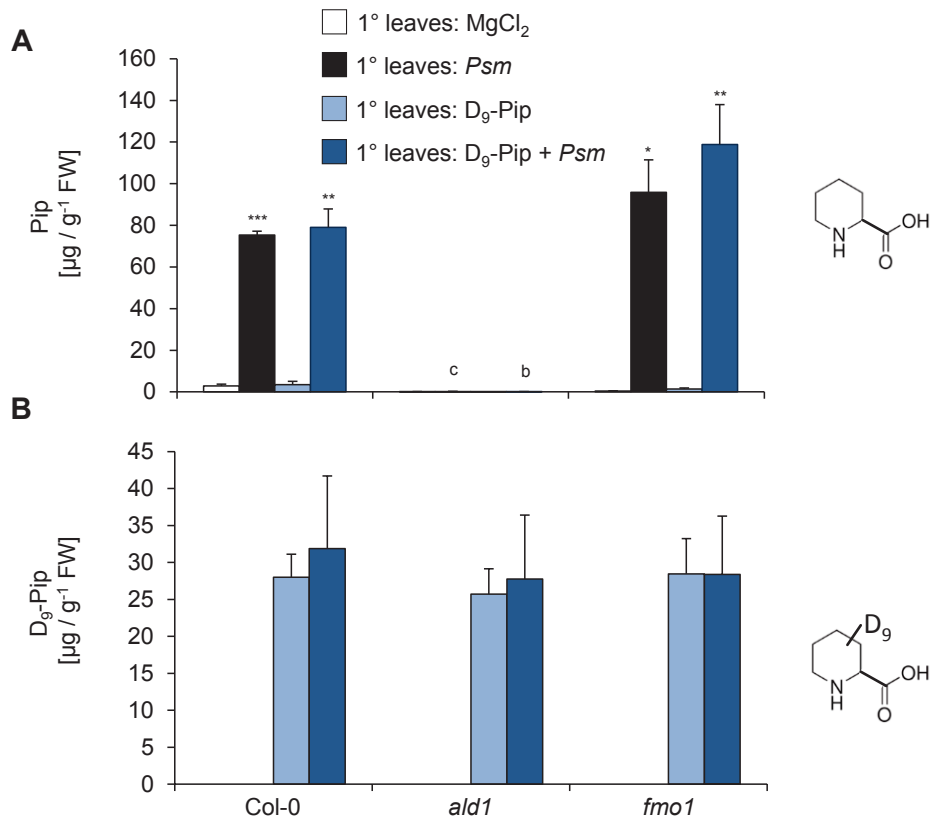


Figure 6.3 Pip and D₉-Pip can be discriminated in infiltrated leaf tissue.

(A) Endogenous levels of Pip after infiltrations with MgCl₂, *Psm*, D₉-Pip, or D₉-Pip + *Psm* in Col-0, *ald1*, and *fmo1* at 48 hpi at the infiltration-site. Asterisks denote statistically significant differences between MgCl₂- and *Psm*, D₉-Pip, or D₉-Pip + *Psm* infiltrated plants of one genotype ***P < 0.001, **P < 0.01, and *P < 0.05. Letters denote statistically differences between the same treatment of Col-0 and the respectively mutant. ^cP < 0.001, ^bP < 0.01, and ^aP < 0.05 (two tailed *t* test).

(B) Levels of D₉-Pip after infiltrations with MgCl₂, *Psm*, D₉-Pip, or D₉-Pip + *Psm* in Col-0, *ald1*, and *fmo1* at 48 hpi at the infiltration-site.

Beside to Pip, the endogenous production of several other amino acids is increased upon *Psm*-infection. Out of those amino acids α-amino adipic acid (Aad) is produced in the highest fold change between MgCl₂ and *Psm* treated leaves (Návarová et al., 2012). Aad is, as well as Pip, a Lys catabolite. Until now, the exact biosynthetic pathway of Aad in Arabidopsis is not fully elucidated and it is suggested that Lys and/or Pip can serve as a precursor for Aad (Zeier, 2013). Via the saccharopine pathway Lys can be converted to α-amino adipic semialdehyde by the LYSINE KETOGLUTARATE

REDUCTASE (LKR) and the SACCHAROPINE DEHYDROGENASE (SDH). α -amino adipic semialdehyde serves as a precursor for Aad (Fig 1.3; Galili et al., 2001; Zeier, 2013). In the second proposed pathway, Pip can serve as precursor for Aad. Thereby, Arabidopsis SACROSINE / PIPECOLATE OXIDASE (SOX) reduces Pip to Δ^1 -piperidine-6-carboxylic acid (P6C) which can be further metabolized to Aad via hitherto not classified enzymes (Fig. 1.3; Goyer et al., 2004; Zeier et al., 2013). However, the fact that *ald1* mutants, which are deficient in Pip biosynthesis (Fig. 6.2; Návarová et al., 2012), are not impaired in pathogen-triggered Aad accumulation indicate that the main source in Arabidopsis for Aad generation is Lys via the LKR/SDH pathway and not Pip (Fig. 6.4A; Návarová et al., 2012). The infiltration with D₉-Pip allowed us to investigate the role of Pip as a precursor for Aad. Consistent with Návarová et al. (2012) we could show that *Psm*-triggered generation of Aad is not dependent on functional ALD1 and FMO1 (Fig. 6.4A). Interestingly, the infiltration of D₉-Pip lead to an endogenous production of deuterium labeled Aad (D₆-Aad). D₆-Aad could be detected by GC/MS-analysis and due to the retention times and the mass spectra discriminated from unlabeled Aad (Fig. S18). The endogenous levels of D₆-Aad were quantitatively just moderate compared to those of Aad and the generation of D₆-Aad was independent of functional ALD1 and FMO1 (Fig. 6.4B), suggesting that a part of endogenous Pip can serve as a precursor for Aad although the main source for Aad generation is Lys and not Pip.

We could demonstrate that in addition to changes of free amino acids upon *Psm* infection (Návarová et al., 2012) also the endogenous levels of N-acetylated and N-formylated free amino acids are increased after *Psm*-infection (Chapter 3). By chemical synthesis, an authentic standard for N-formyl-Pip could be produced (Michael Hartmann and Jürgen Zeier). We used this authentic standard to identify N-formyl-Pip in our GC/MS-analysis for a relative quantification (mass spectra of N-formyl-Pip is shown in Fig. S5H). Thereby, N-formyl-Pip was produced in Col-0 and *fmo1* leaves inoculated with *Psm* and in leaves which were treated by co-infiltration of D₉-Pip + *Psm*, whereas in the Pip-deficient mutant *ald1* just traces of N-formyl-Pip could be detected (Fig. 6.5A). The accumulation of N-formyl-Pip was by trend higher in *fmo1* mutant plants, probably caused by increased production of Pip upon *Psm*-trigger in this mutant (Fig. 6.3; Návarová et al., 2012). Interestingly, also deuterium labeled N-formyl-Pip (D₉-N-formyl-Pip) could be detected after D₉-Pip and D₉-Pip + *Psm* infiltrations (Fig. 6.5B). In Col-0 wild-type and *fmo1* mutant plants the generation of D₉-N-formyl-Pip was thereby significantly increased after the co-infiltration compared to the D₉-Pip

infiltration, indicating that the *Psm*-trigger activates N-formyl-Pip production and that this production is independent from functional FMO1.

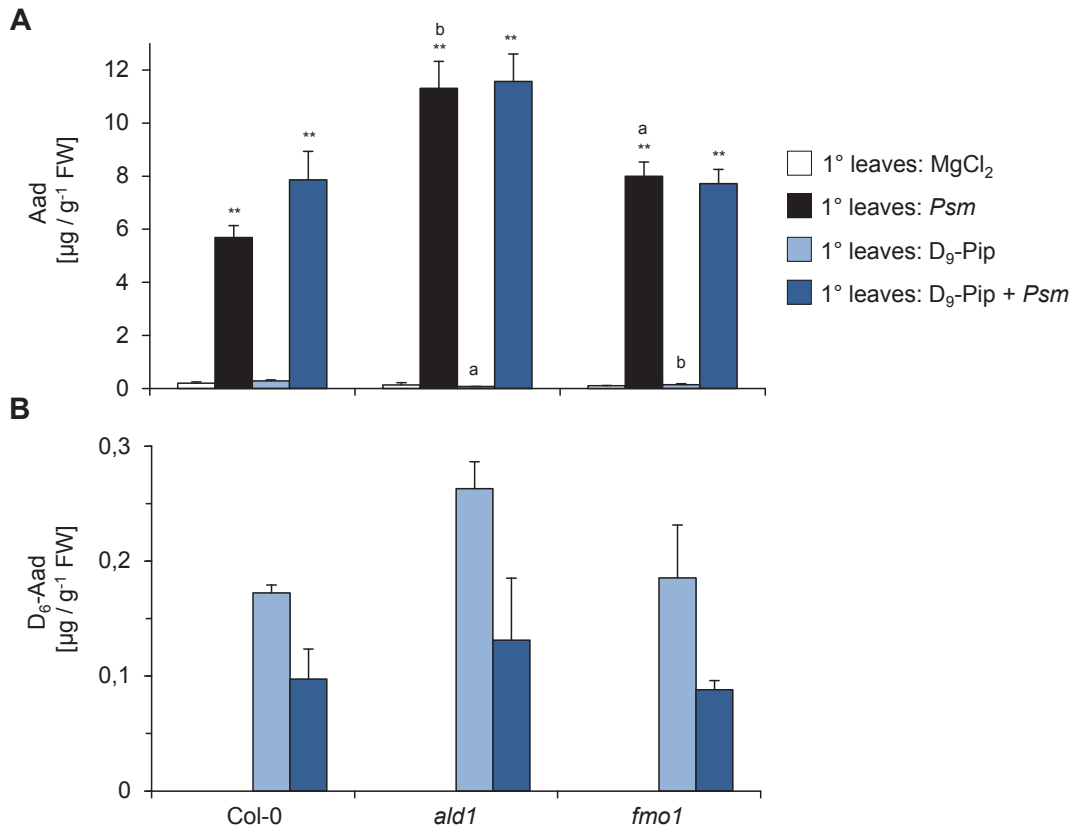


Figure 6.4 Moderate amounts of exogenous fed D₉-Pip can endogenously be converted to D₆-Aad.

(A) Endogenous levels of Aad after infiltrations with MgCl₂, *Psm*, D₉-Pip, or D₉-Pip + *Psm* in Col-0, *ald1*, and *fmo1* at 48 hpi at the infiltration-site. Asterisks denote statistically significant differences between MgCl₂- and *Psm*, Pip, or Pip + *Psm* infiltrated plants of one genotype ***P < 0.001, **P < 0.01, and *P < 0.05. Letters denote statistically differences between the same treatment of Col-0 and the respectively mutant. ^cP < 0.001, ^bP < 0.01, and ^aP < 0.05 (two tailed *t* test).

(B) Levels of D₆-Aad after infiltrations with MgCl₂, *Psm*, D₉-Pip, or D₉-Pip + *Psm* in Col-0, *ald1*, and *fmo1* at 48 hpi at the infiltration-site.

Flavin monooxygenases (FMOs) are in general described for their role in oxygenation processes of metabolites. For example, the Arabidopsis FMO *YUCCA1* is involved in auxin (IAA) biosynthesis by the hydroxylation of the amino group in tryptamine (Zhao et al., 2001). The finding that *fmo1* mutant plants are impaired in SAR establishment downstream of Pip (Návarová et al., 2012; Bernsdorff et al., 2016; Fig. 6.2), suggests that FMO1 could play a role in the generation of oxidized Pip-derived metabolites, with a functional relevance in SAR signaling (Fig. 6.6A). We checked in our metabolite profiling experiments for potential metabolites derived from the fed D₉-

Pip. Indeed, we could find two deuterium-labeled metabolites which are in the following described as deuterium labeled Pip-derived metabolites two and three (D₆-Pip-D2 and D₉-Pip-D3). Both metabolites were only produced in Col-0 and *ald1* after the co-infiltration of D₉-Pip + *Psm* and the infiltration with D₉-Pip alone was not sufficient for the generation of D₆-Pip-D2 and D₉-Pip-D3 (Fig. 6.6B-E). Furthermore, the accumulation of D₆-Pip-D2 and D₉-Pip-D3 could not be observed in *fmo1* mutant plants, which lead to the suggestion that those two until now not identified metabolites could be potential FMO1 products downstream of Pip.

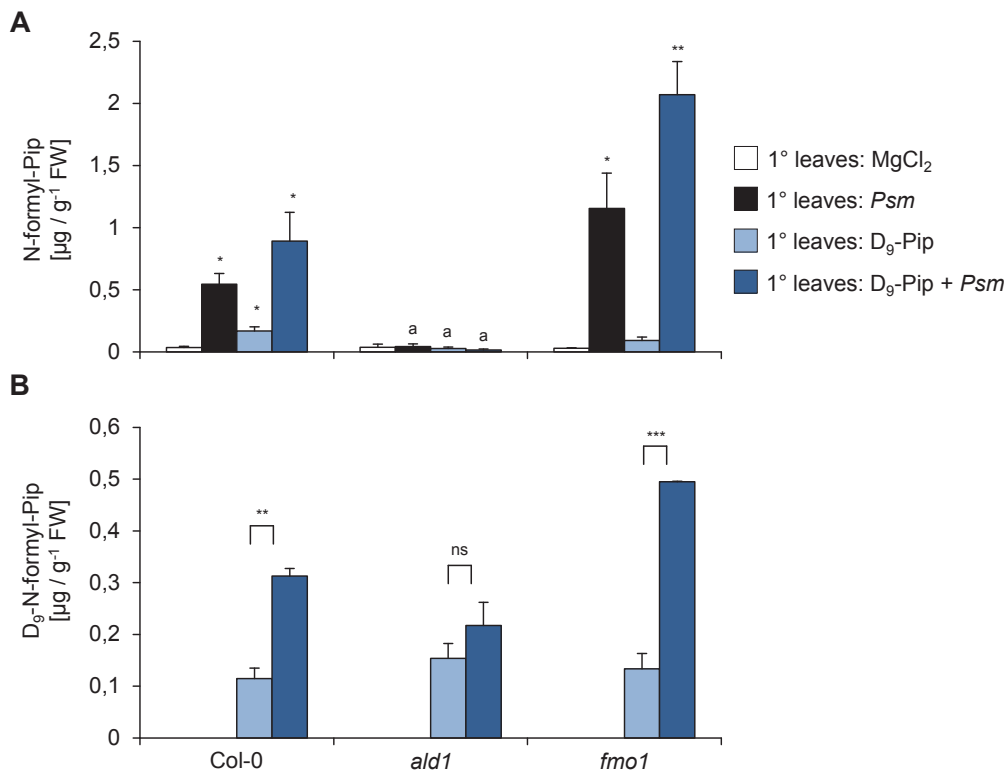


Figure 6.5 Pip can serve as a precursor for N-formyl-Pip.

(A) Endogenous levels of N-formyl-Pip after infiltrations with MgCl₂, *Psm*, D₉-Pip, or D₉-Pip + *Psm* in Col-0, *ald1*, and *fmo1* at 48 hpi at the infiltration-site. Asterisks denote statistically significant differences between MgCl₂- and *Psm*, D₉-Pip, or D₉-Pip + *Psm* infiltrated plants of one genotype ***P < 0.001, **P < 0.01, and *P < 0.05. Letters denote statistically differences between the same treatment of Col-0 and the respectively mutant. ^cP < 0.001, ^bP < 0.01, and ^aP < 0.05 (two tailed *t* test).

(B) Levels of D₉-N-formyl-Pip after infiltrations with MgCl₂, *Psm*, D₉-Pip, or D₉-Pip + *Psm* in Col-0, *ald1*, and *fmo1* at 48 hpi at the infiltration site. Asterisks denote statistically significant differences between D₉-Pip, or D₉-Pip + *Psm* infiltrated plants of one genotype ns = not significant, ***P < 0.001, **P < 0.01, and *P < 0.05

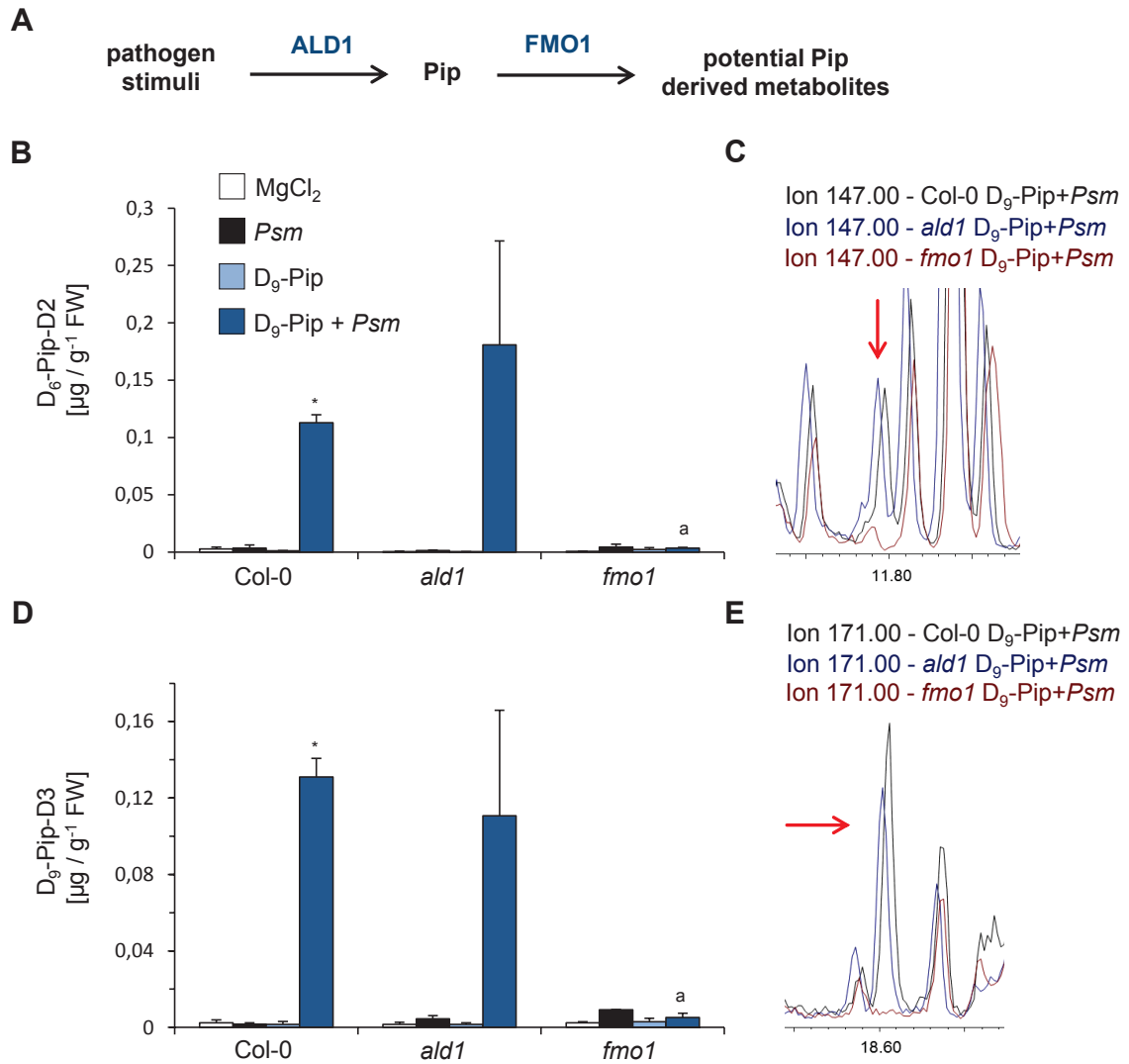


Figure 6.6 **Detection of potential D₉-Pip-derived metabolites generated by FMO1.**

(A) Possible model for the role of FMO1 in the metabolism of Pip-derived metabolites.

(B) Endogenous levels of D₆-Pip-D2 after infiltrations with MgCl₂, *Psm*, D₉-Pip, or D₉-Pip + *Psm* in Col-0, *ald1*, and *fmo1* at 48 hpi at the infiltration-site. Asterisks denote statistically significant differences between MgCl₂- and *Psm*, Pip, or Pip + *Psm* infiltrated plants of one genotype ***P < 0.001, **P < 0.01, and *P < 0.05. Letters denote statistically differences between the same treatment of Col-0 and the respectively mutant. ^cP < 0.001, ^bP < 0.01, and ^aP < 0.05 (two tailed *t* test). **(C)** shows an overlay of single-ion-chromatogram GC/MS-runs [*m/z* 147] from leaf-extracts of Col-0, *ald1* and *fmo1* which were infiltrated with D₉-Pip + *Psm*.

(D) Endogenous levels of D₉-Pip-D3 after infiltrations with MgCl₂, *Psm*, D₉-Pip, or D₉-Pip + *Psm* in Col-0, *ald1*, and *fmo1* at 48 hpi at the infiltration-site. Asterisks denote statistically significant differences between MgCl₂- and *Psm*, Pip, or Pip + *Psm* infiltrated plants of one genotype ***P < 0.001, **P < 0.01, and *P < 0.05. Letters denote statistically differences between the same treatment of Col-0 and the respectively mutant. ^cP < 0.001, ^bP < 0.01, and ^aP < 0.05 (two tailed *t* test). **(E)** shows an overlay of single-ion-chromatogram GC/MS-runs [*m/z* 171] from leaf-extracts of Col-0, *ald1* and *fmo1* which were infiltrated with D₉-Pip + *Psm*.

6.3.3 D₉-Pip can be detected in leaf tissue distal to the site of infiltration

The observation that a local co-infiltration of Pip + *Psm* triggers a partial SAR response in systemic *ald1* leaf tissue (Fig. 6.2) indicated that locally applied Pip in combination with a *Psm*-trigger can partially complement SAR deficiency of *ald1* mutant plants. To investigate if infiltrated D₉-Pip can be transported to systemic leaf tissue, we determined levels of Pip and D₉-Pip in leaves distal to the infiltration site (Fig. 6.7).

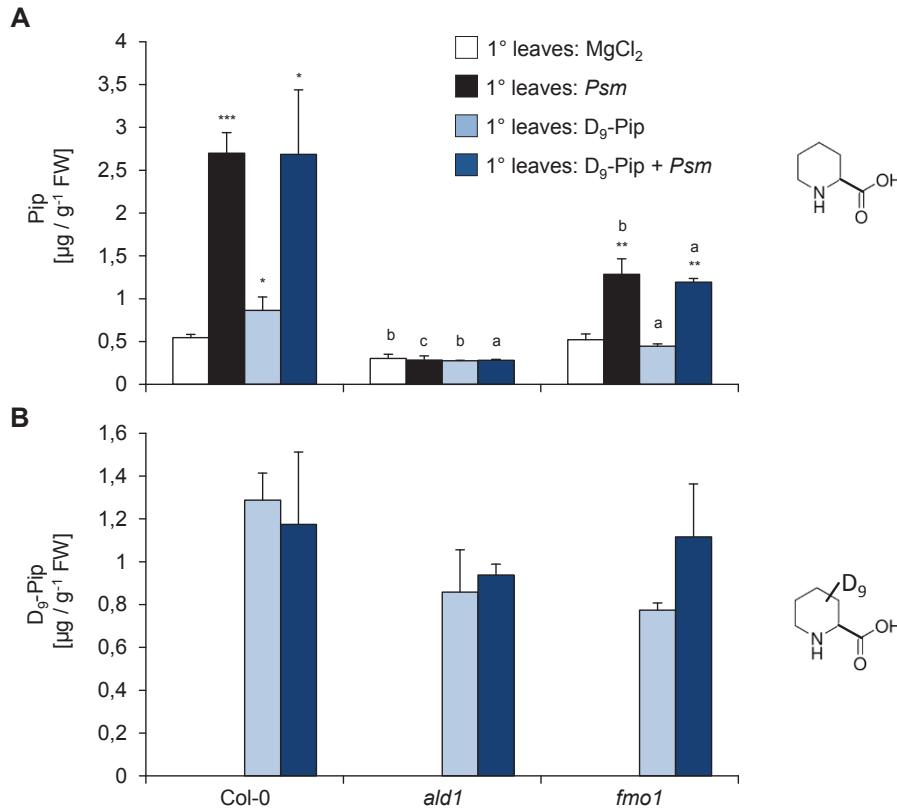


Figure 6.7 D₉-Pip can be detected in leaves distal to the leaves of exogenous application.

(A) Systemic accumulation of Pip after local infiltrations with MgCl₂, *Psm*, D₉-Pip, or D₉-Pip + *Psm* in Col-0, *ald1*, and *fmo1* at 48 hpi. Asterisks denote statistically significant differences between MgCl₂- and *Psm*, Pip, or Pip + *Psm* infiltrated plants of one genotype ***P < 0.001, **P < 0.01, and *P < 0.05. Letters denote statistically significant differences between the same treatment of Col-0 and the respectively mutant. ^cP < 0.001, ^bP < 0.01, and ^aP < 0.05 (two tailed *t* test).

(B) Systemic levels of D₉-Pip after local infiltrations with MgCl₂, *Psm*, D₉-Pip, or D₉-Pip + *Psm* in Col-0, *ald1*, and *fmo1* at 48 hpi.

In systemic Col-0 leaves, unlabeled Pip accumulated after infiltration of local leaves with *Psm* and D₉-Pip + *Psm*. Interestingly, in Col-0 a markedly systemic accumulation of Pip could be observed when plants were locally infiltrated with D₉-Pip (Fig. 6.7A). Pip-deficient *ald1* mutant failed to accumulate Pip in systemic leaves upon

local *Psm* inoculation, as described previously (Návarová et al., 2012), as well as upon local D₉-Pip and D₉-Pip + *Psm* infiltrations. In *fmo1* mutant plants a systemic accumulation of Pip could be observed after *Psm* and D₉-Pip + *Psm* infiltration, but this accumulation was significantly decreased compared to the same treatments in Col-0. Contrary to Col-0, in *fmo1* local infiltration of D₉-Pip was not sufficient to increase Pip levels in systemic leaves (Fig. 6.7A). D₉-Pip could be detected in systemic leaves of Col-0, *fmo1*, and *ald1* plants locally infiltrated with D₉-Pip and D₉-Pip + *Psm* (Fig. 6.7B). D₉-Pip levels in systemic leaf tissue were in the same range after local infiltration from D₉-Pip alone and after the co-infiltration of D₉-Pip and *Psm*, suggesting that exogenous fed Pip can be transported via the vascular system from local to systemic leaves but that this transport is not enriched after *Psm*-infection. Notably, only a small amount (approx. 3 – 4 %) of the locally infiltrated D₉-Pip reached the systemic leaves. In local D₉-Pip-infiltrated leaves concentrations of D₉-Pip were in a range between 25 – 30 µg⁻¹ FW, whereas in systemic leaves only concentrations from 1 – 1.4 µg⁻¹ FW could be determined (Fig. 6.3B; Fig. 6.7B).

6.3.4 A local co-infiltration of Pip and *Psm* leads to a partial activation of defense responses in systemic leaf tissue in *ald1* which is absent in *fmo1*

The collected data so far indicated the co-infiltration of Pip + *Psm* leads to a FMO1-dependent partial SAR response, whereas Pip-infiltration alone is not sufficient to trigger this partial SAR (Fig. 6.2). Moreover, D₉-Pip infiltration in lower leaves leads to a significant transport of D₉-Pip into upper leaves (approx. 4 % of the initially applied substance), and this transport is not further increased by *Psm*-coapplication (Fig. 6.7B). To get further information about the molecular mechanisms which contribute to the partial SAR response in *ald1*, we measured defense responses which are accompanied by the establishment of SAR. The biosynthesis of SA via ICS1 in systemic leaf tissue is indispensable for a strong SAR response (Wildermuth et al., 2001; Bernsdorff et al., 2016), and the positive regulation of SA biosynthesis by PAD4 as well as SA downstream signaling via NPR1 contributing to PAMP-triggered immunity, effector-triggered immunity, and strong SAR (Vlot et al., 2009; Fu and Dong, 2013). We therefore measured the systemic accumulation of free SA and glycosidically-bound SA, triggered by local infiltration of MgCl₂, *Psm*, D₉-Pip, or D₉-Pip + *Psm* in Col-0, *ald1* and *fmo1* (Fig. 6.8). Local *Psm*-inoculation led to systemic accumulation of free and glycosidic bound SA in Col-0, but not in *ald1* and *fmo1*, consistent with previously published studies (Návarová et al., 2012; Bernsdorff et al.,

2016). In agreement with the partial SAR effect upon the co-infiltration in *ald1* (Fig. 6.2), an increased systemic accumulation of free and conjugated SA was detected in *ald1* upon local co-infiltration of D₉-Pip and *Psm*, but local D₉-Pip infiltration alone triggered no systemic SA accumulation (Fig. 6.8). Furthermore, in *fmo1* mutant plants, none of the local infiltrated solutions was sufficient to trigger a systemic SA accumulation.

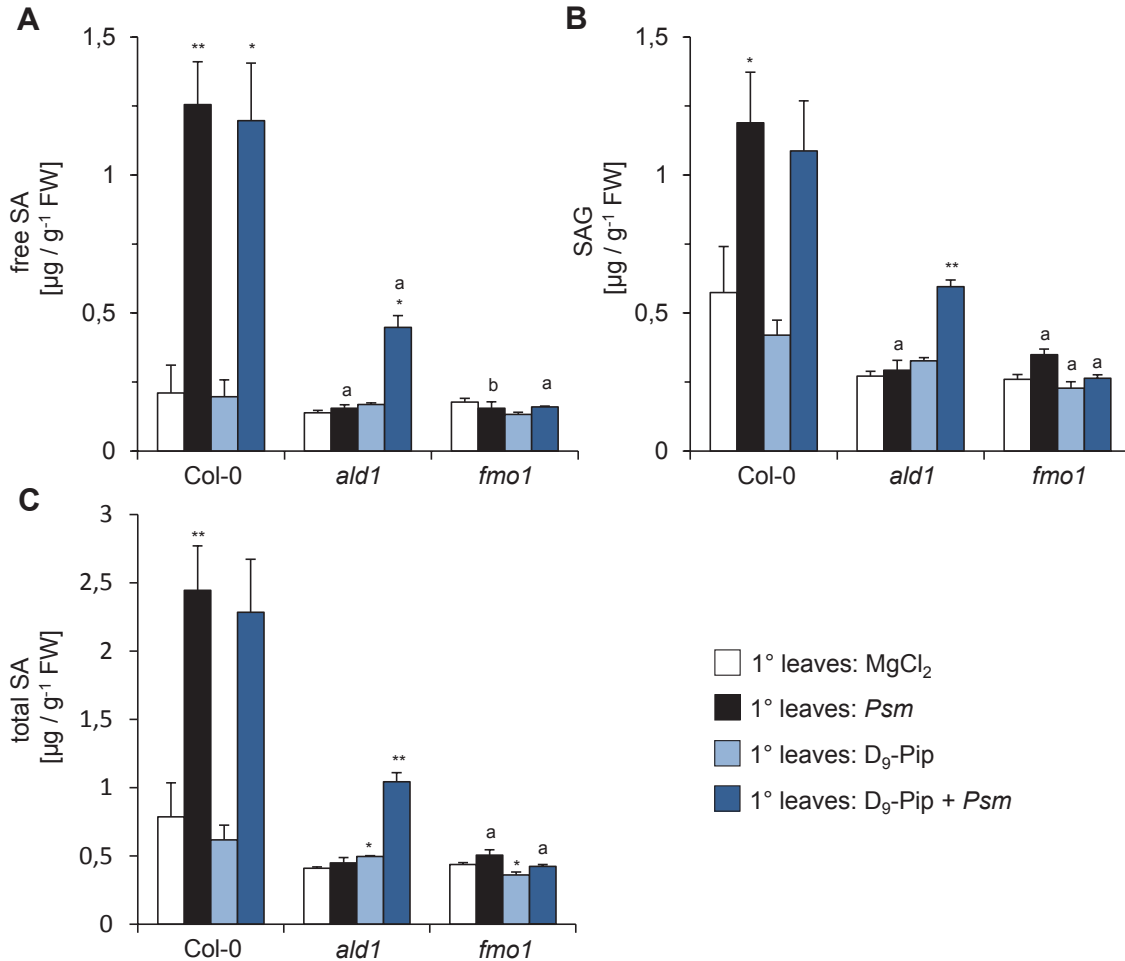


Figure 6.8 The local co-infiltration of D₉-Pip + *Psm* leads to a partial activation of systemic SA-biosynthesis in *ald1* but not in *fmo1*.

(A) Systemic accumulation of free SA after local infiltrations with MgCl₂, *Psm*, D₉-Pip, or D₉-Pip + *Psm* in Col-0, *ald1*, and *fmo1* at 48 hpi.

(B) Systemic accumulation of glycosidic bound SA after local infiltrations with MgCl₂, *Psm*, D₉-Pip, or D₉-Pip + *Psm* in Col-0, *ald1*, and *fmo1* at 48 hpi.

(C) Calculated levels of total SA after local infiltrations with MgCl₂, *Psm*, D₉-Pip, or D₉-Pip + *Psm* in Col-0, *ald1*, and *fmo1* at 48 hpi.

Asterisks denote statistically significant differences between MgCl₂- and *Psm*, Pip, or Pip + *Psm* infiltrated plants of one genotype ***P < 0.001, **P < 0.01, and *P < 0.05. Letters denote statistically differences between the same treatment of Col-0 and the respective mutant. °P < 0.001, °bP < 0.01, and °aP < 0.05 (two tailed *t* test).

The establishment of SAR is closely connected with a transcriptional reprogramming in leaf tissue distal to the inoculation-site. In SAR-activated plants, several genes involved in photosynthesis, primary and secondary metabolism, and growth processes are down regulated (SAR- genes) in systemic leaf tissue, whereas genes involved in different stages of defense signaling are upregulated (SAR+ genes). This transcriptional reprogramming is dependent on Pip, and the systemic transcriptional reprogramming is absent in Pip-deficient *ald1* mutant plants (Bernsdorff et al., 2016). Interestingly, a part of the SAR+ and SAR- genes is still regulated in systemic leaf tissue of SA deficient *sid2* plants. The regulatory effect of those genes is thereby markedly weaker as in the Col-0 wild-type, but significant compared to MgCl₂ infiltrated *sid2* plants, indicating that strong transcriptional reprogramming during SAR activation needs amplification by SA. Therefore, regulation of SAR+ and SAR- genes is not fully dependent on SA signaling, and SAR+ genes can be discriminated in SA-dependent SAR+ genes and partially SA-independent SAR+ genes (Bernsdorff et al., 2016).

To investigate which molecular mechanisms contribute to the partial SAR response in *ald1* after the co-infiltration of Pip + *Psm* (Fig. 6.2), we measured the systemic transcript levels of SA-dependent SAR+ genes *GRXS13*, *ARD3*, and *PR1* and partial SA-independent SAR+ genes *SAG13*, *ALD1*, and *FMO1* in Col-0, *ald1*, and *fmo1* after the four different local infiltrations. Transcript levels of all six genes were increased in systemic leaves of Col-0 after local infiltrations with *Psm* and D₉-Pip + *Psm* (Fig. 6.9). In *ald1* and *fmo1* mutant plants no increased expression triggered by local *Psm*-inoculation of those genes could be observed, in agreement with the previously described roles of ALD1 and FMO1 in biological activated SAR (Mishina and Zeier, 2006; Návarová et al., 2012; Bernsdorff et al., 2016). The local infiltration of D₉-Pip alone was again not sufficient to trigger a systemic defense response in one of the investigated genotypes. Convenient to the partial SAR response and the systemic SA accumulation in *ald1* after the Pip + *Psm* co-infiltration (Fig.6.2; Fig. 6.8) also systemic transcript levels of SA-dependent and partial SA-independent SAR+ genes *GRXS13*, *ARD3*, *PR1*, *SAG13*, and *FMO1* were increased in *ald1* due to the local co-infiltration of D₉-Pip + *Psm*. Moreover, this effect was absent in *fmo1* mutant plants (Fig. 6.9).

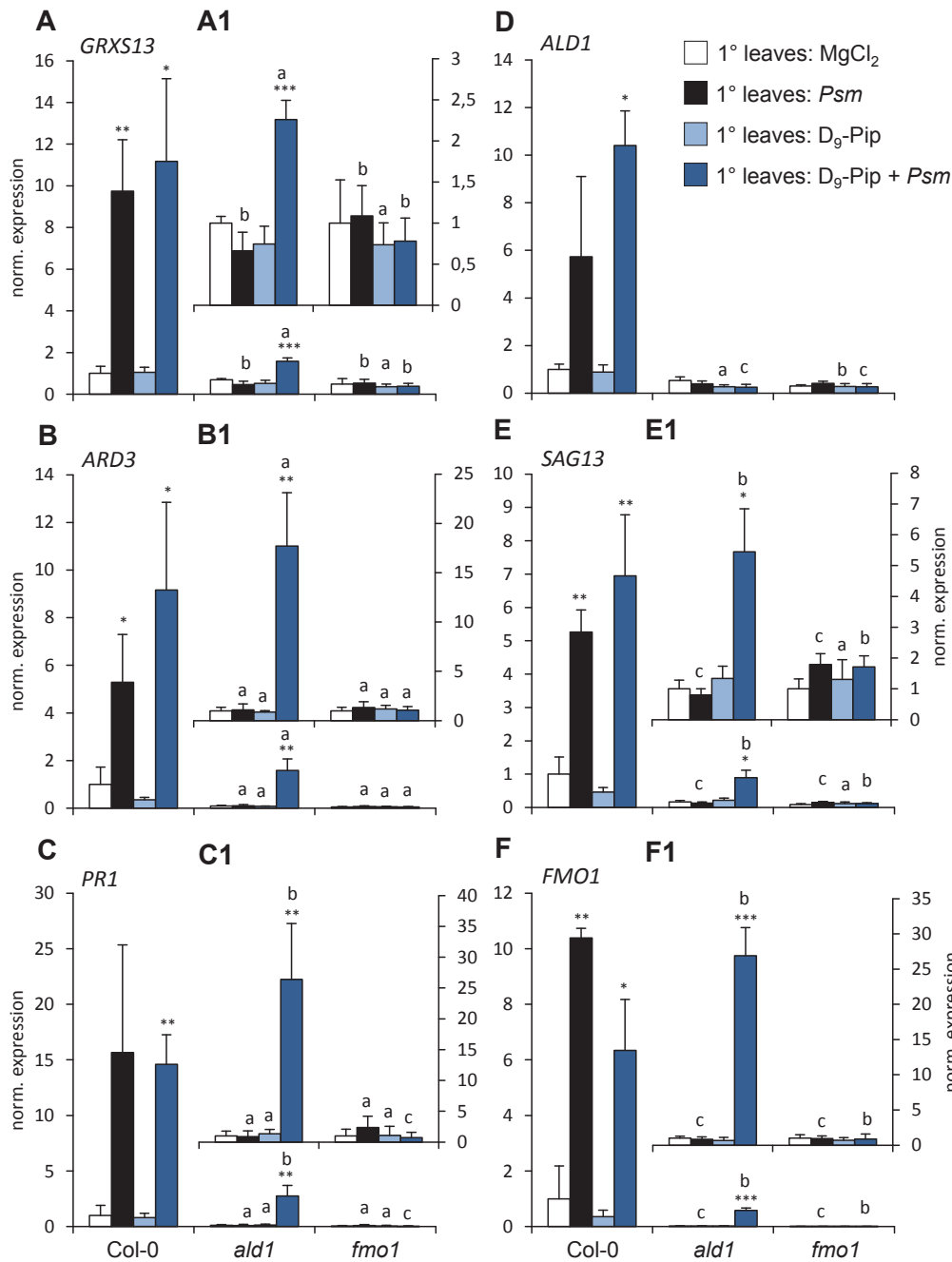


Figure 6.9 The local co-infiltration of D₉-Pip + Psm leads to an increased expression of SA-dependent and SA-independent SAR+ genes in *ald1* but not in *fmo1*.

Transcript levels in systemic leaves of SA-dependent SAR+ genes (A) *GRXS13*, (B) *ARD3*, and (C) *PR1* and partial SA-independent SAR+ genes (D) *ALD1*, (E) *SAG13*, and (F) *FMO1* upon local infiltrations with MgCl₂, Psm, D₉-Pip, or D₉-Pip + Psm in Col-0, *ald1*, and *fmo1* at 48 hpi.

A – F: Expression was normalized to the respective MgCl₂ control expression level in Col-0.

A1 – F1: Expression was normalized to the respective MgCl₂ control expression level in *ald1*.

Asterisks denote statistically significant differences between MgCl₂- and Psm, Pip, or Pip + Psm infiltrated plants of one genotype ***P < 0.001, **P < 0.01, and *P < 0.05. Letters denote statistically differences between the same treatment of Col-0/*ald1* and the respectively mutant. °P < 0.001, °P < 0.01, and °P < 0.05 (two tailed *t* test). SA-dependent and partial SA-independent genes were classified according to Bernsdorff et al. (2016).

The activation of SAR in Arabidopsis upon *Psm* infection is accompanied by an activation of Trp-derived indole metabolism in local and systemic leaf tissue (Stahl et al., 2016; Chapter 5). At the inoculation site more than 20 indolic metabolites, including camalexin, accumulate to high amounts, whereas the levels of only three indolics, ICC, ICA, and I3A, increase in distal leaves. Thereby, the systemic accumulation of indolics is not functionally relevant for SAR establishment but rather a consequence of activated SAR. Consistent with that, SAR-deficient *ald1* and *fmo1* fail to accumulate indolics in systemic leaf tissue and the systemic accumulation of ICC, ICA, and I3A in SA-deficient *sid2* mutant is highly decreased compared to Col-0 (Stahl et al., 2016; Chapter 5). We also measured the systemic accumulation of ICC and ICA in our experimental setup. The local co-infiltration of D₉-Pip + *Psm* triggered a systemic accumulation of ICC and ICA in *ald1* mutant plants but not in *fmo1* (Fig. 6.10), indicating that also signaling processes downstream of SAR establishment are activated due to the co-infiltration.

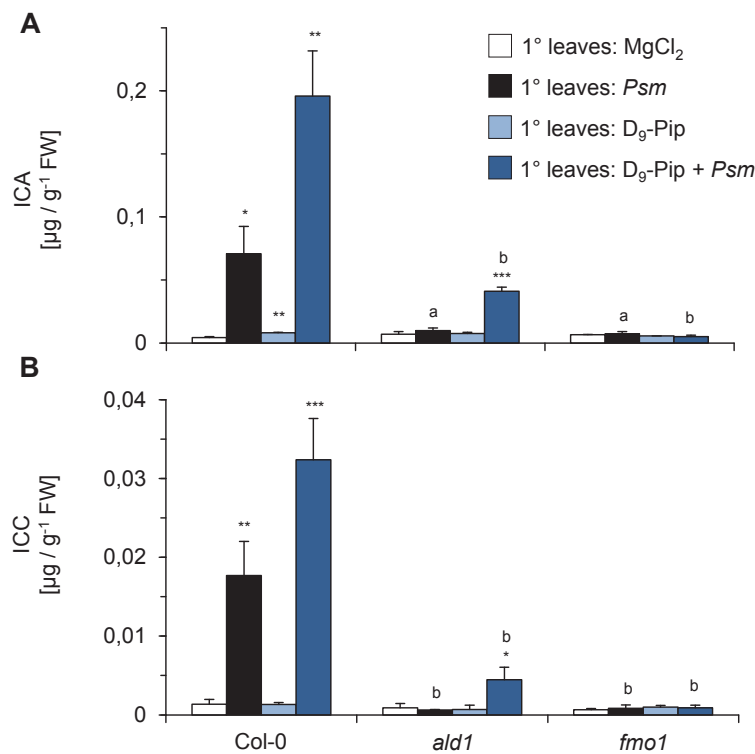


Figure 6.10 The local co-infiltration of D₉-Pip + *Psm* leads to a partial activation of systemic indole metabolism in *ald1* but not in *fmo1*.

Systemic accumulation of ICA (A) and ICC (B) after local infiltrations with MgCl₂, *Psm*, D₉-Pip, or D₉-Pip + *Psm* in Col-0, *ald1*, and *fmo1* at 48 hpi.

Asterisks denote statistically significant differences between MgCl₂- and *Psm*, D₉-Pip, or D₉-Pip + *Psm* infiltrated plants of one genotype ***P < 0.001, **P < 0.01, and *P < 0.05. Letters denote statistically differences between the same treatment of Col-0 and the respectively mutant. ^cP < 0.001, ^bP < 0.01, and ^aP < 0.05 (two tailed *t* test).

As described above, SA deficient *sid2* mutant plants are not completely impaired in systemic defense-signaling which contributes to SAR (Bernsdorff et al., 2016). Consistent with this, a moderate but significant SAR response upon *Psm*-inoculation can be observed in SA deficient *sid2* mutant plants (Fig. 6.11; Bernsdorff et al., 2016). We also measured bacterial multiplication rates in systemic leaves after local infiltration of Pip and co-infiltration of Pip + *Psm* in *sid2* and in a double mutant deficient in both Pip and SA biosynthesis (*sid2ald1*). The co-infiltration of Pip + *Psm* led to partial SAR response in *sid2* comparable to SAR triggered by *Psm*-inoculation in this mutant (Fig. 6.11). As in the *ald1* mutant, a partial SAR response was triggered by local co-infiltration of Pip + *Psm* in *sid2ald1* double mutant, but *Psm*-inoculation alone was not sufficient to trigger that moderate response, underlining the role of Pip as the main regulator for SAR but also showing that for a strong SAR response and for defense-signaling-amplification the systemic de novo synthesis of SA is required.

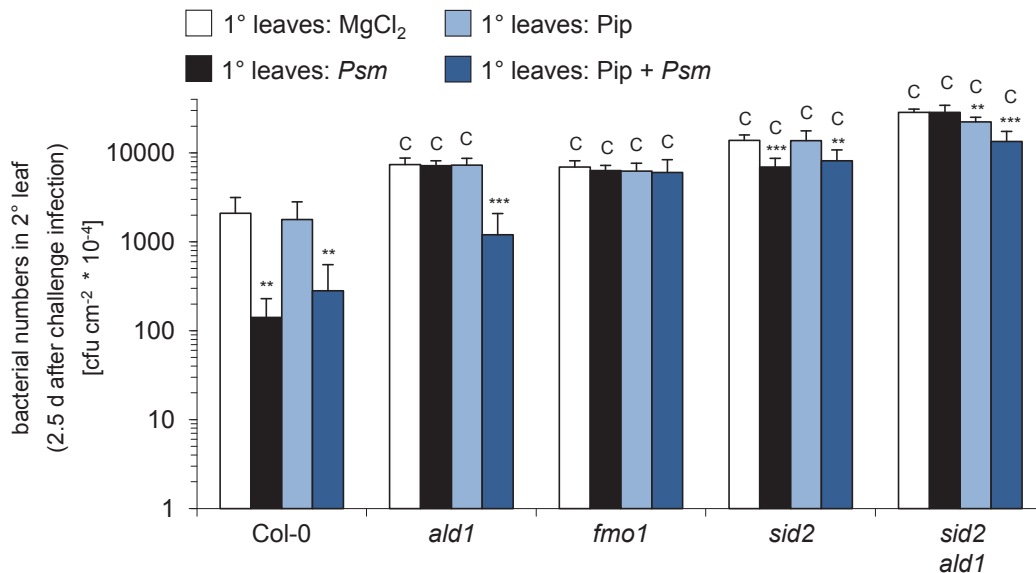


Figure 6.11 SAR upon the co-infiltration of Pip + *Psm* in mutants impaired in Pip and SA signaling.

SAR assay in Col-0, *ald1*, *fmo1*, *sid2*, and *sid2ald1*. Local leaves were infiltrated with either 10 mM MgCl₂, to induce SAR with *Psm* (applied in titers of OD₆₀₀ 0.005), with Pip (1 mM), or with a mixture of Pip + *Psm* (OD₆₀₀ 0.005 and 1 mM, respectively). Two days later three leaves, distal to the site of first infiltration, per plant were infiltrated with *Psm* (applied in titers of OD₆₀₀ 0.001). Bacterial numbers in those leaves were determined 60 h post second infiltration. Bacterial numbers are means from 6 parallel samples, each consisting of three leaf disks. Asterisks denote statistically significant differences between first MgCl₂- and *Psm*, Pip, or Pip + *Psm* infiltrated plants of one genotype ***P < 0.001, **P < 0.01, and *P < 0.05. Letters denote statistically differences between the same treatment of Col-0 and the respectively mutant. ^cP < 0.001, ^bP < 0.01, and ^aP < 0.05 (two tailed *t* test).

6.4 Discussion

In the past, a part of SAR research focused on metabolites with suggested functions in leaf-to-leaf communication and SAR signal amplification. Several metabolites were proposed to have a function in long-distance signaling in SAR establishment, including dehydroabietinal (DA), azelaic acid (AzA), the methyl ester of SA (MeSA), glycerol-3-phosphate (G3P), and pipercolic acid (Pip), but hitherto a transport of one of those metabolites from infected leaf tissue to systemic non-infected leaf tissue in the context of SAR establishment could not be demonstrated (Shah and Zeier, 2013). Upon *Psm*-infection, Pip accumulates in *Psm*-inoculated leaf tissue, in systemic non-inoculated leaf tissue and exclusively also in petiole exudates collected from *Psm*-inoculated leaves (Návarová et al., 2012). Moreover, a moderate but significant systemic accumulation of Pip can be observed in *fmo1* mutants although no increase of *ALD1* transcript can be measured in systemic *fmo1* leaf tissue upon local *Psm*-inoculation (Fig. 6.7A; Fig. 6.9D; Návarová et al., 2012). Notably, in Pip-insensitive *fmo1*, SAR-associated systemic transcriptional reprogramming upon local *Psm*-inoculation is completely abolished (Gruner et al., 2013). Combined with the SAR deficiency of *ald1* and *fmo1* mutant plants those observations made Pip a promising candidate as a long distance signal in SAR establishment.

Here we investigated a possible role of Pip as a SAR long distance signal using a leaf infiltration assay. The comparable analysis of wild-type plants and previously described SAR-deficient mutants, infiltrated with $MgCl_2$, *Psm*, Pip, and Pip + *Psm*, allowed us to investigate the effects of Pip alone and Pip in combination with a *Psm*-stimulus in local leaves and in leaves distal to the infection-site (Fig. 6.1A). Furthermore, the use of deuterium-labeled Pip allowed us to investigate the metabolism of Pip after *Psm*-inoculation.

6.4.1 In *Psm*-infected leaf tissue Pip can be metabolized in FMO1-dependent and -independent manner

Arabidopsis fmo1 mutants are well-described with respect to their deficiency in SAR establishment. Functional *FMO1* is necessary for SAR activation after local recognition of compatible *Psm*, incompatible *Psm avrRpm1*, PAMPs, and for induction of SAR in *Arabidopsis* after oviposition by *Pieris brassica*. Furthermore, transcript levels of *FMO1* are increased in systemic leaf tissue upon those local treatments (Mishina and Zeier, 2006; 2007; Hilfiker et al., 2014). Moreover, it was shown that *FMO1* acts downstream of Pip in SAR establishment, in resistance induction by

exogenously applied Pip, and in the realization of Pip- and *Psm*-mediated defense priming associated with SAR establishment (Návarová et al., 2012; Bernsdorff et al., 2016). However, the exact biochemical function of FMO1 in Arabidopsis immunity is not elucidated yet. In mammalian systems several FMOs are described in oxygenation reactions in biosynthesis of amines and sulfides (Krueger and Williams, 2005; Schugar and Brown, 2015). Furthermore, it could be shown that a bacterial FMO in *Streptomyces maritimus* is involved in the biosynthesis of the antibiotic enterocin (Teufel et al., 2013). A well described FMO in plants is *YUCCA1*. *YUCCA1* is described for a function in the biosynthesis of the phytohormone IAA. Thereby *YUCCA1* is involved in hydroxylation of the amino group in tryptamine and in another branch of IAA metabolism in the conversion of indole-3-pyruvic acid (Zhao et al., 2001; Stepanova et al., 2011). The exogenous application of D₉-Pip in combination with the use of *fmo1* mutant plant allowed us to search for possible Pip-derived metabolites and a potential role of FMO1 in the generation of those metabolites. Indeed we could find several metabolites endogenously produced out of the fed D₉-Pip (Fig. 6.4; Fig.6.5; Fig. 6.6; Fig. 6.12).

Beside to Pip, Aad, a second non-protein amino acid derived from Lys is produced upon *Psm*-infection (Návarová et al., 2012). Here we could show that a slight amount of the fed D₉-Pip can be metabolized to D₆-Aad, but that this conversion from D₉-Pip to D₆-Aad is not pronounced upon *Psm*-infection and is independent of functional FMO1 (Fig. 6.4B; Fig. 6.12). Although only approx. 1 % of the fed D₉-Pip was converted to D₆-Aad (Fig. 6.4B), that indicates that moderate amounts of endogenous Pip can serve as a precursor for Aad. In this pathway Pip is probably reduced to Δ^1 -piperidine-6-carboxylic acid (P6C) via SOX, and P6C can be further metabolized to Aad by until now not classified enzymes (Fig. 1.3; Goyer et al., 2004; Zeier et al., 2013). Notably, the relatively low conversion rate from D₉-Pip to D₆-Aad could also be reasoned by that most of the infiltrated D₉-Pip could not reach the cytoplasm, caused by no efficient amino acid uptake mechanisms from the apoplastic space. However, the fact that Pip-deficient *ald1* mutant plants accumulate Aad upon *Psm*-infection in the same range as wild-type plants indicate that the main source in Arabidopsis for Aad generation is Lys via the LKR/SDH pathway and not Pip (Fig. 6.4A; Návarová et al., 2012). Consistent with this observation, mutants impaired in saccharopine dehydrogenase activity (*lkr-1* and *lkr2*), which is involved in the synthesis of the latest Aad precursor α -amino adipic semialdehyde (Fig 1.3), fail to accumulate Aad upon *Psm*-infection (Návarová et al., 2012; Zeier, 2013). Anyway, biological function of Aad that accumulates upon *Psm*-infection remains to be elucidated, because Aad-deficient

mutants *lkr1* and *lkr2* are not more susceptible to *Psm* and local AaD accumulation has no effect on SAR establishment (Návarová et al., 2012).

A further Pip derived product which could be detected in our experiments was N-formyl-Pip. N-formyl Pip accumulated in Col-0 plants and in *fmo1* mutant plants in leaves inoculated with *Psm* but not in *ald1* mutant plants, indicating that ALD1-derived Pip is the endogenous precursor for N-formyl-Pip formation (Fig. 6.5A). Thereby, the accumulation of N-formyl-Pip was higher in *fmo1* mutant plants compared to Col-0, probably caused by a higher *Psm*-triggered Pip accumulation in this mutant (Fig. 6.3A; Návarová et al., 2012). However, endogenous levels of N-formyl-Pip upon *Psm* inoculation were quite low compared to endogenous Pip levels (approx. 1 % of determined Pip concentrations) (Fig. 6.3A; Fig. 6.5A). Interestingly, labeled N-formyl-Pip (D_9 -N-formyl-Pip) derived from the fed D_9 -Pip could be detected in Col-0, *ald1*, and *fmo1* in leaves which were treated with D_9 -Pip alone and in leaves co-infiltrated with D_9 -Pip + *Psm* (Fig. 6.5B). The endogenous levels of D_9 -N-formyl-Pip were significantly higher in Col-0 and *fmo1* leaves which were co-infiltrated with D_9 -Pip + *Psm*, suggesting that the generation of N-formyl-Pip is positively effected by the pathogen trigger and is not just a consequence of the increased Pip levels upon *Psm*-infection. However, a possible role of acetylated and formylated amino acids and especially of N-formyl-Pip remains to be elucidated and could not be clarified in this study because the enzymes which catalyzes those acylation reactions in response to *Psm* are so far unknown and therefore potential Arabidopsis mutants are not available (Chapter 3).

It was previously discussed that potential FMO1-products could function in Arabidopsis SAR and recent finding that FMO1 acts downstream of Pip in SAR establishment made Pip a promising candidate as a potential substrate for FMO1 (Mishina and Zeier, 2006; Návarová et al., 2012; Zeier, 2013; Bernsdorff et al., 2016). Here, we could detect two metabolites (D_6 -Pip-D2 and D_9 -Pip-D3) that were derived from the fed D_9 -Pip in a FMO1-dependent manner (Fig. 6.6). The generation of D_6 -Pip-D2 and D_9 -Pip-D3 out of D_9 -Pip via FMO1 was thereby dependent on the *Psm* stimulus and infiltration of D_9 -Pip alone was not sufficient to trigger this reaction, probably caused by the fact that *FMO1* transcripts are too low to trigger that reaction in plants which were not *Psm*-inoculated (Mishina and Zeier, 2006; 2007; Gruner et al., 2013). However, observation that those two metabolites were just produced by co-infiltration of D_9 -Pip + *Psm* in Col-0 and *ald1* but not in *fmo1*, combined with previously described functions of FMOs, makes those two metabolites promising candidates for oxidized Pip-derived metabolites generated by FMO1 (Fig. 6.4; Fig. 6.9). A future task will be

the identification of those metabolites produced by FMO1 and the clarification if these metabolites take a functional role in SAR establishment.

6.4.2 A local co-infiltration of Pip and *Psm* can partial complement SAR deficiency of *ald1* mutant plants in a FMO1-dependent manner

Here we could demonstrate that the local co-infiltration of Pip + *Psm* leads to a partial SAR response in systemic *ald1* leaves, whereas *Psm*- or Pip- infiltration alone is not sufficient to trigger SAR in this mutant (Fig. 6.2; Fig. 6.11; Návarová et al., 2012; Bernsdorff et al., 2016). This partial SAR response was fully dependent on functional FMO1, which underlines the role of FMO1 downstream of Pip in the establishment of SAR (Návarová et al., 2012; Bernsdorff et al., 2016). The establishment of partial SAR in *ald1* was accompanied by a partial activation of the systemic accumulation of SA (Fig. 6.8) and a partial systemic increased expression of SA-dependent and – independent SAR+ genes (Fig. 6.9). As well as the partial SAR response, systemic responses due to the local co-infiltration of D₉-Pip + *Psm* could partially complement abolished systemic responses in *ald1* but not in *fmo1*. Recently we could show that as a consequence of SAR establishment, several branches of Trp-derived indole metabolism are activated in distal leaf tissue, resulting in a systemic accumulation of I3A, ICC, and ICA. Furthermore, SAR deficient mutants *ald1* and *fmo1* fail to accumulate those indolics in systemic leaf tissue (Stahl et al., 2016). Here we also measured if abolished systemic accumulation of ICC and ICA in *ald1* is affected by the co-infiltration of D₉-Pip + *Psm* (Fig. 6.10). Indeed, the partial activated SAR-signaling upon the co-infiltration of D₉-Pip + *Psm* in *ald1* resulted also in a partial systemic accumulation of ICC and ICA and consistent with no systemic activated defense signaling upon this treatment in *fmo1*, *fmo1* mutant plants failed to accumulate those indolics in systemic leaf tissue.

Data so far showed, that systemic defense signaling in *ald1* upon local Pip + *Psm* co-infiltration but not after the infiltration of Pip alone is partially activated (Fig. 6.8; Fig. 6.9; Fig. 6.10; Fig. 6.12). Partially activated defense signaling, results in a partial SAR response in *ald1* (Fig. 6.2; Fig. 6.11). This response was absent in *fmo1*. Combined with the assumption that Pip could be a potential long distance signal in SAR establishment, these results suggested that Pip transport from local infected leaves to systemic leaves could be activated upon *Psm*-infection. To test this hypothesis we measured systemic levels of D₉-Pip after local infiltration of D₉-Pip or co-infiltration of D₉-Pip + *Psm* in Col-0, *ald1*, and *fmo1* (Fig. 6.7B). The systemic levels of

D₉-Pip were in the same range after local infiltration of D₉-Pip alone and after D₉-Pip + *Psm* co-infiltration in Col-0, *ald1*, and *fmo1*. Notably, only a small part of the locally infiltrated Pip could be detected in distal leaf tissue. In local D₉-Pip-infiltrated leaves concentrations of D₉-Pip were in a range between 25 – 30 µg⁻¹ FW, whereas in systemic leaves only concentrations from 1 – 1.4 µg⁻¹ FW could be measured (Fig. 6.3B; Fig. 6.7B). The small amounts of Pip which reach the distal leaves in the here used leaf infiltration assay are probably the reason that Pip infiltration alone not increases resistance to *Psm* of distal leaves. If Pip is fed via the root it increases resistance of Col-0 and *ald1* against *Psm*, because Pip concentrations reached in leaves after feeding Pip via the root are in the same range as the levels reached in distal leaves of SAR-activated Col-0 plants (Návarová et al., 2012). However, results indicate that Pip can be transported between leaves via the vascular system, but that the transport of exogenous fed D₉-Pip from local to systemic leaves is not increased upon *Psm*-infection. Systemic defense responses in *ald1* are just activated upon the co-infiltration whereas infiltration of Pip alone is not sufficient to trigger those responses, but in both cases the same amount of fed Pip reaches the systemic leaves (Fig. 6.2; Fig. 6.7 - Fig. 6.12). This could indicate that in addition to Pip, at least one other signal is necessary for SAR establishment. Meanwhile, the observation that co-infiltration of Pip + *Psm* can partial complement SAR deficiency of *ald1* mutant plants in a FMO1-dependent manner underlines that Pip is indispensable for SAR establishment and the role of Pip as the main regulator of SAR in Arabidopsis, which is acting upstream of FMO1 (Návarová et al., 2012; Bernsdorff et al., 2016). We also checked if potential Pip-derived FMO1 products (D₆-Pip-D2 and D₉-Pip-D3; Fig. 6.6) could play a role as possible long-distance signals in SAR establishment. That would assume that D₆-Pip-D2 and D₉-Pip-D3 are transported from local inoculated to distal leaves. However, D₆-Pip-D2 and D₉-Pip-D3 could not be detected in systemic leaves (data not shown), suggesting that these two Pip-derived metabolites are not transported from local to distal leaves. Notably, it also possible that concentrations of D₆-Pip-D2 and D₉-Pip-D3 in systemic leaves were only below the detection level of the used GC/MS-system, because local concentration of these two metabolites were already low in local leaves (<200 ng⁻¹ FW) (Fig. 6.6).

Taken together, with this experimental setup it cannot be exactly clarified if Pip takes a functional role as a long-distance signal in SAR establishment. Here we could just demonstrate that Pip can be transported between leaves (Fig. 6.7B), but the use of whole leaves for GC/MS-analysis reveals no information if the transported Pip stays in the vascular system, in the apoplastic space, or is transferred to site where it is actually

needed within the leaf, or more precisely within the plant cell. For full SAR establishment, the systemic de novo synthesis of SA and Pip is required (Fig. 6.11; Gaffney et al., 1993; Wildermuth et al., 2001; Návarová et al., 2012; Bernsdorff et al., 2016). The biosynthesis of SA via ICS1, as well as the biosynthesis of Pip via ALD1 takes place in the chloroplasts (Garcion et al., 2008; Cecchini et al., 2015a; Friederike Bernsdorff and Jürgen Zeier, personal communication). Therefore, it could be possible that potential SAR signals have to be transmitted to the chloroplasts, but at least have to reach the cytoplasm. Recently it could be shown that Pip is also generated in soybean plants upon aphid-infestation (Klein et al., 2015). In this study, Pip was detected by matrix-assisted laser desorption ionization – mass spectrometry imaging (MALDI-MSI), which reveals information in which area in a leaf Pip is accumulating upon the infestation. A future task for the here described experimental setup could be the use of MALDI-MSI technique, to investigate if the fed D₉-Pip is transferred in distal leaves in a different manner upon *Psm*-stimuli compared to the case were D₉-Pip is fed alone. Anyway, this would assume that at least one other signal in addition to Pip is necessary for SAR establishment.

In the past several metabolites have been proposed to take a function in long distance SAR signaling. In several plant species MeSA is involved in resistance signaling (Park et al., 2007; Dempsey and Klessig, 2012; Shah and Zeier, 2013), but by the use of mutant plants deficient in MeSA generation it could be shown that at least in Arabidopsis MeSA is dispensable for SAR establishment (Attaran et al., 2009). Furthermore, the metabolites DA, G3P, and AzA have been described for a potential role in SAR signaling and all of them need for defense signaling activity the lipid-transfer protein DIR1 (DEFECTIVE IN INDUCED RESISTANCE 1) (Chaturvedi et al., 2012; Chanda et al., 2011; Jung et al., 2009; Cecchini et al., 2015b; Shah and Zeier, 2013). Thereby, DIR1 is only required for SAR establishment when plants are inoculated in the afternoon. *dir1* mutant plants inoculated in the morning with an avirulent *Psm* strain activate SAR in distal leaves to a certain extent, whereas *dir1* mutant plants inoculated in the afternoon fail to establish SAR (Liu et al., 2011b). However, how those metabolites interact with each other in defense signaling remains to be elucidated. It could be possible that for SAR establishment a mixture of several signal molecules is required and that this is the reason why SAR is partially activated upon Pip + *Psm* co-infiltration in *ald1* but not after infiltration of Pip alone, although in both cases the same amount of Pip is transported to systemic leaves (Fig.6.2; Figs. 6.7 – 6.12). To test this hypothesis the use of potential double-mutants, deficient in Pip biosynthesis and DA, G3P, or AzA signaling, under the here described experimental

conditions would be interesting for future experiments. Notably, it is also possible that not only chemical signals functions in SAR establishment. It was shown, that in response to bacterial pathogens, signal propagation from local to distal plant sites can occur via cell-to-cell signal perception. Described signals in the context of this cell-to-cell signaling are H_2O_2 and Ca^{2+} . However, the exact pathways for that signal propagation are not clarified now, but it could be shown that systemic defense signaling via cell-to-cell signal propagation is dependent on functional CALCIUM-DEPENDENT PROTEIN KINASE 5 (CDPK5) (Romeis and Herde, 2014). Moreover, it was shown that systemic defense signaling in Arabidopsis in response to herbivore attack includes slight electric signals (wound-activated surface potential changes - WASPs) (Mousavi et al., 2013). Therefore, it could be possible that in addition to chemical signals also cell-to-cell signal perception or electric signals are required for SAR establishment. A possible reason for this assumed tight regulation of SAR could be that SAR establishment is not only beneficial for a plant. SAR establishment is accompanied by a decrease of primary and secondary metabolism, growth processes, and photosynthesis in systemic leaf tissue (Bernsdorff et al., 2016).

Although the role of Pip as a long-distance in SAR establishment could not be clarified in this study, we summarized results obtained from the co-application of exogenous Pip (Pip_{ex}) and *Psm* via the leaf, combined with previous results for SAR regulation via Pip and FMO1 (Návarová et al., 2012; Bernsdorff et al., 2016), in a plausible model (Fig. 6.12). Thereby, Pip and *Psm* are infiltrated in the apolastic space, but we cannot clarify how much of the exogenous applied Pip reach the cytoplasm. In local leaves (1°) Pip is metabolized to different derivatives. Independently from functional FMO1, Pip can serve as a precursor for N-formyl-Pip and Aad (Fig. 6.4; Fig. 6.5; Fig. S5H; Fig. S18). Thereby the conversion from Pip to Aad is not increased upon *Psm* infection and Pip is not the main source for Aad. The main precursor for Aad is Lys, which is converted via LKR to Aad and this pathway is activated upon *Psm*-infection (Fig. 1.3; Fig. 6.4; Návarová et al., 2012). The conversion of Pip to N-formyl-Pip is activated by *Psm*-inoculation, but enzymes involved in this process are not known yet (Fig. 6.5). In a FMO1-dependent manner, Pip can be metabolized to until now not identified metabolites Pip-D2 and Pip-D3 and also this conversion is strongly activated upon *Psm*-inoculation (Fig. 6.6; Fig. 6.12C).

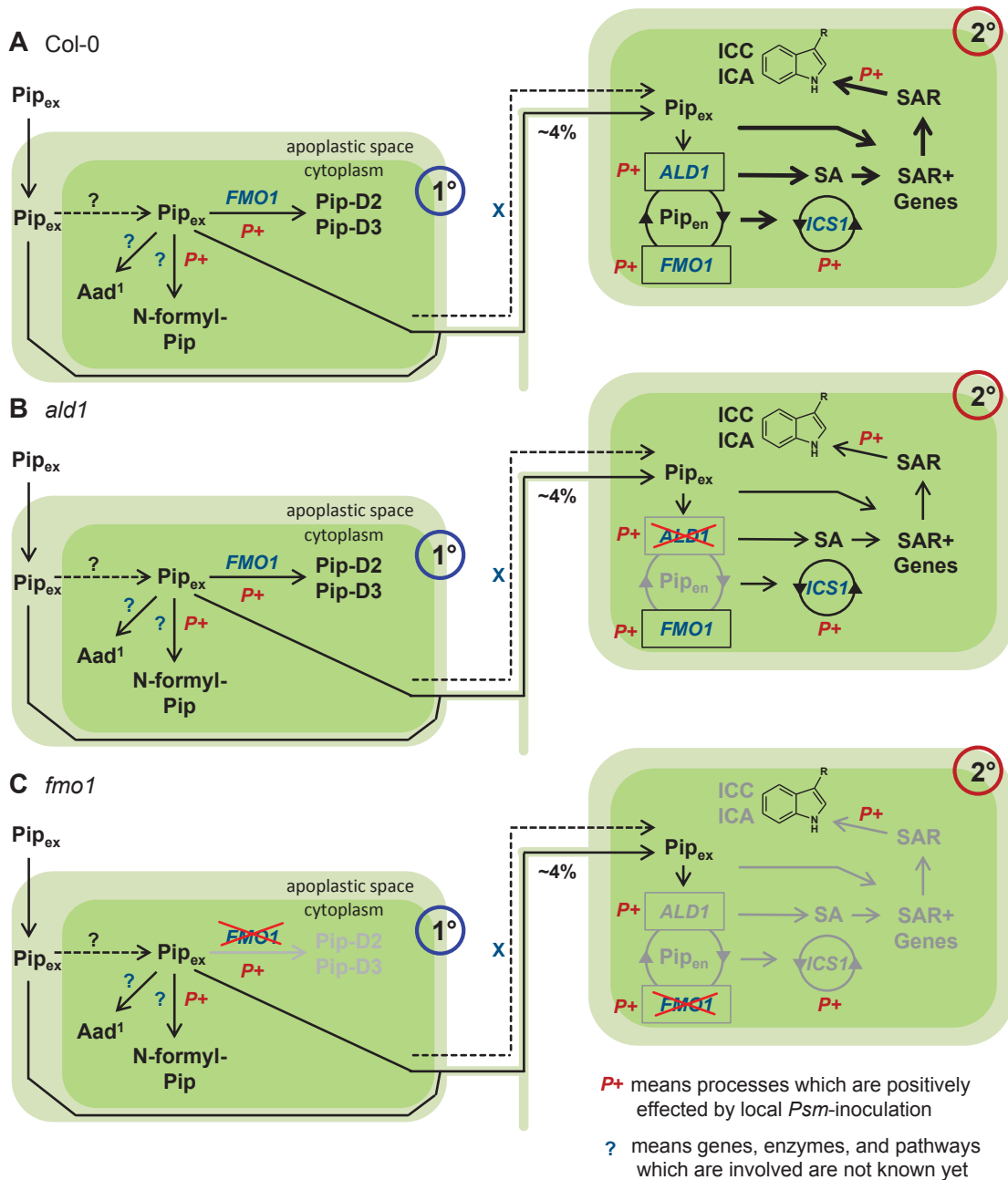


Figure 6.12 Possible model for the transport and metabolism of exogenously applied Pip in combination with *Psm* inoculation in Col-0, *ald1*, and *fmo1*.

Exogenous Pip (Pip_{ex}) and *Psm* are infiltrated in the apolastic space, but we cannot clarify how much Pip_{ex} reach the cytoplasm. At the infection site (**1°**) Pip_{ex} can serve as a precursor for Aad, N-formyl-Pip, and until now not identified Pip-derived metabolites Pip-D2 and Pip-D3. ¹However, Lys and not Pip is the major source for Aad. The generation of N-formyl-Pip, Pip-D2, and Pip-D3 is positively affected upon *Psm*-infection and the generation of Pip-D2 and Pip-D3 is dependent on FMO1. Approx. 4 % of Pip_{ex} can be transported to systemic non-infected leaf-tissue (**2°**). This transport is under the here used experimental conditions not enriched upon *Psm*-inoculation, but can activate the production of endogenous Pip (Pip_{en}) in Col-0. In addition to a *Psm*-triggered stimulus (X), the transported Pip can activate systemic defense responses via SA-dependent and-independent pathways in a FMO1-dependent manner, consistent with established models of SAR-signaling (Návarová et al., 2012; Bernsdorff et al., 2016). A detailed explanation can be found in the text.

However, the exogenously fed Pip can be transported from the leaves where it was applied to systemic not infiltrated leaves (2°), but only approx. 4 % of the applied Pip_{ex} reach systemic leaves. Moreover, the leaf-infiltration assay reveals no information if transported Pip comes from the apoplastic space or from the cytoplasm and Pip-transport is not enriched upon *Psm*-infection (Fig. 6.7B). The transported exogenously applied Pip is sufficient to activate the biosynthesis of endogenous Pip (Pip_{en}) in Col-0, but not in *ald1* and *fmo1* (Fig. 6.7A; Fig. 6.12). However, this transport alone is not sufficient to trigger defense responses in systemic leaf tissue of *ald1* and *fmo1* (Fig. 6.2; Figs. 6.7 – 6.12). In addition to the transported Pip, a further stimulus triggered by local inoculation of *Psm* is needed for activation of defense-responses in systemic leaf tissue of *ald1*, whereas the co-application of Pip_{ex} and *Psm* is not sufficient to partially complement SAR-deficiency of *fmo1* (Fig. 6.12B and C). The molecular mechanisms behind this further assumed stimulus (in the model defined as X) could not be identified in this study and remains to be elucidated. Furthermore, it is possible that this hitherto not identified signal could be generated downstream of functional FMO1. In Col-0, systemic defense response upon the co-infiltration are stronger compared to *ald1* because in addition to exogenously applied Pip the production of Pip_{en} is activated. Anyway, the combination of Pip_{ex} in systemic leaf tissue and a local inoculation of *Psm*, leads to a FMO1-dependent activation of SAR signaling via SA-dependent and – independent pathways consistent with the current models of SAR establishment in Arabidopsis (Fig. 6.2; Figs. 6.7 – 6.12; Návarová et al., 2012; Bernsdorff et al., 2016).

7 Methods

7.1 Plant material and cultivation¹

Arabidopsis thaliana plants, grown on soil, were cultivated in individual pots containing a mixture of soil (Klasmann-Deilmann, Substrat BP3) vermiculite and sand (8:1:1). Plants grown in hydroponic culture (Araponics system) (Tocquin et al., 2003) were cultivated in a medium containing the following nutrients: 1.50 mM Ca(NO₃)₂, 1.25 mM KNO₃, 0.75 mM MgSO₄, 0.50 mM KH₂PO₄, 0.1 mM Na₂O₃Si, 72 μM Fe-EDTA, 50 μM KCl, 50 μM H₃BO₃, 10 μM MnSO₄, 2 μM ZnSO₄, 1.5 μM CuSO₄, 0.075 μM (NH₄)₆Mo₇O₂₄ and the final pH was set up to 6.0 (Gibeaut et al., 1997). The seed-holders were filled with 0.6 % agar. Both systems were cultivated inside a controlled environmental chamber with a 10 h day (9_{AM} to 7_{PM}; photon flux density 100 μmol m⁻² s⁻¹) / 14 h night cycle and relative humidity of 60%. Temperatures during the day and night period were 21 and 18 °C respectively. Experiments were conducted with 5 to 6-week-old, naive and unstressed plants exhibiting a uniform appearance.

The different mutant plants used for this study are listed in table S4. Thereby it is listed if those mutants were described previously, or if they correspond to commercial available T-DNA insertion lines. Homozygous T-DNA insertion lines were identified by PCR according to Alonso et al. (2003) and the primers are listed in table S5. Results for the mutant screen are shown in Fig. S19. Because homozygous *Arabidopsis vte3* mutants are not viable (Cheng et al., 2003), experiments had to be conducted with heterozygous *vte3* mutant plants. All mutants were all generated in the Col-0 background and therefore Col-0 plants were used as control plants. Except for *vte1* mutant, which were generated in the Col-2 background.

7.2 Cultivation and inoculation of bacteria

Pseudomonas syringae pv *maculicola* strain ES4326 (*Psm*), *Psm* carrying the *avrRpm1* avirulence gene (*Psm avrRpm1*) and *Psm* carrying the *luxCDABE* operon from *Photobacterium luminescens* under the control of a constitutive promoter (*Psm-lux*) were grown in King's B medium containing the appropriate antibiotics (Zeier et al., 2004; Fan et al., 2008). Overnight log phase cultures were washed three times with 10 mM MgCl₂ and diluted to different optical densities at 600 nm (OD₆₀₀) for leaf

¹ Published previously under Stahl et al. (2016). Author contributions for the article are listed under "Author contributions Chapter 5" (page 210).

inoculation. The bacterial solutions were infiltrated, between 10 and 12 _{AM}, from the abaxial side into the leaves. For determination of metabolites, quantitative real-time PCR analysis, and for the measurement of nonenzymatic lipid peroxidation via MDA quantification three leaves per plant were infiltrated with a suspension of *Psm* or *Psm avrRpm* at OD₆₀₀ 0.005. As a control same amount of plants was infiltrated with a 10 mM MgCl₂ solution. Additional, for some experiments also same amount of untreated plants was used as control. Regularly two days after this treatment samples from inoculated leaves were harvested, fresh weights were determined and samples were used for the different experiments. Except for time-course analysis, therefore samples from inoculated leaves were taken at time-points as depicted in the respective figures.

7.3 Determination of basal resistance and SAR

For measurement of basal resistance, three leaves per plant were infiltrated with a suspension of *Psm*, *Psm avrRpm1*, or *Psm-lux* at OD₆₀₀ 0.001 between 10 and 12 _{AM}. 2.5 d after the treatment the amount of bacteria in the inoculated leaves was quantified by plating or by luminescence of the *Psm-lux* strain in a leaf disc with defined size and an exposure time of 11 s using a “Sirius” luminometer (Berthold Detection Systems GmbH). Colony forming units (cfu’s) were determined using a generated calculation factor. To induce SAR three lower (1°) leaves per plant were infiltrated with a suspension of *Psm* at OD₆₀₀ 0.005. As a control same amount of plants was infiltrated with a 10 mM MgCl₂ solution. For SAR growth assay two days after the primary treatment three upper leaves (2°) of all plants were infiltrated with a suspension of *Psm* or *Psm-lux* at OD₆₀₀ 0.001. The amount of bacteria in this leaves was quantified as described above.

7.4 flg22 and xanthine/xanthine oxidase treatments

Three leaves per plant were infiltrated with flg22 peptide at a concentration of 100 nM. As a control same amount of plants and leaves was infiltrated with deionized H₂O. The flg22 peptide was synthesized by Mimotopes. To investigate the effect of superoxide, the O₂⁻ producing combination of xanthine (X) and xanthine oxidase (XO) was applied as described previously (Griebel and Zeier, 2010). X and XO were applied at concentrations of 0.5 mM X and 0.5 units ml⁻¹ XO in 20 mM sodium phosphate buffer (pH 6.5). X and XO were obtained from Sigma-Aldrich. Control infiltration was performed with 0.5 mM X in 20 mM sodium phosphate without XO.

7.5 Exogenous application of Pip via the leaf

Three local leaves (1°) per plant were infiltrated with 10 mM MgCl₂, *Psm* suspension (OD₆₀₀ 0.005), D,L-Pip solution (1 mM), or a co-infiltration with *Psm* (OD₆₀₀ 0.005) and Pip solution (1 mM) (for overview of experimental setup see: Fig. S21A). For investigation of the mobility of Pip inside a plant, the function of Pip as a long-distance signal in the establishment of SAR, and the metabolism of Pip in plant immunity the experiments have been conducted with Pip and with deuterium labeled Pip (D₉-Pip; D,L-piperidine-d₉-carboxylic acid; C/D/N ISOTOPES INC.). For the determination of metabolites, local infiltrated leaves (1°) and systemic non-infiltrated leaves (2°) were harvested 48 hpi and fresh weights were determined. SAR was determined as described in 7.3.

7.6 Exogenous application of Pip, SA, and ICA for assessment of basal resistance¹

For metabolite feeding via the root system, plants were supplemented with aqueous solutions of 10 ml of 1mM D,L-Pip or ICA via the soil one day prior to bacterial inoculation (Návarová et al., 2012). ICA (S220027; Sigma Aldrich) was diluted in an equimolar solution of NaOH, and the pH was set to 7.0. Control plants were supplemented with 10 ml of water. For exogenous leaf treatments, solutions of 0.5 mM SA or ICA were infiltrated into three leaves of five-week-old plants. Water was infiltrated as a control treatment. To determine plant resistance to *Psm*, bacterial suspension (OD₆₀₀ 0.001) were infiltrated into the same leaves 4 h later, and bacterial growth was assessed as described above. For metabolite analyses, SA- or water-pretreated leaves received one of the following secondary treatments 4 h after the pre-treatment: *Psm*-infiltration with a suspension of OD₆₀₀ 0.005, mock-infiltration with 10 mM MgCl₂, or no treatment at all. Leaf samples for metabolite analyses were harvested 10h, 24h, and 48h after the second treatment.

¹ Published previously under Stahl et al. (2016). Author contributions for the article are listed under “Author contributions Chapter 5” (page 210).

7.7 Microarray data

Microarray data depicted in table S1, table S2, and table S3, is derived from public available NASC arrays. table S3, NASCARRAYS-454; Wang et al., 2008 and NASCARRAYS-703; Gruner et al., 2013. Table S2, NASCARRAYS-414; Wang et al., 2008. Table S1, NASCARRAYS-414; Wang et al., 2008 and TAIR-ME 00331, Postel et al., 2010.

7.8 Quantitative real-time PCR analysis

RNA isolation, cDNA synthesis, and quantitative real-time PCR analysis were performed as described previously (Návarová et al., 2012). The gene *PTB* (*POLYPYRIMIDIN TRACT BINDING PROTEIN 1*), which is nonresponsive to *P. syringae* infection, was used as a reference gene (Czechowski et al., 2005). The gene-specific primers used in this study are listed in table S6. The expression levels were normalized to those of the reference gene and were expressed relative to value of the gene in MgCl₂-infiltrated leaves.

7.9 Determination of nonenzymatic lipid peroxidation via MDA quantification

Frozen leaf material was homogenized, mixed with 2 ml of 0.1 % trichloroacetic acid (TCA), and centrifuged at 10.000 g for 15 min. 1 ml of the supernatant was mixed with 2 ml of 20 % TCA and 2 ml of 0.5 % thiobarbituric acid (TBA) and the mixture was incubated at 95 °C for 30 min to react MDA with TBA. Thereby a TBA-MDA complex is formed which is reported to have a specific absorbance at 532 nm. The specific absorbance of 532 nm and a nonspecific of 600 nm were measured with an UV-VIS spectrophotometer (UVmini-1240 Shimadzu) and the nonspecific absorbance was subtracted from the specific absorbance. The concentrations of MDA were calculated using Beer-Lambert's equation with an extinction coefficient for MDA of 155 mM⁻¹ cm⁻¹ (Heath and Packer, 1968) and expressed to the fresh weight. Because this assay is described to overestimate the absolute concentration of MDA we normalized data on MDA levels in untreated Col-0 leaves and depicted them as fold-changes.

7.10 Determination of metabolites via GC/MS

Determination of endogenous levels of tocopherols, free SA, glycosidic bound SA, scopoletin, metabolites listed in table 1, and metabolites listed in table S7 was

conducted by vapour-phase extraction procedure and subsequent GC/MS-analysis as described previously by Mishina and Zeier (2006) with minor modifications. The vapour-phase extraction procedure was performed with Porapak-Q absorbent (VCT-1/4X3-POR-Q; Analytical Research Systems). A 4 μ l aliquot was subjected to GC/MS analysis and separated on a gas chromatograph (GC 7890A; Agilent Technologies) equipped with a fused silica capillary column (HP-5MS 30 m x 0.25 mm; J&W Scientific, Agilent Technologies), and mass spectra were recorded with a combined 5975C mass spectrometric detector (Agilent Technologies) in the electron ionization mode. For GC separation the injector temperature was to 250 °C. A constant flow of helium (1.2 ml/min) and the following temperature program were used: 50 °C for 3 min, with 8 °C/min to 240 °C, with 20 °C/min to 320 °C, 320 °C for 10 min. For quantification of metabolites, peaks emanating from selected ion chromatograms were integrated. The corresponding peak areas were expressed relative to the peak area of internal standards, m/z 124 for D₄-SA, m/z 130 for indole-3-propionic acid (IPA), m/z 388 for tocol, and m/z 160 for 6-methyl-coumarin. Detailed information for mass spectra of Trp-derived indolics is given in table 1. Mass spectra of the other quantified metabolites are listed in table S7. Corresponding peak areas of metabolites listed in table 1 were expressed relative to the peak area of IPA, internal standards for the other quantified metabolites are listed in table S7.

7.11 Determination of free amino acids via GC/MS

Determination of Trp, Pip, D₉-Pip, Aad and D₆-Aad was performed as described in Návarová et al. (2012) using the EZ:faast free amino acid kit for GC/MS (Phenomenex).

7.12 Determination of metabolites via HPLC¹

Determination of I3A and I3M was performed by high performance liquid chromatography (HPLC) coupled with fluorescence detection. Homogenized leaf material was mixed with 520 μ l DMSO (containing IPA – 1 ng/ μ l), the mixture was shaken thoroughly for 5 minutes and centrifuged for 20 min at 13200 rpm. 450 μ l of the supernatant was transferred into a new reaction tube and centrifuged again for 5 min at

¹ Published previously under Stahl et al. (2016). Author contributions for the article are listed under “Author contributions Chapter 5” (page 210).

13200 rpm. 400 µl of the supernatant was transferred into a new reaction tube and a 5 µl aliquot was subjected to HPLC analysis. The injected sample mixture was separated on a high-performance liquid chromatograph (1260 Infinity; Agilent Technologies) equipped with a C18 column (Zorbax SB-C18, 2.1x100 mm, 1.8 µm; Agilent Technologies) with water (0.01% formic acid) as solvent A and 98% acetonitrile (2% H₂O; 0.01% formic acid) as solvent B at a flow rate of 0.250 ml/min and at 27 °C (gradient of solvent B: 3% for 4 min, to 9% in 5 min, to 11% in 6 min, to 28% in 15 min, to 60% in 10 min, to 100% in 10 min, 100% for 5 min, to 0% in 2 min, 0% for 4 min, to 3% in 1 min, 3% for 5 min). Peaks were detected with a fluorescence detector (1260 Infinity Fluorescence Detector; Agilent Technologies) by an excitation of 275 nm and an emission of 350 nm. For quantification, the corresponding peaks were integrated and areas were expressed relative to the peak area of the internal standard IPA.

7.13 Accession numbers

Sequence Data from genes described in this study can be found in the Arabidopsis Genome Initiative or GenBank/EMBL databases under the following accession numbers: *TAT7* (At5g53970), *HPPD* (At1g06570), *VTE1* (At4g32770), *VTE2* (At2g18950), *VTE3* (At3g63410), *VTE4* (At1g64970), *VTE5* (At5g04490), *VTE6* (At1g78620), *ETR1* (At1g66340), *DDE2* (At5g42650), *ICS1* (At1g74710), *ABA2* (At1g52340), *CPR5* (At5g64930), *COI1* (At2g39940), *ALD1* (At2g13810), *RBOHD* (At5g47910), *FAD3* (At2g29980), *FAD7* (At3g11170), *FAD8* (At5g05580), *PTB* (At3g01150), *CYP79B2* (At4g39950), *CYP79B3* (At2g22330), *PEN2* (At2g44490), *CYP81F1* (At4g37430), *CYP81F2* (At5g57220), *CYP71A13* (At2g30770), *PAD3* (At3g26830), *PAD4* (At3g52430), *MYB34* (At5g60890), *MYB51* (At1g18570), *MYB122* (At1g74080), *FMO1* (At1g19250), (At2g39940), *NPR1* (At1g64280), *ATF1* (At2g32030), *DIN4* (Atg3g13450), *IVD1* (At3g45300), *NATA1* (At2g39030), *F6`H1* (At3g13610), *GRXS13* (At1g03850), *ARD3* (At2g26400), *PR1* (At2g14610), and *SAG13* (At2g29350).

8 References

- Abeysekara, N.S., Swaminathan, S., Desai, N., Guo, L., and Bhattacharyya, M.K.** (2016). The Plant immunity inducer pipecolic acid accumulates in the xylem sap and leaves of soybean seedlings following *Fusarium virguliforme* infection. *Plant Sci.* **243**, 105-114.
- Adio, A.M., Casteel, C.L., De Vos, M., Kim, J.H., Joshi, V., Li, B., Juéry, C., Daron, J., Kliebenstein, D.J., and Jander, G.** (2011). Biosynthesis and defensive function of N^δ-acetylornithine, a jasmonate-induced *Arabidopsis* metabolite. *Plant Cell*, **23**, 3303-3318.
- Agerbirk, N., and Olsen, C.E.** (2012). Glucosinolate structures in evolution. *Phytochemistry*, **77**, 16–45.
- Ahuja, I., Kissen, R., and Bones, A.M.** (2012). Phytoalexins in defense against pathogens. *Trends Plant Sci.* **17**, 73-90.
- Alonso, J.M., et al.** (2003). Genome-wide insertional mutagenesis of *Arabidopsis thaliana*. *Science*, **301**, 653-657.
- Anderson, J.P., et al.** (2004). Antagonistic interaction between abscisic acid and jasmonate-ethylene signaling pathways modulates defense gene expression and disease resistance in *Arabidopsis*. *Plant Cell*, **16**, 3460–3479.
- Andreae, W.E.** (1952). Effect of Scopoletin on Indoleacetic Acid Metabolism. *Nature*, **170**, 83-84.
- Araujo, W.L., et al.** (2010) Identification of the 2-hydroxyglutarate and isovaleryl-CoA dehydrogenases as alternative electron donors linking lysine catabolism to the electron transport chain of *Arabidopsis* mitochondria. *Plant Cell*, **22**, 1549-1563.
- Arend, M., Schnitzler, J.P., Ehltng, B., Hänsch, R., Lange, T., Rennenberg, H., Himmelbach, A., Grill, E., and Fromm, J.** (2009). Expression of the *Arabidopsis* mutant ABI1 gene alters abscisic acid sensitivity, stomatal development, and growth morphology in gray poplars. *Plant Physiol.* **151**, 2110-2119.
- Ascencio-Ibáñez, J.T., Sozzani R, Lee, T.J., Chu, T.M., Wolfinger, R.D., Cella, R., and Hanley-Bowdoin, L.** (2008). Global analysis of *Arabidopsis* gene expression uncovers a complex array of changes impacting pathogen response and cell cycle during geminivirus infection. *Plant Physiol.* **148**, 436-454.
- Attaran, E., Rostás, M., and Zeier, J.** (2008). *Pseudomonas syringae* elicits emission of the terpenoid (E,E)-4,8,12-trimethyl-1,3,7,11-tridecatetraene in *Arabidopsis* leaves via jasmonate signaling and expression of the terpene synthase TPS4. *Mol. Plant. Microbe Interact.* **21**, 1482-1497.

References

- Attaran, E., Zeier, T.E., Griebel, T., and Zeier J.** (2009). Methyl salicylate production and jasmonate signaling are not essential for systemic acquired resistance in Arabidopsis. *Plant Cell*, **21**, 954-71.
- Axtell, M.J., and Staskawicz, B.J.** (2003). Initiation of RPS2-specified disease resistance in Arabidopsis is coupled to the AvrRpt2-directed elimination of RIN4. *Cell* **112**, 369–377.
- Balmer, A., Pastor, V., Gamir, J., Flors, V., and Mauch-Mani, B.** (2014). The 'prime-ome': towards a holistic approach to priming. *Trends Plant Sci.* **20**, 443-452.
- Baxter, A., Mittler, R., and Suzuki, N.** (2014). ROS as key players in plant stress signalling. *J Exp Bot.* **65**, 1229-1240.
- Bednarek, P.** (2012). Chemical warfare or modulators of defence responses - the function of secondary metabolites in plant immunity. *Curr. Opin. Plant Biol.* **15**, 407-414.
- Bednarek, P., and Osbourn, A.** (2009). Plant-microbe interactions: chemical diversity in plant defense. *Science.* **324**, 746-748.
- Bednarek, P., et al.** (2009). A Glucosinolate Metabolism Pathway in Living Plant Cells Mediates Broad-Spectrum Antifungal Defense. *Science*, **323**, 101-106.
- Bednarek, P., Piślewska-Bednarek, M., Ver Loren van Themaat, E., Maddula, R.K., Svatoš, A., and Schulze-Lefert, P.** (2011). Conservation and clade-specific diversification of pathogen-inducible tryptophan and indole glucosinolate metabolism in Arabidopsis thaliana relatives. *New Phytol.* **192**, 713-726.
- Bednarek, P., Schneider, B., Svatos, A., Oldham, N.J., and Hahlbrock, K.** (2005). Structural complexity, differential response to infection, and tissue specificity of indolic and phenylpropanoid secondary metabolism in Arabidopsis roots. *Plant Physiol.* **138**, 1058-1070.
- Bender, C.L., Alarcón-Chaidez, F., and Gross, D.C.** (1999). *Pseudomonas syringae* phytotoxins: mode of action, regulation, and biosynthesis by peptide and polyketide synthetases. *Microbiol. Mol. Biol. Rev.* **63**, 266-292.
- Bender, J., and Celenza, J.L.** (2009). Indolic glucosinolates at the crossroads of tryptophan metabolism. *Phytochem. Rev.* **8**, 25-37.
- Bergmüller, E., Porfirova, S., and Dörmann P.** (2003). Characterization of an Arabidopsis mutant deficient in γ -tocopherol methyltransferase. *Plant Mol. Biol.* **52**, 1181–1190.
- Bernsdorff, F., Döring A.-C., Gruner, K., Schuck, S., Bräutigam, A., and Zeier, J.** (2016). Pipecolic acid orchestrates plant systemic acquired resistance and defense priming via salicylic acid-dependent and independent pathways. *Plant Cell*, **28**, 102–129.

References

- Binder, S.** (2010). Branched-Chain Amino Acid Metabolism in *Arabidopsis thaliana*. The Arabidopsis Book, **8**, e0137.
- Bisgrove, S.R., Simonich, M.T., Smith, N.M., Sattler, A., and Innes, R.W.** (1994). A disease resistance gene in Arabidopsis with specificity for two different pathogen avirulence genes. Plant Cell, **6**, 927-933.
- Bleecker, A.B., and Kende, H.** (2000). Ethylene: A gaseous signal molecule in plants. Annu. Rev. Cell. Dev. Biol. **16**, 1–18.
- Bleecker, A.B., Estelle, M.A., Somerville, C., and Kende, H.** (1988) Insensitivity to ethylene conferred by a dominant mutation in Arabidopsis thaliana. Science, **241**, 1086–1089.
- Bohman, S., Staal, J., Thomma, B.P., Wang, M., and Dixelius, C.** (2004). Characterisation of an *Arabidopsis-Leptosphaeria maculans* pathosystem: resistance partially requires camalexin biosynthesis and is independent of salicylic acid, ethylene and jasmonic acid signaling. Plant J. **37**, 9-20.
- Boller, T., and He, S.Y.** (2009). Innate immunity in plants: an arms race between pattern recognition receptors in plants and effectors in microbial pathogens. Science, **324**, 742-744.
- Böttcher, C., Chapman, A., Fellermeier, F., Choudhary, M., Scheel, D., and Glawischnig, E.** (2014). The biosynthetic pathway of indole-3carbaldehyde and indole-3-carboxylic acid derivatives in *Arabidopsis thaliana*. Plant Physiol. **165**, 841-853.
- Böttcher, C., Westphal, L., Schmotz, C., Prade, E., Scheel, D., and Glawischnig, E.** (2009). The Multifunctional Enzyme CYP71B15 (PHYTOALEXIN DEFICIENT3) Converts Cysteine-Indole-3-Acetonitrile to Camalexin in the Indole-3-Acetonitrile Metabolic Network of *Arabidopsis thaliana*. Plant Cell. **21**, 1830-1845.
- Bowling, S.A., Clarke, J.D., Liu, Y., Klessig, D.F., and Dong, X.** (1997). The *cpr5* mutant of Arabidopsis expresses both NPR1-dependent and NPR1-independent resistance. Plant Cell, **9**, 1573–1584.
- Bowling, S.A., Clarke, J.D., Liu, Y., Klessig, D.F., and Dong, X.** (1997). The *cpr5* mutant of Arabidopsis expresses both NPR1-dependent and NPR1-independent resistance. Plant Cell, **9**, 1573–1584.
- Brown, P.D., Tokuhiisa, J.G., Reichelt, M., and Gershenzon J.** (2003). Variation of glucosinolate accumulation among different organs and developmental stages of *Arabidopsis thaliana*. Phytochemistry. **62**, 471-481.
- Bruessow, F., Gouhier-Darimont, C., Buchala, A., Metraux, J.P., and Reymond, P.** (2010). Insect eggs suppress plant defence against chewing herbivores. Plant J. **62**, 876-85.

References

- Cahoon, E.B., Hall, S.E., Ripp, K.G., Ganzke, T.S., Hitz, W.D., and Coughlan, S.J.** (2003). Metabolic redesign of vitamin E biosynthesis in plants for tocotrienol production and increased antioxidant content. *Nature Biotechnology*. **21**, 1082–1087.
- Cecchini, N.M., Jung, H.W., Engle, N.L., Tschaplinski, T.J., and Greenberg, J.T.** (2015a). ALD1 Regulates Basal Immune Components and Early Inducible Defense Responses in Arabidopsis. *Mol. Plant Microbe Interact.* **28**, 455-466.
- Cecchini, N.M., Monteoliva, M.I., and Alvarez, M.E.** (2011). Proline dehydrogenase contributes to pathogen defence in Arabidopsis. *Plant Physiol.* **155**, 1947–1959.
- Cecchini, N.M., Steffes, K., Schläppi, M.R., Gifford, A.N., and Greenberg, J.T.** (2015b). Arabidopsis AZI1 family proteins mediate signal mobilization for systemic defence priming. *Nat. Commun.* **6**, 7658.
- Chanda, B., et al.** (2011). Glycerol-3-phosphate is a critical mobile inducer of systemic immunity in plants. *Nat. Genet.* **43**, 421-427.
- Chaouch, S., Queval, G., and Noctor, G.** (2012). AtRbohF is a crucial modulator of defence-associated metabolism and a key actor in the interplay between intracellular oxidative stress and pathogenesis responses in Arabidopsis. *Plant J.* **69**, 613-627.
- Chaerle, L., Lenk, S., Hagenbeek, D., Buschmann, C., and Van Der Straeten, D.** (2007). Multicolor fluorescence imaging for early detection of the hypersensitive reaction to tobacco mosaic virus. *J. Plant Physiol.* **164**, 253-262.
- Charles, A.K.** (1986). Pilocarpic acid receptors in rat cerebral cortex. *Neurochem. Res.* **11**, 521–525.
- Chaturvedi, R., Venables, B., Petros, R.A., Nalam, V., Li, M., Wang, X., Takemoto, L.J., and Shah, J.** (2012). An abietane diterpenoid is a potent activator of systemic acquired resistance. *Plant J.* **71**, 161-172.
- Chen, Y., Shen, H., Wang, M., Li, Q., and He, Z.** (2013). Salicyloyl-aspartate synthesized by the acetyl-amido synthetase GH3.5 is a potential activator of plant immunity in Arabidopsis. *Acta. Biochim. Biophys. Sin. (Shanghai)*. **45**, 827-836.
- Chen, J., Zhang, Y., Wang, C., Lü, W., Jin, J.B., and Hua X.** (2011). Proline induces calcium-mediated oxidative burst and salicylic acid signaling. *Amino Acids*, **40**, 1473–1484.
- Chen, Z., Zheng, Z., Huang, J., Lai, Z., and Fan, B.** (2009). Biosynthesis of salicylic acid in plants. *Plant Signal. Behav.* **4**, 493–496.

References

- Cheng, Z., Sattler, S., Maeda, H., Sakuragi, Y., Bryant, D.A., and DellaPenna, D.** (2003). Highly divergent methyltransferases catalyze a conserved reaction in tocopherol and plastoquinone synthesis in cyanobacteria and photosynthetic eukaryotes. *Plant Cell*, **15**, 2343-2356.
- Chinchilla, D., Zipfel, C., Robatzek, S., Kemmerling, B., Nürnberger, T., Jones, J.D., Felix, G., and Boller, T.** (2007). A flagellin-induced complex of the receptor FLS2 and BAK1 initiates plant defence. *Nature*, **448**, 497-500.
- Clarke, J.D., Aarts, N., Feys, B.J., Dong, X., and Parker, J.E.** (2001). Constitutive disease resistance requires *EDS1* in the *Arabidopsis* mutants *cpr1* and *cpr6* and is partially *EDS1*-dependent in *cpr5*. *Plant J.* **26**, 409-420.
- Collakova, E., and DellaPenna, D.** (2003). The role of homogentisate phytyltransferase and other tocopherol pathway enzymes in the regulation of tocopherol synthesis during abiotic stress. *Plant Physiol.* **133**, 930-940.
- Collins, N.C., Thordal-Christensen, H., Lipka, V., Bau, S., Kombrink, E., Qiu, J.L., Hüchelhoven, R., Stein, M., Freialdenhoven, A., Somerville, S.C., and Schulze-Lefert, P.** (2003). SNARE-protein-mediated disease resistance at the plant cell wall. *Nature*. **425**, 973-977.
- Conrath, U.** (2011). Molecular aspects of defence priming. *Trends Plant Sci.* **16**, 524–531.
- Conrath, U., Beckers, G.J., Langenbach, C.J., and Jaskiewicz, M.R.** (2015). Priming for enhanced defense. *Annu. Rev. Phytopathol.* **53**, 97-119.
- Consonni, C., Bednarek, P., Humphry, M., Francocci, F., Ferrari, S., Harzen, A., Ver Loren van Themaat, E., and Panstruga, R.** (2010). Tryptophan-derived metabolites are required for antifungal defense in the *Arabidopsis mlo2* mutant. *Plant Physiol.* **152**, 1544-1561.
- Costet, L., Fritig, B., and Kauffmann, S.** (2002). Scopoletin expression in elicitor-treated and tobacco mosaic virus-infected tobacco plants. *Physiol. Plant.* **115**, 228-235.
- Cunnac, S., Lindeberg, M., and Collmer, A.** (2009). *Pseudomonas syringae* type III secretion system effectors: repertoires in search of functions. *Curr. Opin. Microbiol.* **12**, 53–60.
- Czechowski, T., Stitt, M., Altmann, T., Udvardi, M.K., and Scheible, W.R.** (2005). Genome-wide identification and testing of superior reference genes for transcript normalization in *Arabidopsis*. *Plant Physiol.* **139**, 5–17.
- D'Auria, J.C.** (2006). Acyltransferases in plants: a good time to be BAHD. *Curr. Opin. Plant Biol.* **9**, 331-340.

References

- de Souza, S.M., Delle Monache, F., and Smânia, A. Jr.** (2005). Antibacterial activity of coumarins. *Z. Naturforsch. C.* **60**, 693-700.
- de Torres Zabala, M., Bennett, M.H., Truman, W.H., and Grant, M.R.** (2009). Antagonism between salicylic and abscisic acid reflects early host-pathogen conflict and moulds plant defence responses. *Plant J.* **59**, 375–386.
- DellaPenna D., and Pogson B.J.** (2006). Vitamin Synthesis in Plants: Tocopherols and Carotenoids. *Annu. Rev. Plant Biol.* **57**, 711–738.
- Delledonne, M., Xia, Y., Dixon, R.A. and Lamb, C.** (1998) Nitric oxide functions as a signal in plant disease resistance. *Nature*, **394**, 585–588.
- Dempsey, D.A., and Klessig, D.F.** (2012). SOS - too many signals for systemic acquired resistance? *Trends Plant Sci.* **17**, 538-545.
- Deuschle, K., Funck, D., Forlani, G., Stransky, H., Biehl, A., Leister, D., van der Graaff, E., Kunze, R., and Frommer, W.B.** (2004). The role of D1-pyrroline-5-carboxylate dehydrogenase in proline degradation. *Plant Cell*, **16**, 3413–3425.
- Ding, Y., Dommel, M., and Mou, Z.** (2016). Abscisic Acid Promotes Proteasome-Mediated Degradation of the Transcription Coactivator NPR1 in *Arabidopsis thaliana*. *Plant J.* (article in press)
- Dixon, R.A.** (2001). Natural products and plant disease resistance. *Nature*, **411**, 843-847.
- Doares, S.H., Narváez-Vásquez, J., Conconi, A., and Ryan, C.A.** (1995). Salicylic acid inhibits synthesis of proteinase inhibitors in tomato leaves induced by systemin and jasmonic acid. *Plant Physiol.* **108**, 1741–1746.
- Dong, X.** (2004). NPR1, all things considered. *Curr. Opin. Plant Biol.* **7**, 547–552.
- Dörmann, P.** (2007). Functional diversity of tocopherols in plants. *Planta*, **225**, 269-276.
- Durrant, W.E., and Dong, X.** (2004). Systemic acquired resistance. *Annu. Rev. Phytopathol.* **42**, 185-209.
- Dyda, F., Klein, D.C., and Hickman, A.D.** (2000). GCN5-Related N-Acetyltransferases: A Structural Overview. *Annu. Rev. Biophys. Biomol. Struct.* **29**, 81-103.
- El Oirdi, M., Trapani, A., and Bouarab, K.** (2010). The nature of tobacco resistance against *Botrytis cinerea* depends on the infection structures of the pathogen. *Environ Microbiol.* **12**, 239-253.

References

- Ellouzi, H., Hamed, K.B., Cela, J., Müller, M., Abdelly, C., and Munné-Bosch, S.** (2013). Increased sensitivity to salt stress in tocopherol-deficient *Arabidopsis* mutants growing in a hydroponic system. *Plant Signal. Behav.* **8**, 2.
- Esteban, R., Olano, J.M., Castresana, J., Fernández-Marín, B., Hernández, A., Becerril, J.M., and García-Plazaola, J.I.** (2009). Distribution and evolutionary trends of photoprotective isoprenoids (xanthophylls and tocopherols) within the plant kingdom. *Physiol. Plant.* **135**, 379-189.
- Fabro, G., Kovács, I., Pavet, V., Szabados, L., and Alvarez, M.E.** (2004). Proline accumulation and *AtP5CS2* gene activation are induced by plant-pathogen incompatible interactions in *Arabidopsis*. *Mol. Plant Microbe. Interact.* **17**, 343–350.
- Falk, J., and Munné-Bosch, S.** (2010). Tocochromanol functions in plants: antioxidation and beyond. *J Exp Bot.* **6**, 1549-1566.
- Fan, J., Crooks, C., and Lamb, C.** (2008). High-throughput quantitative luminescence assay of the growth in planta of *Pseudomonas syringae* chromosomally tagged with *Photorhabdus luminescens luxCDABE*. *Plant J.* **53**, 393-399.
- Farmer, E.E., and Davoine, C.** (2007). Reactive electrophile species. *Curr. Opin. Plant. Biol.* **10**, 380-6.
- Felix, G., Duran, J. D., Volko, S., and Boller, T.** (1999). Plants have a sensitive perception system for the most conserved domain of bacterial flagellin. *Plant J.* **18**, 265–276.
- Felix, G., Regenass, M., and Boller, T.** (1993). Specific perception of subnanomolar concentrations of chitin fragments by tomato cells. Induction of extracellular alkalinization, changes in protein phosphorylation, and establishment of a refractory state. *Plant J.* **4**, 307–316.
- Ferrari, S., Galletti, R., Denoux, C., De Lorenzo, G., Ausubel, F.M., and Dewdney J.** (2007). Resistance to *Botrytis cinerea* induced in *Arabidopsis* by elicitors is independent of salicylic acid, ethylene, or jasmonate signaling but requires PHYTOALEXIN DEFICIENT3. *Plant Physiol.* **144**, 367-379.
- Feys, B.J., Moisan, L.J., Newman, M.A., and Parker, J.E.** (2001). Direct interaction between the *Arabidopsis* disease resistance signaling proteins, EDS1 and PAD4. *EMBO J.* **20**, 5400-5411.
- Flor, H.H.** (1971). Current status of the gene-for-gene concept. *Annu. Rev. Phytopathol.* **9**, 275–296.

References

- Forcat, S., Bennett, M., Grant, M., and Mansfield, J.W.** (2010). Rapid linkage of indole carboxylic acid to the plant cell wall identified as a component of basal defence in *Arabidopsis* against *hrp* mutant bacteria. *Phytochemistry*. **71**, 870-876.
- Frerigmann, H., and Gigolashvili, T.** (2014). MYB34, MYB51, and MYB122 Distinctly Regulate Indolic Glucosinolate Biosynthesis in *Arabidopsis thaliana*. *Mol. Plant*. **7**, 814-828.
- Frerigmann, H., Glawischnig, E., and Gigolashvili, T.** (2015). The role of MYB34, MYB51, and MYB122 in the regulation of camalexin biosynthesis in *Arabidopsis thaliana*. *Front. Plant Sci.* **6**, 654. doi: 10.3389/fpls/2015.00654.
- Frerigmann, H., Pislewska-Bednarek, M., Sanchez-Vallet, A., Molina, A., Glawischnig, E., Gigolashvili, T., and Bednarek, P.** (2016). Regulation of pathogen triggered tryptophan metabolism in *Arabidopsis thaliana* by MYB transcription factors and indole glucosinolate conversion products. *Mol. Plant*. **9**, 682-695.
- Fu, Z.Q., and Dong, X.** (2013). Systemic acquired resistance: turning local infection into global defense. *Annu Rev Plant Biol.* **64**, 839-863.
- Gaffney, T., Friedrich, L., Vernooij, B., Negrotto, D., Nye, G., Uknes, S., Ward, E., Kessmann, H., and Ryals, J.** (1993). Requirement of Salicylic Acid for the Induction of Systemic Acquired Resistance. *Science*, **261**, 754-756.
- Galili, G., Tang, G., Zhu, X., and Gakiere, B.** (2001). Lysine catabolism: a stress and development super-regulated metabolic pathway. *Curr. Opin. Plant Biol.* **4**, 261-266.
- Gamir, J., Pastor, V., Cerezo, M., and Flors, V.** (2012). Identification of indole-3-carboxylic acid as mediator of priming against *Plectosphaerella cucumerina*. *Plant Physiol. Biochem.* **61**, 169-179.
- Garcia, D., Sanier, C., Macheix, J. J., and D'Auzac, J.** (1995). Accumulation of scopoletin in *Hevea brasiliensis* infected by *Microcyclus ulei* (P. Henn.) V. ARX and evaluation of its fungitoxicity for three leaf pathogens of rubber tree. *Physiol. Mol. Plant Pathol.* **47**, 213-223.
- Garcion, C., Lohmann, A., Lamodièrè, E., Catinot, J., Buchala, A., Doermann, P., and Métraux, J.P.** (2008). Characterization and biological function of the ISOCHORISMATE SYNTHASE2 gene of *Arabidopsis*. *Plant Physiol.* **147**, 1279-1287.
- Geng X., Cheng J., Gangadharan A., and Mackey, D.** (2012) The coronatine toxin of *Pseudomonas syringae* is a multifunctional suppressor of *Arabidopsis* defense. *Plant Cell*, **24**, 4763-4774.

References

- Geu-Flores, F., Møldrup, M.E., Böttcher, C., Olsen, C.E., Scheel, D., and Halkier, B.A.** (2011). Cytosolic γ -glutamyl peptidases process glutathione conjugates in the biosynthesis of glucosinolates and camalexin in *Arabidopsis*. *Plant Cell*. **23**, 2456-2469.
- Gibeaut, D.M., Hulett, J., Cramer, G.R., and Seemann, J.R.** (1997). Maximal Biomass of *Arabidopsis thaliana* Using a Simple, Low-Maintenance Hydroponic Method and Favorable Environmental Conditions. *Plant Physiol*. **115**, 317-319.
- Gigolashvili, T., Berger, B. and Flügge, U.I.** (2009). Specific and coordinated control of indolic and aliphatic glucosinolate biosynthesis by R2R3-MYB transcription factors in *Arabidopsis thaliana*. *Phytochemistry. Rev.* **8**, 3-13.
- Glawischnig, E.** (2007). Camalexin. *Phytochemistry*. **68**, 401-406.
- Glawischnig, E., Hansen, B.G., Olsen, C.E., and Halkier, B.A.** (2004). Camalexin is synthesized from indole-3-acetaldoxime, a key branching point between primary and secondary metabolism in *Arabidopsis*. *Proc. Natl Acad. Sci. USA*. **101**, 8245-8250.
- Glazebrook, J.** (2001). Genes controlling expression of defense responses in *Arabidopsis* - 2001 status. *Curr. Opin. Plant Biol.* **4**, 301-308.
- Glazebrook, J., and Ausubel, F.M.** (1994). Isolation of phytoalexin-deficient mutants of *Arabidopsis thaliana* and characterization of their interactions with bacterial pathogens. *Proc. Natl. Acad. Sci. USA*. **91**, 8955–8959.
- Gnonlonfin, G.J.B., Sannic, A., and Brimera, L.** (2012). Review Scopoletin – A Coumarin Phytoalexin with Medicinal Properties. *Crit. Rev. Plant Sci.* **31**, 47-56.
- Gómez-Gómez, L., Felix, G., and Boller, T.** (1999). A single locus determines sensitivity to bacterial flagellin in *Arabidopsis thaliana*. *Plant J.* **18**, 277–284.
- Goyer, A., Johnson, T.L., Olsen, L.J., Collakova, E., Shachar-Hill, Y., Rhodes, D., and Hanson A.D.** (2004). Characterization and metabolic function of a peroxisomal sarcosine and pipicolate oxidase from *Arabidopsis*. *J. Biol. Chem.* **279**, 16947-16953.
- Griebel, T., and Zeier, J.** (2010). A role for β -sitosterol to stigmasterol conversion in plant pathogen interactions. *Plant J.* **63**, 254-268.
- Grun, G., Berger, S., Matthes, D., and Mueller, M. J.** (2007). Early accumulation of non-enzymatically synthesized oxylipins in *Arabidopsis thaliana* after infection with *Pseudomonas syringae*. *Funct. Plant Biol.* **34**, 65-71.
- Gruner, K., Griebel, T., Návarová H., Attaran, E., and Zeier J.** (2013). Reprogramming of plants during systemic acquired resistance. *Front. in Plant Sci.* **4**, 252.

References

- Grusak, M.A., and DellaPenna, D.** (1999). Improving the nutrient composition of plants to enhance human nutrition and health. *Annu. Rev. Plant Physiol. Plant Mol. Biol.* **50**, 133–161.
- Hagemeier, J., Schneider, B., Oldham, N.J., and Hahlbrock K.** (2001). Accumulation of soluble and wall-bound indolic metabolites in *Arabidopsis thaliana* leaves infected with virulent or avirulent *Pseudomonas syringae* pathovar tomato strains. *Proc. Natl Acad. Sci. USA.* **98**, 753-758.
- Halkier, B.A., and Gershenzon, J.** (2006). Biology and biochemistry of glucosinolates. *Annu. Rev. Plant Biol.* **57**, 303-333.
- Hansjakob, A., Riederer, M., and Hildebrandt, U.** (2011). Wax matters: absence of very-long-chain aldehydes from the leaf cuticular wax of the glossy11 mutant of maize compromises the prepenetration processes of *Blumeria graminis*. *Plant Pat.* **60**, 1151–1161.
- Havaux, M., Eymery, F., Porfirova, S., Rey, P., and Dörmann, P.** (2005). Vitamin E Protects against Photoinhibition and Photooxidative Stress in *Arabidopsis thaliana*. *Plant Cell*, **17**, 3451–3469.
- Havaux, M., Lütz, C., and Grimm, B.** (2003). Chloroplast Membrane Photostability in ch1P Transgenic Tobacco Plants Deficient in Tocopherols. *Plant Physiol.* **132**, 300–310.
- Havaux, M., Triantaphylidès, C., and Genty, B.** (2006). Autoluminescence imaging: a non-invasive tool for mapping oxidative stress. *Trends Plant Sci.* **11**, 480-484.
- Heath, R.L., and Packer, L.** (1968) Photoperoxidation in isolated chloroplasts: I. Kinetics and stoichiometry of fatty acid peroxidation. *Arch. Biochem. Biophys.* **125**, 189-198.
- Herde, M., Gärtner, K., Köllner, T. G., Fode, B., Boland, W., Gershenzon, J., Gatz, C., and Tholl, D.** (2008). Identification and regulation of TPS04/GES, an *Arabidopsis* geranylinalool synthase catalyzing the first step in the formation of the insect-induced volatile C₁₆-homoterpene TMTT. *Plant Cell*, **20**, 1152-1168.
- Hilfiker, O., Groux, R., Bruessow, F., Kiefer, K., Zeier, .J, and Reymond, P.** (2014). Insect eggs induce a systemic acquired resistance in *Arabidopsis*. *Plant J.* **80**, 1085-1094.
- Hincha, D.K.** (2008). Effects of α-tocopherol (vitamin E) on the stability and lipid dynamics of model membranes mimicking the lipid composition of plant chloroplast membranes. *FEBS Lett.* **582**, 3687–3692.
- Hiruma, K., Fukunaga, S., Bednarek, P., Pislewska-Bednarek, M., Watanabe, S., Narusaka, Y., Shirasu, K., and Takano, Y.** (2013). Glutathione and tryptophan metabolism are required for *Arabidopsis* immunity during the hypersensitive response to hemibiotrophs. *Proc. Natl Acad. Sci. USA.* **110**, 9589-9594.

References

- Huang, T., Jander, G., and de Vos, M.** (2011). Non-protein amino acids in plant defense against insect herbivores: representative cases and opportunities for further functional analysis. *Phytochemistry*, **72**, 1531-1537.
- Hwang, S.M., Kim, D.W, Lee, B.H., and Bahk, J.D.** (2009). *Arabidopsis cytoplasmic N-acetyltransferase*, as the ortholog of RimL in *E. coli*, controls flowering time via the autonomous pathway. *Plant Sci.* **177**, 593-600.
- Iuchi, S., Kobayashi, M., Taji, T., Naramoto, M., Seki, M., Kato, T., Tabata, S., Kakubari, Y., Yamaguchi-Shinozaki, K., and Shinozaki, K.** (2001). Regulation of drought tolerance by gene manipulation of 9-cis-epoxycarotenoid dioxygenase, a key enzyme in abscisic acid biosynthesis in *Arabidopsis*. *Plant J.* **27**, 325-333.
- Iven, T., König, S., Singh, S., Braus-Stromeier, S.A., Bischoff, M., Tietze, L.F., Braus, G.H., Lipka, V., Feussner, I., and Dröge-Laser, W.** (2012). Transcriptional activation and production of tryptophan-derived secondary metabolites in *Arabidopsis* roots contributes to the defense against the fungal vascular pathogen *Verticillium longisporum*. *Mol. Plant.* **5**, 1389-13402.
- Jirage, D., Tootle, T.L., Reuber, T.L., Frost, L.N., Feys, B.J., Parker, J.E., Ausubel, F.M., and Glazebrook, J.** (1999). *Arabidopsis thaliana* PAD4 encodes a lipase-like gene that is important for salicylic acid signaling. *Proc. Natl Acad. Sci. USA.* **96**, 13583–13588.
- Johansson, O.N., Fantozzi, E., Fahlberg, P., Nilsson, A.K., Buhot, N., Tör, M., and Andersson, M.X.** (2014). Role of the penetration-resistance genes *PEN1*, *PEN2* and *PEN3* in the hypersensitive response and race-specific resistance in *Arabidopsis thaliana*. *Plant J.* **79**, 466-476.
- Jones, J.D.G., and Dangl, J.L.** (2006). The plant immune system. *Nature*, **444**, 323–329.
- Jung, H.W., Tschaplinski, T.J., Wang, L., Glazebrook, J., and Greenberg, J.T.** (2009). Priming in systemic plant immunity. *Science*, **324**, 89-91.
- Kai, K., Mizutani, M., Kawamura, N., Yamamoto, R., Tamai, M., Yamaguchi, H., Sakata, K., and Shimizu, B.** (2008). Scopoletin is biosynthesized via *ortho*-hydroxylation of feruloyl CoA by a 2-oxoglutarate-dependent dioxygenase in *Arabidopsis thaliana*. *Plant J.* **55**, 989-999.
- Kai, K., Shimizu, B., Mizutani, M., Watanabe, K., and Sakata, K.** (2006). Accumulation of coumarins in *Arabidopsis thaliana*. *Phytochemistry*, **67**, 379–386.
- Kaku, H., Nishizawa, Y., Ishii-Minami, N., Akimoto-Tomiyama, C., Dohmae, N., Takio, K., Minami, E., and Shibuya, N.** (2006). Plant cells recognize chitin fragments for defense signaling through a plasma membrane receptor. *Proc. Natl. Acad. Sci. USA.* **103**, 11086-11091.

References

- Kalamaki, M.S., Alexandrou, D., Lazari, D., Merkouropoulos, G., Fotopoulos, V., Pateraki, I., Aggelis, A., Carrillo-López, A., Rubio-Cabetas, M.J., and Kanellis, A.K.** (2009). Over-expression of a tomato N-acetyl-L-glutamate synthase gene (SINAGS1) in *Arabidopsis thaliana* results in high ornithine levels and increased tolerance in salt and drought stresses. *J. Exp. Bot.* **60**, 1859-1871.
- Katsir, L., Schillmiller, A. L., Staswick, P. E., He, S. Y. and Howe, G. A.** (2008). COI1 is a critical component of a receptor for jasmonate and the bacterial virulence factor coronatine. *Proc. Natl. Acad. Sci. USA.* **105**, 7100–7105.
- Kawai, T., and Akira, S.** (2010). The role of pattern-recognition receptors in innate immunity: update on Toll-like receptors. *Nat. Immunol.* **11**, 373-384.
- Kazan, K., and Lyons, R.** (2014). Intervention of Phytohormone Pathways by Pathogen Effectors. *Plant Cell*, **10**, 2285-2309.
- Kim, J.H., Lee, B.W., Schroeder, F.C., and Jander G.** (2008). Identification of indole glucosinolate breakdown products with antifeedant effects on *Myzus persicae* (green peach aphid). *Plant J.* **54**, 1015-1026.
- Klein, A.T., et al.** (2015). Investigation of the Chemical Interface in the Soybean–Aphid and Rice–Bacteria Interactions Using MALDI-Mass Spectrometry Imaging. *Anal. Chem.* **87**, 5294-5301.
- Kliebenstein, D.J., Rowe, H.C., and Denby, K.J.** (2005). Secondary metabolites influence *Arabidopsis/Botrytis* interactions: variation in host production and pathogen sensitivity. *Plant J.* **44**, 25–36.
- Knoester, M., Pieterse, C.M., Bol, J.F., and van Loon, L.C.** (1999). Systemic resistance in *Arabidopsis* induced by rhizobacteria requires ethylene-dependent signaling at the site of application. *Mol. Plant Microbe Interact.* **12**, 720-727.
- Kolattukudy, P.E.** (1981). Structure, biosynthesis, and biodegradation of cutin and suberin. *Ann. Rev. Plant. Physiol.* **321**, 539–567.
- Kolattukudy, P.E.** (1985). Enzymatic penetration of the plant cuticle by fungal pathogens. *Annu. Rev. Phytopathol.* **23**, 223-250.
- Kolattukudy, P.E., Rogers, L.M., Li, D., Hwang, C.-S., and Flaishman, M.A.** (1995). Surface signaling in pathogenesis. *Proc. Natl. Acad. Sci. U S A.* **92**, 4080-4087.
- Koo, A.J.K., Gao, X., Jones, A.D., and Howe, G.A.** (2009). A rapid wound signal activates the systemic synthesis of bioactive jasmonates in *Arabidopsis*. *Plant J.* **59**, 974–986.

References

- Koornneef, A., and Pieterse, C.M.** (2008). Cross talk in defense signaling. *Plant Physiol.* **146**, 839-844.
- Krueger, S.K. and Williams, D.E.** (2005) Mammalian flavin-containing monooxygenases: structure/function, genetic polymorphisms and role in drug metabolism. *Pharmacol. Ther.* **106**, 357–387.
- Kunkel B.N., and Brooks, D.M.** (2002). Cross talk between signaling pathways in pathogen defense. *Curr. Opin. Plant Biol.* **5**, 325-331.
- Lamb, C. and Dixon, R.A.** (1997) The oxidative burst in plant disease resistance. *Annu. Rev. Plant Physiol. Plant Mol. Biol.* **48**, 251–275.
- Lawton, K.A., Potter, S.L., Uknes, S., and Ryals, J.** (1994). Acquired resistance signal transduction in *Arabidopsis* is ethylene independent. *Plant Cell*, **6**, 581-588.
- Lay, F. T. and Anderson, M. A.** (2005). Defensins – Components of the innate system in plants. *Curr. Protein Pept. Sci.* **6**, 85–101.
- Ledford, H.K., Baroli, I., Shin, J.W., Fischer, B.B., Eggen, R.I., and Niyogi, K.K.** (2004). Comparative profiling of lipid-soluble antioxidants and transcripts reveals two phases of photo-oxidative stress in a xanthophyll-deficient mutant of *Chlamydomonas reinhardtii*. *Mol. Genet. Genomics*, **272**, 470-479.
- Léon-Kloosterziel, K., Gil, M.A., Ruijs, G.J., Jacobsen, S.E., Olszewski, N.E., Schwartz, S.H., Zeevaart, J.A.D., and Koornneef, M.** (1996). Isolation and characterization of abscisic acid-deficient *Arabidopsis* mutants at two new loci. *Plant J.* **10**, 655-661.
- Lewis, L. A., et al.** (2015). Transcriptional Dynamics Driving MAMP-Triggered Immunity and Pathogen Effector-Mediated Immunosuppression in *Arabidopsis* Leaves Following Infection with *Pseudomonas syringae* pv tomato DC3000. *Plant Cell*, **11**, 3038-3064.
- Li, Y., Zhang, Z., Jia, Y., Shen, Y., He, H., Fang, R., Chen, X., and Hao, X.** (2008). 3-Acetyl-3-hydroxyoxindole: a new inducer of systemic acquired resistance in plants. *Plant Biotechnol J.* **6**, 301-308.
- Lipka, V., et al.** (2005). Pre- and postinvasion defenses both contribute to nonhost resistance in *Arabidopsis*. *Science*. **310**, 1180-1183.
- Liu, J., Elmore, J.M., Lin, Z.-J.D. and Coaker, G.** (2011a). A receptor-like cytoplasmic kinase phosphorylates the host target RIN4, leading to the activation of a plant innate immune receptor. *Cell Host Microbe*. **9**, 137-146.

References

- Liu, P.P., von Dahl, C.C., and Klessig, D.F.** (2011b). The extent to which methyl salicylate is required for signaling systemic acquired resistance is dependent on exposure to light after infection. *Plant Physiol.* **157**, 2216-2226.
- Loeffler, C., et al.** (2005). B1-phytoprostanes trigger plant defense and detoxification responses. *Plant Physiol.* **137**, 328–340.
- Lotze, M.T., et al.** (2007). The grateful dead: damage associated molecular pattern molecules and reduction/oxidation regulate immunity. *Immunol. Rev.* **220**, 60-81.
- Luis, P., Behnke, K., Toepel, J., and Wilhelm, C.** (2006). Parallel analysis of transcript levels and physiological key parameters allows the identification of stress phase gene markers in *Chlamydomonas reinhardtii* under copper excess. *Plant Cell Environ.* **29**, 2043-2054.
- Maeda H., and DellaPenna D.** (2007). Tocopherol functions in photosynthetic organisms. *Curr. Opin. Plant Biol.* **10**, 260–265.
- Maeda, H., Sage, T.L., Isaac, G., Welti, R., and DellaPenna, D.** (2008). Tocopherols modulate extraplastidic polyunsaturated fatty acid metabolism in *Arabidopsis* at low temperature. *Plant Cell*, **20**, 452-470.
- Malitsky, S., Blum, E., Less, H., Venger, I., Elbaz, M., Morin, S., Eshed, Y., and Aharoni, A.** (2008). The transcript and metabolite networks affected by the two clades of *Arabidopsis* glucosinolate biosynthesis regulators. *Plant Physiol.* **148**, 2021-2049.
- Mao, G., Meng, X., Liu, Y., Zheng, Z., Chen, Z., and Zhang, S.** (2011). Phosphorylation of a WRKY transcription factor by two pathogen-responsive MAPKs drives phytoalexin biosynthesis in *Arabidopsis*. *Plant Cell.* **23**, 1639-1653.
- Mateo, A., Funck, D., Mühlenbock, P., Kular, B., Mullineaux, P.M., and Karpinski, S.** (2006). Controlled levels of salicylic acid are required for optimal photosynthesis and redox homeostasis. *J. Exp. Bot.* **57**, 1795–1807.
- McConn, M., and Browse, J.** (1996). The Critical Requirement for Linolenic Acid Is Pollen Development, Not Photosynthesis, in an *Arabidopsis* Mutant. *Plant Cell*, **8**, 403-416.
- McConn, M., Creelam, R.A., Bell, E., Mullet, J.E., and Browse, J.** (1997). Jasmonate is essential for insect defense in *Arabidopsis*. *Proc. Natl. Acad. Sci. USA.* **94**, 5473-5477.
- Melotto, M., Underwood, W., Koczan, J., Nomura, K., and He, S.Y.** (2006). Plant stomata function in innate immunity against bacterial invasion. *Cell*, **126**, 969-980.

References

- Mène-Safrané, L., Davoine, C., Stolz, S., Majcherczyk, P., and Farmer, E.E.** (2007) Genetic removal of tri-unsaturated fatty acids suppresses developmental and molecular phenotypes of an *Arabidopsis* tocopherol-deficient mutant. Whole-body mapping of malondialdehyde pools in a complex eukaryote. *J. Biol. Chem.* **49**, 35749-35756.
- Mishina, T.E., and Zeier, J.** (2006). The *Arabidopsis* flavin-dependent monooxygenase FMO1 is an essential component of biologically induced systemic acquired resistance. *Plant Physiol.* **141**, 1666-1675.
- Mishina, T.E., and Zeier, J.** (2007). Pathogen-associated molecular pattern recognition rather than development of tissue necrosis contributes to bacterial induction of systemic acquired resistance in *Arabidopsis*. *Plant J.* **50**, 500–513.
- Monaghan, J., and Zipfel, C.** (2012). Plant pattern recognition receptor complexes at the plasma membrane. *Curr. Opin. Plant Biol.* **15**, 349-357.
- Morant, M. et al.** (2014). Metabolomic, Transcriptional, Hormonal, and Signaling Cross-Talk in *Superroot2*. *Mol. Plant.* **3**, 192-211.
- Morrison, R.I.** (1953). The isolation of L-pipecolic acid from *Trifolium repens*. *Biochem. J.* **53**, 474–478.
- Morrissey, J.P., Wubben, J.P., and Osbourn, A.E.** (2000). *Stagonospora avenae* secretes multiple enzymes that hydrolyze oat leaf saponins. *Mol. Plant Microbe. Interact.* **13**, 1041-1052.
- Mosblech, A., Feussner, I., and Heilmann, I.** (2009). Oxylipins: structurally diverse metabolites from fatty acid oxidation. *Plant Physiol. Biochem.* **47**, 511-517.
- Mousavi, S.A., Chauvin, A., Pascaud, F., Kellenberger, S., and Farmer, E.E.** (2013). GLUTAMATE RECEPTOR-LIKE genes mediate leaf-to-leaf wound signalling. *Nature*, **500**, 422-426.
- Mueller, M.J., and Berger, S.** (2009). Reactive electrophilic oxylipins: pattern recognition and signalling. *Phytochemistry*, **70**, 1511-1521.
- Mueller, S., Hilbert, B., Dueckershoff, K., Roitsch, T., Krischke, M., Mueller, M.J., and Berger, S.** (2008). General detoxification and stress responses are mediated by oxidized lipids through TGA transcription factors in *Arabidopsis*. *Plant Cell*, **20**, 768-785.
- Munné-Bosch, S., Schwarz, K., and Alegre, L.** (1999). Enhanced formation of α -tocopherol and highly oxidized abietane diterpenes in waterstressed rosemary plants. *Plant Physiol.* **121**, 1047-1052.

References

- Mur, L.A., Kenton, P., Lloyd, A.J., Ougham, H., and Prats, E.** (2008). The hypersensitive response; the centenary is upon us but how much do we know? *J. Exp. Bot.* **59**, 501-520.
- Nafisi, M., Goregaoker, S., Botanga, C.J., Glawischnig, E., Olsen, C.E., Halkier, B.A., and Glazebrook, J.** (2007). *Arabidopsis* cytochrome P450 monooxygenase 71A13 catalyzes the conversion of indole-3-acetaldoxime in camalexin synthesis. *Plant Cell.* **19**, 2039-2052.
- Nakajima, N., Hiradate, S., and Fujii, Y.** (2001). Plant growth inhibitory activity of L-canavanine and its mode of action. *J. Chem. Ecol.* **27**, 19–31.
- Nambara, E., and Marion-Poll, A.** (2005). Abscisic Acid Biosynthesis and Catabolism. *Annu. Rev. Plant Biol.* **56**, 165–185.
- Návarová, H., Bernsdorff, F., Döring, A.C., and Zeier J.** (2012). Pipecolic acid, an endogenous mediator of defense amplification and priming, is a critical regulator of inducible plant immunity. *Plant Cell*, **24**, 5123-5141.
- Nawrath, C.** (2002). The Biopolymers Cutin and Suberin. *Arabidopsis Book*, **1**, e0021.
- Nawrath, C., and Métraux, J.P.** (1999) Salicylic acid induction-deficient mutants of *Arabidopsis* express PR-2 and PR-5 and accumulate high levels of camalexin after pathogen inoculation. *Plant Cell*, **11**, 1393–1404.
- Pálfi, G., and Dézsi, L.** (1968). Pipecolic acid as an indicator of abnormal protein metabolism in diseased plants. *Plant Soil*, **29**, 285–291.
- Papadopoulou, K., Melton, R.E., Leggett, M., Daniels, M.J., Osbourn, A.E.** (1999). Compromised disease resistance in saponin-deficient plants. *Proc. Natl Acad. Sci. USA.* **96**, 12923-12928.
- Park, S.W., Kaimoyo, E., Kumar, D., Mosher, S., and Klessig, D.F.** (2007). Methyl salicylate is a critical mobile signal for plant systemic acquired resistance. *Science*, **318**, 113–116.
- Pedras, M.S.C., Yaya, E.E., and Glawischnig, E.** (2011). The phytoalexins from cultivated and wild crucifers: chemistry and biology. *Nat. Prod. Rep.* **28**, 1381-1405.
- Peer, M., Stegmann, M., Mueller, M.J., and Waller, F.** (2010). *Pseudomonas syringae* infection triggers de novo synthesis of phytosphingosine from sphinganine in *Arabidopsis thaliana*. *FEBS Lett.* **584**, 4053-4056.
- Peña-Cortés, H., Albrecht, T., Prat, S., Weiler, E.W., and Willmitzer, L.** (1993) Aspirin prevents wound-induced gene expression in tomato leaves by blocking jasmonic acid biosynthesis. *Planta*, **191**, 123–128.

References

- Peng, C., Uygun, S., Shiu, S.H., and Last, R.L.** (2015). The Impact of the Branched-Chain Ketoacid Dehydrogenase Complex on Amino Acid Homeostasis in Arabidopsis. *Plant Physiol.* **169**, 1807–1820.
- Penninckx, I.A.M.A., Eggermont, K., Terras, F.R.G., Thomma, G.P.H.J, De Samblanx G.W, Buchala, A., Metraux, J., Manners, J.M., and Broekaert, W.F.** (1996). Pathogen-induced systemic activation of a plant defensin gene in Arabidopsis follows a salicylic acid-independent pathway. *Plant Cell*, **8**, 2309-2323.
- Perchlik, M., Foster, J., and Tegeder, M.** (2014). Different and overlapping functions of Arabidopsis LHT6 and AAP1 transporters in root amino acid uptake. *J Exp Bot.* **65**, 5193-5204.
- Petersen, M., et al.** (2000). Arabidopsis map kinase 4 negatively regulates systemic acquired resistance. *Cell*, **103**, 1111–1120.
- Pfalz, M., Mikkelsen, M.D., Bednarek, P., Olsen, C.E., Halkier, B.A., and Kroymann J.** (2011). Metabolic engineering in *Nicotiana benthamiana* reveals key enzyme functions in Arabidopsis indole glucosinolate modification. *Plant Cell.* **23**, 716-729.
- Piasecka, A., Jedrzejczak-Rey, N., and Bednarek, P.** (2015). Secondary metabolites in plant innate immunity: conserved function of divergent chemicals. *New Phytol.* **206**, 948-964.
- Pieterse, C.M., Van der Does, D., Zamioudis, C., Leon-Reyes, A., and Van Wees, S.C.** (2012). Hormonal modulation of plant immunity. *Annu. Rev. Cell Dev. Biol.* **28**, 489-521.
- Pieterse, C.M.J., Zamioudis, C., Berendsen, R.L., Weller, D.M., Van Wees, S.C.M. and Bakker, P.A.H.M.** (2014) Induced systemic resistance by beneficial microbes. *Annu. Rev. Phytopathol.* **52**, 347–375.
- Porfirova, S., Bergmüller, E., Tropf, S., Lemke, R., and Dörmann, P.** (2002). Isolation of an Arabidopsis mutant lacking vitamin E and identification of a cyclase essential for all tocopherol biosynthesis. *Proc. Natl. Acad. Sci. U S A.* **99**, 12495–12500.
- Postel, S., Küfner, I., Beuter, C., Mazzotta, S., Schwedt, A., Borlotti, A., Halter, T., Kemmerling, B., and Nürnberger, T.** (2010). The multifunctional leucine-rich repeat receptor kinase BAK1 is implicated in Arabidopsis development and immunity. *Eur. J. Cell Biol.* **89**, 169-174.
- Queval, G., et al.** (2007) Conditional oxidative stress responses in the Arabidopsis photorespiratory mutant *cat2* demonstrate that redox state is a key modulator of daylength-dependent gene expression, and define photoperiod as a crucial factor in the regulation of H₂O₂-induced cell death. *Plant J.* **52**, 640–657.

References

- Rajniak, J., Barco, B., Clay, N.K., and Sattely, E.S.** (2015). A new cyanogenic metabolite in *Arabidopsis* required for inducible pathogen defence. *Nature*, **525**, 376-379.
- Riewe, D., Koochi, M., Lisec, J., Pfeiffer, M., Lippmann, R., Schmeichel, J., Willmitzer, L., and Altmann, T.** (2012). A tyrosine aminotransferase involved in tocopherol synthesis in *Arabidopsis*. *Plant J.* **71**, 850-859.
- Rivas-San Vicente, M., and Plasencia, J.** (2011). Salicylic acid beyond defense: its role in plant growth and development. *J. Exp. Bot.* **62**, 3321–3338.
- Romeis, T., and Herde, M.** (2014). From local to global: CDPKs in systemic defense signaling upon microbial and herbivore attack. *Curr. Opin. Plant Biol.* **20**, 1-10.
- Robert-Seilaniantz, A., Grant, M., and Jones, J.D.** (2011). Hormone crosstalk in plant disease and defense: more than just jasmonate-salicylate antagonism. *Annu. Rev. Phytopathol.* **49**, 317-343.
- Rogers, E.E., Glazebrook, J., and Ausubel, F.M.** (1996). Mode of action of the *Arabidopsis thaliana* phytoalexin camalexin and its role in *Arabidopsis*-pathogen interactions. *Mol. Plant Microbe Interact.* **9**, 748-757.
- Rosenthal, G.A.** (2001). L-Canavanine: A higher plant insecticidal allelochemical. *Amino Acids*, **21**, 319–330.
- Saga, H., Ogawa, T., Kai, K., Suzuki, H., Ogata, Y., Sakurai, N., Shibata, D., and Ohta, D.** (2012). Identification and Characterization of *ANAC042*, a TranscriptionFactor Family Gene Involved in the Regulation of Camalexin Biosynthesis in *Arabidopsis*. *Mol. Plant. Microbe Interact.* **25**, 684-696.
- Sanchez-Vallet, A., Ramos, B., Bednarek, P., López, G., Piślewska-Bednarek, M., Schulze-Lefert, P., and Molina, A.** (2010). Tryptophan-derived secondary metabolites in *Arabidopsis thaliana* confer non-host resistance to necrotrophic *Plectosphaerella cucumerina* fungi. *Plant J.* **63**, 115-127.
- Sandorf, I., and Holländer-Czytko, H.** (2002). Jasmonate is involved in the induction of tyrosine aminotransferase and tocopherol biosynthesis in *Arabidopsis thaliana*. *Planta.* **216**, 173–179.
- Sattler, S.E., Cahoon, E.B., Coughlan, S.J., and DellaPenna, D.** (2003). Characterization of Tocopherol Cyclases from Higher Plants and Cyanobacteria. Evolutionary Implications for Tocopherol Synthesis and Function. *Plant Physiol.* **132**. 2184–2195.

References

- Sattler, S.E., Gilliland, L.U., Magallanes-Lundback, M., Pollard, M., and DellaPenna, D.** (2004). Vitamin E is essential for seed longevity, and for preventing lipid peroxidation during germination. *Plant Cell*, **16**, 1419–1432.
- Sattler, S.E., Mène-Saffrané, L., Farmer, E.E., Krischke, M., Mueller, M.J., and DellaPenna D.** (2006). Nonenzymatic Lipid Peroxidation Reprograms Gene Expression and Activates Defense Markers in Arabidopsis Tocopherol-Deficient Mutants. *Plant Cell*, **18**, 3706–3720.
- Schaeffer, A., Bronner, R., Benveniste, P., and Schaller, H.** (2001). The ratio of campesterol to sitosterol that modulates growth in Arabidopsis is controlled by STEROL METHYLTRANSFERASE 2;1. *Plant J.* **25**, 605–615.
- Schaller, H.** (2003) The role of sterols in plant growth and development. *Prog. Lipid Res.* **42**, 163–175.
- Schenk, S.T., et al.** (2014). N-Acyl-Homoserine Lactone Primes Plants for Cell Wall Reinforcement and Induces Resistance to Bacterial Pathogens via the Salicylic Acid/Oxylipin Pathway. *Plant Cell*, **26**, 2708-2723.
- Schlaeppli, K., Abou-Mansour, E., Buchala, A., and Mauch, F.** (2010). Disease resistance of Arabidopsis to *Phytophthora brassicae* is established by sequential action of indole glucosinolates and camalexin. *Plant J.* **62**, 840-851.
- Schlaeppli, K., Bodenhausen, N., Buchala, A., Mauch, F., and Reymond, P.** (2008). The glutathione-deficient mutant *pad2-1* accumulates lower amounts of glucosinolates and is more susceptible to the insect herbivore *Spodoptera littoralis*. *Plant J.* **55**, 774-786.
- Schmid, N.B., et al.** (2014). Feruloyl-CoA 6'-Hydroxylase1-dependent coumarins mediate iron acquisition from alkaline substrates in Arabidopsis. *Plant Physiol.* **164**, 160-172.
- Schmiesing, A., Emonet, A., Gouhier-Darimont, C., and Reymond, P.** (2016). Arabidopsis MYC Transcription Factors Are the Target of Hormonal SA/JA Crosstalk in Response to *Pieris brassicae* Egg Extract. *Plant Physiol.* (article in press)
- Schneider, C.** (2005). Chemistry and biology of vitamin E. *Mol. Nutr. Food Res.* **49**, 7–30.
- Schugar, R.C., and Brown, J.M.** (2015). Emerging roles of flavin monooxygenase 3 in cholesterol metabolism and atherosclerosis. *Curr. Opin. Lipidol.* **26**, 426-431.
- Schuhegger, R., Nafisi, M., Mansourova, M., Petersen, B.L., Olsen, C.E., Svatos, A., Halkier, B.A., and Glawischnig, E.** (2006). CYP71B15 (PAD3) catalyzes the final step in camalexin biosynthesis. *Plant Physiol.* **141**, 1248-1254.
- Schuhegger, R., Rauhut, T., and Glawischnig, E.** (2007). Regulatory variability of camalexin biosynthesis. *J. Plant Physiol.* **164**, 636-644.

References

- Schuster, J., and Binder, S.** (2005). The mitochondrial branched-chain aminotransferase (AtBCAT-1) is capable to initiate degradation of leucine, isoleucine and valine in almost all tissues in *Arabidopsis thaliana*. *Plant Mol. Biol.* **57**, 241-254.
- Sewelam, N., Jaspert, N., Van Der Kelen, K., Tognetti, V.B., Schmitz, J., Frerigmann, H., Stahl, E., Zeier, J., Van Breusegem, F., and Maurino, V.G.** (2014). Spatial H₂O₂ signaling specificity: H₂O₂ from chloroplasts and peroxisomes modulates the plant transcriptome differentially. *Mol. Plant*, **7**, 1191-1210.
- Shah, J., and Zeier, J.** (2013). Long-distance communication and signal amplification in systemic acquired resistance. *Front Plant Sci.* **4**, 30.
- Singh, P., Yekondi, S., Chen, P.W., Tsai, C.H., Yu, C.W., Wu, K., and Zimmerli, L.** (2014). Environmental history modulates *Arabidopsis* pattern-triggered immunity in a HISTONE ACETYLTRANSFERASE1-dependent manner. *Plant Cell.* **26**, 2676-2688.
- Snyder, B.A., and Nicholson, R.L.** (1990). Synthesis of phytoalexins in sorghum as a site-specific response to fungal ingress. *Science.* **248**, 1637-1639.
- Sønderby, I.E, Geu-Flores, F., and Halkier, B.A.** (2010). Biosynthesis of glucosinolates--gene discovery and beyond. *Trends Plant Sci.* **15**, 283-290.
- Song, J.T., Lu, H., and Greenberg, J.T.** (2004a). Divergent roles in *Arabidopsis thaliana* development and defense of two homologous genes, aberrant growth and death2 and AGD2-LIKE DEFENSE RESPONSE PROTEIN1, encoding novel aminotransferases. *Plant Cell*, **16**, 353–366.
- Song, J.T., Lu, H., McDowell, J.M., and Greenberg, J.T.** (2004b). A key role for ALD1 in activation of local and systemic defenses in *Arabidopsis*. *Plant J.* **40**, 200–212.
- Song, S., et al.** (2014). Interaction between MYC2 and *ETHYLENE INSENSITIVE3* modulates antagonism between jasmonate and ethylene signaling in *Arabidopsis*. *Plant Cell*, **26**, 263-279.
- Spoel, S.H., and Dong, X.** (2012). How do plants achieve immunity? Defence without specialized immune cells. *Nat. Rev. Immunol.* **12**, 89-100.
- Spoel, S.H., et al.** (2003) NPR1 modulates cross-talk between salicylate- and jasmonate-dependent defense pathways through a novel function in the cytosol. *Plant Cell*, **15**, 760–770.
- Stahl, E., Bellwon, P., Huber, S., Schläppi, K., Bernsdorff, F., Vallat-Michel, A., Mauch, F., and Zeier, J.** (2016). Regulatory and Functional Aspects of Indolic Metabolism in Plant Systemic Acquired Resistance. *Mol. Plant.* **9**, 662-681.
- Staswick, P.E., and Tiryaki, I.** (2004). The oxylipin signal jasmonic acid is activated by an enzyme that conjugates it to isoleucine in *Arabidopsis*. *Plant Cell*, **16**, 2117–2127.

References

- Stein, M., Dittgen, J., Sánchez-Rodríguez, C., Hou, B.H., Molina, A., Schulze-Lefert, P., Lipka, V., and Somerville, S.** (2006). *Arabidopsis* PEN3/PDR8, an ATP binding cassette transporter, contributes to nonhost resistance to inappropriate pathogens that enter by direct penetration. *Plant Cell*. **18**, 731-746.
- Stepanova, A.N., Yun, J., Robles, L.M., Novak, O., He, W., Guo, H., Ljung, K., and Alonso, J.M.** (2011). The *Arabidopsis* YUCCA1 flavin monooxygenase functions in the indole-3-pyruvic acid branch of auxin biosynthesis. *Plant Cell*, **23**, 3961–3973.
- Sticher, L., Mauch-Mani, B., and Métraux, J.P.** (1997). Systemic acquired resistance. *Annu. Rev. Phytopathol.* **35**, 235-270.
- Su, T., Xu, J., Li, Y., Lei, L., Zhao, L., Yang, H., Feng, J., Liu, G., and Ren, D.** (2011). Glutathione-indole-3-acetonitrile is required for camalexin biosynthesis in *Arabidopsis thaliana*. *Plant Cell*, **23**, 364-380.
- Suharti, W.S, Nose, A., and Zheng, S.H.** (2016). Metabolite Profiling of Sheath Blight Disease Resistance in Rice: In the Case of Positive Ion Mode Analysis by CE/TOF-MS. *Plant Production Science*. Article posted online, DOI: 10.1080/1343943X.2016.1140006
- Sun, H., Wang, L., Zhang, B., Ma, J., Hettenhausen, C., Cao, G., Sun, G., Wu, J., and Wu, J.** (2014). Scopoletin is a phytoalexin against *Alternaria alternata* in wild tobacco dependent on jasmonate signalling. *J. Exp. Bot.* **65**, 4305-4315.
- Sun, Y., Li, L., Macho, A.P., Han, Z., Hu, Z., Zipfel, C., Zhou, J.M. and Chai, J.** (2013). Structural basis for flg22-induced activation of the *Arabidopsis* FLS2-BAK1 immune complex. *Science*, **342**, 624-348.
- Tal, B. and Robeson, D. J.** (1986). The induction, by fungal inoculation of ayapin and scopoletin biosynthesis in *Helianthus annuus*. *Phytochemistry*, **25**, 77–79.
- Tan, J., Bednarek, P., Liu, J., Schneider, B., Svatos, A., and Hahlbrock, K.** (2004). Universally occurring phenylpropanoid and species-specific indolic metabolites in infected and uninfected *Arabidopsis thaliana* roots and leaves. *Phytochemistry*. **65**, 691-699.
- Teufel, R., et al.** (2013). Flavin-mediated dual oxidation controls an enzymatic Favorskii-type rearrangement. *Nature*, **503**, 552-556.
- Thaler, J., and Bostock, R.** (2004). Interactions between abscisic-acid-mediated responses and plant resistance to pathogens and insects. *Ecology*, **85**, 48–58.

References

- Thibaud-Nissen, F., Wu, H., Richmond, T., Redman, J. C., Johnson, C., Green, R., Arias, J., and Town, C.D.** (2006). Development of Arabidopsis whole-genome microarrays and their application to the discovery of binding sites for the TGA2 transcription factor in salicylic acid-treated plants. *Plant J.* **47**, 152-162.
- Thoma, I., Loeffler, C., Sinha, A.K., Gupta, M., Krischke, M., Steffan, B., Roitsch, T., and Mueller, M.J.** (2003). Cyclopentenone isoprostanes induced by reactive oxygen species trigger defense gene activation and phytoalexin accumulation in plants. *Plant J.* **34**, 363–375.
- Thomma, B.P., Nelissen, I., Eggermont, K., and Broekaert W.F.** (1999). Deficiency in phytoalexin production causes enhanced susceptibility of *Arabidopsis thaliana* to the fungus *Alternaria brassicicola*. *Plant J.* **19**, 163-171.
- Thordal-Christensen, H.** (2003). Fresh insights into processes of nonhost resistance. *Curr. Opin. Plant Biol.* **6**, 351-357.
- Tintor, N., Ross, A., Kanehara, K., Yamada, K., Fan, L., Kemmerling, B., Nürnberger, T., Tsuda, K., and Saijo, Y.** (2013). Layered pattern receptor signaling via ethylene and endogenous elicitor peptides during Arabidopsis immunity to bacterial infection. *Proc Natl. Acad. Sci. USA.* **110**, 6211-6216.
- Tocquin, P., Corbesier, L., Havelange, A., Pieltain, A., Kurtem, E., Bernier, G., and Périlleux, C.** (2003). A novel high efficiency, low maintenance, hydroponic system for synchronous growth and flowering of *Arabidopsis thaliana*. *BMC Plant Biol.* **3**, 2. doi: 10.1186/1471-2229-3-2.
- Torres Zabala, M. de., et al.** (2015) Chloroplasts play a central role in plant defence and are targeted by pathogen effectors. *Nature Plants*, **1**, 15074.
- Torres, M. A., Dangl, J. L., and Jones, J.D.G.** (2002). Arabidopsis gp91phox homologues AtrbohD and AtrbohF are required for accumulation of reactive oxygen intermediates in the plant defense response. *Proc. Natl. Acad. Sci. USA.* **99**, 517-522.
- Tsuba, M., Katagiri, C., Takeuchi, Y., Takada, Y., and Yamaoka, N.** (2002). Chemical factors of the leaf surface involved in the morphogenesis of *Blumeria graminis*. *Physiol. Mol. Plant Pathol.* **60**, 51–57.
- Tsuji, J., Jackson, E.P., Douglas A. Gage, D.A., Hammerschmidt, R., and Somerville S.C.** (1992). Phytoalexin accumulation in Arabidopsis thaliana during the hypersensitive reaction to *Pseudomonas syringae* pv *syringae*. *Plant Physiol.* **98**, 1304–1309.
- Tsuji, J., Zook, M., Hammerschmidt, R., Somerville, S., and Last, R.** (1993). Evidence that tryptophan is not a direct biosynthetic intermediate of camalexin in *Arabidopsis thaliana*. *Physiol. Mol. Plant Pathol.* **43**, 221-229.

References

- Valentin, H.E., et al.** (2006). The *Arabidopsis* vitamin E pathway *gene5-1* mutant reveals a critical role for phytol kinase in seed tocopherol biosynthesis. *Plant Cell*, **18**, 212-224.
- Van Breusegem, F., Bailey-Serres, J., and Mittler, R.** (2008). Unraveling the tapestry of networks involving reactive oxygen species in plants. *Plant Physiol.* **147**, 978–984.
- van Loon, L.C., Geraats, B.P., and Linthorst, H.J.** (2006b). Ethylene as a modulator of disease resistance in plants. *Trends Plant Sci.* **11**, 184-191.
- van Loon, L.C., Rep, M., and Pieterse, C.M.** (2006a). Significance of inducible defense-related proteins in infected plants. *Annu. Rev. Phytopathol.* **44**, 135-162.
- VanEtten, H.D., Mansfield, J.W., Bailey, J.A., and Farmer, E.E.** (1994). Two Classes of Plant Antibiotics: Phytoalexins versus "Phytoanticipins". *Plant Cell*, **6**, 1191-1192.
- Vlot, A.C., Dempsey, D.A., and Klessig, D.F.** (2009). Salicylic Acid, a multifaceted hormone to combat disease. *Annu. Rev. Phytopathol.* **47**, 177-206.
- Vogel-Adghough, D., Stahl, E., Návarová, H., and Zeier J.** (2013). Pipecolic acid enhances resistance to bacterial infection and primes salicylic acid and nicotine accumulation in tobacco. *Plant Signal. Behav.* **8**, 11.
- vom Dorp K., Hölzl, G., Plohm, C., Eisenhut, M., Abraham, M., Weber, A.P., Hanson, A.D., and Dörmann, P.** (2015). Remobilization of Phytol from Chlorophyll Degradation Is Essential for Tocopherol Synthesis and Growth of *Arabidopsis*. *Plant Cell*, **27**, 2846-2859.
- von Malek, B., van der Graaff, E., Schneitz, K., and Keller, B.** (2002). The *Arabidopsis* male-sterile mutant *dde2-2* is defective in the *ALLENE OXIDE SYNTHASE* gene encoding one of the key enzymes of the jasmonic acid biosynthesis pathway. *Planta*, **216**, 187–192.
- Wang, L., Mitra, R.M., Hasselmann, K.D., Sato, M., Lenarz-Wyatt, L., Cohen, J.D., Katagiri, F., and Glazebrook, J.** (2008). The genetic network controlling the *Arabidopsis* transcriptional response to *Pseudomonas syringae* pv. *maculicola*: roles of major regulators and the phytotoxin coronatine. *Mol. Plant-Microbe Interact.* **21**, 1408–1420.
- Wang, X., and Quinn, P.J.** (2000). The location and function of vitamin E in membranes. *Mol. Membr. Biol.* **17**, 143–156.
- Ward J.L., et al.** (2010) The metabolic transition during disease following infection of *Arabidopsis thaliana* by *Pseudomonas syringae* pv. *tomato*. *Plant J.* **63**, 443–457.
- Wasternack, C., and Hause, B.** (2013). Jasmonates: biosynthesis, perception, signal transduction and action in plant stress response, growth and development. An update to the 2007 review in *Annals of Botany*. *Ann Bot.* **111**, 1021-1058.

References

- Weber, H., Chetelat, A., Reymond, P., and Farmer, E.E.** (2004). Selective and powerful stress gene expression in *Arabidopsis* in response to malondialdehyde. *Plant J.* **37**, 877–888.
- West, N.P., Cergol, K.M., Xue, M., Randall, E.J., Britton, W.J., and Payne, R.J.** (2011). Inhibitors of an essential mycobacterial cell wall lipase (Rv3802c) as tuberculosis drug leads. *Chem. Commun.* **47**, 5166-5168.
- Wildermuth, M.C., Dewdney, J., Wu, G., and Ausubel, F.M.** (2001). Isochorismate synthase is required to synthesize salicylic acid for plant defence. *Nature*, **414**, 562-565.
- Worrall, D.** (2003) Sphingolipids, new players in plant signaling. *Trends Plant Sci.* **8**, 317–320.
- Wu, Y., Zhang, D., Chu, J. Y., Boyle, P., Wang, Y., Brindle, I. D., De Luca, V., and Després, C.** (2012). The *Arabidopsis* NPR1 protein is a receptor for the plant defense hormone salicylic acid. *Cell Reports*, **1**, 639-647.
- Xie, D.X., Feys, B.F., James, S., Nieto-Rostro, M., and Turner, J.G.** (1998). COI1: an *Arabidopsis* gene required for jasmonate-regulated defense and fertility. *Science*, **280**, 1091-1094.
- Xu, Y., Chang, P.L.C., Liu, D., Narasimhan, M.L., Kashchandra, G.R., Hasegawa, P.M., and Bressan, R.A.** (1994). Plant defense genes are synergistically induced by ethylene and methyl jasmonate. *Plant Cell*, **6**, 1077-1085.
- Yaeno, T., Matsuda, O., and Iba, K.** (2004). Role of chloroplast trienoic fatty acids in plant disease defense responses. *Plant J.* **40**, 931-941.
- Zacharius, R.M., Thompson, J.F., and Steward, F.C.** (1954). The detection, isolation and identification of L(-)-pipercolic acid in the non-protein fraction of beans (*Phaseolus vulgaris*). *J. Am. Chem. Soc.* **76**, 2908–2912.
- Zamioudis, C. et al.** (2015). Rhizobacterial volatiles and photosynthesis-related signals coordinate MYB72 expression in *Arabidopsis* roots during onset of induced systemic resistance and iron-deficiency responses. *Plant J.* **84**, 309-322.
- Zamioudis, C., Hanson, J., Pieterse, C.M.** (2014). β -Glucosidase BGLU42 is a MYB72-dependent key regulator of rhizobacteria-induced systemic resistance and modulates iron deficiency responses in *Arabidopsis* roots. *New Phytol.* **204**, 368-379.
- Zeier J.** (2013). New insights into the regulation of plant immunity by amino acid metabolic pathways. *Plant Cell Environ.* **36**, 2085-2103.

References

- Zeier, J., Pink, B., Mueller, M.J., and Berger S.** (2004). Light conditions influence specific defense responses in incompatible plant–pathogen interactions: uncoupling systemic resistance from salicylic acid and *PR-1* accumulation. *Planta*. **219**, 673-683.
- Zeng, W., Melotto, M., and He, S.Y.** (2010). Plant stomata: a checkpoint of host immunity and pathogen virulence. *Curr. Opin. Biotechnol.* **21**, 599-603.
- Zhang, Z., Feechan, A., Pedersen, C., Newman, M.A., Qiu, J.L., Olesen, K.L., and Thordal-Christensen, H.** (2007). A SNARE-protein has opposing functions in penetration resistance and defence signalling pathways. *Plant J.* **49**, 302-312.
- Zhao, J., and Last, R.L.** (1996). Coordinate regulation of the tryptophan biosynthetic pathway and indolic phytoalexin accumulation in *Arabidopsis*. *Plant Cell*. **8**, 2235-2244.
- Zhao, Y., Christensen, S.K., Fankhauser, C., Cashman, J.R., Cohen, J.D., Weigel, D., and Chory, J.** (2001). A role for flavin monooxygenase-like enzymes in auxin biosynthesis. *Science*, **291**, 306–309.
- Zhao, Y., Hull, A.K., Gupta, N.R., Goss, K.A., Alonso, J., Ecker, J.R., Normanly, J., Chory, J., and Celenza J.L.** (2002). Trp-dependent auxin biosynthesis in *Arabidopsis*: involvement of cytochrome P450s CYP79B2 and CYP79B3. *Genes Dev.* **16**, 3100-3112.
- Zhou, N., Tootle, T.L., and Glazebrook, J.** (1999). *Arabidopsis PAD3*, a gene required for camalexin biosynthesis, encodes a putative cytochrome P450 monooxygenase. *Plant Cell*. **11**, 2419-2428.
- Zimmermann, P., Hirsch-Hoffmann, M., Hennig, L., and Gruissem, W.** (2004) GENEVESTIGATOR. *Arabidopsis* microarray database and analysis toolbox. *Plant Physiol.* **136**, 2621–2632.
- Zipfel, C.** (2008). Pattern-recognition receptors in plant innate immunity. *Curr. Opin. Immunol.* **20**, 10-16.
- Zipfel, C., Robatzek, S., Navarro, L., Oakeley, E.J., Jones, J.D.G., Felix, G., and Boller, T.** (2004). Bacterial disease resistance in *Arabidopsis* through flagellin perception. *Nature*, **428**, 764–767.
- Zoeller, M., Stingl, N., Krischke, M., Fekete, A., Waller, F., Berger, S., and Mueller M.J.** (2012). Lipid profiling of the *Arabidopsis* hypersensitive response reveals specific lipid peroxidation and fragmentation processes: biogenesis of pimelic and azelaic acid. *Plant Physiol.* **160**, 365-378.

Supplemental Material

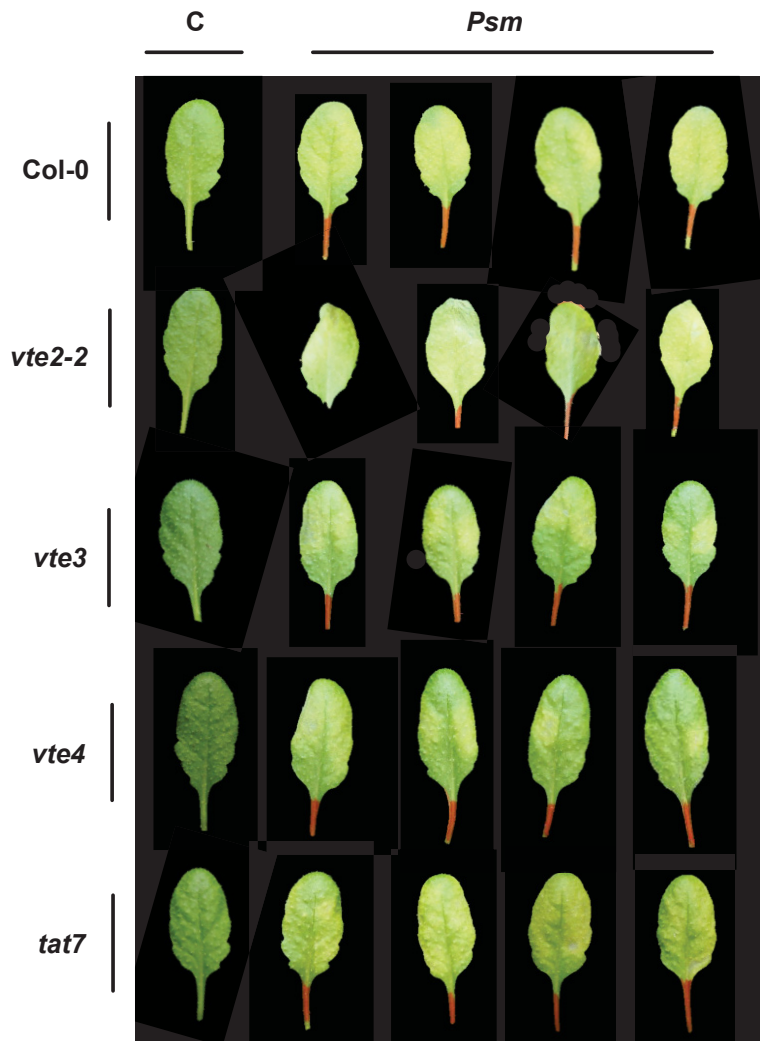


Figure S1. Disease symptoms of *Psm*-inoculated Col-0, *vte2-2*, *vte3*, *vte4*, and *tat7* plants.

Leaves were pictured 3 days post inoculation with *Psm* (applied in titers of OD_{600} 0.001). C (control) means non-infiltrated leaves.

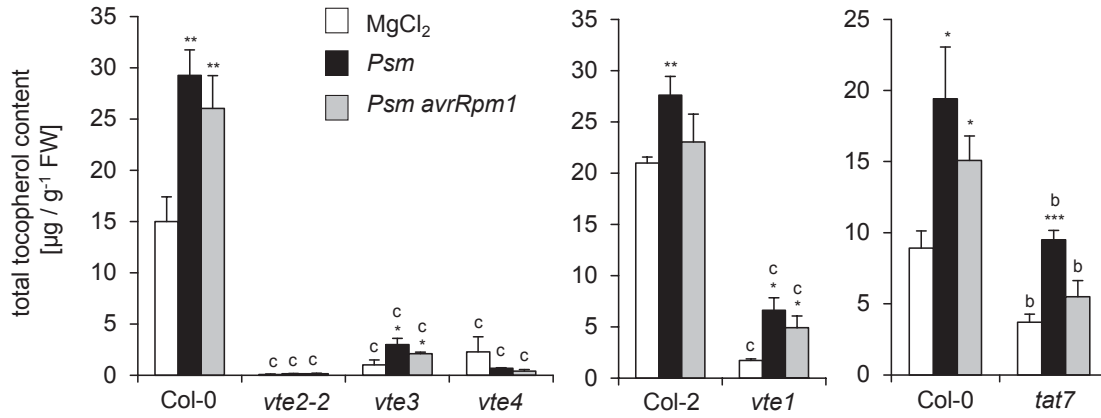


Figure S2. Total tocopherol levels of Col-0, *vte2-2*, *vte3*, *vte4*, Col-2, *vte1*, and *tat7*.

Endogenous levels of α -tocopherol, β -tocopherol, γ -tocopherol, and δ -tocopherol were determined in leaves of Col-0, *vte2-2*, *vte3*, *vte4*, Col-2, *vte1*, and *tat7* plants infiltrated with MgCl₂, *Psm*, or *Psm avrRpm1* at 48 hpi. For information of total tocopherol content levels of different tocopherol forms were summated. Asterisks denote statistically differences between MgCl₂-infiltration and *Psm*- or *Psm avrRpm1*-inoculation. ***P < 0.001, **P < 0.01, and *P < 0.05. Letters denote statistically differences between the same treatment of Col-0 or Col-2 and the respective mutant. ^cP < 0.001, ^bP < 0.01, and ^aP < 0.05 (two tailed *t* test).

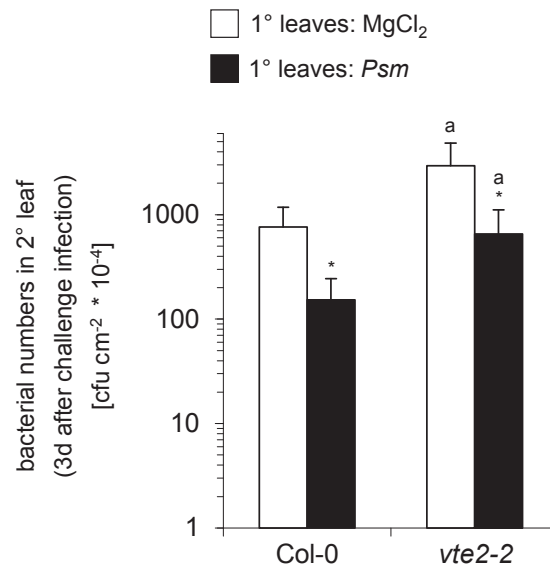


Figure S3. SAR is not impaired in the *vte2-2* mutant.

SAR assay with Col-0 and *vte2-2* mutant plants. Local leaves were infiltrated with either 10 mM MgCl₂ or, to induce SAR, with *Psm* (applied in titers of OD₆₀₀ 0.005). Two days later three leaves, distal to the site of first infiltration, per plant were infiltrated with *Psm* (applied in titers of OD₆₀₀ 0.001). Bacterial numbers in those leaves were determined 60 h post second infiltration. Bacterial numbers are means from 6 parallel samples, each consisting of three leaf disks. Asterisks denote statistically significant differences between first MgCl₂- and *Psm*-infiltrated plants of one genotype ***P < 0.001, **P < 0.01, and *P < 0.05. Letters denote statistically differences between the same treatment of Col-0 and *vte2-2*. ^cP < 0.001, ^bP < 0.01, and ^aP < 0.05 (two tailed *t* test).

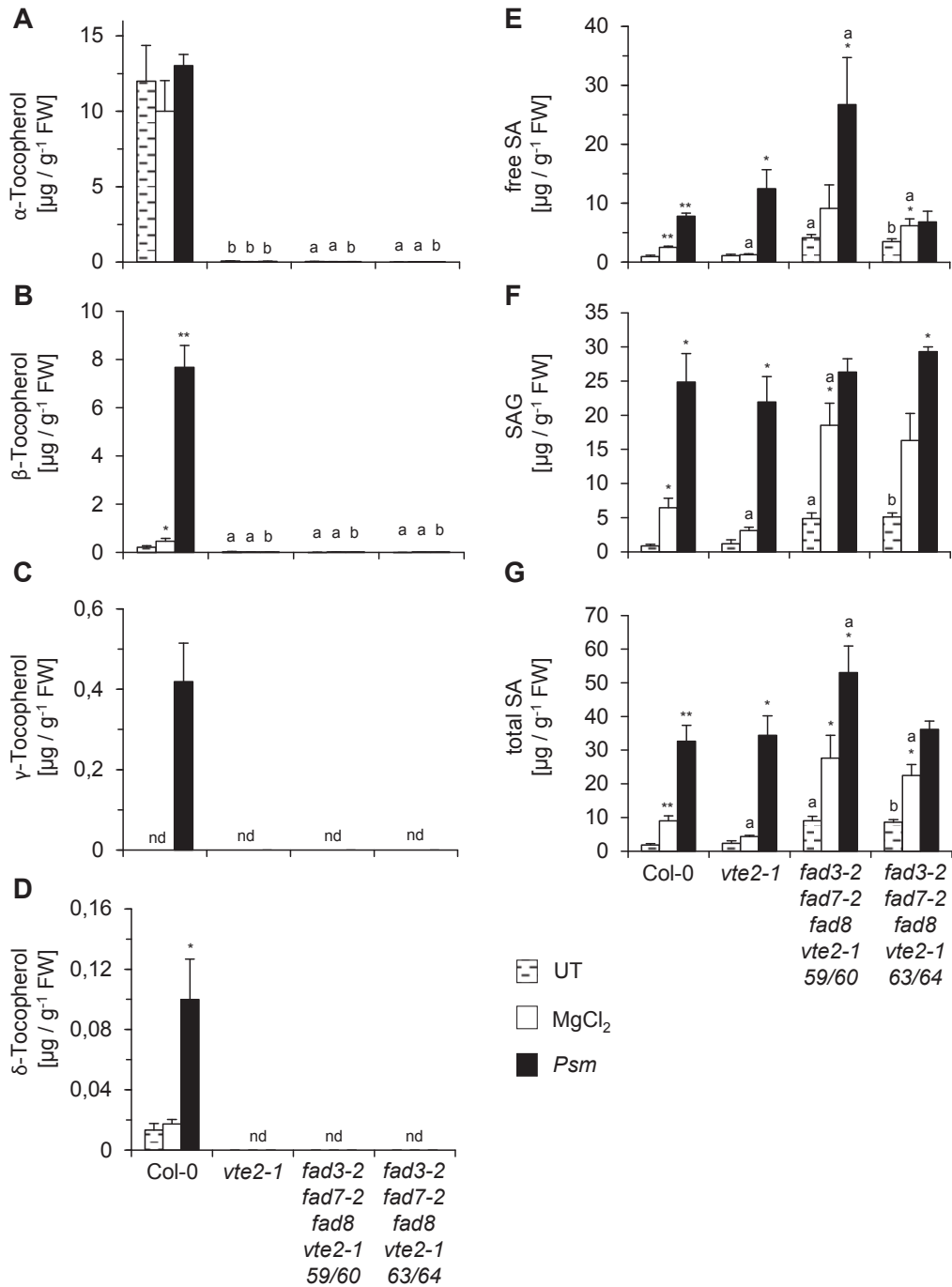
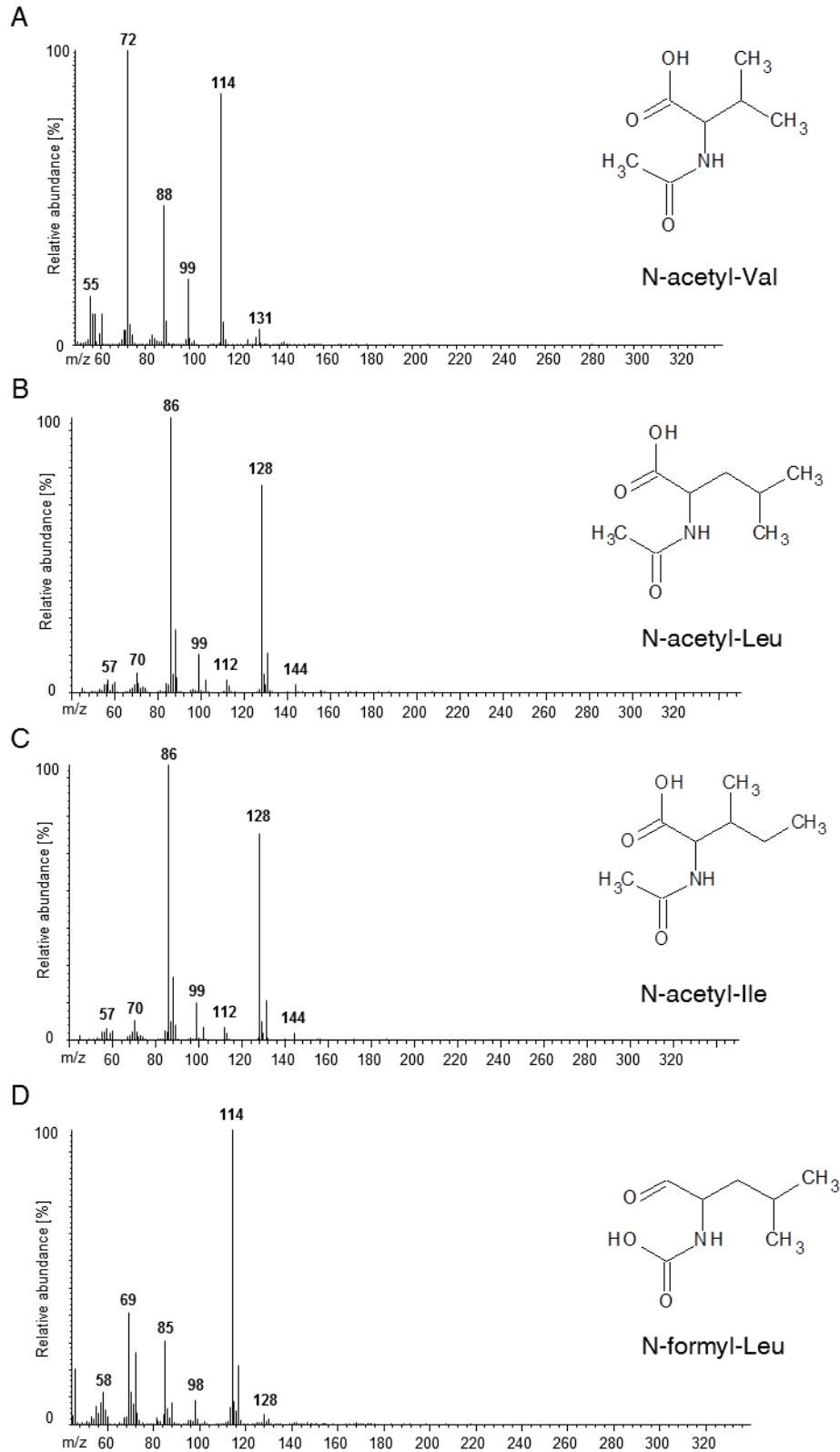
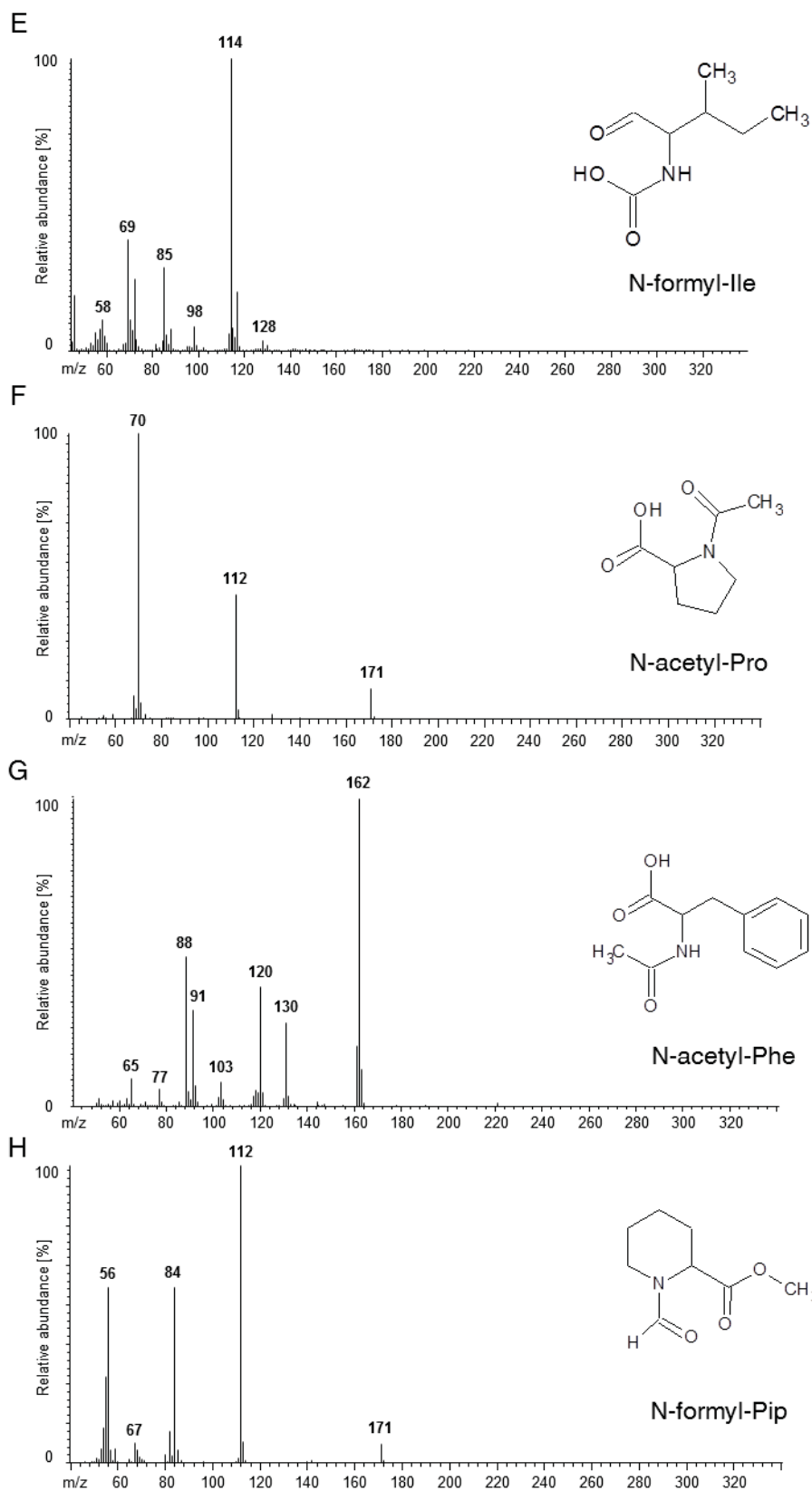


Figure S4. The *vte2-1* and *fad3-2 fad7-2 fad8 vte2-1* mutants are fully impaired in basal and pathogen-triggered tocopherol generation and quadruple mutant lines exhibit increased basal SA levels.

Endogenous levels of (A) α -tocopherol, (B) β -tocopherol, (C) γ -tocopherol, (D) δ -tocopherol, (E) free SA, (F) SAG, and (G) total SA in leaves infiltrated with MgCl₂, *Psm*, or untreated leaves at 48 hpi in *Col-0* and *vte2-1* and two lines of the quadruple mutant *fad3-2 fad7-2 fad8 vte2-1*. Asterisks denote statistically differences between untreated leaves and MgCl₂-infiltrated leaves or statistically differences between MgCl₂-infiltration and *Psm*-inoculation. ***P < 0.001, **P < 0.01, and *P < 0.05. Letters denote statistically differences between the same treatment of *Col-0* and the respective mutant. ^cP < 0.001, ^bP < 0.01, and ^aP < 0.05 (two tailed *t* test).





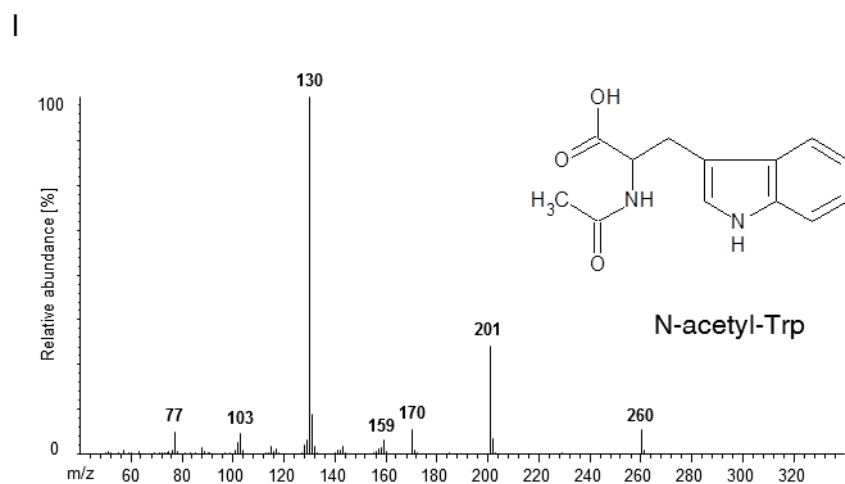


Figure S5. Mass spectra and structure of the identified N-acetylated and N-formylated amino acids

(A) N-acetyl-Val, **(B)** N-acetyl-Leu, **(C)** N-acetyl-Ile, **(D)** N-formyl-Leu, **(E)** N-formyl-Ile, **(F)** N-acetyl-Pro, **(G)** N-acetyl-Phe, **(H)** N-formyl-Pip, and **(I)** N-acetyl-Trp. Mass-spectra were recorded in the in the electron ionization mode.

A

Metabolite	Col-0_Psm_time course															
	Col-0, 8 hpi, local leaves				Col-0, 24 hpi, local leaves				Col-0, 48 hpi, local leaves				Col-0, 48 hpi, systemic leaves			
	MgCl ₂ [ng / g FW]	Psm [ng / g FW]	ratio P / M		MgCl ₂ [ng / g FW]	Psm [ng / g FW]	ratio P / M		MgCl ₂ [ng / g FW]	Psm [ng / g FW]	ratio P / M		MgCl ₂ [ng / g FW]	Psm [ng / g FW]	ratio P / M	
N-acetyl-Val	23.2 ± 6.1	23.7 ± 3.9	1	43.0 ± 19.6	52.7 ± 5.0	1.2		19.0 ± 0.5	121.6 ± 31.5	6.4**		19.3 ± 3.3	20.7 ± 4.1	1.1		
N-acetyl-Leu	6.1 ± 1.1	7.7 ± 2.8	1.2	12.5 ± 4.9	14.0 ± 0.9	1.1		13.9 ± 5.5	63.6 ± 16.2	4.6**		7.5 ± 3.2	10.0 ± 3.0	1.3		
N-acetyl-Ile	6.7 ± 2.7	9.1 ± 1.7	1.4	18.9 ± 7.7	30.1 ± 5.1	1.6		14.0 ± 4.1	127.0 ± 48.3	9.1*		7.4 ± 3.1	8.9 ± 1.4	1.2		
N-formyl-Leu	13.4 ± 3.4	13.6 ± 4.1	1	41.9 ± 11.2	172.9 ± 91.4	4.1		42.0 ± 4.2	646.8 ± 321.0	15.4*		15.3 ± 3.4	15.2 ± 1.3	1		
N-formyl-Ile	10.5 ± 5.0	18.5 ± 8.3	1.8	39.1 ± 25.9	69.7 ± 36.2	1.8		33.9 ± 5.4	276.3 ± 138.5	8.2*		15.4 ± 10.4	8.7 ± 1.3	0.6		
N-acetyl-Pro	259.5 ± 15.4	321.7 ± 33.5	1.2*	469.8 ± 156.5	810.2 ± 140.6	1.7*		847.1 ± 139.6	2167.4 ± 521.8	2.6*		289.9 ± 106.3	317.8 ± 56.9	1.1		
N-acetyl-Phe	3.3 ± 0.9	3.3 ± 0.5	1	7.4 ± 1.0	12.6 ± 1.8	1.7*		6.8 ± 1.8	70.9 ± 26.3	10.4*		4.1 ± 0.8	4.9 ± 1.0	1.2		
N-formyl-Pip	13.8 ± 4.5	21.0 ± 8.2	1.5	42.5 ± 8.7	107.5 ± 42.7	2.5		43.2 ± 16.0	544.3 ± 188.7	12.6*		23.2 ± 14.1	23.6 ± 6.5	1		
N-acetyl-Trp	9.5 ± 2.4	15.9 ± 4.8	1.7	21.1 ± 10.0	25.4 ± 3.3	1.2		36.4 ± 8.0	122.9 ± 41.9	3.4*		6.7 ± 2.3	12.2 ± 6.7	1.8		
scopoletin	3.2 ± 0.2	2.5 ± 0.6	0.8	6.0 ± 2.3	15.6 ± 5.5	2.6*		9.2 ± 3.0	50.8 ± 10.2	5.5**		1.5 ± 0.4	1.5 ± 0.5	1		

B

Metabolite	Col-0_Psm avrRpm1_time course															
	Col-0, 8 hpi, local leaves				Col-0, 24 hpi, local leaves				Col-0, 48 hpi, local leaves				Col-0, 48 hpi, systemic leaves			
	MgCl ₂ [ng / g FW]	Psm avrRpm1 [ng / g FW]	ratio Avr / M		MgCl ₂ [ng / g FW]	Psm avrRpm1 [ng / g FW]	ratio Avr / M		MgCl ₂ [ng / g FW]	Psm avrRpm1 [ng / g FW]	ratio Avr / M		MgCl ₂ [ng / g FW]	Psm avrRpm1 [ng / g FW]	ratio Avr / M	
N-acetyl-Val	23.2 ± 6.1	25.4 ± 7.1	1.1	43.0 ± 19.6	42.2 ± 16.0	1		19.0 ± 0.5	45.4 ± 9.4	2.4**		19.3 ± 3.3	19.4 ± 2.8	1		
N-acetyl-Leu	6.1 ± 1.1	8.9 ± 3.6	1.5	12.5 ± 4.9	12.0 ± 2.6	1		13.9 ± 5.5	18.9 ± 4.5	1.4		7.5 ± 3.2	9.3 ± 2.4	1.2		
N-acetyl-Ile	6.7 ± 2.7	16.1 ± 6.7	2.4	18.9 ± 7.7	16.5 ± 7.3	0.9		14.0 ± 4.1	34.0 ± 7.4	2.4*		7.4 ± 3.1	9.3 ± 0.9	1.3		
N-formyl-Leu	13.4 ± 3.4	25.1 ± 10.7	1.9	41.9 ± 11.2	38.5 ± 16.6	0.9		42.0 ± 4.2	169.1 ± 61.3	4.0*		15.3 ± 3.4	14.3 ± 7.4	0.9		
N-formyl-Ile	10.5 ± 5.0	12.4 ± 8.2	1.2	39.1 ± 25.9	17.6 ± 9.4	0.5		33.9 ± 5.4	94.4 ± 49.2	2.8		15.4 ± 10.4	9.9 ± 3.1	0.6		
N-acetyl-Pro	259.5 ± 15.4	326.3 ± 139.3	1.3	469.8 ± 156.5	608.5 ± 95.8	1.3		847.1 ± 139.6	1028.8 ± 197.9	1.2		289.9 ± 106.3	384.5 ± 104.0	1.3		
N-acetyl-Phe	3.3 ± 0.9	8.1 ± 2.5	2.5*	7.4 ± 1.0	9.5 ± 4.3	1.3		6.8 ± 1.8	19.3 ± 3.1	2.8**		4.1 ± 0.8	3.7 ± 0.8	0.9		
N-formyl-Pip	13.8 ± 4.5	52.1 ± 9.1	3.8**	42.5 ± 8.7	51.4 ± 4.8	1.2		43.2 ± 16.0	114.6 ± 28.7	2.7*		23.2 ± 14.1	19.7 ± 8.0	0.8		
N-acetyl-Trp	9.5 ± 2.4	12.2 ± 8.6	1.3	21.1 ± 10.0	20.5 ± 11.2	1		36.4 ± 8.0	75.0 ± 16.9	2.1*		6.7 ± 2.3	18.7 ± 0.9	2.8**		
scopoletin	3.2 ± 0.2	5.1 ± 2.2	1.6	6.0 ± 2.3	9.1 ± 7.7	1.5		9.2 ± 3.0	22.6 ± 4.0	2.5*		1.5 ± 0.4	1.6 ± 0.8	1.1		

0 - 10	10 - 50	50 - 150	150 - 300	300 - 500	500 - 1000	1000 - 2500	> 2500
--------	---------	----------	-----------	-----------	------------	-------------	--------

[ng / g FW]

Figure S6. Temporal patterns of the accumulation of the identified metabolites in Arabidopsis (Col-0) after inoculation with *Psm* and *Psm avrRpm1*.

Figure-legend is given on the next page.

Supplemental Material

Legend for figure S6:

Accumulation patterns were determined at the infection-site 8, 24, and 48 hpi, and in systemic leaves 48 hpi. Mean Values for the endogenous levels of the identified metabolites are given in [ng / g FW].

(A) Ratio *P* / M means the fold-change between the *Psm*-inoculated and MgCl₂-infiltrated leaves.

(B) Ratio *Avr* / M means the fold-change between the *Psm avrRpm1*-inoculated and MgCl₂-infiltrated leaves.

Asterisks denote statistically differences between *Psm* (*P*), *Psm avrRpm1* (*Avr*) and MgCl₂ (*M*) samples (two tailed *t*-test; ****P* < 0.001, ***P* < 0.01 and **P* < 0.05).

Metabolite	Col-0_ 48 hpi local leaves					sid2_ 48 hpi_ local leaves				
	MgCl ₂ [ng / g FW]	<i>Psm</i> [ng / g FW]	ratio <i>P</i> / <i>M</i>	<i>Psm avrRpm1</i> [ng / g FW]	ratio <i>Avr</i> / <i>M</i>	MgCl ₂ [ng / g FW]	<i>Psm</i> [ng / g FW]	ratio <i>P</i> / <i>M</i>	<i>Psm avrRpm1</i> [ng / g FW]	ratio <i>Avr</i> / <i>M</i>
N-acetyl-Val	37.6 ± 16.1	119.0 ± 34.7	3.2 *	90.8 ± 19.6	2.4 *	37.9 ± 5.6	146.1 ± 50.6	3.9 *	49.3 ± 17.9	1,3
N-acetyl-Leu	46.8 ± 17.2	88.6 ± 16.2	1.9 *	28.8 ± 3.4	0,6	34.0 ± 5.9	91.7 ± 23.9	2.7 *	37.6 ± 11.4	2,4
N-acetyl-Ile	46.5 ± 28.8	101.8 ± 28.9	2,2	64.0 ± 16.1	1,4	37.4 ± 10.2	151.7 ± 55.6	4.1 *	85.9 ± 19.1	2,3 *
N-formyl-Leu	106.8 ± 88.1	1793.9 ± 506.1	16.8 **	348.3 ± 74.1	3.3 *	107.1 ± 19.6	2396.4 ± 1486.8	22,4	581.6 ± 170.1	5.4 **
N-formyl-Ile	133.5 ± 108.7	1469.6 ± 357.2	11.0 **	270.2 ± 40.1	2	119.0 ± 20.9	1755.7 ± 938.6	15.0 *	509.5 ± 146.5	4.3 *
N-acetyl-Pro	659.2 ± 203.7	5215.8 ± 214.8	7.9 ***	2548.1 ± 848.1	3.9 *	667.5 ± 97.8	4408.3 ± 1178.0	6.6 **	2958.7 ± 487.9	4.4 **
N-acetyl-Phe	10.7 ± 3.9	50.9 ± 11.4	4.8 **	18.8 ± 9.6	1,8	6.1 ± 0.7	122.0 ± 49.3	20.0	36.2 ± 5.1	5.9 ***
N-formyl-Pip	117.5 ± 72.6	1051.5 ± 273.6	8.9 **	208.0 ± 49.7	1,8	109.0 ± 5.0	1549.1 ± 853.5	14.2 *	405.8 ± 75.7 a	3.7 ***
N-acetyl-Trp	32.6 ± 13.9	291.8 ± 148.9	8.9 *	115.5 ± 71.0	3,5	76.1 ± 15.7 a	423.8 ± 116.6	5.6 **	188.3 ± 28.9	2.5 **
scopoletine	5.5 ± 4.0	39.2 ± 14.7	7.1 *	31.7 ± 7.3	5.8 **	3.5 ± 0.8	127.7 ± 65.5	36.5	50.7 ± 12.4	14.5 **

Figure S7. Accumulation of the identified acylated amino acids in the SA-biosynthesis mutant *sid2* after inoculation with *Psm* and *Psm avrRpm1*.

Mean Values for the endogenous levels of the identified metabolites are given in [ng / g FW]. Leaves for the extraction were harvested 48 h after the inoculation. Ratio *P* / M means the fold-change between *Psm*-inoculated and MgCl₂-infiltrated leaves. Ratio *Avr* / M means the fold-change between *Psm avrRpm1*-inoculated and MgCl₂-infiltrated leaves.

Asterisks denote statistically differences between *Psm* (*P*), *Psm avrRpm1* (*Avr*) and MgCl₂ (*M*) samples (two tailed *t*-test; ****P* < 0.001, ***P* < 0.01 and **P* < 0.05). Letters denote statistically differences between the same treatment of Col-0 and *sid2* (^c *P* < 0.001, ^b *P* < 0.01, and ^a *P* < 0.05; two tailed *t* test).

Supplemental Material

Metabolite	Col-0_ 48 hpi local leaves					aba2-1_ 48 hpi_ local leaves				
	MgCl ₂ [ng / g FW]	<i>Psm</i> [ng / g FW]	ratio P / M	<i>Psm avrRpm1</i> [ng / g FW]	ratio Avr / M	MgCl ₂ [ng / g FW]	<i>Psm</i> [ng / g FW]	ratio P / M	<i>Psm avrRpm1</i> [ng / g FW]	ratio Avr / M
N-acetyl-Val	37.6 ± 16.1	119.0 ± 34.7	3.2 *	90.8 ± 19.6	2.4 *	68.8 ± 21.5	108.1 ± 60.4	1,6	102.6 ± 15.4	1,5
N-acetyl-Leu	46.8 ± 17.2	88.6 ± 16.2	1.9 *	28.8 ± 3.4	0,6	73.5 ± 28.2	148.5 ± 88.1	2	100.0 ± 17.3 b	1,4
N-acetyl-Ile	46.5 ± 28.8	101.8 ± 28.9	2,2	64.0 ± 16.1	1,4	99.3 ± 24.4	157.7 ± 82.7	1,6	146.7 ± 93.5	1,5
N-formyl-Leu	106.8 ± 88.1	1793.9 ± 506.1	16.8 **	348.3 ± 74.1	3.3 *	329.5 ± 120.3	2714.5 ± 2176.8	8,2	545.8 ± 438.5	1,7
N-formyl-Ile	133.5 ± 108.7	1469.6 ± 357.2	11.0 **	270.2 ± 40.1	2	356.2 ± 128.0	2202.3 ± 2138.0	6,2	649.7 ± 174.9 a	1,8
N-acetyl-Pro	659.2 ± 203.7	5215.8 ± 214.8	7.9 ***	2548.1 ± 848.1	3.9 *	1724.1 ± 384.4 a	5888.1 ± 1636.4	3,4	2798.3 ± 602.1	1,6
N-acetyl-Phe	10.7 ± 3.9	50.9 ± 11.4	4.8 **	18.8 ± 9.6	1,8	8.6 ± 1.3	25.6 ± 15.8	3	21.8 ± 4.1	2.5 **
N-formyl-Pip	117.5 ± 72.6	1051.5 ± 273.6	8.9 **	208.0 ± 49.7	1,8	217.9 ± 55.1	1003.5 ± 823.6	4,6	369.6 ± 38.8	1.7 *
N-acetyl-Trp	32.6 ± 13.9	291.8 ± 148.9	8.9 *	115.5 ± 71.0	3,5	117.1 ± 27.3 b	461.3 ± 341.9	3,9	205.0 ± 36.9	1,8
scopoletine	5.5 ± 4.0	39.2 ± 14.7	7.1 *	31.7 ± 7.3	5.8 **	8.2 ± 1.1	62.5 ± 16.4	7.6 **	52.7 ± 28.5	6,4

Metabolite	Col-0_ 48 hpi local leaves					nced3_ 48 hpi_ local leaves				
	MgCl ₂ [ng / g FW]	<i>Psm</i> [ng / g FW]	ratio P / M	<i>Psm avrRpm1</i> [ng / g FW]	ratio Avr / M	MgCl ₂ [ng / g FW]	<i>Psm</i> [ng / g FW]	ratio P / M	<i>Psm avrRpm1</i> [ng / g FW]	ratio Avr / M
N-acetyl-Val	15.5 ± 0.75	68.3 ± 27.5	4.4 *	52.0 ± 16.1	3.4 *	31.7 ± 5.0 b	119.4 ± 40.8	3.8 *	67.6 ± 24.1	2,1
N-acetyl-Leu	11.5 ± 1.1	100.3 ± 51.2	8.7 *	71.1 ± 22.4	6.2 *	23.4 ± 7.5 a	190.4 ± 139.3	8,1	108.9 ± 59.6	4,6
N-acetyl-Ile	11.0 ± 1.7	145.3 ± 76.9	13.2 *	94.2 ± 27.8	8.6 *	24.7 ± 5.6 a	185.5 ± 113.0	7,5	100.1 ± 63.7	4,1
N-formyl-Leu	37.5 ± 5.9	854.5 ± 469.0	22.8 *	437.6 ± 57.6	11.7 ***	71.5 ± 26.3	1011.1 ± 301.0	14.1 **	192.2 ± 117.3 a	2,7
N-formyl-Ile	34.0 ± 3.2	311.7 ± 157.5	9.2 *	172.2 ± 20.9	5.1 ***	60.8 ± 22.8	472.0 ± 227.9	7.8 *	102.9 ± 42.9	1,7
N-acetyl-Pro	414.2 ± 28.9	2064.8 ± 812.3	5.0 *	1323.4 ± 741.9	3,2	1030.0 ± 128.3 b	3251.5 ± 291.3	3.2 ***	3005.0 ± 566.2	2,9
N-acetyl-Phe	1.5 ± 0.3	30.9 ± 15.5	20.6 *	37.6 ± 15.8	25.1 *	6.0 ± 1.8 a	91.8 ± 60.7	15,3	29.5 ± 18.2	4,9
N-formyl-Pip	18.2 ± 1.4	222.9 ± 112.8	12.2 *	126.9 ± 87.5	7	43.3 ± 10.6 a	514.3 ± 158.1	11.9 **	106.6 ± 61.6	2,5
N-acetyl-Trp	8.0 ± 1.1	54.3 ± 18.4	6.8 *	45.1 ± 5.6	5.6 ***	17.8 ± 4.7 a	81.2 ± 19.2	4.6 **	27.5 ± 9.7	1,5
scopoletine	1.2 ± 0.5	32.6 ± 4.3	27.2 ***	31.0 ± 1.4	25.8 ***	2.2 ± 0.8	48.4 ± 9.7	22 **	33.4 ± 3.9	15,2

Metabolite	Col-0_ 48 hpi local leaves					abi1_ 48 hpi_ local leaves				
	MgCl ₂ [ng / g FW]	<i>Psm</i> [ng / g FW]	ratio P / M	<i>Psm avrRpm1</i> [ng / g FW]	ratio Avr / M	MgCl ₂ [ng / g FW]	<i>Psm</i> [ng / g FW]	ratio P / M	<i>Psm avrRpm1</i> [ng / g FW]	ratio Avr / M
N-acetyl-Val	15.5 ± 0.75	68.3 ± 27.5	4.4 *	52.0 ± 16.1	3.4 *	13.2 ± 5.0	67.2 ± 43.8	5,1	132.0 ± 65.7	10
N-acetyl-Leu	11.5 ± 1.1	100.3 ± 51.2	8.7 *	71.1 ± 22.4	6.2 *	7.1 ± 1.2 a	131.1 ± 87.6	18,5	233.7 ± 127.3	32,9
N-acetyl-Ile	11.0 ± 1.7	145.3 ± 76.9	13.2 *	94.2 ± 27.8	8.6 *	8.4 ± 6.0	154.5 ± 107.4	18,4	300.5 ± 134.0	35,8
N-formyl-Leu	37.5 ± 5.9	854.5 ± 469.0	22.8 *	437.6 ± 57.6	11.7 ***	23.6 ± 11.7	769.5 ± 564.3	32,6	716.1 ± 324.7	30,4
N-formyl-Ile	34.0 ± 3.2	311.7 ± 157.5	9.2 *	172.2 ± 20.9	5.1 ***	21.5 ± 8.2	241.1 ± 172.3	11,2	318.2 ± 118.4	14,8 *
N-acetyl-Pro	414.2 ± 28.9	2064.8 ± 812.3	5.0 *	1323.4 ± 741.9	3,2	408.6 ± 135.8	1773.0 ± 1229.2	4,3	2043.6 ± 902.6	5
N-acetyl-Phe	1.5 ± 0.3	30.9 ± 15.5	20.6 *	37.6 ± 15.8	25.1 *	1.7 ± 0.2	64.7 ± 17.1	38,1	94.6 ± 60.0	55,6
N-formyl-Pip	18.2 ± 1.4	222.9 ± 112.8	12.2 *	126.9 ± 87.5	7	16.2 ± 3.4	347.6 ± 135.1	21,5	399.0 ± 178.6	24,6
N-acetyl-Trp	8.0 ± 1.1	54.3 ± 18.4	6.8 *	45.1 ± 5.6	5.6 ***	6.1 ± 1.8	65.4 ± 22.8	10,7 *	82.9 ± 33.1	13,6
scopoletine	1.2 ± 0.5	32.6 ± 4.3	27.2 ***	31.0 ± 1.4	25.8 ***	1.2 ± 0.3	29.0 ± 10.7	24,2	38.8 ± 36.1	32,3

[ng / g FW]							
0 - 10	10 - 50	50 - 150	150 - 300	300 - 500	500 - 1000	1000 - 2500	> 2500

Figure S8. Accumulation of the identified acylated amino acids in ABA-signaling deficient mutant plants after inoculation with *Psm* and *Psm avrRpm1*.

- (A) *aba2-1*
- (B) *nced3*
- (C) *abi1*

Mean Values for the endogenous levels of the identified metabolites are given in [ng / g FW]. Leaves for the extraction were harvested 48 h after the inoculation. Ratio P / M means the fold-change between *Psm*-inoculated and MgCl₂-infiltrated leaves. Ratio Avr / M means the fold-change between *Psm avrRpm1*-inoculated and MgCl₂-infiltrated leaves.

Asterisks denote statistically differences between *Psm* (P), *Psm avrRpm1* (Avr) and MgCl₂ (M) samples (two tailed *t*-test; ***P < 0.001, **P < 0.01 and *P < 0.05). Letters denote statistically differences between the same treatment of Col-0 and the respective mutant (^c P < 0.001, ^b P < 0.01, and ^a P < 0.05; two tailed *t* test).

Supplemental Material

Metabolite	Col-0, 48 hpi, local leaves			<i>ald1</i> , 48 hpi, local leaves			<i>fmo1</i> , 48 hpi, local leaves		
	MgCl ₂ [ng / g FW]	<i>Psm</i> [ng / g FW]	ratio <i>P</i> / <i>M</i>	MgCl ₂ [ng / g FW]	<i>Psm</i> [ng / g FW]	ratio <i>P</i> / <i>M</i>	MgCl ₂ [ng / g FW]	<i>Psm</i> [ng / g FW]	ratio <i>P</i> / <i>M</i>
N-acetyl-Val	14.2 ± 3.6	101.3 ± 6.3	7.1 **	14.5 ± 2.3	217.2 ± 21.2 b	14.9 **	24.7 ± 3.5	338.9 ± 62.2 a	13.7 *
N-acetyl-Leu	18.7 ± 5.8	130.4 ± 8.6	7 **	16.7 ± 3.6	319.9 ± 41.7	19.2 **	30.1 ± 5	588.9 ± 150.7 a	19.6 *
N-acetyl-Ile	7.5 ± 3.2	161.8 ± 18	21.6 **	11.7 ± 5.2	351.9 ± 77.4	30.1 *	18.8 ± 7.7	592.4 ± 188.9	31.5 *
N-formyl-Leu	40.7 ± 18.4	1524.2 ± 602.8	37.4	37.9 ± 14.8	2814.1 ± 895	3.1	203.1 ± 63.9	6539.1 ± 86.2	32.2 **
N-formyl-Ile	46.6 ± 20.9	612.1 ± 223.7	13.1	36.4 ± 15.3	1158.1 ± 345.8.9	31.8	123 ± 43.9	2275.3 ± 370.2	18.5
N-acetyl-Pro	489.4 ± 151.2	2780.6 ± 135.1	5.7 ***	393.3 ± 105	5590.9 ± 589.9 a	14 **	500.1 ± 128.9	6402.4 ± 1291.8 a	12.8 *
N-acetyl-Phe	3.1 ± 1.2	77.5 ± 18.4	25 *	4.8 ± 1.8	114.7 ± 35.5	23.9 *	7.6 ± 2.8	190.7 ± 57.3	25.1 *
N-formyl-Pip	35.9 ± 10.8	544.2 ± 107.4	15.2 *	36.9 ± 32.2	43.3 ± 25.2 a	1.2	29.5 ± 4.5	± 350.1	39.1 *
N-acetyl-Tip	14.7 ± 1.1	93.8 ± 36.6	6.4	24.2 ± 3.9	171.4 ± 62.1	7.1	22.4 ± 5.2	122.5 ± 61.4	5.5

[ng / g FW]							
0 - 10	10 - 50	50 - 150	150 - 300	300 - 500	500 - 1000	1000 - 2500	> 2500

Figure S9. Accumulation of the identified acylated amino acids in *ald1* and *fmo1* after inoculation with *Psm* and *Psm avrRpm1*.

Mean Values for the endogenous levels of the identified metabolites are given in [ng / g FW]. Leaves for the extraction were harvested 48 h after the inoculation. Ratio *P* / *M* means the fold-change between *Psm*-inoculated and MgCl₂-infiltrated leaves.

Asterisks denote statistically differences between *Psm* (*P*) and MgCl₂ (*M*) samples (two tailed *t*-test; ****P* < 0.001, ***P* < 0.01 and **P* < 0.05). Letters denote statistically differences between the same treatment of Col-0 and the respective mutant (^c*P* < 0.001, ^b*P* < 0.01, and ^a*P* < 0.05; two tailed *t* test).

Supplemental Material

Metabolite	Col-0, 48 hpi, local leaves			<i>atf1</i> , 48 hpi, local leaves		
	MgCl ₂	<i>Psm</i>	ratio	MgCl ₂	<i>Psm</i>	ratio
	[ng / g FW]		P / M	[ng / g FW]		P / M
N-acetyl-Val	5.5 ± 1	49 ± 0.8	8.9 ***	9.4 ± 3.1	70.6 ± 12.7 a	7.5 *
N-acetyl-Leu	4 ± 2.1	30.8 ± 10.2	7.7	12 ± 2.2	27.1 ± 5.5	2.3
N-acetyl-Ile	13.4 ± 4.6	38.4 ± 6.9	2.9 *	9.9 ± 0.6	29 ± 9.4	2.9
N-formyl-Leu	27 ± 15.8	338.3 ± 143.7	12.3	46.4 ± 19.4	185.8 ± 116.2	4.0
N-formyl-Ile	18.2 ± 9.7	134.9 ± 51.6	7.4	20.4 ± 4.4	93.2 ± 32.6	4.6
N-acetyl-Pro	661.7 ± 253.7	2014.1 ± 306.4	3.1 *	600.9 ± 209.4	1812.7 ± 16.7	3.0 **
N-acetyl-Phe	4.7 ± 1.3	51.2 ± 7.6	10.9 **	4.7 ± 0.9	56.9 ± 7.1	12.1 *
N-formyl-Pip	53.6 ± 24.7	248 ± 66.6	4.6 *	68 ± 8.9	220.5 ± 117	3.2
N-acetyl-Trp	20.9 ± 9.2	161.8 ± 18.4	7.7 *	17.1 ± 6.6	127.8 ± 38.2	7.5
free SA [µg / g FW]	0.81 ± 0.2	1.91 ± 0.33	2.4 *	0.81 ± 0.1	1.7 ± 0.22	2.1

Metabolite	Col-0, 48 hpi, local leaves			<i>ugt79b5</i> , 48 hpi, local leaves		
	MgCl ₂	<i>Psm</i>	ratio	MgCl ₂	<i>Psm</i>	ratio
	[ng / g FW]		P / M	[ng / g FW]		P / M
N-acetyl-Val	5.5 ± 1	49 ± 0.8	8.9 ***	10.2 ± 1.9	82.9 ± 4.5 b	8.1 ***
N-acetyl-Leu	4 ± 2.1	30.8 ± 10.2	7.7	10.4 ± 5.5	30.3 ± 7.2	2.9
N-acetyl-Ile	13.4 ± 4.6	38.4 ± 6.9	2.9 *	13.4 ± 4.6	48.8 ± 6.2	3.6 *
N-formyl-Leu	27 ± 15.8	338.3 ± 143.7	12.3	36.1 ± 10.9	229.2 ± 43.3	6.3 *
N-formyl-Ile	18.2 ± 9.7	134.9 ± 51.6	7.4	22.8 ± 4.4	94.3 ± 18.2	4.1 *
N-acetyl-Pro	661.7 ± 253.7	2014.1 ± 306.4	3.1 *	592.1 ± 175.9	1880 ± 853.2	3.2
N-acetyl-Phe	4.7 ± 1.3	51.2 ± 7.6	10.9 **	4.6 ± 1	44.3 ± 12.8	9.6 *
N-formyl-Pip	53.6 ± 24.7	248 ± 66.6	4.6 *	82.5 ± 26.6	259.6 ± 46.1	3.1 *
N-acetyl-Trp	20.9 ± 9.2	161.8 ± 18.4	7.7 *	39.7 ± 14.7	98.3 ± 6.9	2.5 *
free SA [µg / g FW]	0.81 ± 0.2	1.91 ± 0.33	2.4 *	1.51 ± 0.79	1.73 ± 0.45	1.1

Metabolite	Col-0, 48 hpi, local leaves			<i>nata1</i> , 48 hpi, local leaves		
	MgCl ₂	<i>Psm</i>	ratio	MgCl ₂	<i>Psm</i>	ratio
	[ng / g FW]		P / M	[ng / g FW]		P / M
N-acetyl-Val	5.5 ± 1	49 ± 0.8	8.9 ***	8.9 ± 2.9	87.1 ± 10.6 a	9.8 **
N-acetyl-Leu	4 ± 2.1	30.8 ± 10.2	7.7	9.9 ± 2.8	46.7 ± 29	4.7
N-acetyl-Ile	13.4 ± 4.6	38.4 ± 6.9	2.9 *	12.5 ± 2.3	44 ± 28.7	3.5
N-formyl-Leu	27 ± 15.8	338.3 ± 143.7	12.3	41.9 ± 5.8	231.3 ± 114.4	5.5
N-formyl-Ile	18.2 ± 9.7	134.9 ± 51.6	7.4	21.2 ± 4.9	105.5 ± 46.3	4.9
N-acetyl-Pro	661.7 ± 253.7	2014.1 ± 306.4	3.1 *	568.5 ± 80.7	1791 ± 64.6	3.2 **
N-acetyl-Phe	4.7 ± 1.3	51.2 ± 7.6	10.9 **	6.7 ± 2.3	36.2 ± 9.6 a	5.4 *
N-formyl-Pip	53.6 ± 24.7	248 ± 66.6	4.6 *	87.3 ± 18.1	259.7 ± 131.6	3.0
N-acetyl-Trp	20.9 ± 9.2	161.8 ± 18.4	7.7 *	25.1 ± 9.9	69.7 ± 6.9 a	2.8 *
free SA [µg / g FW]	0.81 ± 0.2	1.91 ± 0.33	2.4 *	0.98 ± 0.19	1.82 ± 0.76	1.9

[ng / g FW]							
0 - 10	10 - 50	50 - 150	150 - 300	300 - 500	500 - 1000	1000 - 2500	> 2500

Figure S10. Accumulation of the acylated amino acids in *atf1*, *ugt79b5*, and *nata1* mutant plants after inoculation with *Psm*.

(A) *atf1*; (B) *ugt79b5*; (C) *nata1*

Mean Values for the endogenous levels of the identified metabolites are given in [ng / g FW]. Leaves for the extraction were harvested 48 h after the inoculation. Ratio *P* / *M* means the fold-change between *Psm*-inoculated and MgCl₂-infiltrated leaves.

Asterisks denote statistically differences between *Psm* (*P*) and MgCl₂ (*M*) samples (two tailed *t*-test; ****P* < 0.001, ***P* < 0.01 and **P* < 0.05). Letters denote statistically differences between the same treatment of Col-0 and the respective mutant (^c*P* < 0.001, ^b*P* < 0.01, and ^a*P* < 0.05; two tailed *t* test).

Supplemental Material

A

Metabolite	Col-0, 48 hpi, local leaves			<i>din4-a</i> , 48 hpi, local leaves			<i>din4-c</i> , 48 hpi, local leaves		
	MgCl ₂ [ng / g FW]	<i>Psm</i> [ng / g FW]	ratio P / M	MgCl ₂ [ng / g FW]	<i>Psm</i> [ng / g FW]	ratio P / M	MgCl ₂ [ng / g FW]	<i>Psm</i> [ng / g FW]	ratio P / M
N-acetyl-Val	21.7 ± 6.5	29 ± 3.7	1.3	13.9 ± 1.5	26.7 ± 5.8	1.9	18.6 ± 3.8	58.3 ± 9.3 a	3.1
N-acetyl-Leu	1.6 ± 0.4	13 ± 2.1	8.1 *	3.3 ± 0.5	21.8 ± 5.2	6.6 *	8.7 ± 0.2 c	33.4 ± 5.4 a	3.8 *
N-acetyl-Ile	3.2 ± 0.6	13.8 ± 1.4	5.8 *	3.7 ± 0.4	17.8 ± 1.8	4.8 *	6.1 ± 0.2 a	29.9 ± 5.1 a	4.9 *
N-formyl-Leu	4.3 ± 1.1	49.1 ± 18.1	11.4	9.1 ± 2.5	145.4 ± 47.8	15.9	8.7 ± 2.0	157.6 ± 27.8 a	18.1 *
N-formyl-Ile	4.2 ± 0.9	29.3 ± 13.4	7.0	9.1 ± 2.2 a	68.8 ± 25	7.6	7.2 ± 2.5	63.8 ± 13.4	8.9
N-acetyl-Pro	190.1 ± 42.9	630.5 ± 131.2	3.3	279.5 ± 46.6 c	1316.2 ± 78.9 a	4.7 **	271.1 ± 122.2	1456.5 ± 208 a	5.4 *
N-acetyl-Phe	1.5 ± 0.4	6.9 ± 2.2	4.6	2.1 ± 0.1	13.5 ± 5.3	6.4	1.4 ± 0.1	28.5 ± 2.2 b	20.3 **
N-formyl-Pip	8.4 ± 1.6	72.1 ± 21.4	8.6 *	11.1 ± 1	108.1 ± 19.4 a	9.7	20.5 ± 6	90.8 ± 21.7	4.4
N-acetyl-Trp	24.1 ± 7.1	63.4 ± 5.1	2.6 *	46.1 ± 7.1	93.9 ± 24	2.0	36.6 ± 5.9	122.9 ± 24.4	3.4
SA [µg / g FW]	0.16 ± 0.3	1.25 ± 0.14	7.8 *	0.2 ± 0.05	1.9 ± 0.25 a	9.5	0.21 ± 0.03	2.34 ± 0.39 a	11.1 *

B

Metabolite	Col-0, 48 hpi, local leaves			<i>ivd1-a</i> , 48 hpi, local leaves			<i>ivd1-b</i> , 48 hpi, local leaves		
	MgCl ₂ [ng / g FW]	<i>Psm</i> [ng / g FW]	ratio P / M	MgCl ₂ [ng / g FW]	<i>Psm</i> [ng / g FW]	ratio P / M	MgCl ₂ [ng / g FW]	<i>Psm</i> [ng / g FW]	ratio P / M
N-acetyl-Val	21.7 ± 6.5	29 ± 3.7	1.3	12.9 ± 2.5	20.9 ± 2.6	1.6 *	30 ± 14.4	54.2 ± 8.2	1.8
N-acetyl-Leu	1.6 ± 0.4	13 ± 2.1	8.1 *	3.3 ± 0.9	13.5 ± 3.7	4.1	5.2 ± 2.5	34.3 ± 4.5 a	6.6 **
N-acetyl-Ile	3.2 ± 0.6	13.8 ± 1.4	5.8 *	3.6 ± 1.1	12.7 ± 3.9	3.5	6.4 ± 2.4	25.9 ± 1.8 a	4.0 **
N-formyl-Leu	4.3 ± 1.1	49.1 ± 18.1	11.4	3.6 ± 0.9	34.3 ± 12.9	9.5	20.6 ± 7.8	350.4 ± 122.6	17.0
N-formyl-Ile	4.2 ± 0.9	29.3 ± 13.4	7.0	3.3 ± 1.3	19.5 ± 6.9	5.9	15.8 ± 4.2	147.2 ± 42.8	9.3 *
N-acetyl-Pro	190.1 ± 42.9	630.5 ± 131.2	3.3	131.9 ± 41.3	697.6 ± 146.7	5.3 *	721.6 ± 220.1	3565.9 ± 545.4 a	4.9 *
N-acetyl-Phe	1.5 ± 0.4	6.9 ± 2.2	4.6	1.2 ± 0.1	39.6 ± 6.4 a	33.0 *	4.9 ± 0.8 a	25.3 ± 7.1 a	5.2 *
N-formyl-Pip	8.4 ± 1.6	72.1 ± 21.4	8.6 *	9.9 ± 2.5	62.9 ± 7.6	6.4 **	21 ± 1.6 a	252.8 ± 7.5 b	12.0 ***
N-acetyl-Trp	24.1 ± 7.1	63.4 ± 5.1	2.6 *	51.2 ± 4 a	394.7 ± 29.3 b	7.7 **	53.9 ± 8.1	102.1 ± 14	1.9
SA [µg / g FW]	0.16 ± 0.3	1.25 ± 0.14	7.8 *	0.08 ± 0.01 a	1.49 ± 0.21	18.6 *	0.6 ± 0.04 b	3.99 ± 0.07 b	6.7 ***

[ng / g FW]							
0 - 10	10 - 50	50 - 150	150 - 300	300 - 500	500 - 1000	1000 - 2500	> 2500

Figure S11. Accumulation of the acylated amino acids in *din4-a*, *din4-c*, *ivd1-a* and *ivd1-b* mutant plants after inoculation with *Psm*.

(A) *din4-a* and *din4-c*; **(B)** *ivd1-a* and *ivd1-b*

Mean Values for the endogenous levels of the identified metabolites are given in [ng / g FW]. Leaves for the extraction were harvested 48 h after the inoculation. Ratio P / M means the fold-change between *Psm*-inoculated and MgCl₂-infiltrated leaves.

Asterisks denote statistically differences between *Psm* (P) and MgCl₂ (M) samples (two tailed *t*-test; ***P < 0.001, **P < 0.01 and *P < 0.05). Letters denote statistically differences between the same treatment of Col-0 and the respective mutant (^cP < 0.001, ^bP < 0.01, and ^aP < 0.05; two tailed *t* test).

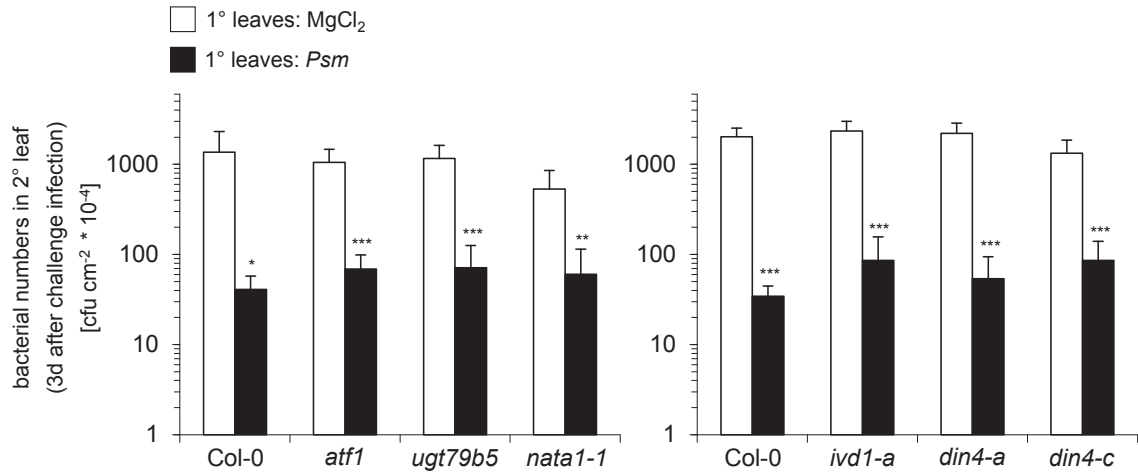


Figure S12. SAR in *atf1*, *ugt79b5*, *nata1*, *ivd1*, *din4-a*, and *din4-c*.

Local leaves were infiltrated with either 10 mM MgCl₂ or, to induce SAR, with *Psm* (applied in titers of OD₆₀₀ 0.005). Two days later three leaves, distal to the site of first infiltration, per plant were infiltrated with *Psm* (applied in titers of OD₆₀₀ 0.001). Bacterial numbers in those leaves were determined 60 h post second infiltration. Bacterial numbers are means from 6 parallel samples, each consisting of three leaf disks. Asterisks denote statistically significant differences between first MgCl₂- and *Psm*-infiltrated plants of one genotype ***P < 0.001, **P < 0.01, and *P < 0.05. Letters denote statistically differences between the same treatment of Col-0 and the respective mutant. ^cP < 0.001, ^bP < 0.01, and ^aP < 0.05 (two tailed *t* test).

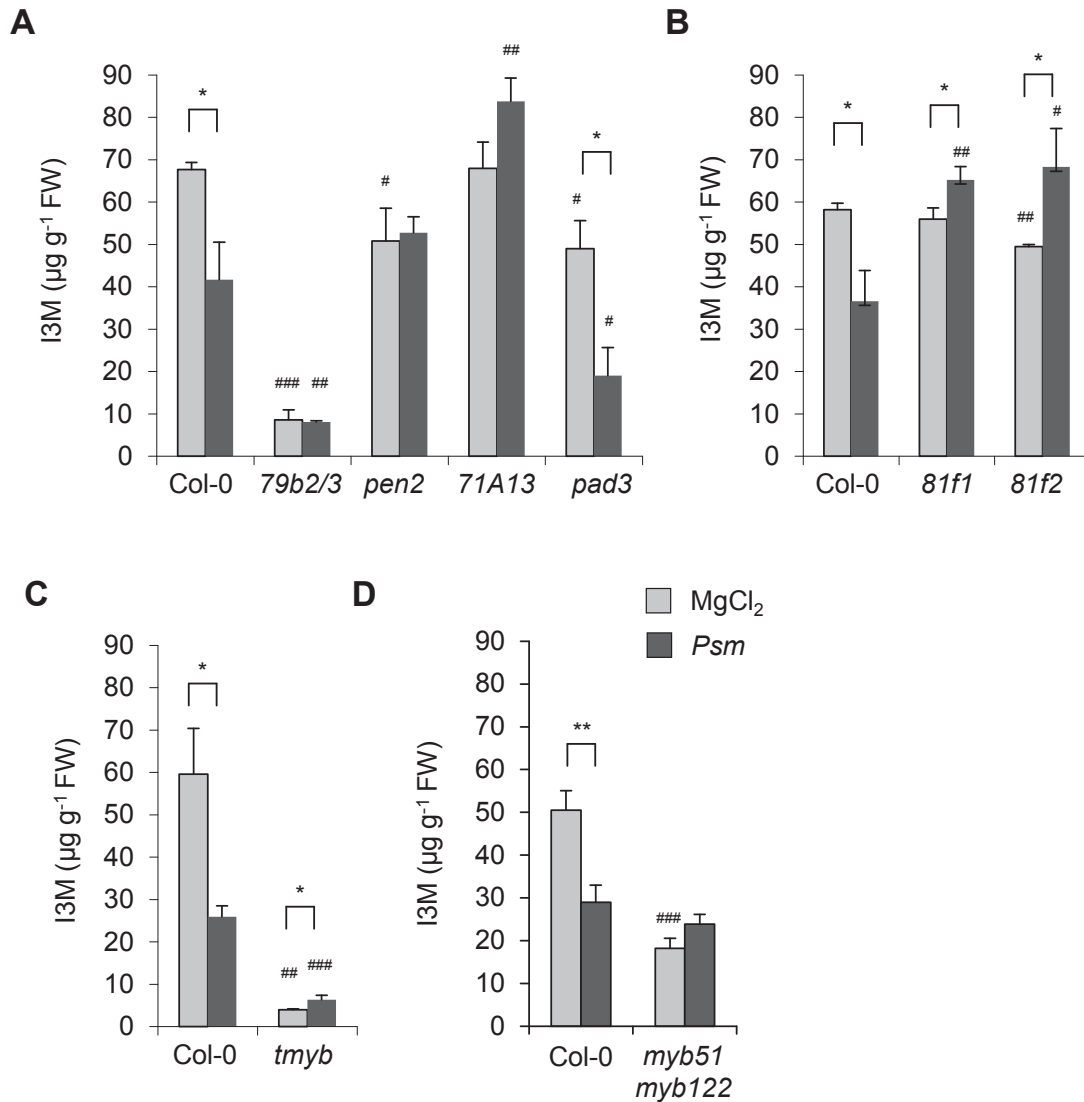


Figure S13. Impact of *P. syringae*-inoculation on the levels of the main Arabidopsis indole glucosinolate I3M in the Col-0 wild-type and different mutant plants.

(A) Col-0, *cyp79b2/b3*, *pen2*, *cyp71A13*, and *pad3*.

(B) Col-0, *cyp81f1*, and *cyp81f2*.

(C) Col-0 and *myb34/51/122* (*tmyb*).

(D) Col-0 and *myb51 myb122*.

Leaves of soil-grown plants were inoculated with *P. syringae* pv. *maculicola* (*Psm*)- or infiltrated with a 10 mM MgCl₂ mock-control solution. Levels of I3M in treated leaves were determined at 48 hpi. Data represent the mean ± SD of at least three replicate samples. Asterisks denote statistically significant differences between MgCl₂ and *Psm* treatment in one genotype (*** $P < 0.001$, ** $P < 0.01$, * $P < 0.05$; two tailed t test). Hash symbols denote statistically significant differences between the same treatment of Col-0 and the corresponding mutant (#### $P < 0.001$, ### $P < 0.01$, # $P < 0.05$; two tailed t test).

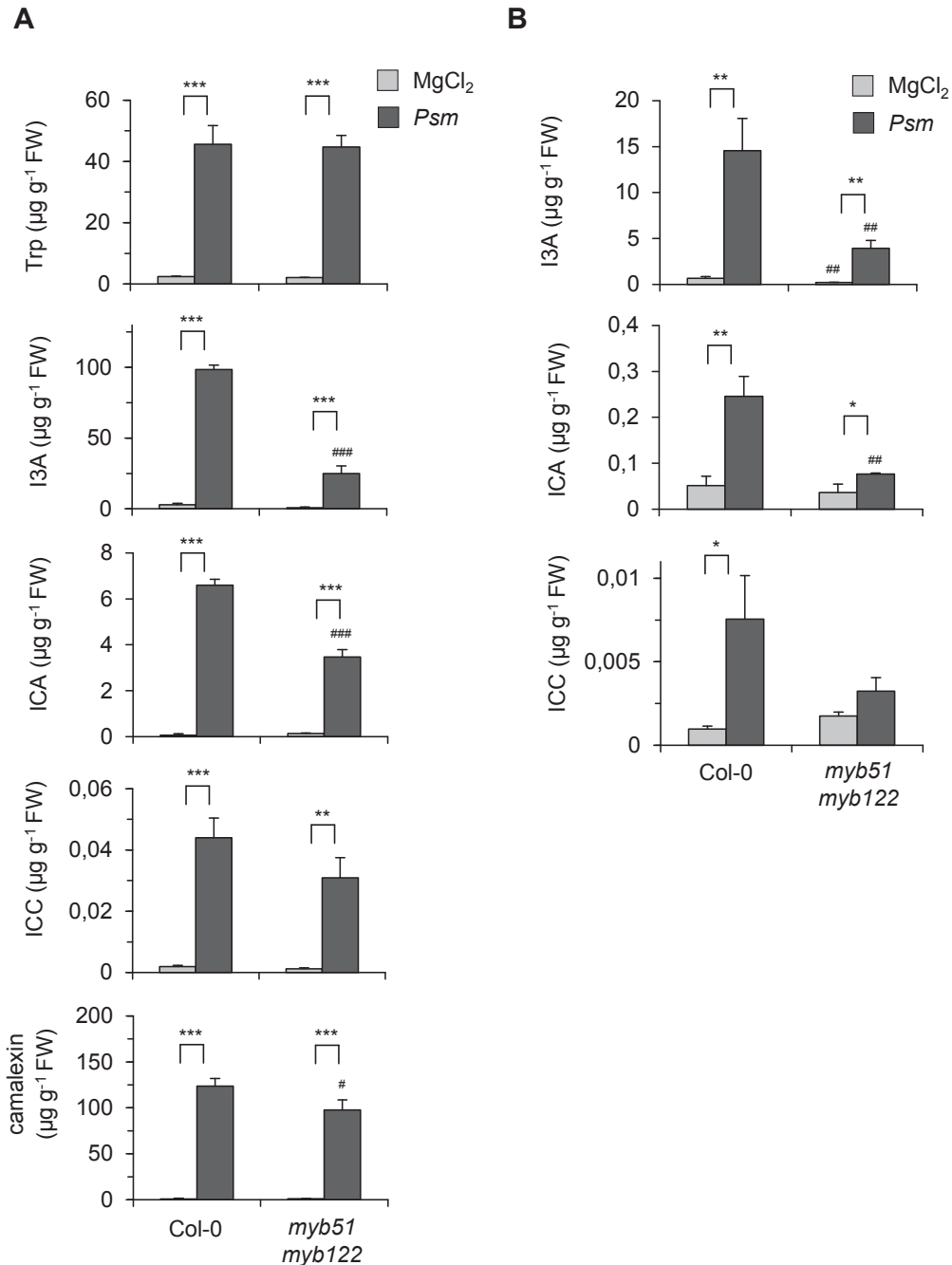


Figure S14. *P. syringae*-induced indole accumulation in soil-grown Col-0 and *myb51 myb122* double mutant plants in **(A)** inoculated leaves and **(B)** in leaves distal from the inoculation site.

(A) Levels of Trp, I3A, ICA, ICC, and camalexin in *Psm*-inoculated and MgCl₂-infiltrated leaves of Col-0 and *myb51 myb122* plants at 48 hpi. Data represent the mean ± SD of three replicate samples. Asterisks denote statistically significant differences between MgCl₂ and *Psm* treatments in one genotype (*** $P < 0.001$, ** $P < 0.01$, * $P < 0.05$; two tailed *t* test). Hash symbols on *myb51 myb122* bars denote statistically significant differences between similarly treated wild-type and mutant samples (### $P < 0.001$, ## $P < 0.01$, # $P < 0.05$; two tailed *t* test)

(B) Levels of I3A, ICA, and ICC in Col-0 *myb51 myb122*, in upper (2°) leaves after *Psm*-inoculation or MgCl₂-infiltration of lower (1°) leaves at 48 hpi. Details as described in (A).

Supplemental Material

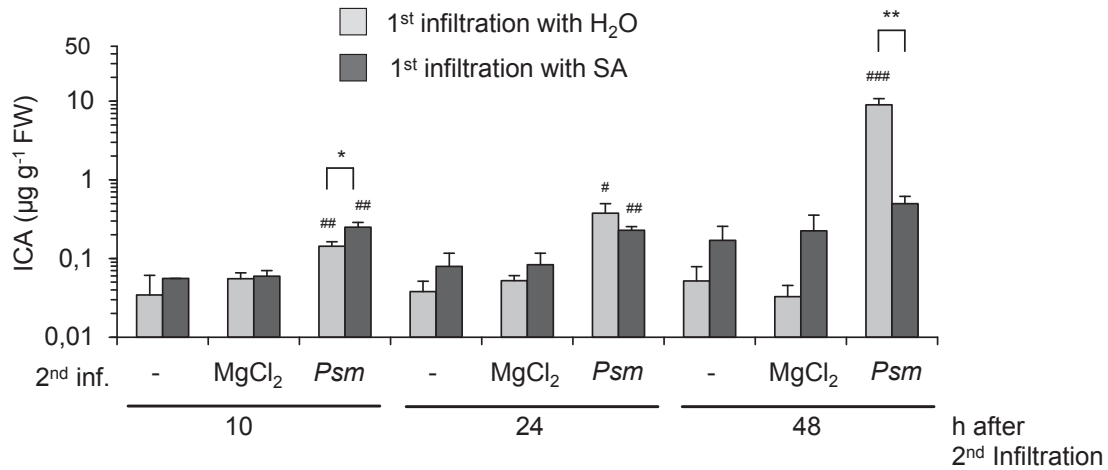


Figure S15. Impact of exogenous salicylic acid on basal and inducible levels of ICA in leaves of Col-0 plants. Please note the logarithmic scaling of the y-axis.

Three leaves of soil-grown Col-0 plants were first infiltrated with H₂O (light bars) or 0.5 mM SA solution (dark bars) (1st infiltration/inf.). 4 hours later, the same leaves were subject to a second infiltration (2nd inf.) with a 10 mM MgCl₂ (mock) solution or a suspension of *Psm*. For a third batch of plants, leaves were kept untreated (-) after the first infiltration. The leaves were harvested at the indicated times after the second treatment. Data represent the mean ± SD of three biological replicate leaf samples from different plants. Asterisks denote statistically significant differences between the respective H₂O and SA treatments (* P < 0.05, ** P < 0.01, *** P < 0.001, two tailed *t* test). Hash symbols above a *Psm*-sample indicate whether statistically significant differences exist between the secondarily mock- or *Psm*-treated samples that received the same first treatment. Analogously, hash symbols above a MgCl₂-sample indicate whether statistically significant differences exist between the secondarily mock-treated and the untreated (-) samples (### P < 0.001, ## P < 0.01, # P < 0.05; two tailed *t* test).

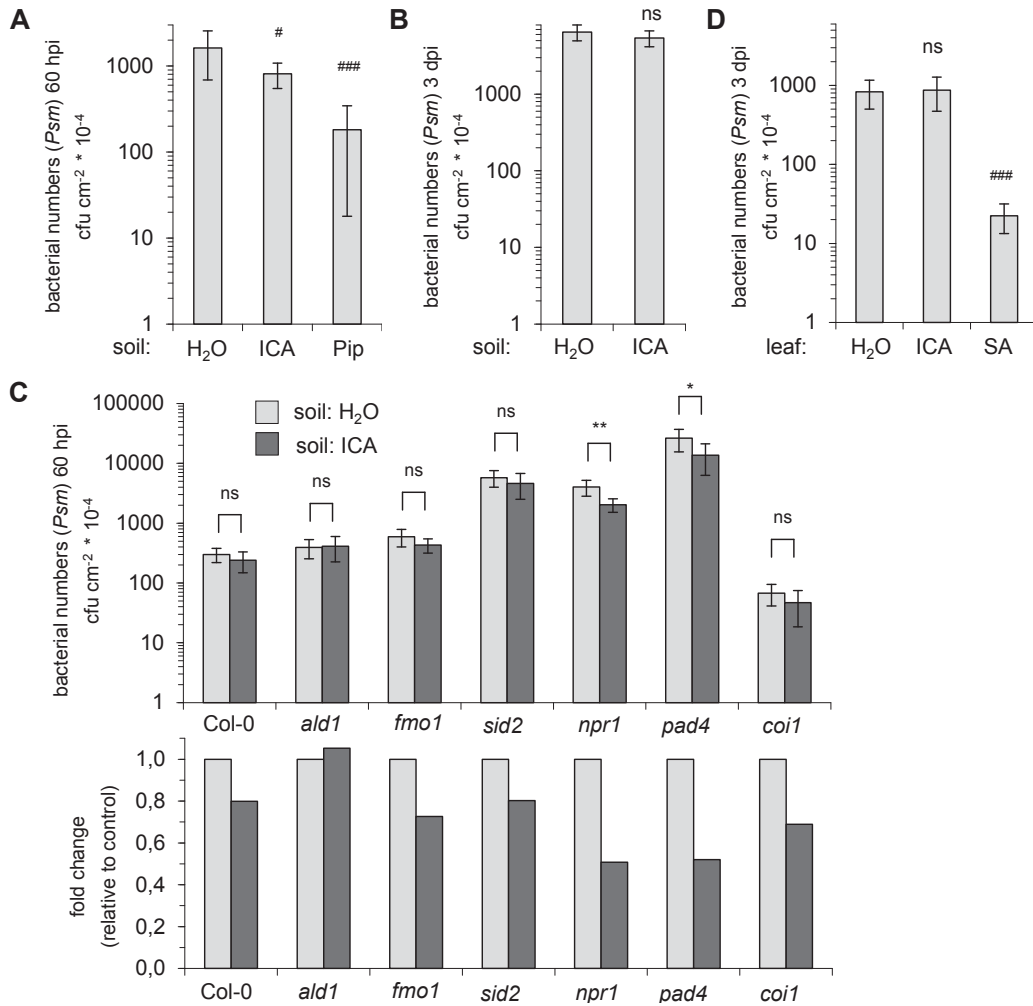


Figure S16. Exogenous application of ICA to Arabidopsis has only marginal influences on plant resistance to *P. syringae*.

(A-C) ICA was applied through the soil, and one day later leaves were inoculated with *Psm*. 60 h later, bacterial growth was assessed. **(D)** ICA was infiltrated into leaves, and 4 hours later, *Psm* inoculation and growth determination was performed.

(A) Pre-treatment of individual soil-grown Col-0 plants with water, 10 μ mol ICA, or 10 μ mol pipecolic acid (Pip). Hash symbols denote statistically differences between the water control and the chemical pre-treatments (### $P < 0.001$, # $P < 0.05$, ns: not significant; two tailed *t* test).

(B) Independent experiment with water- or 10 μ mol ICA-pre-treated Col-0 plants.

(C) Another independent experiment with water- or 10 μ mol ICA-treated Col-0 and different mutant plants impaired in plant defense signalling. Asterisks denote statistically significant differences between ICA-pre-treated and water-control samples (* $P < 0.05$, ** $P < 0.01$, ns: not significant; two tailed *t* test). The lower graph depicts the fold changes of bacterial growth in water- vs. ICA-pre-treated plants.

(D) 0.5 mM ICA, 0.5 mM SA, or H₂O was pre-infiltrated into Col-0 leaves. 4 hours later, the same leaves were challenge-inoculated with *Psm*, and bacterial growth assessed 3 days later. Statistical analyses as described in (A).

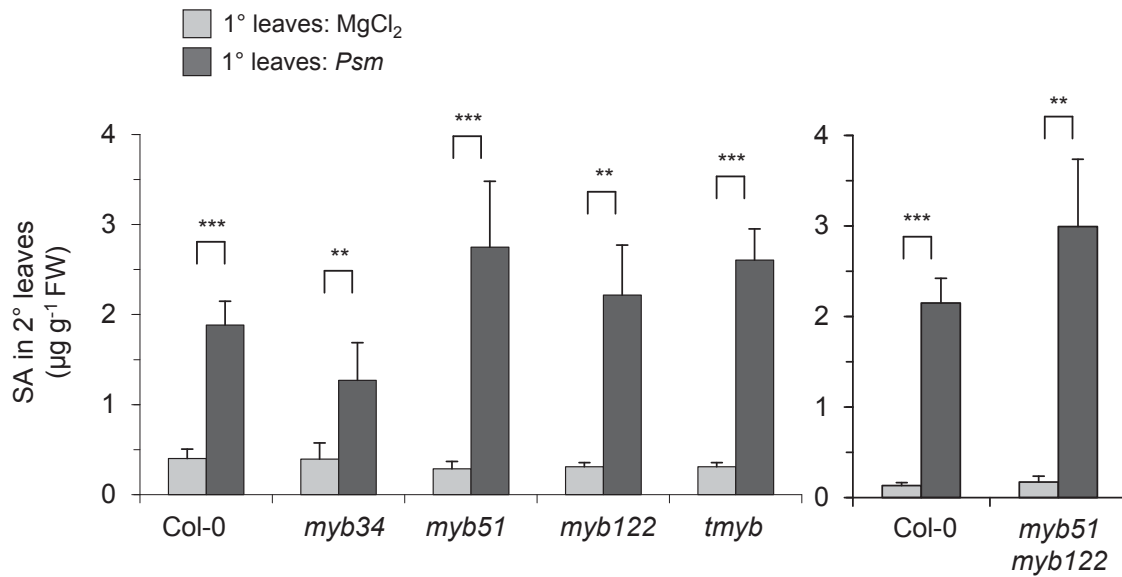


Figure S17. Systemic accumulation of SA in soil-grown Col-0, *myb34*, *myb51*, *myb122*, *myb51 myb122*, and *myb34/51/122 (tmyb)* after *P. syringae*-inoculation.

SA levels were determined in upper (2°) leaves after *Psm*-inoculation or MgCl₂-infiltration of lower (1°) leaves at 48 hpi. Data represent the mean ± SD of at least three replicate samples. Asterisks denote statistically differences between MgCl₂- and *Psm*-treatments in one genotype (*** $P < 0.001$, ** $P < 0.01$, * $P < 0.05$, ns: no significant differences; two tailed *t* test).

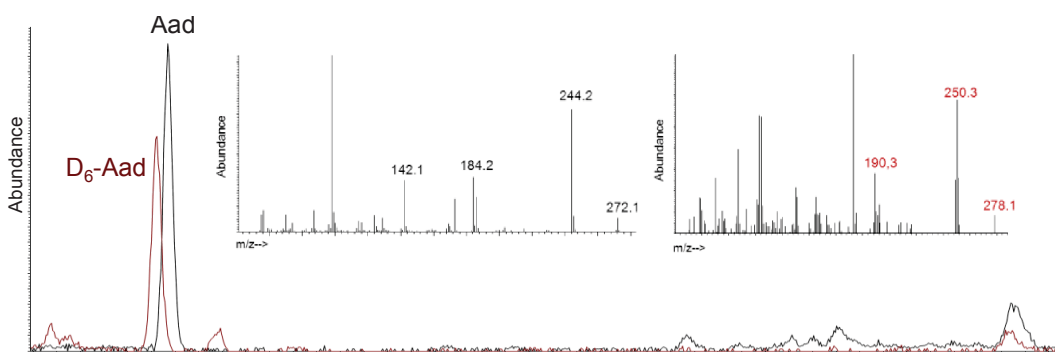
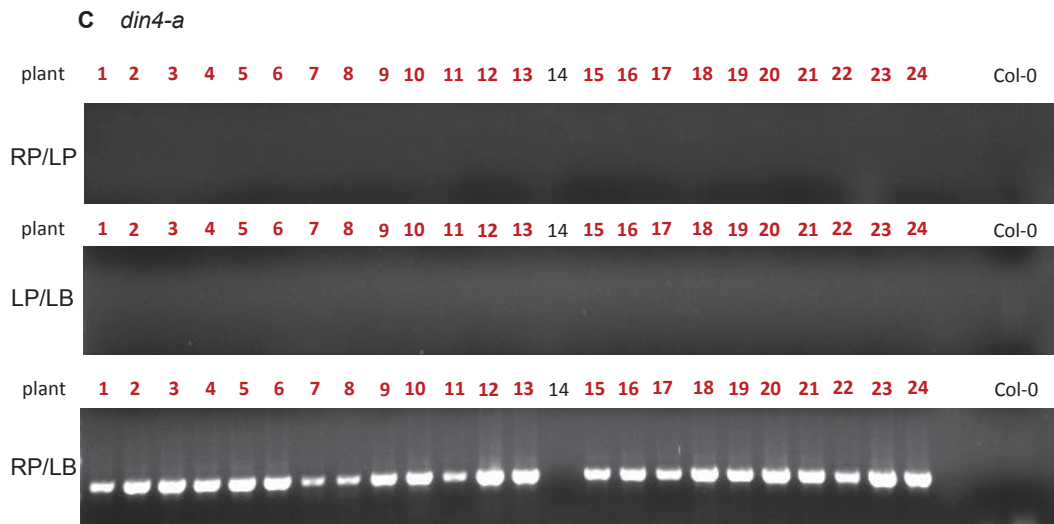
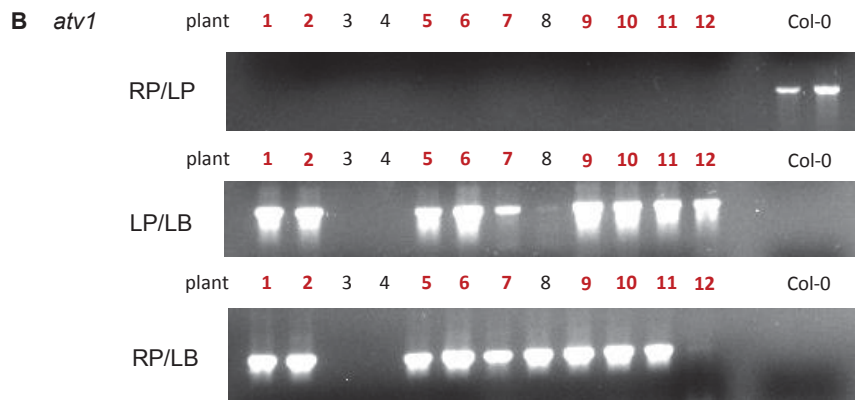
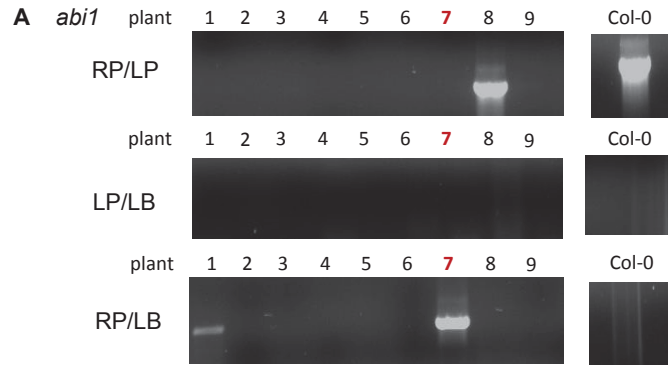


Figure S18. Chromatograms and mass-spectra of Aad and D₆-Aad.

Single-ion-chromatograms for Aad [*m/z* 244] and D₆-Aad [*m/z* 250] and mass-spectra for both metabolites. Mass-spectra were recorded in the in the electron ionization mode.

Supplemental Material

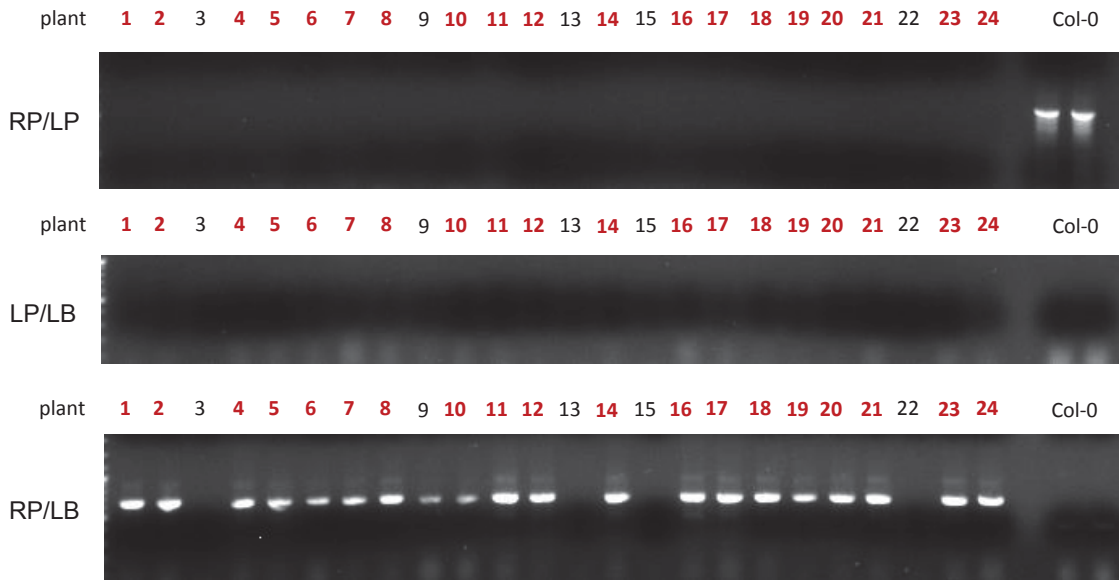


Supplemental Material

D *din4-c*



E *ivd1-a*



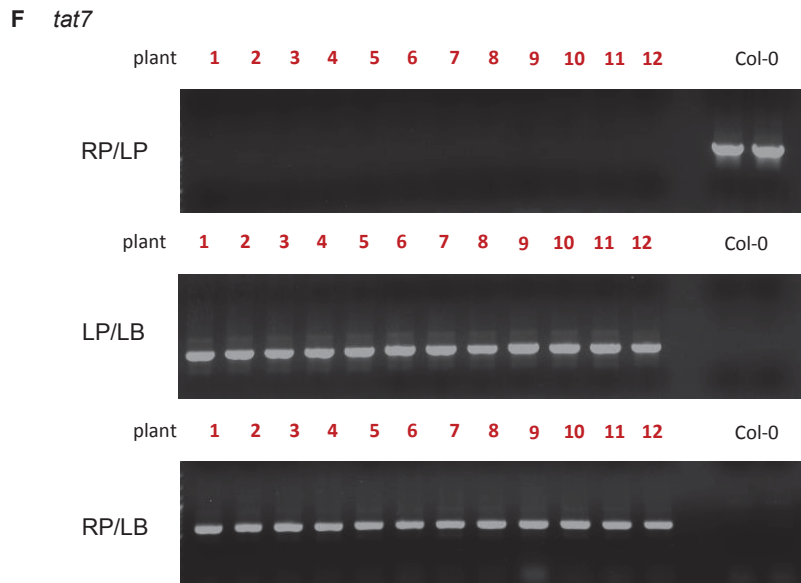


Figure S19. Results for the mutant screen described under 7.1.

(A) *abi1*, (B) *atf1*, (C) *din4-a*, (D) *din4-c*, (E) *ivd1*, (F) *tat7*.

Homozygous T-DNA insertion lines were identified by PCR according to Alonso et al. (2003) and the primers are listed in table S5. Homozygous plants are highlighted in red.

Supplemental Material

Table S1: Expression of genes involved tocopherol-biosynthesis in leaves inoculated with *Pst avr* (24 hpi) and *Psm* (24 and 32 hpi).

Gene	AGI code	expression ratio	expression ratio	expression ratio
		<i>Pst avr</i> / MgCl ₂ (24 hpi)	<i>Psm</i> / MgCl ₂ (24 hpi)	<i>Psm</i> / MgCl ₂ (32 hpi)
<i>TAT7</i>	At5g53970	7.78	3.50	11.84
<i>HPPD</i>	At1g06570	2.92	3.16	7.16
<i>VTE2</i>	At2g18950	3.95	8.56	5.49
<i>VTE3</i>	At3g63410	0.38	0.73	0.14
<i>VTE1</i>	At4g32770	1.4	0.67	0.7
<i>VTE4</i>	At1g64970	1.07	1.45	1.52
<i>VTE5</i>	At5g04490	0.47	0.88	0.52
<i>VTE6</i>	AT1g78620	0.89	1.36	0.67

Values describe the ratios between the expression in *Pst avr*- or *Psm*-inoculated leaves and MgCl₂-infiltrated leaves.

Table S2: Expression of genes involved in acetylation of amino acids in leaves inoculated with *Psm* (24 and 32 hpi).

Gene	AGI code	expression ratio	expression ratio
		<i>Psm</i> / MgCl ₂ (24 hpi)	<i>Psm</i> / MgCl ₂ (32 hpi)
<i>ATF1</i>	At2g32030	6.38	3.55
<i>DIN4</i>	At3g13450	6.14	1.73
<i>IVD1</i>	At3g45300	7.44	2.37
<i>NATA1</i>	At2g39030	6.60	5.44

Values describe the ratios between the expression in *Psm*-inoculated leaves and MgCl₂-infiltrated leaves.

Supplemental Material

Table S3: Expression of indolic pathway genes in *P. syringae* pv. *maculicola*-inoculated (1°) leaves¹ at 24 hpi and in non-inoculated, systemic (2°) leaf tissue² of Arabidopsis Col-0 plants at 48 hpi, according to microarray analyses.

Gene	AGI code	expression in 1° leaves (24 hpi) ¹			expression in 2° leaves (48 hpi) ²		
		Mock (mean ± SD)	<i>Psm</i> (mean ± SD)	ratio <i>P/M</i>	Mock (mean ± SD)	<i>Psm</i> (mean ± SD)	ratio <i>P/M</i>
<i>CYP79B2</i>	At4g39950	219.0 ± 20.5	2245.7 ± 606.0	10.3	101.0 ± 16.8	61.0 ± 4.3	0.6
<i>CYP79B3</i>	At2g22330	268.0 ± 10.2	178.8 ± 58.7	0.7	120.6 ± 10.6	49.5 ± 0.3	0.4
<i>CYP71A13</i>	At2g30770	33.9 ± 14.3	3630.8 ± 503.7	107.1	9.4 ± 0.1	43.2 ± 0.4	4.6
<i>PAD3</i>	At3g26830	34.2 ± 12.5	1984.1 ± 258.9	58.0	8.3 ± 0.8	165.3 ± 79.2	20.0
<i>PEN2</i>	At2g44490	747.4 ± 141.1	587.6 ± 19.1	0.8	519.7 ± 134.8	592.1 ± 10.0	1.1
<i>MYB34</i>	At5g60890	74.5 ± 11.0	19.1 ± 11.2	0.3	58.9 ± 10.5	14.0 ± 2.6	0.2
<i>MYB51</i>	At1g18570	23.8 ± 8.3	184.4 ± 47.2	7.7	11.8 ± 1.1	43.1 ± 8.3	3.7
<i>MYB122</i>	At1g74080	5.0 ± 6.1	98.9 ± 29.8	19.8	8.0 ± 0.2	8.3 ± 0.2	1.0
<i>CYP81F1</i>	At4g37430	42.6 ± 6.5	2187.2 ± 432.1	51.3	13.2 ± 0.4	15.2 ± 0.5	1.2
<i>CYP81F2</i>	At5g57220	13.7 ± 5.6	24.6 ± 14.9	1.8	9.0 ± 1.0	15.6 ± 2.5	1.7
<i>CYP81F3</i>	At4g37400	27.2 ± 4.4	23.0 ± 1.7	0.8	11.8 ± 0.8	13.7 ± 1.5	1.2
<i>CYP81F4</i>	At4g37410	3.3 ± 2.1	3.0 ± 3.0	0.9	10.8 ± 1.4	9.0 ± 0.2	0.8

Means (± SD) of normalized expression values and the ratios of *Psm* (*P*)/mock (*M*) expression values are given.

¹: NASCARRAYS-454; Wang et al., 2008.

²: NASCARRAYS-703; Gruner et al., 2013.

Supplemental Material

Table S4: Mutant-lines used in this study.

Mutant	Line
<i>aba2-1</i>	Léon-Kloosterziel et al., 1996
<i>abi1</i>	SALK_076909C
<i>ald1</i>	Návarová et al., 2012
<i>atf1</i>	SALK_039930C
<i>coi1</i>	Staswick and Tiryaki, 2004
<i>cpr5-2</i>	Bowling et al., 1997
<i>cyp71a13</i>	Nafisi et al., 2007
<i>cyp79b2 cyp79b3</i>	Zhao et al., 2002
<i>cyp81f1</i>	SALK_031939
<i>cyp81f2</i>	Bednarek et al., 2009
<i>dde2</i>	von Malek et al., 2002
<i>din4-a</i>	GK-475G11
<i>din4-c</i>	SALK_088551C
<i>etr1</i>	Bleecker et al., 1988
<i>f6'h1</i>	Kai et al., 2008
<i>fad3-2 fad7-2 fad8 vte2-1</i>	Mène-Saffrané et al., 2007
<i>fmo1</i>	Mishina and Zeier, 2006
<i>ivd1-a</i>	Sail_586_C09
<i>ivd1-b</i>	GK-756G02
<i>myb122</i>	SALK_022993
<i>myb34</i>	Frerigmann and Gigolashvili, 2014
<i>myb34 myb51 myb122</i>	Frerigmann and Gigolashvili, 2014
<i>myb51</i>	Frerigmann and Gigolashvili, 2014
<i>myb51 myb122</i>	Frerigmann et al., 2015
<i>nata1</i>	Adio et al., 2011
<i>nced3</i>	GK-129B08
<i>npr1</i>	NASCID: N3801
<i>pad3-1</i>	Glazebrook and Ausubel, 1994
<i>pad4-1</i>	Jirage et al., 1999
<i>pen2-2</i>	Lipka et al., 2005
<i>rbohD</i>	Torres et al., 2002
<i>sid2-1</i>	Nawrath and Métraux, 1999
<i>sid2 ald1</i>	Bernsdorff et al., 2016
<i>tat7</i>	SALK_141402C
<i>ugt79b5</i>	GK-345H07
<i>vte1</i>	Porfirova et al., 2002
<i>vte2-1</i>	Mène-Saffrané et al., 2007
<i>vte2-2</i>	Havaux et al., 2005
<i>vte3</i>	SALK_031151C
<i>vte4</i>	Bergmüller et al., 2003

Supplemental Material

Table S5: Primer used in this study for the identification of homozygous T-DNA insertion lines.

Mutant	Line	sequences 5' to 3'	
		LP	RP
<i>abi1</i>	SALK_076909C	CTCGGTGGCTACTAGATGCAG	CAGAATTGAGTTTGGGAATCG
<i>atf1</i>	SALK_039930C	TGGGTAAATTGGATAAACCAATTG	CTAGTGTAAGGCTCCACGTG
<i>cyp81f1</i>	SALK_031939	CATACAACCACACAACCGTTG	CCTCCCAAATCTCTGGATCTC
<i>din4-a</i>	GK-475G11	TTTGGTTCGAAAAAGACAACG	TGCTGATGTGGTTAAAATCCC
<i>din4-c</i>	SALK_088551C	ATAGGGTCACGGATTGTTC	TTTGCAGGAAGGAATATCGTG
<i>ivd1-a</i>	Sail_586_C09	ATTGTATCGCATTTTATGGCG	AGATCATTTTGAATTGGCATG
<i>ivd1-b</i>	GK-756G02	AATCTGCAAAGCAACCACAAC	ACCTGCAGAGGAATATGGAGG
<i>myb122</i>	SALK_022993	AGCAGAAGGGTTGAAGAAAGG	GGGAGATTCTGAAGAGGTATG
<i>nced3</i>	GK-129B08	ACAGAGGCTCTCCTCCGTAAC	GTCAGCCACGAGAAGCTACAC
<i>tat7</i>	SALK_141402C	CTACCAAAGCAAGATGACCG	AGTTGCACCGAAACACTCAAC
<i>ugt79b5</i>	GK-345H07	TGAGGAATCCAACATCGAAAC	TCCTTATGGAAACGACGTCAC

Table S6: Primers used in this study for quantitative real-time PCR analysis.

Gene	AGI code	FW (5' to 3')	RV (5' to 3')
<i>PTB</i>	At3g01150	GATCTGAATGTTAAGGCTTTAGCG	GGCTTAGATCAGGAAGTGTATAGTCTCTG
<i>TAT7</i>	At5g53970	CTCGGAATGGGAGACCCAAC	GGGAAGACCCGACGGTAGTAG
<i>HPPD</i>	At1g06570	TTGCCAGGGTTCGAGCGTGT	TCGGCGTTCCAACGTCGTC
<i>VTE1</i>	At4g32770	TCCGGACTCCTCACAGTGGGTAA	AAAGTAGTCGTCGAATGGTGAGCC
<i>VTE2</i>	At2g18950	AATGCCACTGCGGGTCAGCC	GCACCTGCAAATCCAATCACAGAGC
<i>VTE3</i>	At3g63410	CCGGTGACTCTCCTCTCCAGGTC	TCCCAGGAGGAAGCGTCCCAA
<i>VTE4</i>	At1g64970	GAAACGTGGCTGTGGCGGCT	AGGAAGCTAACCCAGTAACCCGGCA
<i>F6'H1</i>	At3g13610	TGATATCTGCAGGAATGAAACC	CGAATCGAGCCATAAAGAG
<i>GRXS13</i>	At1g03850	GGTTGAGATTGGTGAAGAAGAC	GCCATTAATATGAGCAGCCA
<i>ARD3</i>	At2g26400	CATGGACTTATGTGAGGTGTG	ACATCAAAGTATCCACTTCCTG
<i>PR1</i>	At2g14610	GTGCTCTTGTCTTCCCTCG	GCCTGGTTGTGAACCCCTTAG
<i>ALD1</i>	At2g13810	GTGCAAGATCCTACCTTCCCGGC	CGGTCTTGGGGTCATAGCCAGA
<i>SAG13</i>	At2g29350	GCGACAACATAAGGACGA	CTTCATTTGCTTCTCCAACAC
<i>FMO1</i>	At1g19250	TCTTCTGCGTGCCGTAGTTTC	CGCCATTTGACAAGAAGCATAG

Supplemental Material

Table S7: Metabolites quantified via GC/MS as described under 7.10.

compound	RT (min)	<i>m/z</i>	IST (<i>m/z</i>)	CF
SA	11.5	152, <u>120</u> , 92	D ₄ -SA (124)	1.1
α-tocopherol	31.6	<u>430</u> , 165	tocol (388)	1
β-tocopherol	31.2	<u>416</u> , 191, 151	tocol (388)	1
γ-tocopherol	31.9	<u>416</u> , 191, 151	tocol (388)	1
δ-tocopherol	30.8	<u>402</u> , 177, 137	tocol (388)	1
scopoletin	23.3	<u>192</u> , 149, 69	6-methyl-coumarin (160)	1
N-acetyl-Val	11.9	131, <u>114</u> , 99, 88, 72	D ₄ -SA (124)	1
N-acetyl-Leu	13.3	131, <u>128</u> , 99, 88, 86, 69	D ₄ -SA (124)	1
N-acetyl-Ile	13.5	131, <u>128</u> , 99, 88, 86, 69	D ₄ -SA (124)	1
N-formyl-Leu	12.9	<u>114</u> , 85, 69	D ₄ -SA (124)	1
N-formyl-Ile	13.1	<u>114</u> , 85, 69	D ₄ -SA (124)	1
N-acetyl-Pro	15.1	171, <u>112</u> , 70	D ₄ -SA (124)	1
N-acetyl-Phe	19.1	<u>162</u> , 120, 88	IPA (130)	1
N-formyl-Pip	15.2	171, <u>112</u> , 84, 67, 56	D ₄ -SA (124)	1
N-acetyl-Trp	26.9	260, 201, <u>130</u>	IPA (130)	1
3-carboxybenzaldehyde	14.1	164, <u>133</u> , 105, 77, 51	D ₄ -SA (124)	1

Metabolites which were quantified via GC/MS as described under 7.10. *m/z* describes typical masses of the mass spectra of the listed metabolites. Underlined bold masses were used for peak integration and substance quantification. Under IST is listed which internal standard were used for the quantification of the respective metabolite.

Curriculum vitae

Current Address

Dipl.-Biol. Elia Stahl
Heinrich-Heine University Düsseldorf
Institute for Plant Molecular Ecophysiology
Department of Biology
Building 26.13 Level 00 Room 68
Universitätsstr. 1
D-40225 Düsseldorf - Germany
phone: +49-(0)211-81-13401
e-mail: elia.stahl@uni-duesseldorf.de

Personal Data

Born: 31.01.1985 in Werdohl.
Nationality: German.

Education / Experience

since 04/2013	Ph.D scholarship in CEPLAS graduate school. CEPLAS – Cluster of Excellence in Plant Science Institute: “Institute for Plant Molecular Ecophysiology” (Group of Prof. Dr. Jürgen Zeier) Title of the Ph.D project: “Functional, Regulatory and Evolutionary Aspects of Stress-Inducible Plant Metabolic Pathways”
2011 – 2012	Diploma thesis Institute: “Institute for Plant Molecular Ecophysiology” (Group of Prof. Dr. Jürgen Zeier) Title: “Investigations for the role of tocopherols in plant-pathogen interactions in <i>Arabidopsis thaliana</i> .”
2006 - 2011	Study of biology Heinrich-Heine Universität – Düsseldorf

Further Qualification

- Languages: German (native)
English
French (basic knowledge; Level A1.1)
- 10-11.03.2016 Participation in the workshop: “Get into Teaching for Doctoral Researchers”.
- 02-03.07.2015. Participation in the workshop: “Optimizing Writing Strategies for Publishing Research in English”.
- 12.05.2015. Participation in the workshop: “Discussing (in) Science – How to succeed in (interdisciplinary) discussions, debates and meetings”.

- 12-14.01.2015. Participation in the workshop: "Biostatistics".
- 07-08.10.2014. Participation in the workshop: "RNA Sequencing for Beginners".
- 08-09.05.2014. Participation in the workshop: "Presenting Science – How to own the stage on (international) Conferences, for Doctoral and Postdoctoral Researchers".
- 14.01.2013. Participation in the workshop: "Good Scientific Practice for Doctoral Researchers".

Teaching Experience

- **Teaching assistant:**
 - laboratory practice in plant-environment interactions for master students; Düsseldorf 2014
 - laboratory practice in plant-environment interactions for master students; Düsseldorf 2013
 - microscopy for biology students in botany (bachelor level); Düsseldorf 2013
- **Supervision of individual students:**
 - supervision of a 3 months bachelor thesis project; Düsseldorf 2015
 - supervision of a 9 month master thesis project; Düsseldorf 2014
 - supervision of a 10 week lab practical project for an exchange student from Michigan State University (supported by the "*German Academic Exchange Service*"; DAAD); Düsseldorf 2013
 - supervision of a 6 week lab practical project; Düsseldorf 2013

Conferences / Symposia

- 10-11.09.2015. CEPLAS Young Researchers Excursion to KeyGene and Bayer Crop Science. (Wageningen, Nunhem; Netherlands).
- 06-09.09.2015. PR Proteins and Induced Resistance against Pathogens and Insects Meeting. (Aachen; Germany).
Oral presentation: "Tocopherols contribute to basal resistance against *Pseudomonas syringae* in *Arabidopsis*"
- 18-19.05.2015. CEPLAS Symposium at Rautenstrauch-Joest-Museum (Cologne; Germany).
Oral presentation: "Tocopherols contribute to basal resistance against *Pseudomonas syringae* in *Arabidopsis*"
- 29-30.09.2014. CEPLAS Young Researchers Retreat at Physikzentrum Bad Honnef (Germany).
Oral presentation: "Biosynthetic, regulatory and functional aspects of indolic metabolism in plant systemic acquired resistance"

- 03-10.08.2014. Summerschool – “Recent advances investigating structure and function of plant membranes: from microscopy analysis to transport measurements” at Beijing Forestry University (Beijing; China).
- 06-10.07.2014. XVI International Congress on Molecular Plant-Microbe Interactions. (Rhodes; Greece)
Poster presentation: “Tocopherols contribute to basal resistance against *Pseudomonas syringae* in Arabidopsis”
- 15-16.05.2014. CEPLAS Symposium at Townhouse Düsseldorf (Germany).
Poster presentation: “Biosynthetic, regulatory and functional aspects of indolic metabolism in plant systemic acquired resistance”
- 13-14.11.2013. CEPLAS Young Researchers Retreat at Haus Neuland (Bielefeld; Germany) and excursion to SAATEN UNION Biotec GmbH.
Oral presentation: “Regulatory, functional and evolutionary aspects of stress-inducible plant metabolic pathways”

Publications

Stahl, E., Bellwon, P., Huber, S., Schläppi, K., Bernsdorff, F., Vallat-Michel, A., Mauch, F., Neier, R., and Zeier, J. (2016). Regulatory and functional aspects of indolic metabolism in plant systemic acquired resistance. *Molecular Plant*, **6**, 662-681.

Sewelam, N., Jaspert, N., Van Der Kelen, K., Tognetti, V.B., Schmitz, J., Frerigmann, H., **Stahl, E.**, Zeier, J., Van Breusegem, F., and Maurino, V.G. (2014). Spatial H₂O₂ Signalling Specificity: H₂O₂ from Chloroplasts and Peroxisomes Modulates the Plant Transcriptome Differentially. *Molecular Plant*, **7**, 1191-1210.

Vogel-Adghough, D., **Stahl, E.**, Návarová, H., and Zeier J. (2013). Pipecolic acid enhances resistance to bacterial infection and primes salicylic acid and nicotine accumulation in tobacco. *Plant Signaling & Behavior*, **8**, 11.

Acknowledgements

First of all, I would like to thank my mentor and supervisor Prof. Jürgen Zeier for the opportunity to work in his lab, for the interesting research-topic, and for interesting and inspiring discussions. Furthermore, I would like to thank the second member of my PhD committee Prof. Vlada B. Urlacher for inspiring discussions regarding my research project.

For personal and scientific support during the work in Lab I thank all former and present members of the Zeier lab.

I thank the CEPLAS graduate school for organization of the scientific training program and funding. Moreover, I thank all members of CEPLAS for inspiring discussions and fun during meetings and symposia.

I thank Tamara Gigolashvili and Henning Frerigmann for providing *myb34*, *myb51*, *myb51 122*, and *tmyb* seeds, Pavel Bednarek for allocating *cyp81f2-1* seeds and authentic I3A standard, Volker Lipka for providing *pen2-2* seeds, Peter Dörmann for providing *vte1*, *vte2-2*, and *vte4* seeds, and Laurent Mène-Saffrané for providing seeds of *vte2-1*, *vte2-1 fad3-2 fad7-2 fad8*, and for inspiring discussions regarding the tocopherol project.

Finally, I like to thank my family and friends for their support during the last three years and especially for their considerateness towards the end of the thesis.

Eidesstattliche Versicherung

Erklärung gemäß der Promotionsordnung vom 20.03.2015 der Mathematisch-Naturwissenschaftlichen Fakultät der Heinrich-Heine Universität Düsseldorf.

Ich versichere an Eides statt, dass ich die vorliegende Dissertation eigenständig und ohne unerlaubte Hilfe unter Beachtung der "Grundsätze zur Sicherung guter wissenschaftlicher Praxis" an der Heinrich-Heine-Universität Düsseldorf angefertigt habe. Die Dissertation habe ich in dieser oder in ähnlicher Form noch bei keinem anderen Institut eingereicht. Ich habe bisher keine erfolglosen Promotionsversuche unternommen.

Düsseldorf, den _____

Elia Stahl

Author contributions Chapter 5

Manuscript title: Regulatory and Functional Aspects of Indolic Metabolism in Plant Systemic Acquired Resistance.

Authors: Elia Stahl^{1,4}, Patricia Bellwon², Stefan Huber¹, Klaus Schlaeppi^{2,5}, Friederike Bernsdorff¹, Armelle Vallat-Michel³, Felix Mauch², and Jürgen Zeier^{1,4,*}.

¹Department of Biology, Heinrich Heine University Düsseldorf, Universitätsstraße 1, 40225 Düsseldorf, Germany.

²Plant Biology Section, University of Fribourg, Route Albert Gockel 3, 1700 Fribourg, Switzerland.

³Institut de Chimie, Université de Neuchâtel, Avenue Bellevaux 51, 2007 Neuchâtel, Switzerland.

⁴Cluster of Excellence on Plant Sciences (CEPLAS), Heinrich Heine University Düsseldorf, Universitätsstraße 1, D-40225 Düsseldorf, Germany.

⁵Present address: Agroscope Institute for Sustainability Sciences, Reckenholzstrasse 191, CH-8046 Zürich, Switzerland.

*Correspondence: Jürgen Zeier (juergen.zeier@uni-duesseldorf.de).

Published in *Molecular Plant*, 2016, **9**, 662-681.

Author contributions: Elia Stahl, Patricia Bellwon, Stefan Huber, Klaus Schlaeppi, Friederike Bernsdorff., and Jürgen Zeier performed and evaluated the experiments. Armelle Vallat-Michel provided expertise in liquid chromatography analyses, and Felix Mauch provided supervision and feedback. Elia Stahl assisted Jürgen Zeier in manuscript preparation and writing. Jürgen Zeier designed the research, wrote the manuscript, and secured funding.

Düsseldorf, den _____

Jürgen Zeier